SPECTROSCOPIC CHARACTERISATION OF ELECTROCHEMICAL BIOSENSOR INTERFACES

A thesis for the degree of

Doctor of Philosophy

submitted to the Faculty of Engineering

University of Glasgow

by

Pamela Louise Foreman

July 1998

ProQuest LLC.
789 East Eisenhower Parkway
P.O. Box 1346
Ann Arbor, MI 48106 – 1346

"If only I had known. I would have been a locksmith."

Albert Einstein.

ABSTRACT

The work presented in this thesis investigates the composition of various glucose and glutamate biosensor interfaces using the novel combination of electrochemical and spectroscopic techniques.

Initially glucose sensors were prepared by electro-entrapment of the enzyme glucose oxidase (GOx) within thin, non-conducting films of poly(phenylene diamine) (p(pd)). Their electrochemical responses to glucose over the range 0 - 100 mmol dm^{-3} were examined as a function of electrode material, method of enzyme entrapment, enzyme solution concentration and solution oxygen concentration. Additionally, sensors were prepared with a lipid layer below the polymer-enzyme sensing layer to complement the size exclusion properties of the p(pd) films and, hence, minimise further the proportion of the current response due to interfering electro-active species such as ascorbate. For the first time, x-ray photoelectron spectroscopic (XPS) and Fourier Transform infra-red (FT-iR) spectroscopic analysis of the same samples (prepared on gold electrodes) at two different take-off angles, not only corroborated the electrochemical results, but also suggested the microenvironment of the polymer and enzyme within the sensing layer, i.e. the enzyme may 'stand proud' of the polymer matrix. Such analyses also allowed information to be extracted about the kinetic parameters of the system including estimates for the amount of enzyme present within the immobilised polymer matrix.

In order to quantify the XPS results, the polymer matrix was changed to poly(fluorophenol), (p(fp)), which also forms a thin, non-conducting film but its fluorine content has a higher intensity on the XPS spectra. Identical experiments to those prepared with p(pd) films were performed and the results indicated that with this polymer the enzyme appeared to be 'buried' within the film.

Finally, the high operating potentials and corresponding interfering signals associated with electropolymerised enzyme electrodes led to the development of hydrogel based systems which operate at much lower potentials and have a greatly increased signal to noise ratio. Glutamate sensors were prepared using the osmium based hydrogel, poly(vinylpyridine)-containing Os(dimethylbipyridine)$_2$Cl$_2$, in both single and bienzyme layer formats. The most effective method was the bienzyme system which contained the polymer, both immobilised GOx and 'wired' soybean peroxidase (SBP) and was held together with a crosslinker of polyethyleneglycol diglycidyl ether (PEGDGE).

ACKNOWLEDGEMENTS

First and foremost, I would like to thank Dr. Jon Cooper, my supervisor, for introducing me to the world of Bioelectronics and teaching me that electronic engineering can be a lot more interesting than just resistors and capacitors. His constant help, support and encouragement have been invaluable throughout my years at Glasgow University. I would also like to thank Dr. Graham Beamson and the rest of the staff at RUSTI, Daresbury Laboratories for their help with the XPS measurements.

Special thanks go to Bill Monaghan and (my wee pal) Mary Robertson for their ever-ready advice and assistance on absolutely any topic (work or personal!). Without their guidance and good nature the project would have become infinitely more difficult. Thanks also to May McCallum who arrived at the start of the writing-up process and managed to keep me in good spirits. I'd like to acknowledge all the other members of the technical staff throughout the department who have helped me over the years, including Mark Dragsness, Dave Clifton and Bill Ward.

Also deserving of a large thank you are the rest of the members of the cast of 'Biolab: The Movie': Chris Cotton for keeping me continually 'entertained' with his musical talents, Andrew Glidle for his essential help on all matters technical, Alun Griffiths for paving the way before me, Brendan Casey, Thierry de Lumley Woodyear (in Austin), Nic Green, Charlotte Hadyoon, Scott McKendry, Marcus Swann, Lili Cui, James Davis, Eric Johannson, Mike Hughes, Dave Bakewell, Kalok Chan and Mary McGoldrick for their exceptionally good company. And, of course, a huge thanks to Steffen Archer for suffering me 24 hours a day! Additionally, I would like to say thanks to my flatmates Judith Boffey and Mhairi Douglas for years of fun and moans!

Finally, I would like to thank my family for their help, support, rational thinking and financial security over the past nine years and would like to reassure them that my student days are finally over!

GLOSSARY

CV	cyclic voltammetry/voltammogram
DAB	diamino benzene
ESCA	Electron Spectroscopy for Chemical Analysis
FAD	flavin adenine dinucleotide
FT-iR	Fourier Transform Infra-red Spectroscopy
GIR	grazing incidence reflectance
GLOx	glutamate oxidase
GOx	glucose oxidase
MCT	mercury cadmium telenide
PBS	phosphate buffered saline
PEGDGE	poly(ethyleneglycol) diglycidyl ether
p(fp)	poly(*m*-fluorophenol)
pO_2	partial pressure of oxygen
POs-EA	poly(vinylpyridine)-containing $Os(dimethylbipyridine)_2Cl_2$
p(pd)	poly(*o*-phenylenediamine)
p(py)	polypyrrole
RO	reverse osmosis
RUSTI	Research Unit for Surfaces Transforms and Interfaces
SAM	self assembled monolayer
SBP	soybean peroxidase
SEM	scanning electron microscope
TOA	take off angle
XPS	X-ray Photoelectron Spectroscopy

CONTENTS

CHAPTER 1 - INTRODUCTION

In recent years the development of analytical science and its application to biotechnology has progressed remarkably, encouraged by the ever-increasing demand for superior medical detection systems applicable to a wide range of commercial markets. This need has driven widespread research into the field of biosensors and their subsequent commercialisation.[1-4]

The most lucrative markets are those which have a requirement for diagnostic kits, as the need for detection at increasingly lower limits is escalating in many diverse areas. One of the largest potential diagnostic markets is that of clinical testing [5] [6, 7] e.g. in hospital wards or emergency rooms, where size and physical robustness, biocompatibility, accuracy, sensitivity, speed of response, ease of use and cost are just some of the considerations that must be addressed when designing the devices.[8-12] Ultimately, patients themselves should be able to use the biosensors in the monitoring and control of some treatable conditions, such as diabetes. With the development of hand-held biosensor-based blood glucose monitors such as Precision Q.I.D. (MediSense) and OneTouch (LifeScan) home management of diabetes has become a reality. A selection of the most widely used commercially available glucose monitoring sensors, using both optical and electrochemical analyte recognition methods, are shown in Figure 1.1.[13-16]

Figure 1.1 - A selection of the glucose home monitoring systems available commercially around the world to date. Although some rely on optical recognition methods whilst other rely on electrochemical recognition methods, there are some common factors such as the test strip layout and the digital read-out screen.

Additionally, the significant advances made in engineering devices of micron (and nanometer) scales, and the current development of micromachining technologies, have contributed to the progression of small, reliable, integrated medical devices, making the eventual goal, production of a fully functional 'laboratory on a chip', a distinct possibility within the next few years. [9, 17, 18]

This thesis investigates the construction of enzyme sensors and applies the results to the construction of micro-biosensors to measure, during surgery, the levels of the important neurotransmitter, glutamate, which has been implicated in a variety of disorders including selective neuronal injury through cerebral ischaemia.[19-24] In contrast to previous work[25-43] which has concentrated on the optimisation of these sensors through the measurement of their response, the work described in this thesis is primarily concerned with the spectroscopic characterisation of biosensing interfaces, using both X-ray Photoelectron Spectroscopy (XPS) and Fourier Transform Infra-red Spectroscopy (FT-iR) to determine both the interfacial and bulk properties of the polymer-enzyme constructions.

1.1 Biosensors

A biosensor is an analytical device incorporating a biological material which is either immobilised or retained in a functional contact with a transducer surface in order to monitor the local environment.[11] The fundamental characteristic of such a device is that the biological material should be able to produce a quantitative signal in response to a challenge from a specific analyte. There are a wide variety of biological materials, transducer types and sensing mechanisms that can be applied to the composition of a biosensor. For example, enzymes, antibodies and nucleic acids are all suitable as biologically-sensitive materials, capable of producing a specific recognition reaction for a particular analyte.[1, 9, 44-51] The types of sensing strategy and transducer that are presently being developed to convert the biological reaction into a measurable signal include electrochemical, optical, piezo-electric, acoustic and immunological techniques.[1, 11, 47, 52-60] However, irrespective of the sensing method, the biologically functionalised transducer should be able to fulfil the following criteria: high specificity for the analyte of interest, fast response times, stable over the concentration and temperature ranges required and be suitable for miniaturisation. A generalised diagram of the composition and operation of a typical electrochemical biosensor is shown in Figure 1.2.[61]

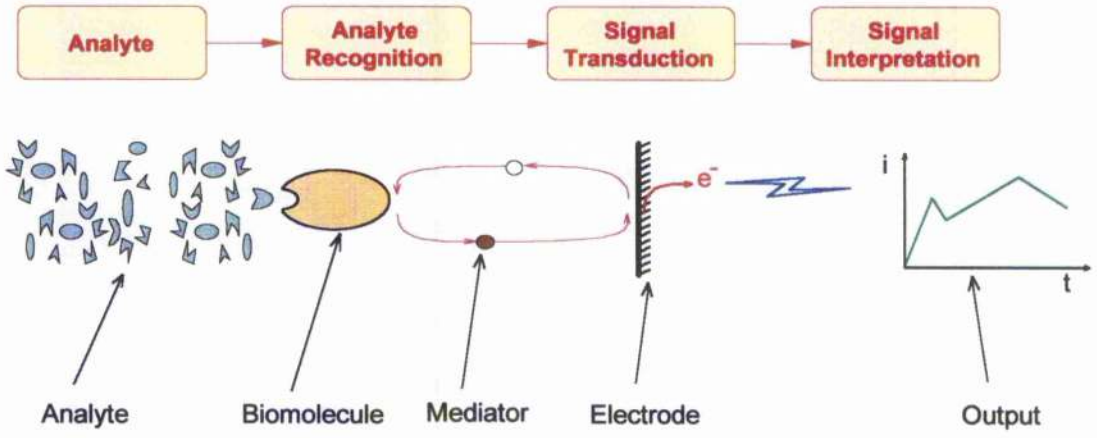

Figure 1.2 - Schematic diagram showing the operation of a typical 'mediated' electrochemical biosensor. The biomolecule, which is specific for only one particular analyte, produces a reaction, the product of which is carried by the mediator molecule to the electrode surface where it can react. A redox reaction occurs at the surface allowing the mediator to be changed from its reduced (filled) form to its oxidised (empty) form, resulting in a transfer of electrons i.e. the electrochemical signal due to analyte.

The majority of enzyme biosensors existing today use the basic concept of the electrochemical biosensor which was first conceived in 1962 by Leyland Clark,[62] who proposed that biomolecules could be immobilised within a matrix in close proximity to a detector system to form a selective electrochemical enzyme-electrode. The transducer surface is responsible for the conversion of the biomolecular recognition process into an electrical signal, such that a quantitative relationship between the measured signal and the bulk substrate concentration can be derived.

1.1.1 Protein Structure and Enzyme Activity

As described above, enzymes are frequently used as the biological component of electrochemical biosensors and play a significant role in recognition of specific analytes and, more importantly, in electron transfer i.e. signal transduction. Additionally, the nature of the spectroscopic techniques used throughout this work to analyse the polymer-enzyme interface of the enzyme biosensors require that a short description of the structure and function of enzymes be presented in this chapter.

Almost all chemical reactions in biological systems are catalysed by specific macromolecules called enzymes.[63] All pure enzymes are proteins and each has a well defined three dimensional structure, the fundamental units of which are amino acids. [64] There are twenty different naturally occurring amino acids, each with a distinctive structure, determined by the side chain (R) bonded to the central (α) carbon atom. When a number of amino acids join together they do so through the formation of a peptide bond between the amino and carboxyl groups, with the elimination of one molecule of water through a condensation reaction. The resulting polymer is known as a polypeptide chain and is shown in Figure 1.3.

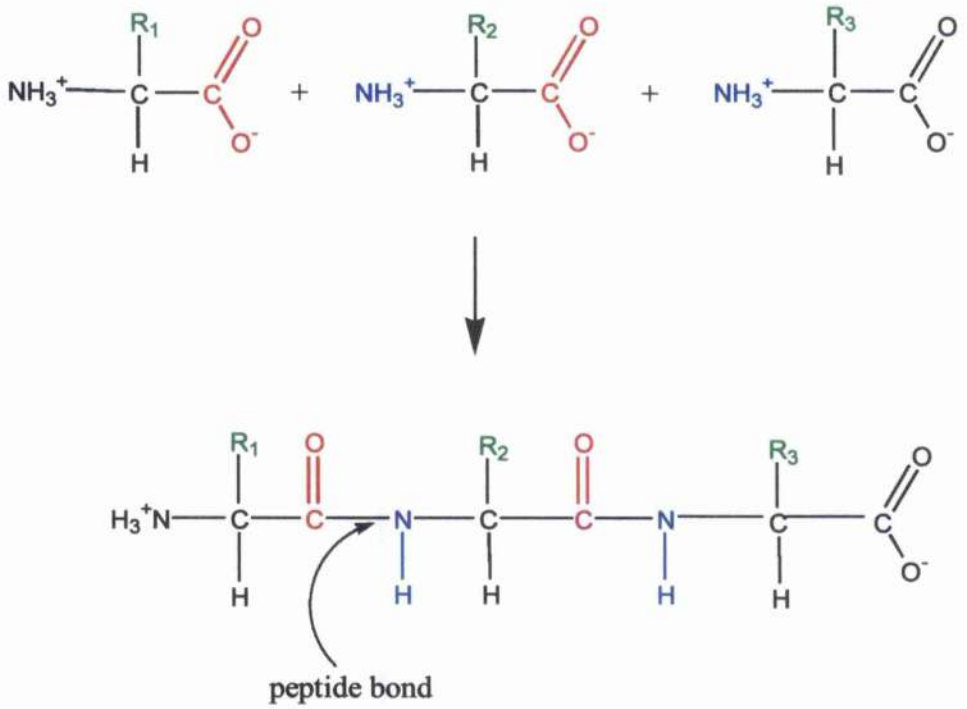

Figure 1.3 - Two or more amino acids connect via a peptide bond to form a polypeptide chain. The peptide bond is formed by a condensation reaction between the amino and carboxyl groups, which releases a water molecule and forms a covalent bond between them. This is known as the primary sequence of the protein structure.

The sequence of amino acids in a protein, as the polypeptide chain, determines the three dimensional conformation of the protein, which itself largely determines the properties and activities of specific proteins. This three-dimensional structure of the protein can be described in terms of different levels of folding, each of which is constructed from the preceding one in 'hierarchical' fashion.[65] Thus, the amino acid sequence is known as the protein's primary structure; the secondary structure being its first-level folding and describes certain regular conformations that can form by hydrogen bonding between relatively small segments of the protein sequence. The two most common secondary structural elements are the α-helix and β-pleated sheet.[66] In the α-helix, the amino acids are coiled into a right-handed helix which forces the atoms of the polypeptide backbone to pack closely at the centre of the helix with the side chains projecting outwards. In the β-sheet the polypeptide chain is almost fully extended and several segments of the chain lie side by side. A further level of folding, the tertiary structure, is imposed on this to give the final three-dimensional conformation of the protein. This can be viewed as three-dimensional

'packing' of secondary structural elements and is directly related to the protein function, e.g. enzymatic, structural. Often proteins with similar functions have similar tertiary structures but different primary structures, e.g. antibodies[67]. The tertiary structure arises from the fact that hydrophobic side chains will become buried within the core of the protein, whilst hydrophilic amino acids will exist on the surface of the protein. Some proteins are formed by the association of more than one polypeptide chain. The interaction between such chains is known as the quaternary structure of the protein, as is the case for haemoglobin [66].

The particular chemical, physical and biological properties of a protein depend upon its surface conformation. The folding of the polypeptide chain creates sites on the surface with a particular 'shape', chemical reactivity and electrostatic profile, which are determined by the nature and arrangement of the amino acid side groups.[63, 64, 66, 67] At these sites, other molecules can be selectively bound and interact with the protein. For proteins that function as enzymes, this area is known as the active site and the specificity of the enzyme is determined by the structure of these sites. The active site of an enzyme often takes the form of a cleft or crevice in the tertiary structure, providing a domain which is relatively small in comparison to the overall enzyme volume. In addition to the amino-acid chain, enzymes contain a portion of material which is non-polypeptide, called a prosthetic group and enzymes are classified on the chemical nature of this prosthetic group.[64] Historically enzymes have been classified on the chemical nature of this prosthetic group which is strongly associated with their function. Examples include metalloproteins[64] which contain a metal ion such as iron (e.g. haem peroxidases) and flavoproteins[64] which contain a flavo-nucleotide group (e.g. flavo oxidases). The enzymes discussed in this thesis fall into the latter category, and contain tightly bound flavin adenine dinucleotide (FAD) groups which can be oxidised and reduced readily, i.e. they catalyse redox reactions.

In general, an enzyme's function is to specifically catalyse the substrate molecules with which the enzyme is interacting; allowing the formation of an enzyme-substrate complex which breaks down to form the free enzyme and the reaction products.

Figure 1.4 shows the 'lock-and-key' model of the interaction of substrate and enzyme. The active site is complementary in shape to that of the substrate alone.[66, 68]

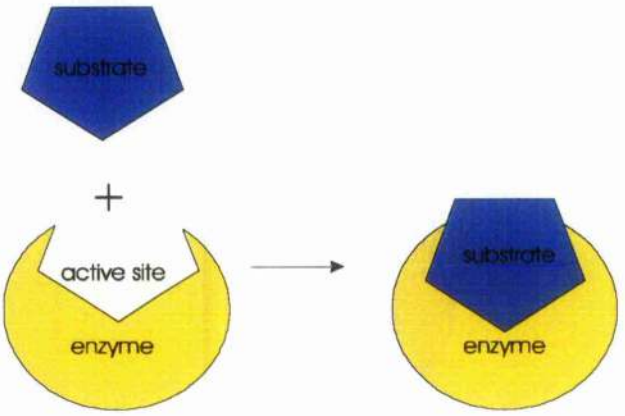

Figure 1.4 - Lock-and-key model of the interaction of substrates and enzymes. The active site of the enzyme alone is complementary in shape to that of the substrate.

It is this substrate-enzyme interaction that provides the basis for electron transfer and, hence, signal transduction corresponding to measurement of the analyte of interest. More recently the 'lock and key' model, which is rather simplistic, has been updated to the 'hand and glove' model, where there is a structural rearrangement of the protein during binding, allowing the substrate to 'fit' into the active site more closely.

1.1.2 Amperometric Sensing Strategy

There are three main methods of electrochemical detection that have been applied to biosensing, namely amperometric, potentiometric and conductimetric analysis. The work performed throughout this thesis uses amperometric techniques but descriptions of all three are described by Sethi.[11]

Electrodes analysed in this work rely upon the amperometric[69] detection of enzymatically produced or consumed electro-active species in the sample to be analysed by measuring the current generated at a working electrode (held at a

constant potential with respect to a reference electrode) as a result of the oxidation or reduction of the electro-active species. A diagrammatic representation of a typical electrochemical experimental set-up is shown in Figure 1.5.[70]

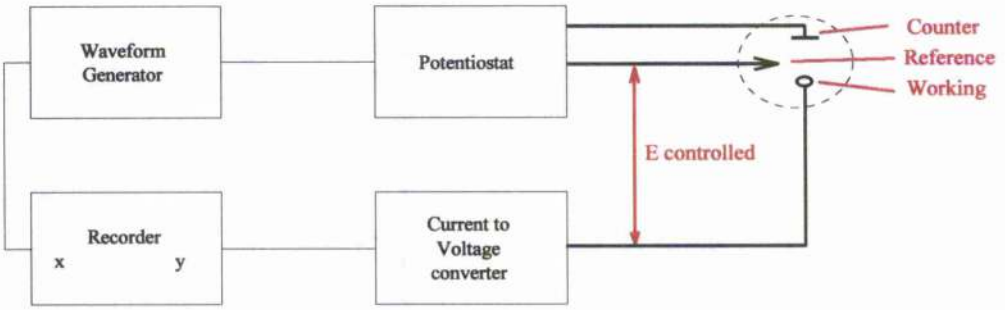

Figure 1.5 shows the typical instrumentation used for electrochemical experiments. The working electrode is the electrode at which the reaction of interest takes place. The potentiostat applies the desired potential between the working and reference electrodes and the current required to sustain the reaction at the working electrode is provided by the auxiliary electrode. This arrangement prevents large currents from passing through the reference electrode that could change its potential.

Electrochemical biosensors generally require the use of a redox enzyme, particularly those belonging to either the oxidase or dehydrogenase subclasses of oxido-reductase enzymes.[60, 64, 68] These enzymes catalyse reactions which produce or consume electro-active co-factors which can be electrochemically detected at the electrode. Flavo-oxidase enzymes, for example, catalyse the oxidation of reduced analytes and in doing so, utilise oxygen as an electron acceptor to produce a stoichiometric amount of either water (4 electron oxidation) or hydrogen peroxide, H_2O_2 (2 electron oxidation). Hydrogen peroxide can be detected, at gold electrodes, by anodic oxidation at potentials greater than +600 mV *vs.* Ag|AgCl reference electrode, or alternatively, oxygen consumption can be measured by cathodic reduction at -650 mV *vs.* Ag|AgCl.[46] By changing the electrode material, for example to carbon or platinum, the electrode potentials required vary accordingly, due to the variation in electric properties of different materials.[71, 72] The generalised scheme for these reactions is shown in Equations (1.1) and (1.2).

$$\text{Substrate}_{(RED)} + \text{Enzyme}_{(OX)} \longrightarrow \text{Product}_{(OX)} + \text{Enzyme}_{(RED)} \quad \textbf{(1.1)}$$

$$\text{Enzyme}_{(RED)} + \text{Co} - \text{substrate}_{(OX)} \longrightarrow \text{Enzyme}_{(OX)} + \text{Co} - \text{product}_{(RED)} \quad \textbf{(1.2)}$$

A typical configuration of an electrochemical enzyme-electrode can be best illustrated through an understanding of the amperometric glucose electrode. Since the home-testing of whole blood glucose of diabetic patients represents the largest potential market for clinical applications of biosensors, the development of glucose electrodes has consequently been one of the major driving forces in the field of biosensor research.[73-81] [82-85] The electrodes are based upon the reaction catalysed by the flavo-enzyme glucose oxidase (GOx) which is shown in Equations (1.3) - (1.5).

$$\text{glucose} + \text{GOx}_{(FAD)} \longrightarrow \text{gluconolactone} + \text{GOx}_{(FADH_2)} \quad \textbf{(1.3)}$$

$$\text{GOx}_{(FADH_2)} + O_2 \longrightarrow \text{GOx}_{(FAD)} + H_2O_2 \quad \textbf{(1.4)}$$

$$H_2O_2 \longrightarrow O_2 + 2H^+ + 2e^- \quad \textbf{(1.5)}$$

Glucose oxidase[86] has been particularly useful for the development of biosensors as it is both robust and stable and is, therefore, well suited to immobilisation procedures. The enzyme catalyses the oxidation of glucose, using oxygen as a mediator, to produce gluconolactone (the product) and H_2O_2 (the co-product). The hydrogen peroxide is subsequently detected electrochemically by oxidation at the electrode surface at a potential of +700 mV *vs.* Ag|AgCl. This is shown in Equation (1.5) and diagrammatically in Figure 1.6.

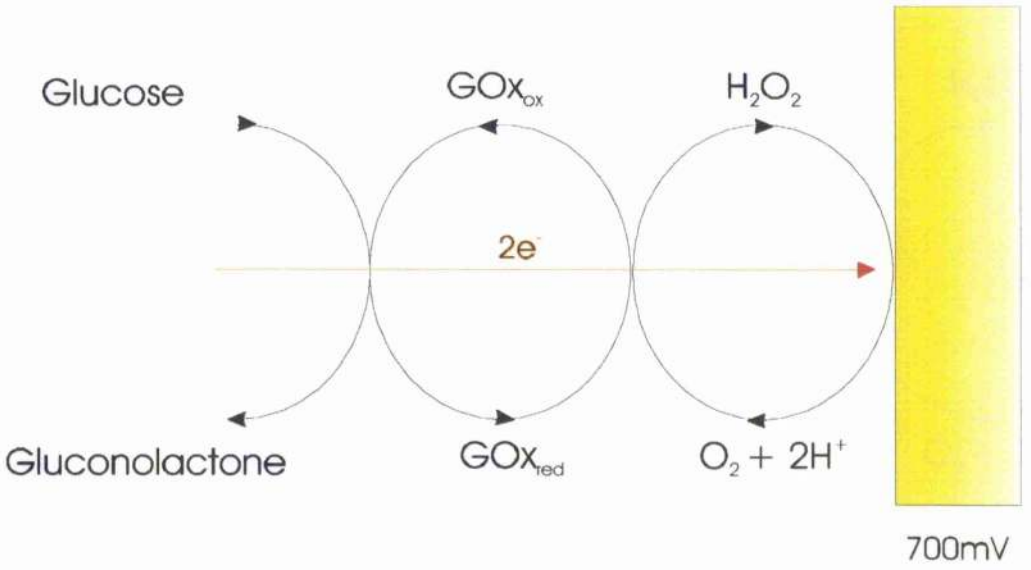

Figure 1.6 - Diagram illustrating the amperometric mode of transduction in a glucose enzyme electrode. The H_2O_2 produced is oxidised at the electrode surface and produces a current proportional to the concentration of glucose in the bulk solution.

Although the glucose electrodes are the most widely researched (and hence advanced) biosensors, the work in this thesis uses their operation to provide a model system for the further development of an amperometric glutamate biosensor. Since the enzyme glutamate oxidase (GLOx)[87, 88] also has FAD redox centre, the same sensing principles can be applied to the detection of glutamate, i.e. the hydrogen peroxide produced from the reaction catalysed by GLOx is oxidised at the electrode surface at +700 mV *vs.* Ag|AgCl, producing a current attributable to the concentration of glutamate in the bulk solution. The reaction scheme is shown in Equations (1.6) - (1.8).

$$\text{glutamate} + O_2 + H_2O \xrightarrow{\text{GLOx}} \alpha - \text{ketoglutaric acid} + NH_3 + H_2O_2 \quad \textbf{(1.6)}$$

$$\text{glutamate} + H_2O + GLOx_{(OX)} \longrightarrow \alpha - \text{ketoglutaric acid} + NH_3 + GLOx_{(RED)} \quad \textbf{(1.7)}$$

$$GLOx_{(RED)} + O_2 \longrightarrow GLOx_{(OX)} + H_2O_2 \quad \textbf{(1.8)}$$

Such an electrode configuration is termed a first generation amperometric sensor[46] since it uses oxygen as a natural electron acceptor or mediator. However, such a biosensing arrangement has a dependency on the concentration of oxygen in the

sample solution which, for biological fluids, can be low and variable.[59, 89] In order to overcome this problem a second generation of amperometric electrodes have been developed[46] which use a metal co-ordinated organic compounds, such as ferrocene and its derivatives, as an electron mediator. [11, 85, 90] This reduces the oxygen dependency of the sensor and also allows the electrode potential to be reduced (which has important consequences in decreasing sensor "interference" (see section 1.1.4)). In order to improve the sensor performance further, third generation biosensors are currently being developed in which the reduced enzyme is re-oxidised directly at a modified electrode surface.[46] These do not require the action of a mediator, allowing electrons to be transferred directly from the enzyme to the electrochemical surface, for example via redox polymers[91-94] (see Section 1.1.6) or via short chain self assembled monolayers (SAM's).[95] However, the one potential drawback of the self-assembled systems is that the enzyme is required to be 'organised' at the electrode surface, involving complex immobilisation strategies. This often results only in monolayer coverage and, hence, associated low currents.

1.1.3 Immobilisation of Enzymes in Polymer Films

To meet specific applications, biosensors require control over the molecular structure at the surface of an electrode. Previously, the concept of immobilisation of enzymes onto solid electrode surfaces has been realised using a variety of techniques including adsorption, covalent binding, cross-linking and entrapment within a porous matrix.[46, 60, 96] Electrochemical polymerisation[97-101] has also been used successfully to immobilise enzymes at transducer surfaces without altering the catalytic reaction. However, such a design necessitates not only that the analyte of interest must diffuse through the membrane before reacting but also that the reaction product must diffuse through the matrix before it can be detected at the electrode surface. Thus, changes in the diffusional properties of the layer will alter the size of the analyte response. Additionally, the thickness of the membrane layer will influence both the organisation of the immobilised enzyme and the resulting electrochemical response.[75]

A variety of organic polymers have been utilised as entrapment matrices and, depending upon their function, they can be applied to different sensor configurations. For example, polymeric gels, functional polymers, electrically conducting polymers and redox mediators[96] have all previously been used in biosensing configurations providing distinct properties.

Electropolymerisation of both conducting and non-conducting polymers possesses a number of advantages over other immobilisation techniques for the entrapment of enzymes at electrode surfaces. These advantages include the relative simplicity of the immobilisation procedure, control over the polymerisation parameters and the ability to localise the deposition allowing, for example, different enzymes to be retained at adjacent micro-electrodes.[46, 102] To form the polymer-enzyme membrane, a suitable monomer from an (enzyme-containing) solution is electrochemically oxidised at a fixed potential to form either a conducting or non-conducting polymer on the surface, entrapping the enzyme as it polymerises.

All of the enzyme-electrodes discussed in this chapter were prepared by entrapment of the enzymes within electrochemically polymerised non-conducting polymers. Formation of poly-o-phenylenediamine (p(pd)) films[103-108] is a self-limiting process which produces a very thin insulating polymer layer and so produces a matrix which enables fast diffusion of substrates and products to and from the enzyme. At present there are two possible polymerisation pathways for p(pd) films as reported by Oyama[109] and Yano[108]. Oyama suggests that the phenylene diamine monomers polymerise through what is known as a 'ladder polymer' formation as shown in Figure 1.7 while Yano reports a slightly different, and more 'branched', structural composition also shown in Figure 1.7.

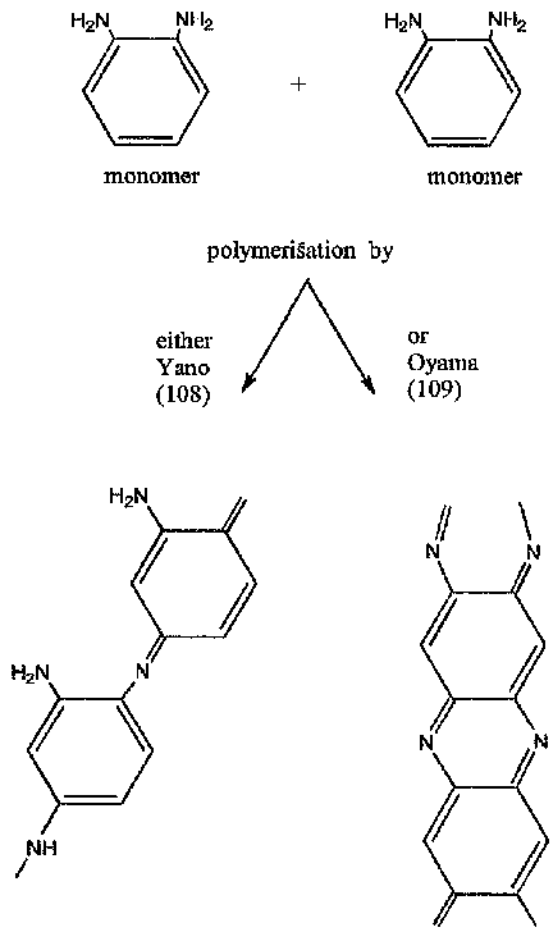

Figure 1.7 - The two different polymerisation mechanisms for poly(phenylenediamine) as reported by Oyama[109] and Yano[108]. In both instances the phenylenediamine monomers are joined through their amide groups but the formation known as a 'ladder' structure, produces a more linear polymer than the branched structure of Yano.

A second type of thin, insulating polymer films were employed in this work, poly(fluorophenol), whose polymerisation is similar to that of phenols.[97, 110] The attachment of a fluorine side group on the *meta*-position necessitates that the polymerisation of fluorophenol proceeds as shown in Figure 1.8.

During the electrochemical polymerisation, the fluorophenol monomer dissociates to form its anion which can be oxidised to produce a radical capable of either of the following reaction schemes: (a) reaction with impurities or other solution species to produce side products or (b) reaction with a further monomer of fluorophenol to produce either the *para*- or *ortho*-linked dimeric radical. Further oxidation and loss of a proton gives the neutral dimer. Subsequent reactions then produce oligomers

and finally polymeric material at the electrode surface. Therefore, fluorophenol polymerisation occurs at either the *para* or *ortho* position of the monomer depending upon both the distribution of electrons and/or the stability of the benzene ring due to the side groups. This may be a contributory factor in the difficulties of producing consistent and even films.

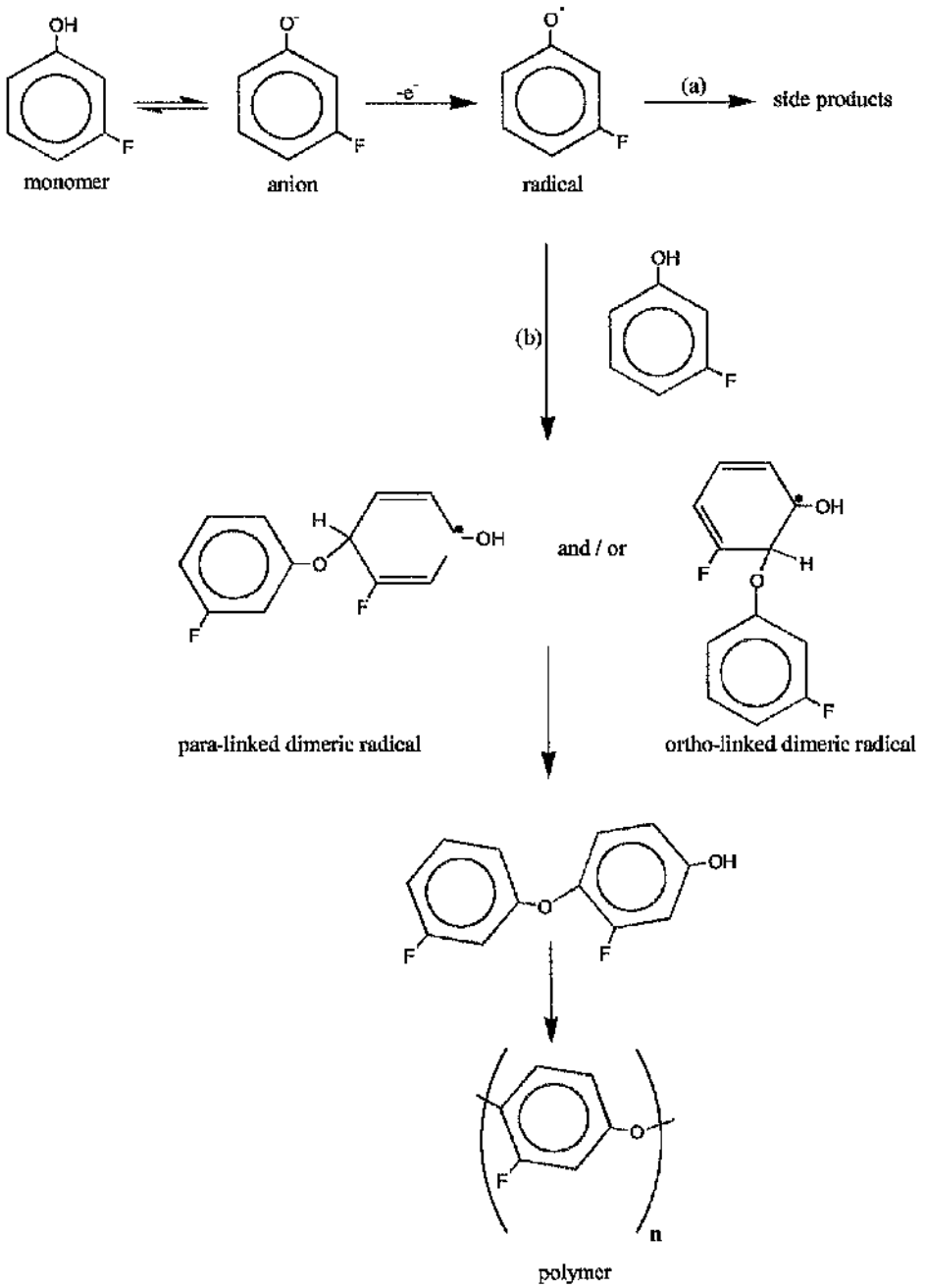

Figure 1.8 - The mechanism of electropolymerisation of fluorophenol. The monomers join together by firstly forming anions, which oxidise to form radicals, and subsequently reacting with other radicals to form the polymeric matrix. The monomers can join by either the *para* or *ortho* positions depending upon the electron distribution around the benzene ring and the attached side groups. As the polymer grows the enzyme is entrapped within the forming matrix.

The formation of insulating films prevents polymerisation on any part of the electrode that has already been coated, thus providing inherently uniform coverage of the surface, regardless of its geometry. However, the thickness and "compactness" of the film can be significantly affected by the length of the polymerisation process, the applied potential used and the material of the working electrode. The attachment of the polymer to the electrode surface is likely to occur due to physical, electrostatic and/or hydrophobic interactions between the matrix and the *rough* electrode surface.[101]

1.1.4 Elimination of Interfering Signals

The specificity of amperometric biosensors for both *in vivo* and *in vitro* applications is limited due to electro-active species present in the biological fluid of interest. Typically, biosensors are operated in complex matrices such as blood or extracellular fluid which contain electro-active substances such as ascorbate, urate and dopamine.[60, 111] The electrode surface of the sensor will, therefore, not only oxidise the desired product (e.g. H_2O_2 formed in the enzymatic oxidation of glucose by glucose oxidase) but also any other species present which are oxidisable at the working potential. Since the concentrations of these interferents are constantly changing in body fluids, it is essential to minimise their contributions in order to maximise the current and hence the 'signal:noise' ratio measured by the sensor.

Electropolymerised films have been employed to serve the dual purpose of immobilisation of enzymes at the transducer surface and also to act as a barrier for effective discrimination against common interferents.[101] The choice of polymer for enzyme entrapment, therefore, has to take into consideration its permselectivity. Various polymer systems and combinations of composite layers have previously been examined for their permselective properties, including exclusion of interferents on a size selective basis[104, 112], discrimination using the polarity of additional species (e.g. lipids)[107], repulsion using charged matrices[113] and reaction with a

secondary enzyme.[43] However, the literature contains little evidence for the mechanism of selectivity for both conducting and non-conducting films.

It has been reported by Sasso *et al* [106]that hydrogen peroxide-detecting sensors based on the electropolymerisation of poly(o-phenylenediamine) films on platinum electrodes in which the enzyme is incorporated in the polymer film show interference-free responses, making them suitable for detecting substrates in biological fluids. Work in this thesis has applied this to glucose sensors and their response to ascorbic acid, one of the most common interferents in biological fluids, measured.

An alternative or additional technique for elimination of interference allows the working potential to be reduced to a value at which the electro-active species are not oxidised. This requires a method of analyte detection which can be performed at these low working potentials. One such method is described in Chapters 5 & 6 where the enzyme is 'wired' to the surface using an osmium redox polymer.[114] This system measures the reduction of the osmium centres of the polymer at the electrode surface which can take place at potentials of approximately 0 mV *vs.* Ag|AgCl. At such low operating potentials the spurious signal due to interferents should be virtually removed from the sensor response.

1.1.5 Oxygen Dependence

Since the aim of this work is to characterise and produce glucose and glutamate sensors for measurements *in vivo*, it is essential that their operation should be stable under physiological conditions. One factor which is consistently variable in these circumstances is the partial pressure of oxygen (pO_2) in blood (as discussed in Section 1.1.2). This variation throughout the body is highlighted by the values reported by O'Neill[115] for glucose detection in brain or subcutaneous tissue where the range of O_2 tension is 5 - 50 μmol dm^{-3}.

The glucose sensor, as discussed previously in Section 1.1.2, illustrates the system's dependence on the concentration of oxygen in the sensing environment. Equations (1.3) - (1.5) show that since the mechanism of electrochemical signal generation relies on the oxidation of H_2O_2 formed from the reaction of oxygen with reduced enzyme, changes in ambient oxygen tension may mimic changes in glucose concentration, undermining the reliability of the sensor to monitor glucose. Therefore, the sensitivity of the sensors prepared by immobilisation of glucose oxidase within p(pd) films on gold electrodes i.e. Au/p(pd)/GOx sensors, to glucose were evaluated under aerobic and anaerobic conditions.

1.1.6 Osmium Hydrogel Based Sensors

In general, on examination of either direct enzyme attachment or physisorption to the bare electrode surface, the electrochemical response observed is poor, suggesting that either the enzyme is denatured or the active site is located sufficiently far from the outer surface of the enzyme to be electrically inaccessible. To overcome these problems it would be useful to form a direct electrical or 'electrochemical' contact between the electrode and the enzyme.[93, 116, 117]

An alternative system is also described in this thesis which allows the enzyme to be retained in close contact to the electrode by electrochemically 'wiring' the enzyme to the electrode with a redox polymer. This enables charged states associated with the biomolecular activity to move directly from the enzyme, through the polymer, to the electrode. Thus, the system is effectively oxygen independent.[117-121]

1.1.6.1 Direct Wired Osmium-based Glutamate Sensors

One of the enzymes discussed in this thesis is glutamate oxidase (GLOx)[87, 88] which is known to contain 2 moles of FAD per mole of enzyme as a prosthetic group but whose crystallographic structure is not yet known. Glutamate oxidase catalyses the reaction of glutamate, in the presence of oxygen and water, with a subsequent two

electron equivalent reduction of a single oxygen molecule, resulting in the production of one molecule of hydrogen peroxide (H_2O_2) and ammonia. This is shown in Equations (1.6).- (1.8).

Although the molecular oxygen is reproduced as a co-product in this reaction, there must be an excess of oxygen in the environment since the regenerated oxygen is not sufficient to sustain the reaction. The hydrogen peroxide produced as a result of the GLOx catalysed reaction can be measured amperometrically and, using the stoichiometric relationship in Equations (1.7) & (1.8), used to quantify the concentration of glutamate. By immobilising the enzyme to an electrode surface which is held at a potential above +700 mV *vs.* Ag|AgCl, the H_2O_2 can be electrochemically oxidised (at pH 7.0) as shown in Equation (1.9).

$$H_2O_2 \rightarrow 2H^+ + O_2 + 2e^- \qquad \textbf{(1.9)}$$

When considered together, Equations (1.6) - (1.9) show the relationship between the measured bioelectrochemical current and the amount of glutamate in solution. This system is another example of the first generation sensors described previously in Section 1.1.2.

This can be applied to the development of glutamate sensors by using a cross-linked redox polyelectrolyte network of poly(vinylpyridine) containing Os(dimethylbipyridine)$_2$Cl$_2$,[91, 122] to which the GLOx is wired, forming an electron conducting hydrogel on the surface of the electrode. The GLOx has a residual negative charge on its surface at pH 7.0 (isoelectric point estimated to be pH 6.2)[87] and so is able to form an electrostatic complex with the positively charged redox polymer. There is also an electrostatic component causing the adsorption of the polymer onto the electrode surface. Carbon electrodes were employed in this study because it has been found that polycationic segments of the polymer strongly adsorb to such surfaces.[116] It is, therefore, these electrostatic interactions between the polymer and the electrode and the enzyme and the polymer that form the basis for the enzyme wiring.

The hydrogel formed is water soluble and is capable of expanding into the 'folds' or 'channels' of the protein which binds the FAD active sites. The polymer has, on average, between 100 - 200 redox sites per 10^5 Daltons molecular weight and, therefore, when it swells and occupies the protein cavities, should consistently provide at least one redox site in close proximity to the active site able to accept electrons from the reduced $FADH_2$ centre (see also Figure 1.9(b))[116]. The biologically generated electrons are then preferentially conducted or transported to the electrode surface along redox pathways defined by the osmium polymer, either by moving along the same redox chain or hopping between chains. Therefore, such electrodes are not limited by the rate of diffusion of substrate and/or product through the sensing layer and it has been reported that any limitation in the maximum steady-state response is likely to be due to redox polymer kinetics rather than enzyme kinetics.[92]

If, however, the electrode environment is of high ionic strength, which would be probable if the sensor was immersed in physiological fluids, then the electrostatic interaction between the polymer and enzyme is likely to be disrupted or 'shielded' by the high excess charge in solution.[116] This results in a loss of polymer flexibility and, therefore, limits the usefulness of the system for carrying current. In order to keep the enzyme completely bound at high ionic strength, a crosslinker of poly(ethylene glycol) diglycidyl ether (PEGDGE 400) was introduced.[123] This reacts with the primary amines on both the redox polymer and the enzyme surface and so adds covalent links to the electrostatic polymer-enzyme complex (see Figure 5.1). The concept of enzyme wiring is shown in Figure 1.9(a) and the corresponding electron transport mechanism can be seen in Figure 1.9(b). The effect of varying the percentage of crosslinker used is investigated elsewhere, in Chapter 6.

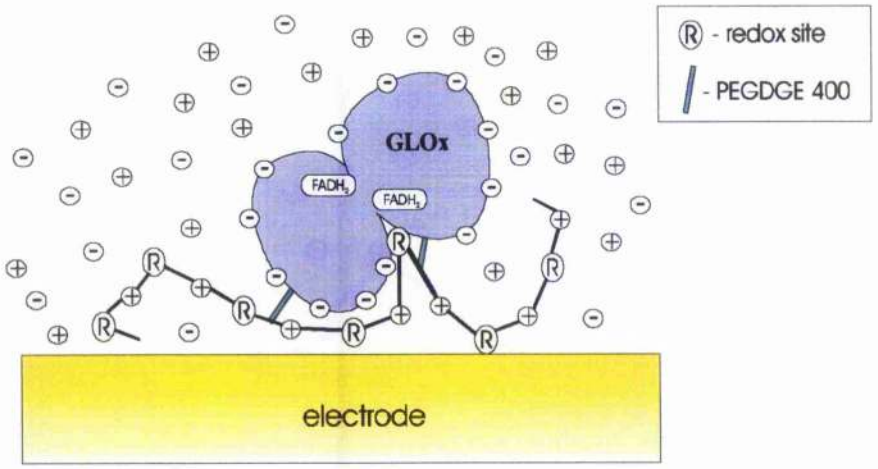

Figure 1.9(a) Wiring of the redox enzyme glutamate oxidase. Redox centres of the polycationic osmium polymer that is electrostatically and covalently bound to the enzyme, relays electrons through the polymer to the electrode surface onto which a section of the polymer is adsorbed. Covalent links (see Figure 5.1) are added to the polymer/enzyme electrostatic interaction by the crosslinker PEGDGE.

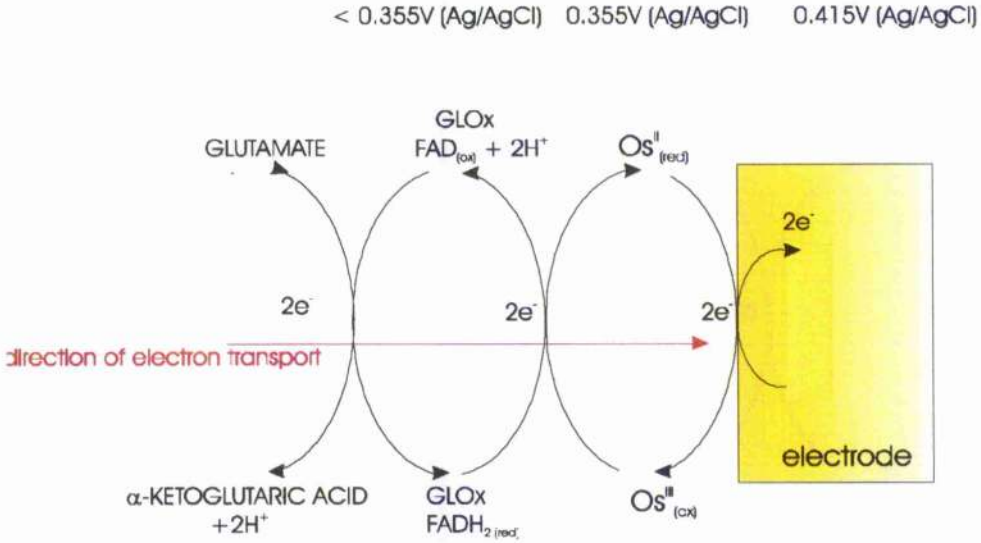

Figure 1.9(b) - Electron transfer stages in the electro-oxidation of glutamate on a wired glutamate oxidase electrode. The half potentials of each stage are shown using experimentally estimated values.

The choice of the electrode potential is important in the design and operation of all amperometric sensors. When considering sensors based upon osmium hydrogels, a value which is sufficiently high to allow the oxidation of the redox sites in the polymer, must be chosen. Whilst the rate of electron transfer between the polymer and the electrode will increase, as a function of increased potential, there is also a

need to maintain as low a potential as possible, so as to minimise the signal from oxidisable interferents (e.g. ascorbate, urate) present in real biological samples.

The final choice of the electrode potential is discussed in the context of Figure 1.9(b), which shows the catalytic activity of GLOx schematically. Whilst the redox potential of GLOx is not known, the fact that the reaction scheme shown works (see Chapter 5 & 6), indicates that the E_0 for $FAD/FADH_2$ within the enzyme must be < 355 mV (a fact that is corroborated by the potential for $FAD/FADH_2$ in GOx, which is ca. -400 mV *vs.* Ag|AgCl).[95] Thus, as GLOx has an E_0 which is lower than that for the polymer, the enzyme-hydrogel-electrode system can be seen as a biomolecular wire, transferring electrons from the catalysed oxidation of glutamate, via the biological environment to the instrumentation.

1.1.6.2 Single Layer, Bienzyme, Osmium-based Glutamate Sensors

The responses of the electrodes described in section 1.1.6.1 above, where the enzyme is directly wired to the electrode, were considerably greater than those from conventional H_2O_2 monitoring amperometric sensors. However, they have the disadvantage that the sensing potential is required to be in excess of +400 mV *vs.* Ag|AgCl. At such high potentials a variety of interfering species e.g. ascorbate (as mentioned previously), are likely to be simultaneously electro-oxidised at the electrode surface, causing the signal to noise ratio to fall.[121] Therefore, in order to reduce the size of the biochemically interfering signal, it is desirable that the electrode potential should be lowered as far as possible.[124] As a consequence a second system employing a single layer, bienzyme electrode was also developed allowing a glutamate dependent signal to be measured at +50 mV *vs.* Ag|AgCl.

This alternative arrangement is based upon the co-immobilisation of wired soybean peroxidase (SBP) and hydrogen peroxide-producing glutamate oxidase whose redox centres are not wired. As previously shown, the three-dimensional redox polymer network used to contain the enzymes is poly(vinylpyridine) containing

Os(dimethylbipyridine)$_2$Cl$_2$. (Identical sensors can be prepared using horseradish peroxidase as the wired enzyme).[125-128]

The principle of the wired SBP electrodes[129] relies upon electrons being relayed from the electrode surface to the SBP enzyme through the redox hydrogel network. In contrast with the single enzyme osmium preparation, see Section 1.1.6.1, where the glutamate dependent current is generated by the oxidation of Os^{II} to Os^{III}, in this case a reduction current is measured at the electrode surface, with the electron transfer sequence for the wired SBP glutamate electrodes being shown in Figure 1.10.

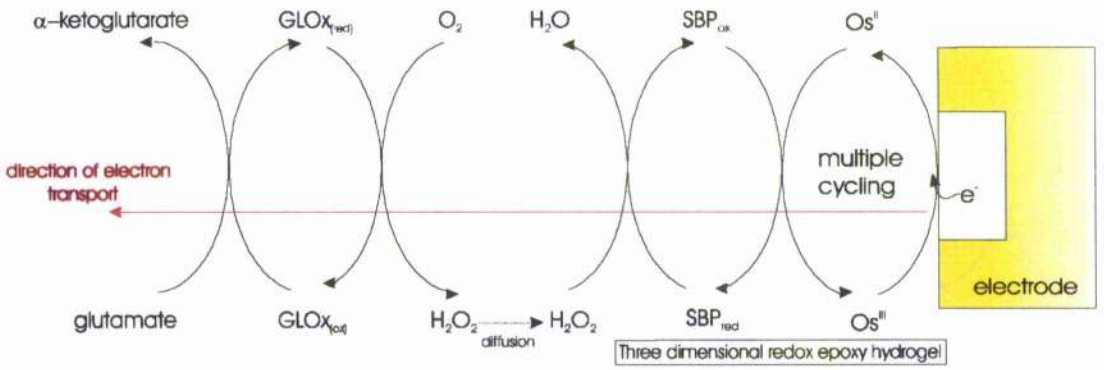

Figure 1.10 - The sequence of electron transport through the wired soybean peroxidase-based glutamate sensor. The reaction of glutamate with GLOx produces hydrogen peroxide which is reduced by the SBP and subsequently oxidises the osmium redox centres of the polymer. The electrons are measured at the electrode surface as a reduction current.

In either the single- or bi-enzyme systems, glutamate can readily diffuse through the hydrogel in order to react with the immobilised GLOx. The H_2O_2 generated from this reaction, in the presence of oxygen, (see Equation (1.6)) diffuses to the electrically wired SBP where it is reduced to water, as shown in Equation (1.10), with the subsequent oxidation of the enzyme.

$$H_2O_2 + 2e^- + 2H^+ \xrightarrow{SBP} 2H_2O \qquad \textbf{(1.10)}$$

The oxidised form of the SBP, whose active sites are in close proximity to the polymer redox sites, acts as an electron acceptor for the reduced form of the polymer, and to complete the cycle, the Os^{III} sites are finally reduced at the electrode surface, which is held at a potential of +50 mV *vs.* Ag|AgCl.

Although this analytical arrangement has the advantage of low interference from ascorbate, in contrast to the direct (or single-) enzyme-wired electrodes, these sensors are dependent upon oxygen to form the hydrogen peroxide. This will result in a competition between the oxygen and the Os^{III} sites to obtain the electrons from the reduced GLOx.

1.1.6.3 Glutamate Microsensors Based Upon Wired Enzymes

Microelectrodes are defined as electrodes whose dimensions are small enough that their properties are a function of their size[130] and they possess many advantages for the probing of chemicals in environments where space is limited. Therefore, miniaturisation of glutamate sensors in order to develop microsensors is of importance when considering the measurement of glutamate in small volumes both *in vivo* and *in vitro.* Such measurements are of clinical interest because of the role that glutamate plays in neurological and psychiatric disorders. The limited space available for measuring glutamate *in vivo* must be taken into consideration when preparing the electrodes i.e. they must be small enough to be placed within the brain without affecting the size and specificity of the current response. The use of single layer, bienzyme wired GLOx microelectrodes, prepared using the technique described previously, possess significant advantages over the macroelectrode sensors, the most notable of which is their ability to rapidly attain steady-state conditions via radial (as opposed to planar) mass transport.[130] As the dimensions of the electrode are reduced so the time taken for diffusion at the surface of the electrode is reduced accordingly. This can be illustrated by considering that the majority of species have diffusion coefficients in the range 10^{-5} - 10^{-6} cm^2 s^{-1} which corresponds to a diffusion rate of approximately 10 μm per second. This deviation from planar diffusion gives rise to higher steady-state responses than observed for equivalent systems on macroelectrodes.

1.1.7 Model for Enzymes Immobilised in Thin Films

Kinetic analyses of the data obtained during this work can be performed when the enzyme is restricted within a thin polymer membrane, particularly if the thickness of the polymer film is small compared with the thickness of the reaction layer (i.e. the enzyme). In the experiments described in this thesis, it is clear that both the films (p(pd) or p(fp)) and enzyme (GOx or GLOx) layers are thin (approximately 10 nm)[29, 131] and that under these circumstances it is unlikely that there will be an unequal distribution of both substrate and product concentration within the film. Therefore, it is relatively easy to derive expressions for the current response of the sensors in terms of the enzyme kinetic parameters and substrate concentrations. The following expression, Equation (1.11), for theoretical steady state response of enzymes entrapped within thin, non-conducting polymer membranes has been published by Bartlett *et al.*, providing a well-established model to characterise the response of a biosensor as a function of a variety of physico-chemical parameters, including partition coefficients and enzyme surface concentration.[132-134]

$$\frac{nF\Lambda\alpha}{I_{obs}} = \frac{K_m}{k_{cat}K_S S_\infty e_\Sigma l} + \frac{1}{k_{cat}e_\Sigma l} + \frac{1}{kK_A a_\infty e_\Sigma l} \qquad \textbf{Equation (1.11)}$$

Such analyses have considerable advantage over the previously used Lineweaver-Burke model which only describes the kinetic behaviour of enzymes in solution and does not take into account the mass transfer characteristics of immobilised enzymes.[63-66] In order to contrast the two models, Equation (1.11) can be rearranged into a form comparable to the Lineweaver-Burke model. This rearranged form is shown in Equation (1.12).

$$\frac{I}{nAF} = \frac{S_\infty}{m + cS_\infty} \qquad \textbf{Equation (1.12)}$$

where $1/m = \alpha K_S k_{cat} e_\Sigma l / K_m$ and $1/c = \alpha k_{cat} e_\Sigma l / (1 + k_{cat}/kK_A a_\infty)$ and both are independent of $[S_\infty]$. Note that n is the number of electrons transferred (in this case,

n=2), F is the Faraday constant, A is the electrode area, K_m and k_{cat} are the enzyme kinetic parameters for the oxidation of glucose, k is the rate constant for the oxidation of hydrogen peroxide, l is the thickness of the polymer film (estimated as 10 nm for p(pd) and p(fp)) and e_T is the amount of enzyme within the polymer film. K_A and K_S are the partition coefficients into the polymer film for the bulk concentration a_∞ of oxygen and the bulk concentration S_∞ of glucose. The parameter α describes the balance between the detection of H_2O_2 at the electrode surface and its loss to the bulk solution, which has previously been estimated as 0.5.[29, 133]

This Equation (1.11) has been used by Bartlett [132-134] to model the responses of enzymes in non-conducting polymer films where the growth of the film is self-limiting and the film thickness is limited to the approximate thickness of a monolayer of enzyme, e.g. 10 nm for poly(phenol). Glucose oxidase and flavocytochrome b_2 cytochrome c oxidase immobilised in poly(phenol) have both been studied using this model.[132, 134] In addition it has been used to investigate some preliminary results for GLOx immobilised in p(pd).[29, 135]

The following sections of this chapter (i.e. Sections 1.2 - 1.4) explain the principles underlying the electrochemical and spectroscopic methods used to compliment the electrochemical results by characterising the composition of the polymer-enzyme sensing layer for each of the biosensor types described in the previous section.

1.2 Electrochemical Techniques

There are a variety of electroanalytical techniques which have previously been developed in order to study both organic and inorganic as well as biological reaction mechanisms[136-140]. Those methods that are used to measure the electrode currents as a function of the voltage applied to the electrochemical cell are termed voltammetric techniques and can be used to provide detailed information about the reaction. Two of the most commonly used voltammetric methods are those of chronoamperometry[138] and cyclic voltammetry.[70] This section provides an

overview of the principles behind the chronoamperometric and cyclic voltammetric analyses.

1.2.1 Chronoamperometry

Chronoamperometric experiments are performed by applying a potential step to the working electrode (in a conventional three-electrode cell) and monitoring the response of the system as a function of time. The initial potential should be such that the species of interest is not oxidised/reduced so that when the potential is stepped to a value where oxidation/reduction is known to occur, a current profile is produced with respect to the reaction at the electrode surface. Immediately following the step, a large current is detected which falls steadily with time. This arises since the magnitude of the current is dependent upon the rate of diffusion of species to the surface. The concentration gradients shortly after the step are very large but as the species has time to diffuse to the surface and become depleted the diffusion layer thickness increases causing a subsequent falling-off of the current. The Cottrell equation, Equation (1.13), describes the current response as a function of time (and electrode area)[138].

$$i = \frac{nFAD^{1/2}c_R t^{1/2}}{\pi^{1/2}} \qquad \textbf{Equation (1.13)}$$

The measured current has two components; a non-Faradaic component arising from a redistribution of charged and polar species at the electrode surface and a Faradaic current resulting from an exchange of electrons between the electrode and the species in solution.[60, 140] The non-Faradaic current can be regarded as the background or baseline current value and the Faradaic current is the one of primary interest in the investigation of electrode reactions.

For the purpose of obtaining sensor calibration curves, when the current stabilises to a consistently low background value, know aliquots of analyte are introduced into the test solution and the current responses recorded in a similar manner. Such an

experiment produces a calibration curve (current *vs.* time) similar to that shown in Figure 1.11 where the redox current is proportional to the concentration of analyte.

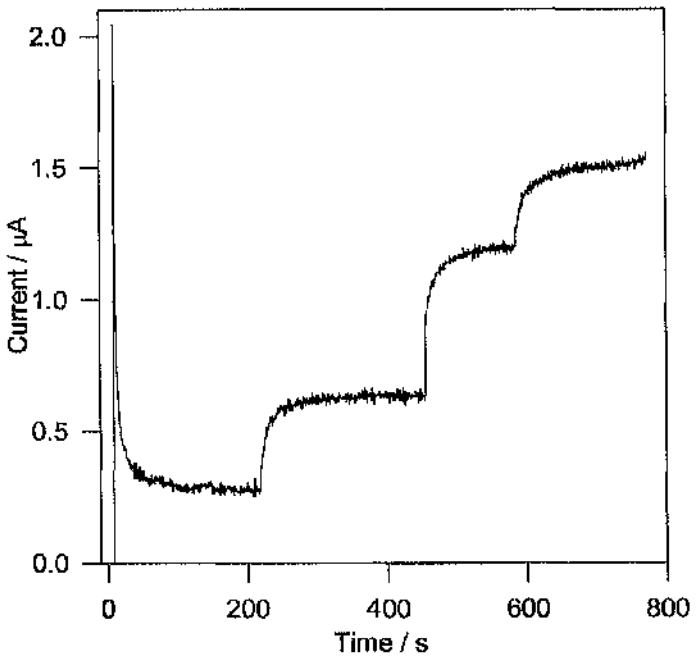

Figure 1.11 - A typical current-time plot obtained from a chronoamperometric experiment. The plot shown here was recorded as part of a calibration experiment on a Au/p(pd)/GOx glucose sensor (area 1 cm^2). Additions of known concentrations of glucose were added (represented by the arrows) after the current response had settled to a constant value. The working electrode was maintained at +700 mV *vs.* Ag|AgCl in order to oxidise the hydrogen peroxide produced from the glucose-GOx reaction.

1.2.2 Cyclic Voltammtery

In contrast to chronoamperometry where the potential to the working electrode is switched between two values, cyclic voltammetry is a technique which is based upon the measurement of current at the working electrode whilst the potential applied to it is scanned between two values, firstly in a positive direction and then the direction of the sweep is reversed and the electrode potential is scanned back to the original value. Linear sweep voltammetry[137] is a related method where the potential is scanned in one direction only. Consider the reaction in Equation (1.14) and the CV in Figure 1.12(b)

$$A \rightarrow B + ne^- \qquad \textbf{(1.14)}$$

As the potential is scanned positively, when a value is reached such that the electrode is highly oxidising, the current increases as the amount of A, which is present at the surface, is oxidised. The current will continue to increase until the diffusion layer is depleted of A causing the current to peak. At this point the current starts to decay as the size of the diffusion layer for A increases. Then when the potential is switched to negative, for the reverse scan, the current slowly increases (negatively) until the potential is sufficiently reducing for the layer of B, which is produced on the forward scan and has accumulated at the surface, to be reduced. This continues until all the A has been reduced and a peak in the reduction current is observed. Once again, as the diffusion layer for B thickens with a build-up of A again, the current falls until the initial potential is reached and the scanning stops.

Cyclic voltammetry is a powerful technique, particularly for initial characterisation studies of a new redox system, as there is a wealth of information to be extracted from the resulting cyclic voltammogram (CV) on the redox behaviour of the system over a wide potential range. The CV is a display of current versus potential and because the potential varies linearly with time, the x-axis can also be thought of as a time axis.

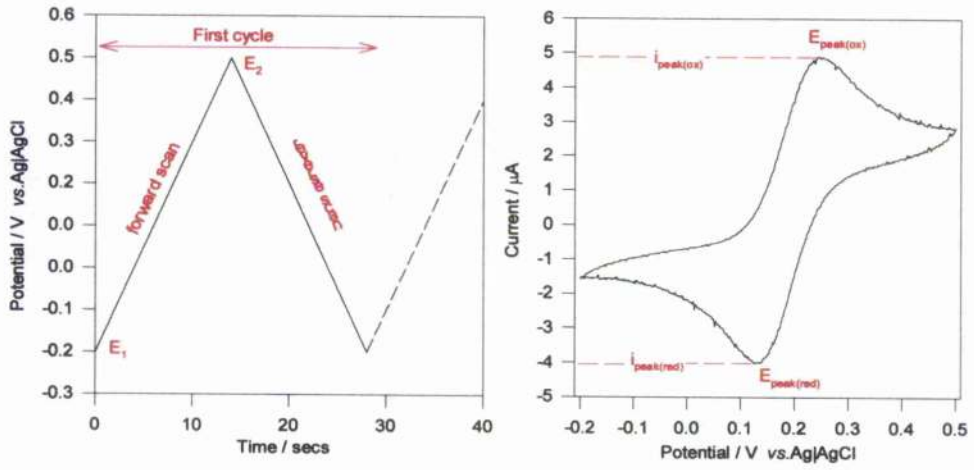

Figure 1.12 shows the input signal and results for cyclic voltammetry of potassium ferricyanide ($K_4Fe(CN)_6$) on a platinum electrode. The plot in (a) shows the excitation signal i.e. a triangular potential waveform with switching potentials at -0.2 and 0.5 V (*vs.* Ag|AgCl) and (b) shows the resulting CV with some of the parameters highlighted i.e. peak oxidation and reduction current, $i_{peak(ox)}$ and $i_{peak(red)}$, and peak oxidation and current potentials, $E_{peak(ox)}$ and $E_{peak(red)}$.

The plot in Figure 1.12(a) shows the variation of the applied potential as a function of time and Figure 1.12(b) shows the resulting cyclic voltammogram obtained for potassium ferricyanide ($K_4Fe(CN)_6$) on a platinum electrode.[70]

Quantification of the CV can produce information on the kinetic parameters of the system.[70, 140]. The parameters of significant interest are peak oxidation and reduction currents ($i_{peak(ox)}$ and $i_{peak(red)}$) and peak oxidation and reduction potentials ($E_{peak(ox)}$ and $E_{peak(red)}$) which give rise to the peak separation (ΔE_{peak}) for use in determining the reversibility of the system and the formal electrode potential of the redox couple (E_o') for use in subsequent potential step experiments. The rate at which the potential is scanned, ν, is also of importance when considering the time scale of the experiment and the magnitude of the parameters on the CV. Additionally, the choice of the location of the redox species i.e. whether either in solution or surface bound, can affect the scan rate and, hence, the magnitude of the parameters of the system.[138, 140]

1.3 X-ray Photoelectron Spectroscopy (XPS)

The most widely used spectroscopic technique for surface characterisation is that of X-ray Photoelectron Spectroscopy (XPS) *aka.* Electron Spectroscopy for Surface Analysis (ESCA).[141-147] Its popularity can be attributed to the unambiguous nature of the data collected and the high resolution and information content obtainable. The basic concept of XPS was conceived as far back as 1914 but modern day techniques were developed principally by Seigbahn in Uppsala, Sweden in the 1960's.[148] The phenomena of photoemmission and the photoelectric effect[149] provide the fundamental theory for surface analysis using XPS. When the sample to be examined is placed in a high vacuum and irradiated with photons of sufficiently high energy (for ESCA the photon source is in the X-ray energy range), the atoms on the surface emit photoelectrons after direct transfer of energy from the photon to the core-level electron. The emitted electrons are subsequently detected by an electron spectrometer[143] which separates them according to their kinetic energy and displays

them on a digital screen as element-specific spectra. This basic concept is shown as a schematic diagram in Figure 1.13 (a) and (b).

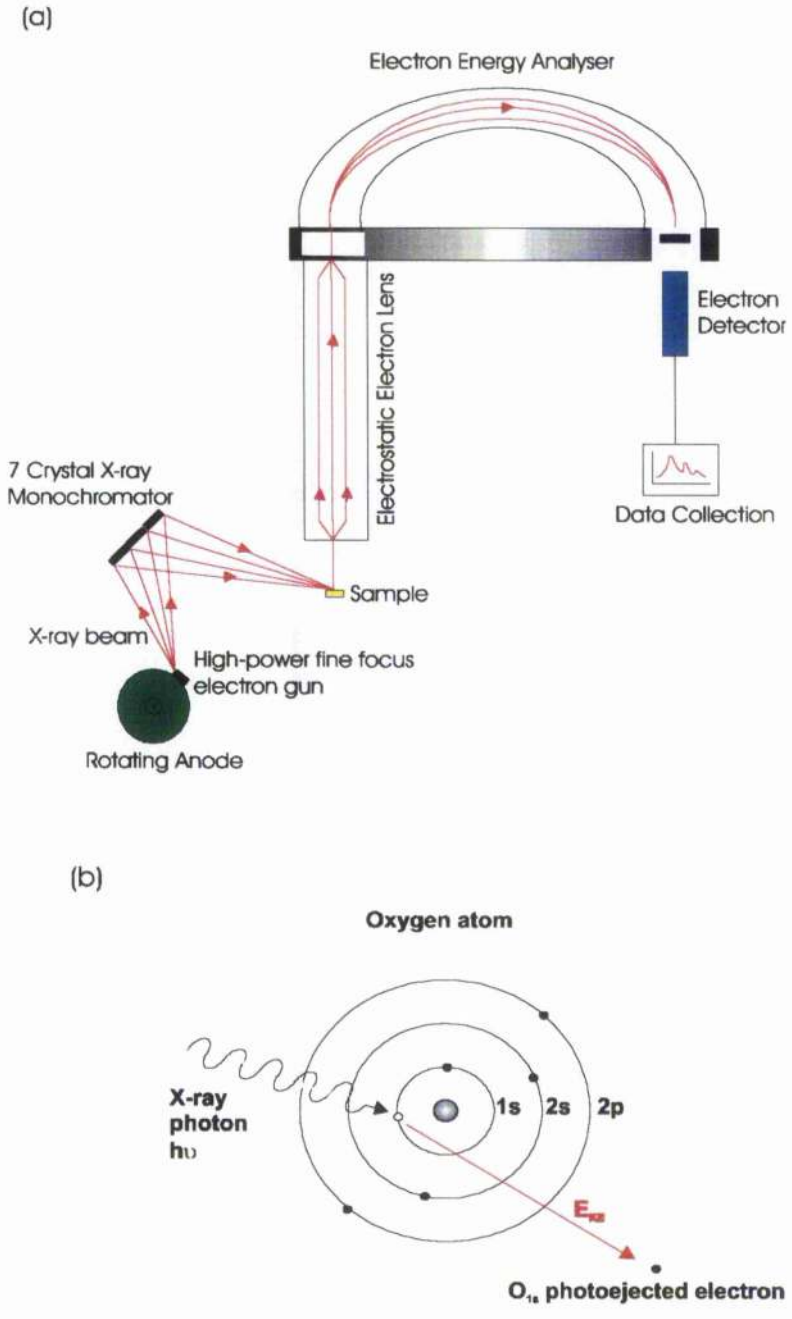

Figure 1.13 Figure 1.13 (a) Schematic of the Xray Photoelectron Spectroscopy apparatus showing the incident x-rays and the collection method of the results and (b) the X-ray photon transfers its energy to a core-level electron imparting enough energy for the electron to leave the atom.

The measured kinetic energy with which the photoelectrons are emitted from the surface region can be described by Equation (1.15)[141, 150]

$$E_K = h\upsilon - E_B - \phi \qquad \textbf{Equation (1.15)}$$

where E_K is the kinetic energy of the emitted electrons (measured during the ESCA experiment), $h\nu$ is the energy of the X-ray source (a known value), E_B is the binding energy of the electron in the atom (which is a function of the type of atom and its environment) and ϕ is the spectrometer work function (a constant for a given analyser). The ability to accurately measure the kinetic energies of the photoelectrons permits the determination of their binding energies (i.e. the parameter which thereby provides valuable chemical information on the surface configuration). The detector counts the number of photoelectrons at the individual binding energies and since each element has a characteristic set of binding energies, this allows discrete differentiation of the components on the surface of the sample.

Covalent and ionic bonds between atoms in the sample will effect the charge distribution within the atom which causes the elemental binding energies to shift in relation to the free neutral atom. The size of this shift is dependent upon the functional group bound to the atom (i.e. its chemical environment), allowing identification of specific bond types.[141, 143, 145, 151] For example, consider the bonding within amino acids (see Figure 1.3), where there are typical Carbon (C1s) binding energies for the acid group (COOH) at 289.0 eV while the value decreases to 286.0 eV for the amine group (C-NH_2). These chemical shifts can be observed for every element in the periodic table, with the exception of hydrogen, but it is the applicability to the second row elements including carbon, nitrogen and oxygen that makes ESCA such an important structural tool for organic interfaces (particularly those used in biosensors and bioelectronics).

The XPS spectra obtained from experiments provide information only on atomic species that are present within approximately 10 nm[141] of the sample surface. Although the incident X-rays can penetrate through the sample to extensive depths,

the escape length is determined by the kinetic energy of the emitted photoelectron. Only those electrons in close proximity to the surface will be able to sustain sufficient energy to escape. Within this distance it is possible to adjust the depth of sample being analysed by altering the angle of the emitted photoelectrons, known as the take-off angle (TOA). This function of the XPS analysis, which is based upon a variation in sampled depth (d or d'), according to a sine function, is termed depth profiling and is shown in Figure 1.14.[141, 145]

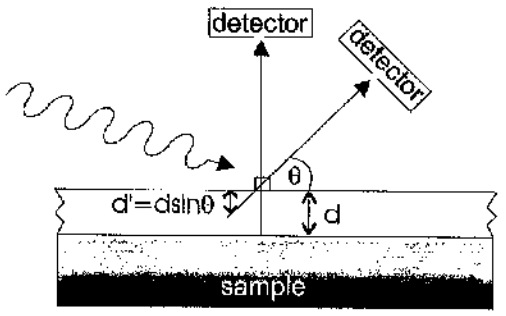

Figure 1.14 - Schematic diagram showing the effect of varying the take-off angle of the photoelectrons on depth of penetration into the sample and, hence, the information about the sample composition.

By changing the take-off angle it is possible to obtain information on the surface composition as a function of depth. At a shallow TOA, e.g. 10°, information is acquired from the outermost layers of the sample, whilst at a steeper TOA of e.g. 90°, the composition below the surface can be analysed. This is of interest for the studies performed in this work where it may be advantageous to know the position of the enzyme within the sensing layer. For example, within a thin polymer-enzyme film, where the size of the enzyme approximates to the thickness of the film. There are two possible models for the polymer-enzyme micro-environment, in which the enzyme is either *proud of* or *buried within* the entrapment matrix. Figure 1.15 shows a representation of the relationship between TOA and penetration depth. A low TOA provides increased surface sensitivity but less structural information. This information is of value in considering the role of the polymer-enzyme film as a permselective membrane (see Chapter 2) and its ability to exclude ions from the electrode surface.

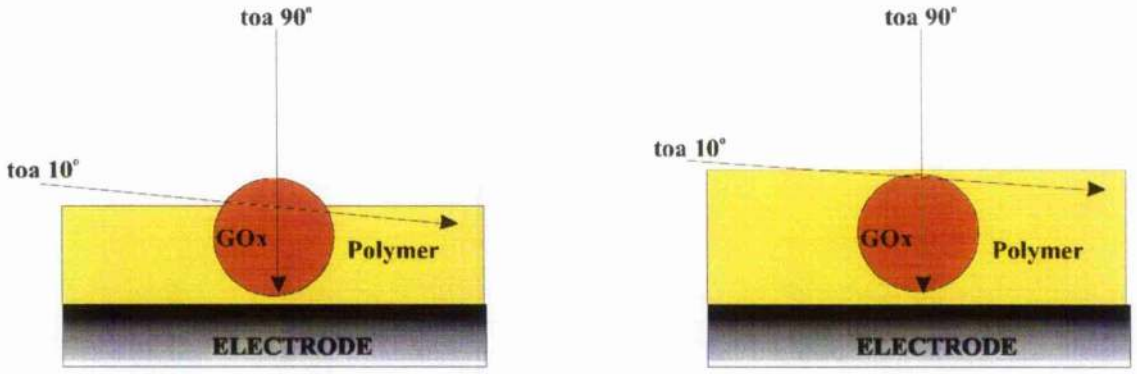

Figure 1.15 illustrates the two compositional models that the enzyme can employ when entrapped within the polymer matrix and the effect the TOA has on the amount of each measured with XPS. The enzyme can either be *proud of* or *buried within* the polymer layer. At a shallow TOA of 10° information on the surface of the sample is obtained while a steeper TOA of 90° allows information on the structure below the sample to be collected. (See Chapter 2 for details)

When examining samples using XPS it is usual to initially take a spectrum over a wide range of energies (a survey spectrum) before performing detailed analyses on the particular areas of interest for the individual sample. Figure 1.16 shows an example of one such survey spectrum for a composite sample containing both polymer and enzyme, which has been carried out over a wide range of binding energies, allowing the size and position of individual elemental peaks to be compared before obtaining higher resolution information/spectra for the elements of interest. Figure 1.16 uses the examples of the carbon C(1s) and gold Au(4f) peaks to illustrate this, to allow for a more in depth analysis of the elemental composition of the sample surface.

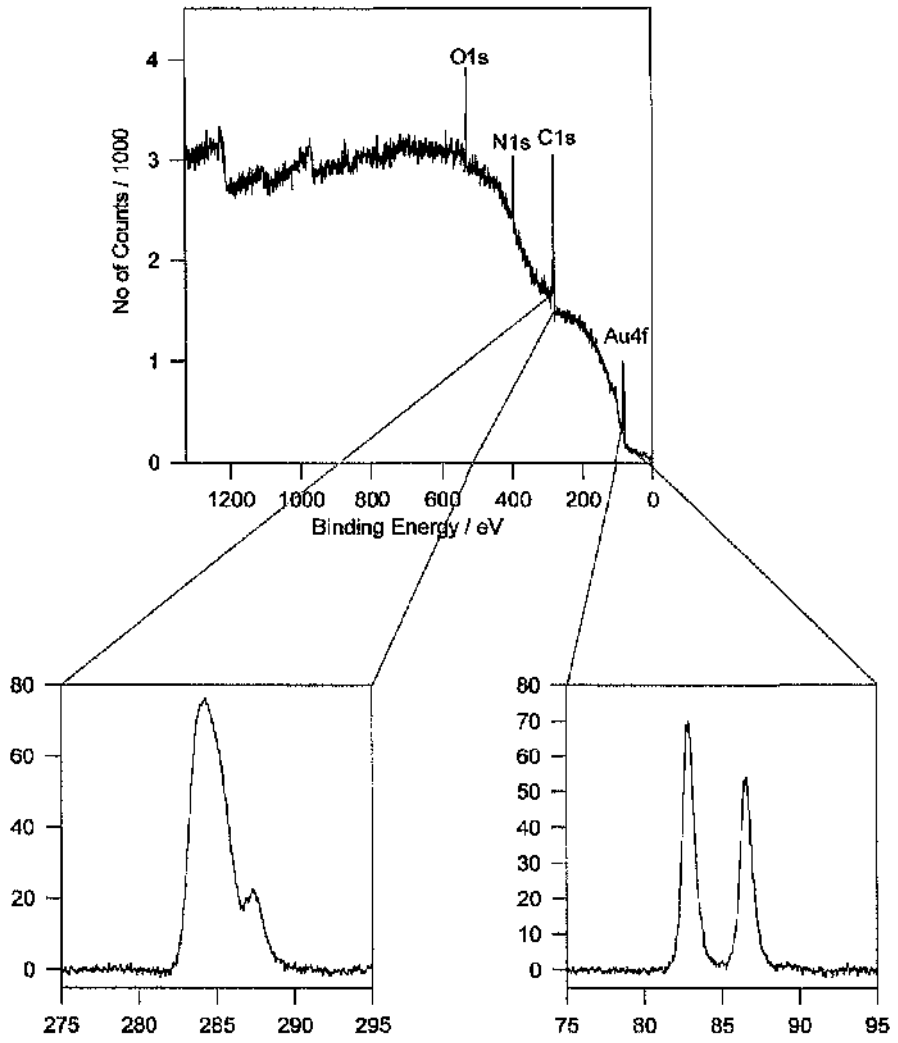

Figure 1.16 - A typical survey spectrum for the samples examined in the context of this thesis showing the individual component peaks over a wide range of binding energies. Particular regions such as the carbon C(1s) and gold Au(4f) can be expanded in order to obtain more detailed information of the individual elemental composition of the sample. (See Chapter 2 for more details)

The ESCA facility used for the analysis of samples prepared in this thesis is the SCIENTA ESCA300 X-ray photoelectron spectrometer (8 kW Al K(alpha) and Cr K(beta) dual source) which is located in the Research Unit for Surfaces Transforms and Interfaces (RUSTI) at the Daresbury Laboratories (Daresbury, U.K.). The combined features of high spectral intensity, high energy resolution (0.25 eV) and high spatial resolution (25 microns) of the machine mean that it can carry out detailed studies of structure, bonding, reactivity and dynamics of surfaces and interfaces. The XPS equipment is shown in Figure 1.17.

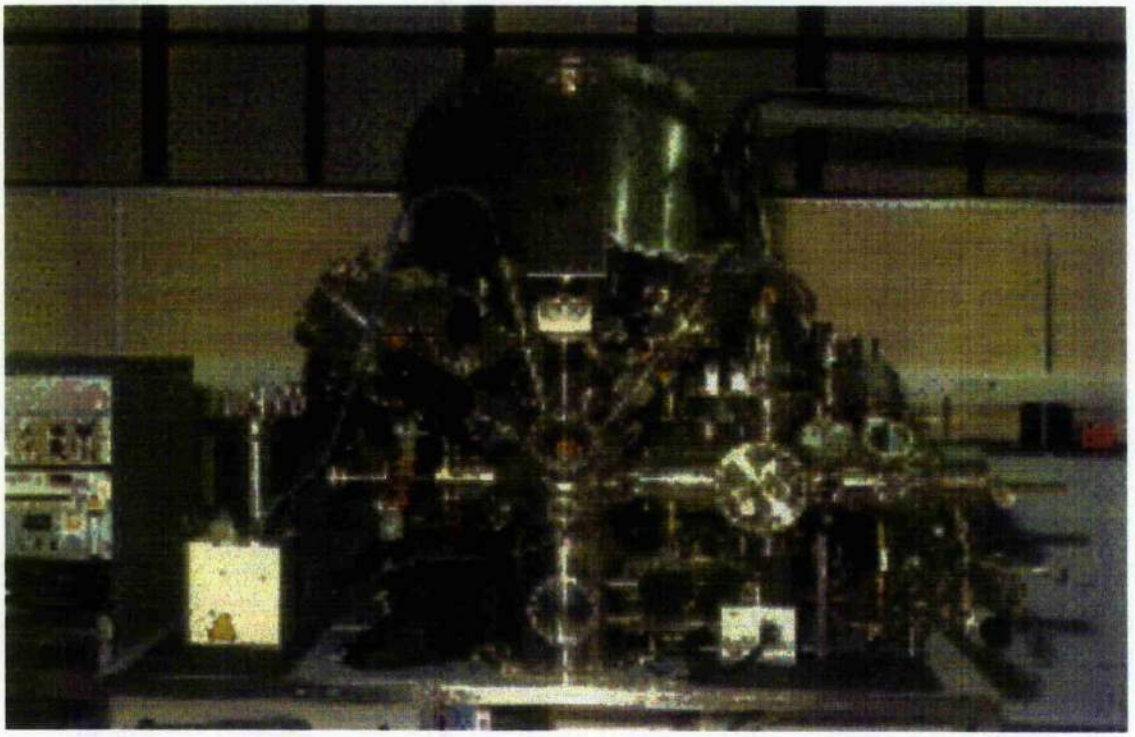

Figure 1.17 shows the SCIENTA ESCA300 X-ray photoelectron spectrometer facility at the Daresbury Laboratory (Daresbury, U.K) used for the analysis of the polymer-enzyme sensing layers of sensors prepared as described throughout this thesis.

1.4 Fourier Transform Infra-Red Spectroscopy (FT-iR)

Surface analysis using the XPS technique described in the preceding section is a powerful analytical tool for both qualitative and quantitative analysis of interfaces. However, other analytical methods can yield important complimentary and/or corroborative information regarding the composition of the bulk of the sample. Therefore, this section details the use of the technique of Fourier Transform Infra-red spectroscopy in the examination of biosensor interfaces.[152-156]

In considering this technique, when light from an infra-red source is passed through a sample of an organic compound some frequencies will be absorbed, whilst others are transmitted without absorption. Particular combinations of atoms in the sample adsorb light of know frequency (or energy) to produce an infra-red spectrum characteristic of the bonds within that functional group. When describing the

appearance of different adsorption bands in the spectra it is important to consider the fundamental molecular movements associated with all chemical bonds. Although chemical bonds are able to undergo a variety of movements such as stretching, twisting and rotating, it is the vibrational changes within the molecule which have absorption energies observable within the infra-red region of the electromagnetic spectrum.[152, 155]

Using the simple example of a diatomic molecule to illustrate the principle of iR adsorption, it is possible to state the selection rules which must be followed before incident iR radiation can be absorbed by any polyatomic molecule.[157] For example, in a diatomic molecule with masses m_1 and m_2 and separated by a distance r, as shown in Figure 1.18, a directional dipole moment will be set up due to the difference in electric charge between the two masses.

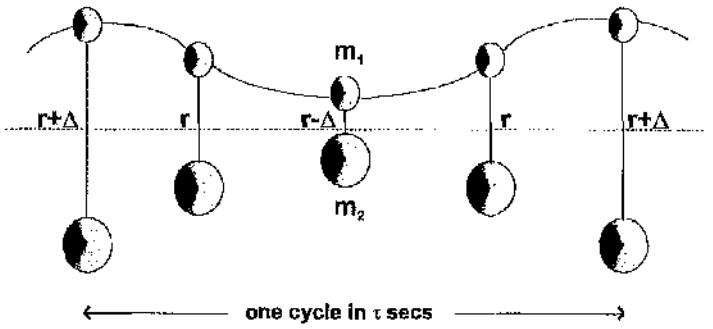

Figure 1.18 - Vibration of a diatomic molecule showing the frequency required before adsorption of the iR radiation can occur.

As the molecule is constantly in a state of vibration, the separation of masses, r, will be constantly and periodically changing, therefore setting up an alternating electric field of particular frequency, $f = 1/\tau$. If the incident iR radiation is of the same frequency then the vibrating molecule will adsorb that radiation.

Each bond within a continuously vibrating organic molecule has its own characteristic frequency arising from both stretching and bending vibrations. The stretching frequencies are due to vibrational changes in bond length, whilst the

bending frequencies involve vibrational changes in bond angle. A greater amount of energy is required to stretch the bond between two atoms than to bend it, and, as a consequence, the stretching adsorptions appear at higher frequencies on the iR spectra than the bending adsorptions for the same bond. In addition, the vibrational frequency of a bond increases when the bond strength increases and the mass of either of the atoms involved in the bond decreases. For example, the frequency associated with an alkene (C=C) and a carbonyl (C=O) group stretches are higher than those for an alkane (C-C) and an alcohol (C-O) group stretches respectively.[152]

For molecular assemblies containing a large number of atoms and bonds (such as proteins and polymers) there are many associated vibrational frequencies. For a non-linear molecule with N atoms, the number of vibrational degrees of freedom is ($3N$ - 6) which, provided they satisfy the conditions for adsorption described above, will produce characteristic vibrational frequencies somewhere within the iR spectra. Additionally, for linear molecules, the degrees of rotational freedom are reduced to ($3N$ - 5) since only two degrees of rotational freedom are required.[152, 157, 158] The diagram in Figure 1.19 shows the possible vibrational modes of both non-linear and linear molecules using water and carbon dioxide as simple examples to illustrate these points.

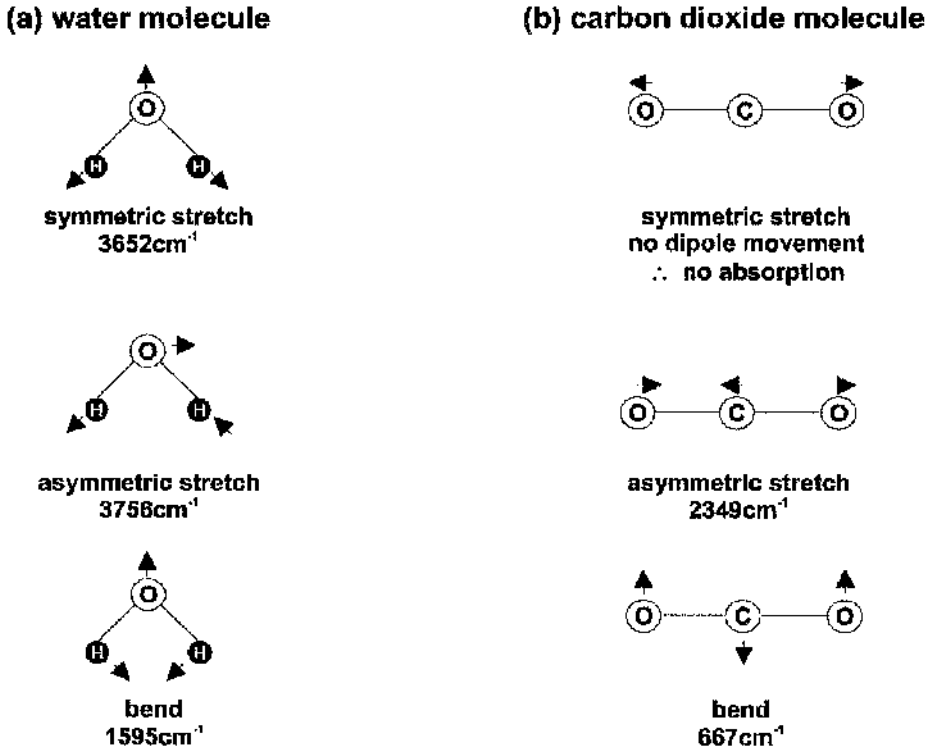

Figure 1.19 - The fundamental modes of vibration of (a) a non-linear polyatomic molecule of water and (b) a linear polyatomic molecule of carbon dioxide. The magnitude of their adsorption wavenumbers varies as a function of the mode of vibration e.g. a symmetric water stretch will adsorb at 3652 cm^{-1} whilst a bending of the same water molecule will show up as an adsorption at 1595 cm^{-1} on the iR spectrum.

The intensity of an adsorption band is dependent upon the magnitude of the dipole change during the vibration; the larger the change, the stronger the adsorption band. The band intensity of a particular functional group also depends on the number of the groups present in the sample (molecule) being studied and on neighbouring atoms/groups. This has particular relevance for the studies performed within this thesis which involve the examination of proteins entrapped within polymeric films.[155, 159-167]

In this context, Chapter 3 specifically studies the construction of a sensing layer consisting of glucose oxidase immobilised within a non-conducting electropolymerised film of poly-*o*-phenylenediamine. Both the enzyme and the polymer are made up of many functional groups and chemical bonds which, due to considerable overlap, can make differentiation difficult using an FT-iR spectrum of

the sample. The structural similarities between the amino acids e.g. C-N, C-C, C=C, which form the complex protein and the repetitive monomer chains of the polymer are responsible for producing overlapping peaks on the respective spectra. This task is made more difficult by the fact that there are roughly equivalent amounts of organic (polymer) and biological (protein) material within the biosensor interface. However, as is shown in Chapter 3, it is possible to determine peaks characteristic of specific functional groups in both spectra.

When attempting to extract information on the protein content of a biosensor-polymer sample, the particular peaks to examine correspond to the following functional groups which are present in proteins: C=O, -COOH, COO^-, O-H, N-H, NH_3^+ and S-H. The most useful energies of the spectrum to study are those corresponding to the peptide bonds (see Figure 1.3) within the enzyme molecules, which produce a strong characteristic signal. The peptide bonds have three associated modes of vibration giving rise to three individual peaks on the iR spectrum; amide I, amide II and amide III. The amide I band is the strongest of the three and is usually associated with the C=O stretch between 1600 - 1700 cm^{-1}. The amide II band, found between 1500 - 1600 cm^{-1}, is a strongly coupled interaction between C-N stretch and N-H bend vibrations and finally, the amide III is a weak peak due to secondary N-H bend vibrations, found between 1200 - 1300 cm^{-1}. The absorption values for these vibrations should vary as the concentration of the protein on the sample surface is varied.[152, 155, 158, 164]

A similar breakdown of the absorption spectra can be adopted for the poly-*o*-phenylenediamine polymer, the structure of which can be seen in Figure 1.7. The groups to examine on this spectrum are those at approximately 1500 cm^{-1} characteristic of the benzene-like structure of the polymer backbone and 1650 cm^{-1} which is indicative of the presence of secondary amines on the branches of the polymer.[168]

The principle of FT-iR operation is based upon infrared light from a p-polarised light source passing through a scanning Michelson interferometer[152] such that a Fourier

Transformation of the energy gives a plot of intensity versus frequency. When a sample is placed in the beam, it absorbs particular frequencies (as described above), so that their intensities are reduced in the interferogram and the subsequent Fourier Transform is the infrared adsorption spectrum of the sample. The most fundamental component of the iR spectrometer is, therefore, the Michelson interferometer whose function can be understood with reference to Figure 1.20.

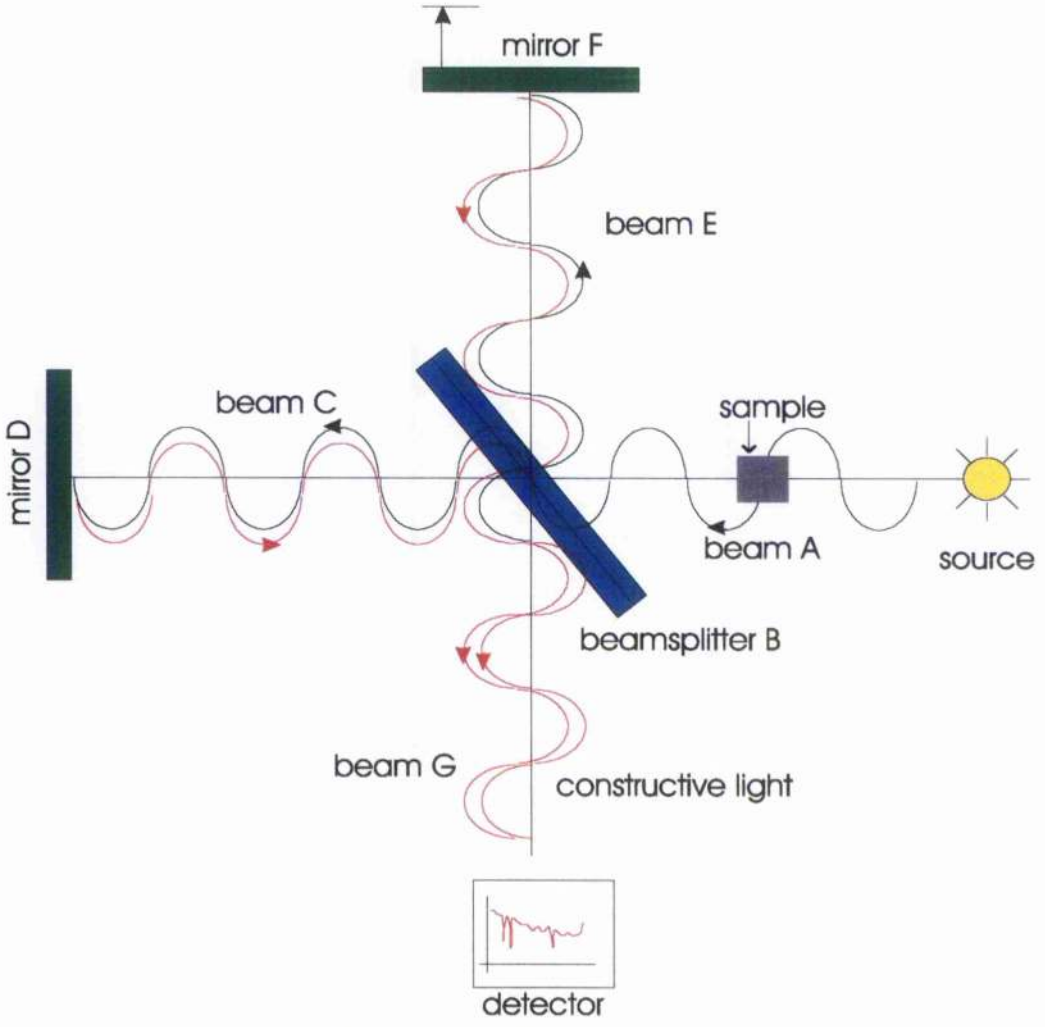

Figure 1.20 shows a schematic of a Michelson interferometer illustrating the reflective pathway of the incident light before it is detected. In the FT-iR spectrometer the sample is placed between the source and the beamsplitter.

Light from the source strikes the beamsplitter B (usually KBr or CsI coated with germanium for iR applications), which is designed to split beam A exactly in half. One half is transmitted, as beam C, to the plane mirror D and reflected there back to

beamsplitter B; the other half of beam A is reflected, as beam E, to another plane mirror F, where it is reflected back to B. Both these beams are recombined as beam G (by reflection and transmission respectively) and passed to the detector. Depending upon the position of mirror F (it is moved in the direction shown in the diagram) either constructive or destructive interference patterns, i.e. light and dark images, will reach the detector and then a Fourier Transform can be applied to this pattern to produce the intensity dependent iR spectrum for a particular sample.

For analysis of thin coatings on metal surfaces or samples with a very smooth surface the iR spectrometer is used in grazing incidence reflectance (GIR) mode.[154, 169, 170] When operated in this mode the incident angle of the iR beam (with respect to the surface) can be varied from 10° (near normal) to 85° (grazing angle) depending upon the thickness of the sample. It is generally found that the thinner the sample the larger the incident angle that is applied in order to obtain information at as great a depth of the sample as possible.

1.6 Outline of Thesis Structure

The work presented in this thesis has been separated into five main chapters, each addressing glucose or glutamate sensors which have been either prepared with a different polymer or analysed using distinct techniques.

Chapter 2 presents the electrochemical analysis of glucose sensors prepared by electropolymerisation of poly(phenylene diamine) and glucose oxidase. The construction of the sensing layer was investigated by varying both the concentration and method of enzyme immobilisation. Also studied was the effect of oxygen on the sensor response and the method of elimination of interferents such as ascorbate. Finally, these results were applied to the preparation of glutamate sensors.

Chapter 3 uses the spectroscopic techniques of X-ray Photoelectron Spectroscopy (XPS) and Fourier Transform Infra-red Spectroscopy (FT-iR) to examine the polymer-enzyme interface of the sensors prepared in Chapter 2.
Chapter 4 applies the techniques described in Chapters 2 & 3 i.e. electrochemical and spectroscopic analyses, to the responses and polymer-enzyme interfaces of glucose sensors prepared by electropolymerisation of poly(fluorophenol) and glucose oxidase. The effect of varying the polymer enables enhanced quantification of the interface.

Chapter 5 introduces the concept of direct electron transfer through the use of osmium hydrogel based glutamate sensors and examines their electrochemical response optimisation. Additionally, their responses were investigated when operated under low oxygen conditions and in the presence of interfering species.

Chapter 6 examines the composition of the glutamate sensors described in Chapter 5 using cyclic voltammetry, XPS and FT-iR to determine the effect of the crosslinking agent that is required to hold the system together.

Chapter 7 contains the conclusions of the project along with suggestions for future work.

CHAPTER 2 - ELECTROCHEMICAL ANALYSIS OF POLY(*o*-PHENYLENEDIAMINE) BASED SENSORS

In this thesis a variety of glucose and glutamate polymer-enzyme electrodes were prepared in order to examine different sensor configurations. The effect of varying transducer material, immobilisation matrix and biological sensing element were all investigated for glucose sensors and used as a model for the development of glutamate sensors. In addition, an understanding of the polymer-enzyme structure in the context of the spectroscopic studies performed in Chapter 3 was obtained. This chapter describes the construction of glucose specific electrodes by immobilisation of the enzyme glucose oxidase (GOx) within an electrochemically formed non-conducting polymer film of poly-*o*-phenylenediamine (p(pd)). The work compliments premium research accomplished both in our laboratory using microelectrodes[29], as well as that of others[103, 106, 107, 171]. The method of enzyme immobilisation was varied in order to maximise the electrode response. Also assessed was the sensors' ability to eliminate interfering substances and their sensitivity to glucose for different concentrations of oxygen in solution.

Using the results from the glucose sensors, glutamate electrodes were similarly prepared by immobilisation of glutamate oxidase (GLOx) within poly-*o*-phenylenediamine films and their responses modelled using previously described algorithms[29, 132]. The work provides information which becomes relevant in the context of the data present in Chapter 3.

2.1 Experimental

2.1.1 Materials

Ortho-phenylenediamine (1,2,-benzenediamine) (P-9029) was purchased from Sigma (Poole, England) and was used without any further purification. Phosphate buffer solutions (40 mmol dm^{-3}) were prepared from stock solutions of disodium hydrogen phosphate and sodium dihydrogen phosphate (Sigma). Potassium chloride (KCl) was added to the buffers (50 mmol dm^{-3}) as the supporting electrolyte, and the pH of the buffer was adjusted to pH 7.4. All solutions were freshly prepared using reverse osmosis (RO) ultrapure water (Millipore, U.K). Stock solutions of *D*-glucose (G-7528), *L*-glutamic acid (G-6904), ascorbic acid (A-5960), prepared in appropriate buffers immediately prior to use, and *L*-α-phosphatidylcholine (P-6638), 100 mg ml^{-1} prepared in chloroform, were all purchased from Sigma. Glucose oxidase, GOx, (EC 1.1.3.4., 245 U mg^{-1}) from *Aspergillus niger* was a gift from MediSense (Birmingham, U.K.). Glutamate oxidase, GLOx, (EC 1.4.3.11.., from *Streptomyces sp.*, 30 U mg^{-1}) was a gift from Yamasa Shoyu (Chiba, Japan). Both enzymes were prepared as buffered solutions and stored at -20°C. Oxygen-free nitrogen was purchased from BOC (U.K.)

Gold working electrodes were fabricated using standard photolithographic techniques, as described in section 2.1.2. The materials used, titanium (Ti), palladium (Pd) and gold (Au) were purchased from Goodfellows (Cambridge, U.K.). Platinum 'bulk' macroelectrodes (MF-2013) encased in plastic, inside diameter 1.6 mm and outer 3 mm, were purchased from BAS Technicol, Cheshire. The Ag|AgCl reference electrode (MF-2063) was also purchased from BAS.

2.1.2. Methods

2.1.2.1. Preparation of substrates:

Electrodes used were either polycrystalline or evaporated gold electrodes. The evaporated surfaces were produced, using a well established 'recipe' on a Plassys QD1 automated electron-beam evaporation system, by deposition of a Ti/Pd/Au (10/10/100 nm) multi-layer onto a glass substrate. The particular recipe of metals was chosen as it provided excellent adhesion of the metal to the glass substrate, and good electrochemical stability even at high oxidative potentials in aqueous solutions. Large scale electrodes (1 cm x 2 cm) were fabricated using scribed glass slides which could be 'snapped' (after surface functionalisation) to give two identical (1 cm^2) electrodes, either for electrochemical studies or for XPS.

In all cases, the gold was cleaned immediately prior to polymer deposition: the evaporated surfaces were cleaned by a reactive ion etch for 5 minutes (50 mT, 20 sccm and 10 W) in first oxygen and then argon using a PlasmaFab ET340, whilst polycrystalline platinum was polished with alumina slurry (0.3 μm grain size) and sonicated in reverse osmosis water for 5 minutes Prior to functionalisation, gold slides were stored in RO water, in order to reduce the amounts of adsorbed hydrocarbon contamination.

2.1.2.2. Electrochemical Apparatus:

All electrochemical measurements were performed using a PC-controlled PAR 273 potentiostat (EG&G Princeton Applied Research, UK). DC cyclic voltammetry[70] and chronoamperometry[138] were carried out in a three-chamber all-glass cell incorporating a conventional three-electrode configuration. One of these chambers accommodated the working electrode (e.g. polycrystalline gold), a platinum counter electrode was in the second and the final chamber, connected to the others by a glass frit, held a Ag|AgCl reference (3.0 mmol dm^{-3} NaCl). On occasions, polymer films were grown in a single chamber with all three electrodes within the same cell.

2.1.2.3. Enzyme Electrode Preparation:

The following different arrangements of enzyme electrode were prepared: Au/p(pd)/GOx, Pt/p(pd)/GOx and Au/p(pd)/GLOx. The Au/p(pd)/GOx electrodes were constructed using enzyme solution concentrations of 10 mg ml^{-1} and 1 mg ml^{-1}, employing three variations on the immobilisation method. The first involved a 5 minute preadsorption of enzyme onto the bare gold electrode followed by electropolymerisation from a solution of 300 mmol dm^{-3} o-phenylenediamine[172] (prepared in 40 mmol dm^{-3} phosphate buffer). The polymerisation reaction was initiated by a potential step from 0 mV *vs.* Ag|AgCl to 650 mV *vs.* Ag|AgCl and maintained at this value for 10 minutes. As the growth of non-conducting polymers is self-limiting, the anodic polymerisation current falls to a steady-state value, close to zero, after a few minutes.[106] This can be used as an indication of the thickness of polymer film on the electrode surface. The second immobilisation method followed the reverse pattern i.e. a 10 minute electropolymerisation of p(pd) followed by a 5 minute postadsorption of GOx. The third type of films were grown by a 10 minute co-polymerisation from a solution containing both *o*-phenylenediamine monomer and glucose oxidase (at concentrations of both 10 mg ml^{-1} and 1 mg ml^{-1}). The same procedure of co-polymerisation was adopted for the Pt/p(pd)/GOx electrodes.

The experiments using Pt/lipid/p(pd)/GOx electrodes were prepared by adding initially a 5 µl drop of the phosphatidylcholine solution onto the platinum surface and allowing it to dry before polymerising the p(pd) film containing GOx as above.

The Pt/p(pd)/GOx sensors prepared for the interference and oxygen-tension measurements were polymerised from a solution containing 300 mmol dm^{-3} phenylenediamine and 5 mg ml^{-1} glucose oxidase.

The Pt/p(pd)/GLOx electrodes were prepared in the same manner but using a solution of 300 mmol dm^{-3} *o*-phenylenediamine containing 13 µg ml^{-1} glutamate oxidase.

2.1.2.4. Electrochemical Measurements:

Amperometric current profiles of the sensors were measured in response to known solution concentrations of the analyte of interest, i.e. glucose or glutamate. The working electrode was maintained at a potential of +700 mV *vs.* Ag|AgCl and the current response recorded for successive aliquots of glucose (in the concentration range 0 - 100 mmol dm^{-3}) or glutamate (in the concentration range of 0 - 25 mmol dm^{-3}). The current value was allowed to stabilise to a steady-state value after each addition. For the Au/p(pd)/GOx sensors the effect of varying the concentration of enzyme in the monomer solution was monitored by examining the effect it had on the sensor response.

2.1.2.5. Interference Measurements:

Electrochemical measurements were made when the Pt/p(pd)/GOx sensors were exposed to physiological concentrations of the electro-active interferent ascorbic acid (0 - 0.4 mmol dm^{-3}).[173] The electrodes were poised at +700 mV *vs.* Ag|AgCl and the current profiles in response to the ascorbate recorded. In order to examine the effect of varying the polymer growth conditions, electrodes were tested which had films grown for 10 minutes, 1 hour, 2 hours and 24 hours.

The scanning electron microscopic analysis of the p(pd) films was performed using a Hitachi S-800 electron microscope. Samples were prepared by depositing a thin layer of gold-palladium before loading into the microscope.

2.1.2.6. Effect of Partial Pressure of Oxygen:

The Pt/p(pd)/GOx sensors described above were used to measure electrochemical responses to glucose under varying solution conditions. The experimental apparatus used to monitor the level of oxygen (pO_2) in solution consisted of a platinum circular Clark-type working electrode and a Ag|AgCl ring reference electrode, mounted in a perspex block containing a vent to allow de-gassing with nitrogen (N_2). The oxygen electrode was maintained at a constant potential of -650 mV *vs.* Ag|AgCl and the amperometric current response was measured before and after a 20 minute nitrogen purge and also after a 20 minute period of air recirculation.

The data from the electrochemical measurements was collected on a Viglen personal computer and analysed using the graphical package SigmaPlot.

2.2 Results and Discussion

This section is concerned with the investigation of the kinetic behaviour of glucose sensors, constructed by immobilisation of the enzyme within an electropolymerised non-conducting film. Their electrochemical responses under both aerobic and anaerobic conditions are discussed in the context of the importance of the influence of interferents. Having characterised the glucose electrodes, electrochemical measurements were also obtained for a glutamate sensor modelled on the operation of the glucose sensor.

2.2.1 Electrochemical Analysis of the Enzyme - Polymer Film Growth

Glucose sensors were prepared, as described previously, employing three different immobilisation configurations whilst maintaining identical monomer and enzyme solution concentrations. Electrochemical assays were performed on samples prepared using three possible electropolymerisation protocols with measurements being made for glucose concentrations in the range 0 - 100 mmol dm^{-3}. The results for the electro-immobilisations, performed at two different solution concentrations are shown in Figure 2.1 (a) and (b).

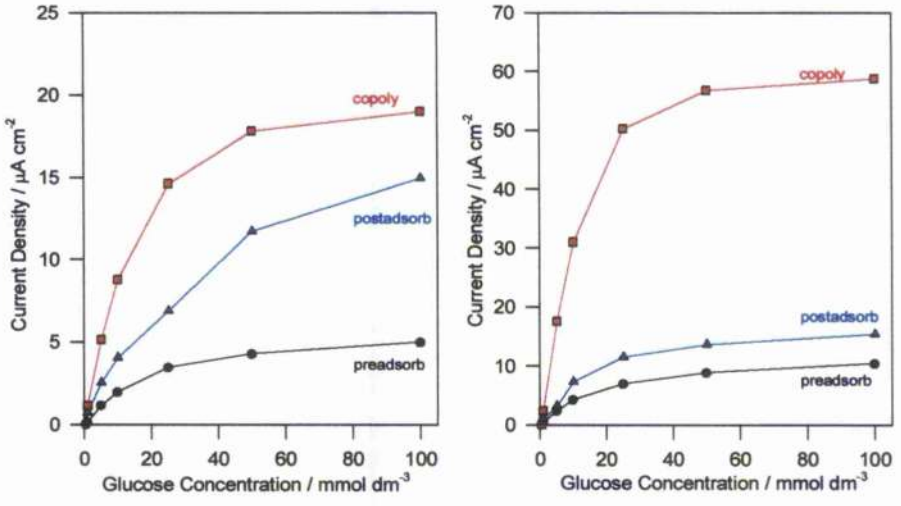

Figure 2.1 - Electrochemical assay responses for electrodes prepared (as described in section 2.1.2) by preadsorption, copolymerisation and postadsorption from enzyme solutions of both (a) 10 mg ml^{-1} and (b) 1 mg ml^{-1}.

The results in Figure 2.1(a) show the variation in sensor response for the different polymer-enzyme protocols prepared with a GOx solution concentration of 10 mg ml^{-1}. Figure 2.1(b) shows the same pattern of results for a GOx solution concentration of 1 mg ml^{-1}. In both cases the electrode responses follow a similar trend with respect to the protocol used, with the preparation technique involving polymerisation from a solution containing both monomer and enzyme yielding the highest electrode responses. Current responses are lowest when the GOx has been preadsorbed onto the surface prior to the polymer growth. This could suggest either that the polymer layer suppresses diffusion of the glucose to the electrode or that there is poor adhesion between the GOx and the gold surface. However, the latter theory has been shown not to be the case[174, 175]. For the technique when polymer growth is followed by a GOx postadsorption, the current values appear to be larger, although still substantially lower than those prepared using the copolymerisation technique. This may be attributed again to poor diffusion of the reaction product, i.e. the H_2O_2, through the polymer to the electrode surface and/or bad adhesion of the GOx to the polymer. The latter theory may be supported by the fact that the electrodes are stored in buffer solution for a few hours prior to assaying which increases the likelihood of GOx desorption into solution. Therefore, in order to obtain maximal

enzyme loading in the polymer layer, the sensor should be prepared by electropolymerisation from a solution containing both monomer and enzyme.

Surprisingly, it can be seen from Figure 2.1 that the current response for the sensor prepared from a 1 mg ml^{-1} GOx solution is larger than that obtained from the electrode prepared with 10 mg ml^{-1} GOx. A possible explanation for this effect could be that as the concentration of enzyme on the surface i.e. the surface density of enzyme, increases, the diffusion pathway of the enzymatically produced H_2O_2 to the electrode surface is restricted; thus reducing the magnitude of the electrode response and rendering it limited by the concentration of product at the surface as a function of enzyme density/ease of diffusion.

This effect was observed by O'Neill[105] using a similar system based upon GOx immobilised within a film of poly-o-phenylenediamine at platinum electrodes and also by Fortier[176] using a conducting polymer, polypyrrole, system of Pt/p(py)/GOx. O'Neill found that by increasing the GOx concentration from 1 mg ml^{-1} to 5 mg ml^{-1} the V_{max} value decreased and this drop was attributable to a severe depletion of oxygen at the film/solution interface at high GOx concentrations. However, this feature of enzyme loading was found to have an advantageous effect on the sensor selectivity in such a manner that greater loading yielded the highest glucose:ascorbate ratio. (see section 2.2.3).

Therefore, having established an optimum method of enzyme immobilisation on gold substrates the remainder of the glucose systems that were examined were prepared using platinum substrates. Additionally, during the preliminary stages of this work a set of clinical *in vivo* electrodes were donated to the laboratory which were fabricated in platinum and, therefore, encouraged the development of glucose sensors based on platinum electrodes.

2.2.2 - Electrochemical Glucose Assay Results on Platinum Electrodes

Glucose sensors of composition Pt/p(pd)/GOx (prepared using the copolymerisation technique described above) were constructed with GOx solution concentrations of 10 mg ml^{-1} and 1 mg ml^{-1} and their response to varying concentrations of glucose measured at 700 mV *vs.* Ag|AgCl. Their responses are shown in Figure 2.2.

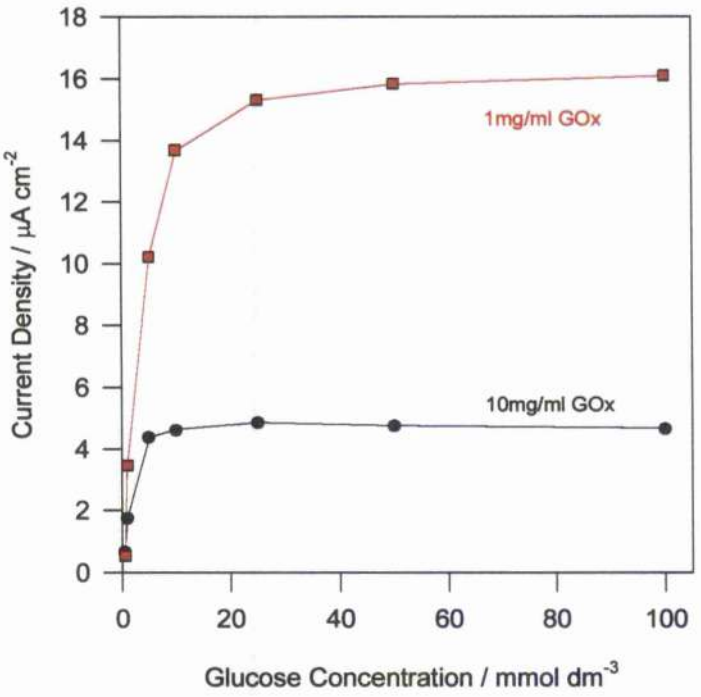

Figure 2.2 - Glucose assay results for Pt/p(pd)/GOx electrodes prepared (as described in section 2.1.2) with 10 mg ml^{-1} and 1 mg ml^{-1} GOx.

The graph in Figure 2.2 follows the same trend as those in Figure 2.1 i.e. the current response is greater for smaller enzyme loading. Kinetic analysis of the data in Figure 2.2 was carried out using an algorithm which describes the general kinetic behaviour for the response of amperometric enzyme electrodes.[29, 132] As discussed in Section 1.1.7, the analysis generally provides a good model for the observed results when the enzyme is restricted within a thin polymer membrane, particularly if the thickness of the polymer film is small compared with the thickness of the reaction layer i.e. the enzyme. In the experiments described in this chapter, it is known that both the p(pd) film and enzyme layer are thin; approximately 10 nm.

Therefore, it is feasible to apply the following expression for theoretical steady state response of enzymes entrapped within non-conducting/thin polymer membranes[29, 132, 134] shown in Equation 2.1.

$$\frac{nFA\alpha}{I_{obs}} = \frac{K_m}{k_{cat}K_S S_\infty e_\Sigma l} + \frac{1}{k_{cat}e_\Sigma l} + \frac{1}{kK_A a_\infty e_\Sigma l} \qquad \textbf{Equation (2.1)}$$

This can be rearranged into a form similar to the Lineweaver-Burke plot which is most commonly used to determine enzyme kinetics. This is shown in Equation 2.2.

$$\frac{I}{nAF} = \frac{S_\infty}{m + cS_\infty} \qquad \textbf{Equation (2.2)}$$

where $1/m = \alpha K_S k_{cat} e_\Sigma l / K_m$ and $1/c = \alpha k_{cat} e_\Sigma l / (1 + k_{cat}/kK_A a_\infty)$ and both are independent of $[S_\infty]$. Values for these kinetic parameters for the Pt/p(pd)/GOx sensors are shown in Table 2.1.

Electrode Type	$\frac{K_S k_{cat} e_\Sigma}{K_m}$ / s^{-1}	$\frac{k_{cat} e_\Sigma}{(1 + k_{cat}/kK_A a_\infty)}$ / mol cm^{-3} s^{-1}	$\frac{K_m}{K_S(1 + k_{cat}/kK_A a_\infty)}$ / mmol cm^{-3}
Pt/p(pd)/GOx (10 mg/ml)	28.01	1.73×10^3	16.19
Pt/p(pd)/GOx (1 mg/ml)	84.34	86.36×10^3	0.98

Table 2.1 - Comparison of kinetic parameters obtained from the analysis of the data in Figure 2.2 using the expression in Equation (2.2) which characterises enzymes immobilised within thin polymer films.

The values in the second column of Table 2.1, which are equivalent to the V_{max} parameter of the traditional Lineweaver-Burke analysis, show an increase when the

enzyme solution concentration was reduced from 10 to 1 mg ml^{-1} which is as expected from previous results in this chapter. Similarly, the values in the third column, equivalent to the K_m value, show a corresponding decrease, indicating a reduction of the dynamic range of the electrode. The values in Table 2.1 were also compared with literature values for other enzyme electrodes analysed using the same immobilisation model. Caruana[110, 134] used this model to analyse GOx immobilised at a platinum surface within a film of polyphenol. The kinetic parameters obtained using polyphenol, after electrode area compensation, are lower than those obtained for the polyphenylenediamine. Therefore, it may be surmised that since the biological component (enzyme) in the two GOx based systems is identical they have same K_m and k_{cat} values and if the enzyme surface concentration, e_{Σ}, was the same then the deciding factor in the kinetic analysis would be the partition coefficients K_S and K_A for the polymers.

Figure 2.3 (a) and (b) shows the current response of the Pt/p(pd)/GOx sensors and a best-fit curve plotted using values obtained from Equation (2.2). The solid curve represents the current responses measured during experimentation and the broken curve represents the non-linear least-squares best fit of Equation (2.2) to the data using the Marquardt-Levenburg algorithm implemented by SigmaPlot. (The Marquardt-Levenberg algorithm finds the parameters of the independent variable(s) that give the best fit between the equation and the data. This algorithm seeks the values of the parameters that minimise the sum of the squared differences between the values of the observed and predicted values of the dependent variable.)[177]

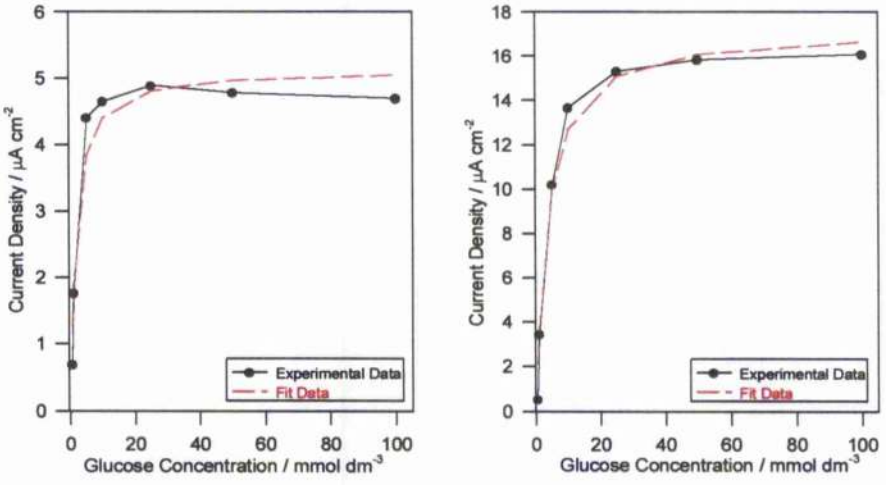

Figure 2.3 - Current responses for the Pt/p(pd)/GOx electrodes (prepared as described in section 2.1.2) with enzyme concentrations of (a) 10 mg ml^{-1} and (b) 1 mg ml^{-1}. The solid line ——— is the experimental data and the broken line ------- is the best fit line.

The advantage of using Equation (2.2) for fitting the data over the standard Lineweaver-Burke,[64] double reciprocal plot is that it incorporates parameters which describe the system in much greater detail. However, further analysis of the data is problematic without accurate estimates for e_{Σ}, and k_{cat} of the immobilised enzyme. Lineweaver-Burke plots are primarily a solution based model where diffusion/mass transport is not restricted and, therefore, is often limiting. At surfaces and for immobilised systems, other parameters must be introduced and become more important, hence Equation (2.1).

2.2.3 - Effect of Ascorbate on Sensor Response

In this section both gold and platinum electrodes were used due to the variety of techniques utilised in observing the effect of electrochemical interferents on electrode response and also because the polymer films can take on various forms on different electrode materials.

2.2.3.1 Increasing Polymerisation Time of Au/p(pd)/GOx Sensors

In terms of the application of the enzyme electrodes to studies involving determination of glucose *in vivo,* the effect of interferents is of prime importance.

The relative permselectivity of the polymer films described in this chapter was investigated by correlation between polymerisation time and the ascorbic acid response observed in the physiological range 0 - 1 mmol dm^{-3}.

Investigations into altering the polymerisation time from 10 minutes up to 24 hours showed that the response to ascorbic acid decreased as the p(pd) polymerisation time was increased. This suggests that there is some mechanism connected to a prolonged polymer growth mechanism that enables it to function as a better barrier to electrochemical interferents. The graph shown in Figure 2.4 shows this trend.

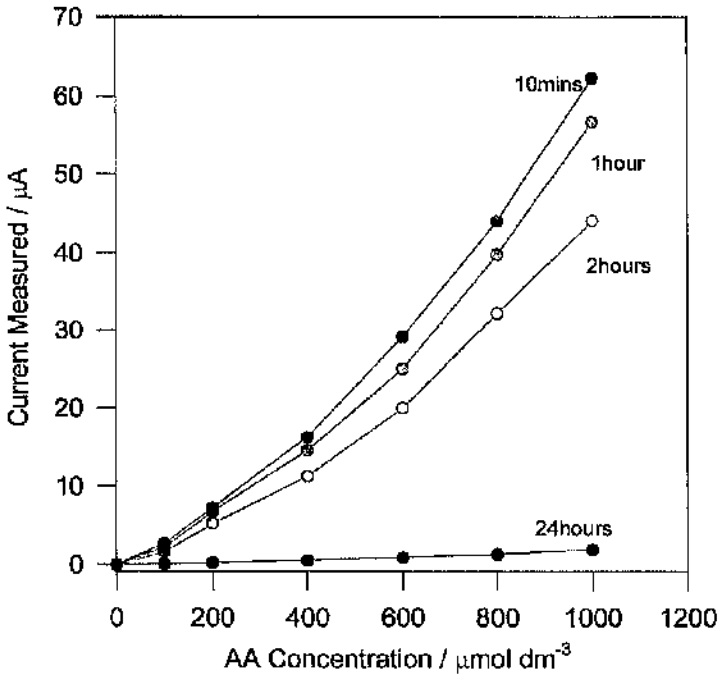

Figure 2.4 - Variation in current response of Au/p(pd)/GOx electrodes (prepared as described in section 2.1.2) in response to ascorbate. Electrodes have polymerisation times of 10 mins, 1 hour, 2 hours and 24 hours.

At present, little is known about the orientation of the individual monomers within the poly-*o*-phenylenediamine film except that it grows to a self-limiting thickness of approximately 10 nm after 10 minutes growth.[106] One possible explanation for this apparent signal reduction may be that prolonged polymerisation allows the polymer to 'backfill' i.e. grow into any 'gaps' in the film that formed during the initial

minutes of growth. Another possibility is that the films become more evenly and, hence, densely packed as the film is grown for extended periods of time.

In order to examine the surface of the polymer, scanning electron microscopy (SEM) was performed on the p(pd)-covered gold surface both before and after repeated exposure to 10 mmol dm^{-3} ascorbic acid for 10 minutes. Typical results can be seen in Figure 2.5.

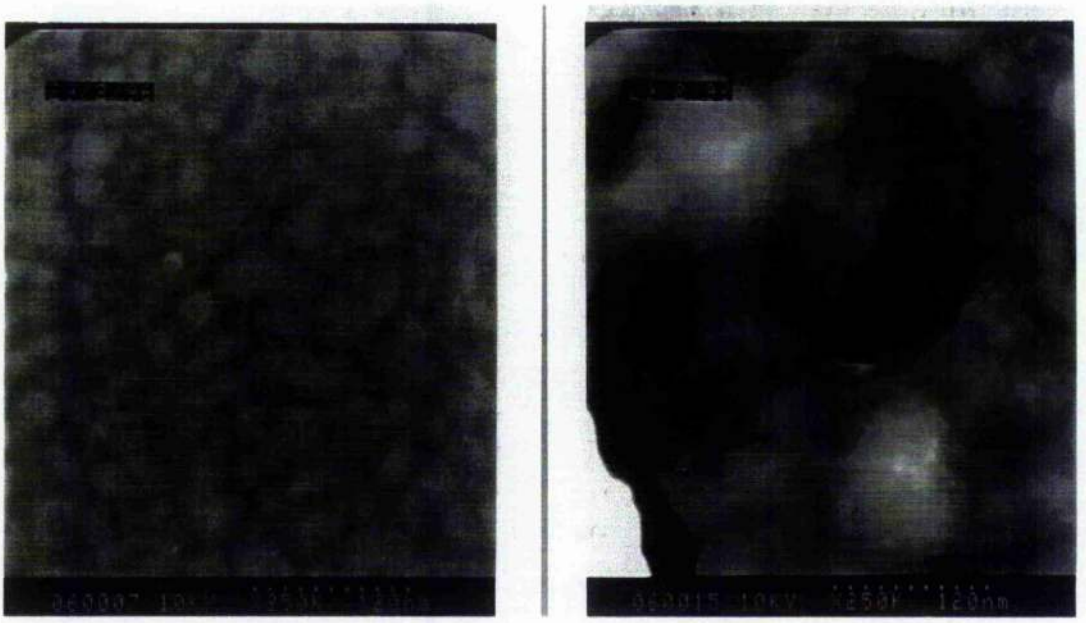

Figure 2.5 - Scanning Electron Micrographs of the p(pd)/GOx films (prepared as described in section 2.1.2) on gold both before (a) and after (b) prolonged exposure to ascorbic acid.

The SEM photographs show what appears to be a uniform layer of the polymer on the gold surface before ascorbate exposure (Figure 2.5(a)). After exposure some degradation of the polymer matrix can be observed which takes the form of 'holes' in the uniform coverage. This result is supported by the work carried out (as part of an undergraduate project) which showed an increase in signal response to ascorbate on multiple assays.

Therefore, it seems that the relative permselectivity of the p(pd) films to ascorbic acid, when the enzyme is present, can be effectively decreased by increasing the

polymer growth time. This effect, however, is negated by the fact that on multiple exposure to ascorbate the polymer starts to break down and thus increases the interfering signal response again. This problem was also addressed using X-ray Photoelectron Spectroscopy (XPS), the results of which can be found in Chapter 3. The XPS measurements provide evidence that there is indeed some structural alteration to the polymer layer as the polymerisation time is increased.

2.2.3.2 Effect of Introducing Lipids into the p(pd) Layer

It has been shown by Wang[107] that the introduction of lipids into the p(pd) matrix is effective at improving the selectivity of amperometric glucose sensors based upon platinum substrates. Lipid coatings are known to offer discriminative properties based on the polarity of their surface/coating[131, 178-180] and so the combination of such hydrophobic layers with the size exclusion features of p(pd) films apparently offers remarkable improvements in the selectivity of glucose biosensors made in this way. The lipid layer acts as a host layer for the growing p(pd) and immobilised enzyme, allowing passage of the small hydrogen peroxide to the electrode surface whilst preventing the ascorbate reaching the surface by using its combined polarity and size effects.

Figure 2.6 compares the glucose response and ascorbate response for sensors prepared with a mixed p(pd)-lipid layer.

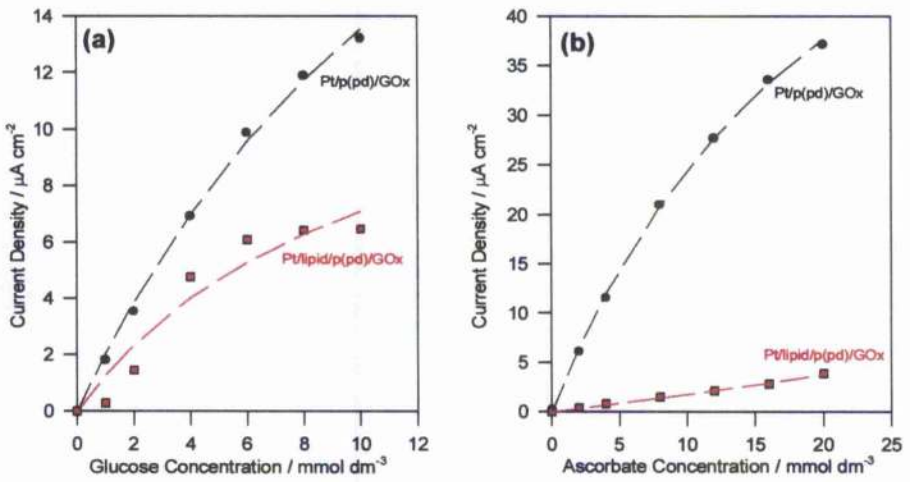

Figure 2.6 - Calibration plots for (a) glucose response (0 - 100 mmol dm^{-3}) and (b) ascorbic acid (0 - 0.4 mmol dm^{-3}) at both p(pd) only and the p(pd)-lipid glucose electrodes (prepared as described in section 2.1.2).

The plot in Figure 2.6(a) compares the current response versus substrate concentration for successive additions of glucose, as obtained at both p(pd) and p(pd)-lipid glucose electrodes. Although the steady state response of the sensors are consistently high, it appears that the response experiences almost a 50% decrease when the lipid is introduced into the polymer film. However, Figure 2.6(b) shows that the p(pd)-lipid structure offers substantially improved discrimination against the otherwise interfering oxidisable interferent ascorbic acid. The response to ascorbate is reduced by approximately 85% when the lipid is incorporated within the polymer layer and, more importantly, there is a corresponding rise from 0.48 to 3.07 in the signal to noise ratio (for responses due to 10 mmol dm^{-3} glucose and 12 mmol dm^{-3} ascorbate) . This improved selectivity is obtained at the expense of maximum analyte sensitivity and, therefore, it is essential that further experimentation be performed which examines the effect of varying the concentration and type of lipid used. However, the results in this section offer an example of methods that can be used to improve the signal to noise ratio of glucose sensors prepared with polyphenylenediamine films.

2.2.4 - Oxygen Dependence of the Pt/p(pd)/GOx Sensors

The oxygen dependence of glucose sensors is of considerable significance for the application of such sensors in biological systems where oxygen availability is severely restricted.[59, 89] Preliminary tests have been performed on Pt/p(pd)/GOx electrodes for the effect on the glucose response when operated under air-saturated i.e. aerobic and nitrogen-saturated i.e. anaerobic conditions. Their response to glucose in the range 0 - 50 mmol dm^{-3} was measured firstly under air-saturated conditions then the solution was nitrogen-purged for approximately 20 minutes to remove oxygen and the responses measured under nitrogen-saturated conditions. Finally oxygen was reintroduced into the solution by bubbling air through for approximately 20 minutes and the responses measured again in an air-saturated environment. Figure 2.7 shows the profile of the glucose response of a Pt/p(pd)/GOx sensor under such conditions. The plots have been normalised to zero current density although some current density was maintained after extensive degassing, most probably attributable to variations in the polymer structure.

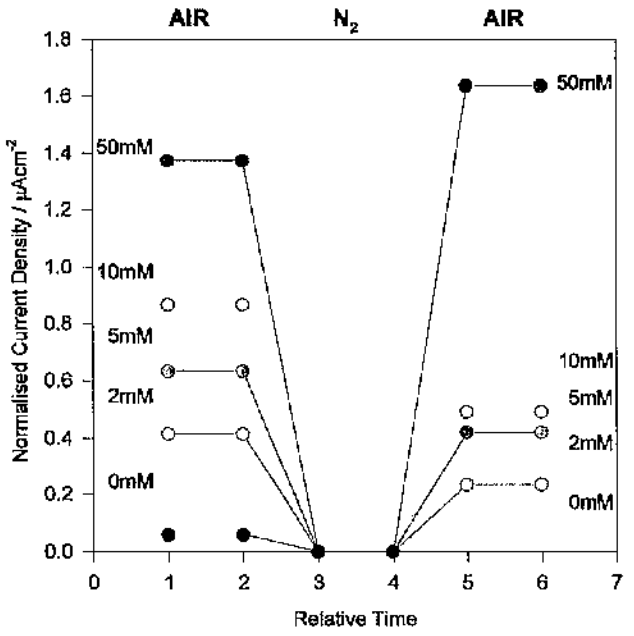

Figure 2.7 - Amperometric steady state response of Pt/p(pd)/GOx sensor (prepared as described in section 2.1.2) to glucose in the range 0 - 50 mmol dm^{-3} under air, nitrogen and air-saturated conditions.

It can be seen from the current profiles in Figure 2.7 that the introduction of nitrogen to the sensor environment, assuming approximately oxygen-free conditions, significantly decreases the sensor response over the whole range of glucose concentrations. On recirculation of oxygen into the system in the form of bubbled air, it was possible to regain between 34 - 44% of the original response values (with the exception of the 50 mmol dm^{-3} response). Contrary to the expected result, the responses under oxygen-free conditions did not fall to zero and, in fact, a surprisingly high response was observed. This may be due to insufficient nitrogen purging but recently O'Neill[115] has reported that there appears to be evidence to suggest that at low oxygen concentrations the response of Pt/p(pd)/GOx microelectrode sensors are effectively independent of the oxygen present in solution. This implies that mechanisms other than reaction of solution oxygen with reduced enzyme are responsible for the signal generated. One possible mechanism is the formation of a platinum oxide layer[181-184] at the electrode surface, perhaps due to hydrolysis of water, which is sufficient to imitate the solution oxygen required for hydrogen peroxide detection systems. Alternative hypotheses are that some oxygen becomes dissolved and/or entrapped within the polymer layer itself and can be used as a reserve supply or that the electrode surface acts as some form of mediator for the current. Continued research into this area is currently being carried out and is essential for the development of *in vivo* sensing.

2.2.5 - Application of p(pd) Films to Glutamate Sensors

Although the majority of this thesis concentrates on producing a well characterised glucose biosensor, the ultimate aim is to take the results obtained and apply them to other enzyme systems. Therefore, it is important to demonstrate that the glucose systems described above can be applied to biosensing of other important substrates, in this case glutamate. Electrodes were constructed by immobilising glutamate oxidase within an electropolymerised film of p(pd) and the response of the Au/p(pd)/GLOx sensor to glutamate in the range 0 - 25 mmol dm^{-3} was observed. A typical calibration plot for these sensors is shown in Figure 2.8.

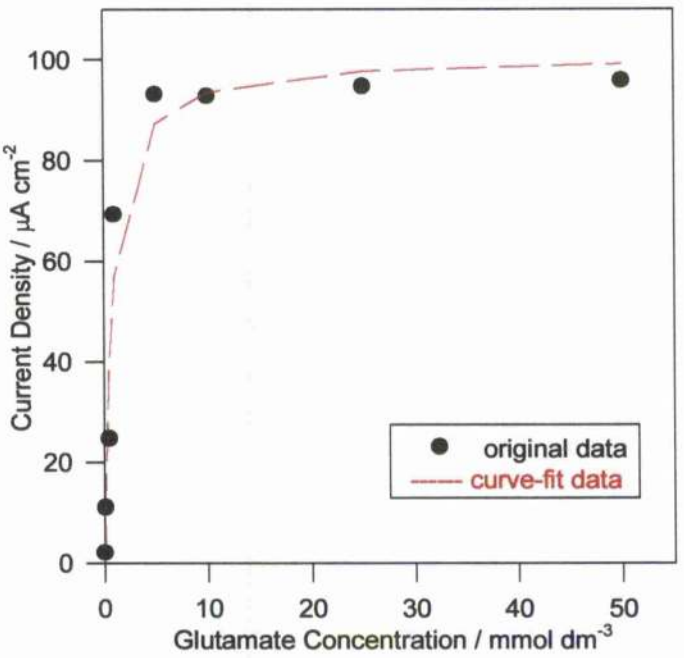

Figure 2.8 - Electrochemical current response for Au/p(pd)/GLOx electrode (prepared as described in section 2.1.2) in response to glutamate in the range 0 - 25 mmol dm^{-3} Fitting performed to Equation (2.2) for enzymes immobilised within thin polymer films.

The data points displayed in Figure 2.8 show the response of the sensor to glutamate and the broken curve is a best-fit curve for the data using the complex fit Equation (2.2) for enzymes immobilised within thin polymer films, which describes the current not only in terms of the enzyme kinetic parameters and substrate concentrations but also involves more advanced parameters such as diffusion coefficients. The values of the kinetic parameters obtained from the analysis i.e. $\frac{K_S k_{cat} e_\Sigma}{K_m}$ and $\frac{k_{cat} e_\Sigma}{(1 + k_{cat}/kK_A a_\infty)}$, were found to be 45.89 s^{-1} and 60.17 mol cm^3 s^{-1} respectively, and can be compared with those in Table 2.1 for the enzyme glucose oxidase. This analysis provides a K_m equivalent term of 1.31m mol cm^{-3} which can be compared to the value obtained, using a Michaelis-Menten kinetic model, of 0.7 mmol dm^{-3} for the K_m of the enzyme which agrees with the range quoted in the references[32] (depending upon the sensor configuration). The important characteristic to extract from this result is simply that various enzymes, including glutamate oxidase, are able to be immobilised within p(pd) films without any loss of

function and can operate successfully as biosensors capable of detecting their particular analyte of interest.

2.3 Summary

To summarise the work completed in this chapter, glucose sensors have been successfully designed which maximise the sensor response and combine the size exclusion properties of the p(pd) films with the polarising effect of lipid layers in order to increase the signal to noise ratio. The method of preparing the polymer-enzyme layer which produced the greatest signal to noise ratio was that of copolymerisation from a solution containing both enzyme and monomer. Additionally, it was found that the relationship between enzyme solution and surface concentration was such that a greater solution concentration produced a larger electrode response. However, this relationship reached a point where increased enzyme loading produced a reduction in current response, most probably due to restriction of the analyte diffusion pathway.

By preparation on platinum substrates in this manner, the investigation of the sensors under aerobic conditions showed that they were able to operate efficiently under low oxygen conditions, allowing them to be considered for use in the development of *in vivo* sensors.

Finally, it has also been shown that such a sensor construction can be used for detection of other important analytes such as glutamate.

CHAPTER 3 - SPECTROSCOPIC ANALYSIS OF POLY(*o*-PHENYLENEDIAMINE) BASED GLUCOSE SENSORS

Previously, three different strategies have been used to immobilise enzymes within polymers for electrochemical biosensing interfaces; (a) preadsorption of the enzyme onto the transducer surface followed by electrodeposition of a layer of polymer (or other binding matrix)[106]; (b) copolymerisation from a solution containing enzyme and polymer[132]; (c) postadsorption of the enzyme on top of the polymer layer[185]. In the literature the performance of electrodes prepared using these methods has been assessed solely by looking at their electrochemical response to the analyte of interest.[97] Although this can indicate which method is best for maximising the current response of the sensor it does not provide any information on the biomolecular composition of the polymer-enzyme interface. Therefore, this chapter illustrates the use of two different spectroscopic techniques to analyse the composition of the polymer/enzyme layer of glucose biosensors prepared under different conditions.

In this respect, the techniques used were X-ray photoelectron spectroscopy (XPS)[141] and Fourier Transform Infra-Red Spectroscopy (FT-iR)[152] which provide surface and bulk elemental analysis of the sensing interface respectively. The resulting spectra can supply both qualitative and quantitative information on the sensor configuration and can be correlated with electrochemical assay results (Chapter 2) in order to ascertain detail on the structure and composition of the sensor interface.

In this chapter both techniques are used to provide both quantitative and qualitative analysis of the distribution of enzyme and polymer within the sensing layer. Although both techniques have a broader potential for quantitative analysis, the results presented in this chapter are limited because of our inability to distinguish spectroscopically between the polymer and enzyme spectra. In contrast, the system described in Chapter 4 which uses the polymer film polyfluorophenol is analysed in

more detail using a more advanced fitting technique to arrive at the percentage of both enzyme and polymer on the surface. This can be confidently performed because the polymer spectra can be easily differentiated from the enzyme spectra by its fluorine content.

3.1 Experimental

In this chapter glucose enzyme-electrodes, prepared by the immobilisation of glucose oxidase within a film of poly-*o*-phenylenediamine, were examined using the techniques of XPS and FT-iR. Chapter 2, section 2.1.1, describes the materials required in the preparation of the samples whilst the methods section, 2.1.2, describes the procedures required for their production. The experimental section of this chapter provides an overview of the procedures required in performing both the analytical techniques described above.

3.1.1 Methods:

3.1.1.1 Sample Preparation:

The same samples were used for both the XPS and FT-iR analyses and were of area 1 cm^2 which was sufficiently large enough to obtain relevant information on the surface composition. To keep the amount of surface contamination to a minimum, all samples were stored under phosphate buffer (50 mmol dm^{-3}) immediately after preparation and analyses were obtained as quickly as possible (usually < 1 day). In addition to the polymer-enzyme combination samples being analysed, reference samples for both the polymer and enzyme alone were prepared. The p(pd) reference samples were prepared by electropolymerisation at a potential of +700 mV *vs.* Ag|AgCl from a solution containing 300 mmol dm^{-3} phenylenediamine for 10 minutes. The enzyme reference samples were prepared by adsorption of protein, whilst cycling the electrode between 0 - 700 mV *vs.* Ag|AgCl for 30 minutes in a

solution containing 10 mg ml^{-1} glucose oxidase (prepared in 50 mmol dm^{-3} phosphate buffer). Previous tests indicated that electrosorption of the enzyme reference sample was found to yield the greatest amount of enzyme on the electrode surface.

3.1.1.2 XPS Analysis:

All the XPS spectra were collected using the high-resolution SCIENTA ESCA 300 spectrometer located at RUSTI, Daresbury Laboratories (Warrington, U.K.). The instrument consists of an AlKα rotating anode source producing radiation of energy 1487 eV which is then monochromated before being projected onto the sample. The photoelectrons are then collected at the detector, after being separated according to their energy using an electrostatic hemispherical electron energy analyser. The slit width of the source was maintained at 0.8 mm to obtain a consistent sampling area and the take of angle was varied from 10° to 90° for each sample measured. Prior to measurement, each sample was rinsed in RO water, blown dry and immediately loaded into the sample chamber of the instrument. All measurements were performed with a pressure of ca. 10^{-9} Torr in the main vacuum chamber.

Analysis of each sample was performed by first taking a wide survey scan spectrum covering a wide range of approximately 1300 eV (between 0 and 1300 eV) and then collecting high resolution spectra over smaller ranges (20 eV) at specific features/regions found in the survey spectrum. As the samples were insulated from the analyser due to their glass substrate, flood-gun energy[141] was required to compensate for the build up of positive charge from photoelectron emission. Therefore, before analysis, the individual spectra obtained had to be corrected for the offset due to the flood-gun electron kinetic energy using the Au(4f) energy as a reference.

3.1.1.3 Quantification and Curve Fitting of XPS Peaks:

As discussed in previous sections, the ESCA spectra contain peaks which can be associated with particular elements, the area under which is related to the amount of element present. By measuring the peak areas and correcting them for instrumental

factors, such as detector sensitivity, the percentage of each element can be determined.[150]

The spectra obtained from the samples were prepared for analysis by firstly shifting in the x-axis to compensate for flood-gun charging effects and then by subtraction of a linear baseline. The curve fitting procedure for the samples in this chapter is simplistic since there are no distinguishing features to discriminate between enzyme and polymer on the carbon C(1s) spectra (although more 'effective' fitting of polymer-enzyme compositions can be seen in Chapter 4). By manually varying the percentages of both the reference polymer C(1s) and enzyme C(1s) spectra, adding them together and fitting them to the sample C(1s) spectrum, it is possible to achieve the 'best-fit' spectrum and hence an estimate of the percentage of both components in the sample. The fit used features characteristic of energies at the high end of the carbon spectra (>285 eV) in order to eliminate the effect of hydrocarbon contamination[145] which is visible at the lower energies (ca. 285 eV). Fitting was performed using the SigmaPlot package.

3.1.1.4 FT-iR Analysis:

The instrument used to collect the spectra was a BOMEM MB-102 FT-iR spectrometer with a mercury cadmium telenide (MCT) detector running BOMEM GRAMS/32 (Version 4.04) software (Gallactic Industries Corporation). Specular reflectance mode[152, 186] using p-polarised light at an incident angle of 80° (grazing angle) was employed and spectra were recorded at a 4 cm^{-1} resolution with an iris aperture of 8 mm.

Nitrogen purging was maintained throughout the experiments to flush the atmosphere of any water molecules which produce strong adsorption bands at 3300 cm^{-1} and 1600 cm^{-1}.[187] The spectrometer output data is recorded as transmission spectra and converted into absorbance data before analysis. As for the XPS technique, reference spectra were also collected for samples comprising of pure polymer and enzyme only.

3.1.1.5 Quantification and Curve Fitting of FT-iR Spectra:

Before the composite spectra could be deconvoluted into their component polymer and enzyme parts, the data was processed into a form which allowed reliable comparison between samples. The first step involved conversion of the transmission data into percentage absorbance using the relationship in Equation (3.1).

$$abs = -\log\left(trans/_{100}\right). \qquad \textbf{Equation (3.2)}$$

Subsequently a cubic baseline was subtracted from the data (providing an approximation of the sloping background)[157]. The final stage of data manipulation involved a normalisation routine for differences in sample area, carried out using an absorbance value at a non-absorbing wavenumber (i.e. 2000 cm^{-1}) and multiplication of the data by this correction factor.

Having obtained the data in a processable format, spectra in the range 1400 - 1750 cm^{-1} were examined in order to investigate the polymer and enzyme features in closer detail. As with the XPS spectra fitting, SigmaPlot was used to vary estimates of the percentage of each component in the sample until a 'best fit' to the sample spectra was obtained. This type of analysis was performed for each sample and the percentages compared for the different electrode preparations.

3.2 Results and Discussion

This section contains information obtained on the construction of the sensing interface of glucose biosensors using the two spectroscopic techniques of XPS and FT-iR. The results compliment each other and provide an informative picture of the distribution within the polymer-enzyme structure. This analysis can be used qualitatively to compare similar samples and quantitatively, with respect to references, to provide numerical solutions for individual samples. This is similar to the study performed by Griffiths *et al.*[164] examining GOx immobilised within over-oxidised polypyrrole (p(py)) films.

3.2.1 - XPS Analysis

The method of enzyme immobilisation within p(pd) films was varied and the effect on the composition of the sensing layer examined using XPS. The three immobilisation methods were investigated, as described in Chapter 2, which were

- preadsorption of enzyme onto the gold electrode followed by polymerisation
- copolymersiation from a solution containing both enzyme and polymer
- polymerisation followed by postadsorption of enzyme.

Samples were prepared using each of the three methods for enzyme solution concentrations of 10 mg ml^{-1} and 1 mg ml^{-1}.

The results are presented in sections, each dealing with particular aspects of the polymer/enzyme interface highlighted by the XPS technique (the first two deal with specific experimental practicalities whilst the latter two concern results):

- the effect of the take-off angle i.e. observed spectral differences as a function of depth
- the role of surface contamination in fitting data
- the effect of variation of enzyme solution concentration
- the effect of variation of the method of enzyme immobilisation.

3.2.1.1 - Effect of Take-off Angle on Surface Composition:

The data for each sample was acquired at two take-off angles of 10° and 90° from the surface, and results used to demonstrate how the polymer-enzyme composition varies as a function of sample depth.[141] Qualitatively, the shape of the response curves, with respect to TOA, can reveal much about the compositional organisation of the surface. For these experiments the gold Au(4f) spectra were used as reference spectra against which the C(1s) and N(1s) spectra could be corrected for flood-gun shift in the x-direction (i.e. binding energy). As the samples are all thin organic films, the Au(4f) spectra can also act as a guide to the proportion of the gold substrate that can be observed through the polymer and, therefore, give an indication as to the structure of the immobilised enzyme within the polymer. (See diagram in Figure 1.15)

Figure 3.1 shows the Au(4f) spectra obtained at take off angles of both 10° and 90° for the sample prepared by copolymerisation from a solution of 10 mg ml^{-1} GOx.

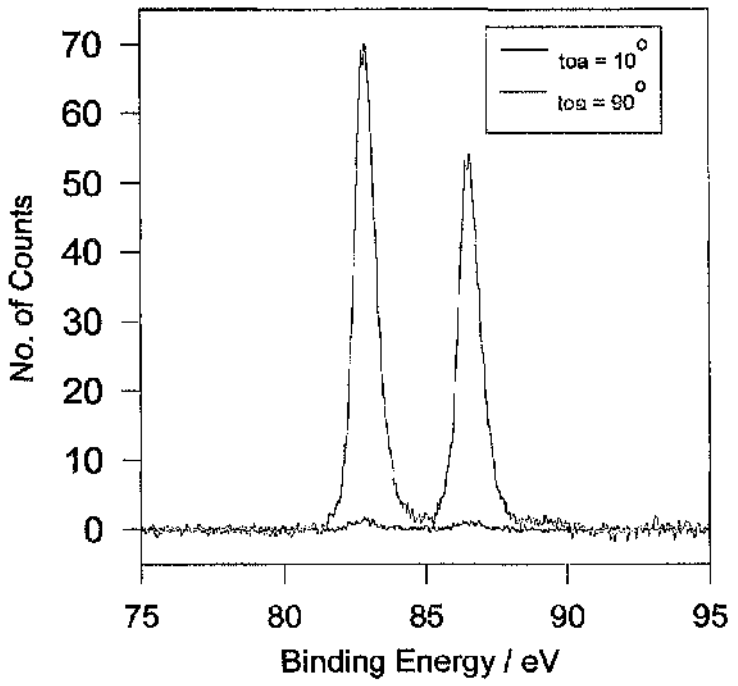

Figure 3.1 - The XPS spectral effect of varying the take-off angle for the example of a Au/p(pd)/GOx sample (prepared as described in section 3.1.1.). At a shallow TOA very little gold is seen, whilst at an angle which allows the full depth of the sample to be examined, the gold substrate can be seen.

It can be seen in Figure 3.1 that as the take-off angle is varied from 10° to 90° the amount of gold visible through the polymer-enzyme layer is greatly increased. This illustrates the variation in the sample depth which can be probed using this technique. At a shallow TOA of 10° only the gold energies visible in the top layer of the sample surface are counted. If the polymer-enzyme film is relatively uniform (in thickness and, hence, surface coverage) then the insulating layer that it forms on the surface should prevent any signal from the gold substrate being recorded. However, a small gold signal is observed which may be indicative of the fact that the polymer film is thin, or that the surface coverage is uneven.

When the TOA is changed to 90°, the gold signal is much stronger, a result explained by the fact that X-rays are able to penetrate through the entire depth of the sample, allowing photoelectrons to be counted from the underlying gold. Therefore, this attribute of XPS can provide valuable information about the molecular positioning of the individual components of the sample under examination. (Radhakrishnan *et al.* have similarly shown the dependence of molecular positioning with respect to TOA)[188]

3.2.1.2 - Surface Contamination:

One of the major disadvantages of using XPS as an analytical technique for samples prepared using thin polymer films is the adventitious (and variable) peaks that appear on the spectra caused by contamination on the sample surface. All efforts were made to ensure that the samples were kept as clean as possible, but inevitably there will be an unavoidable component of 'dirt' from their surroundings. This 'dirt' normally takes the form of hydrocarbon adsorption onto the surface and can be seen at the low energy end of the C(1s) spectra but once the sample is in the spectrometer further contamination can occur by the adsorption of residual gases. Interestingly, the contamination has very little nitrogen, as evidenced by the lack of the N(1s) spectrum, which helps to enable it to be distinguished from the enzyme (see Chapter 4).

In order to illustrate this problem with respect to the work performed in this chapter, the carbon C(1s) spectra for one sample at TOA's of 10° and 90° were examined at lower energies where the contamination is most likely to be visible. The representative sample chosen to demonstrate the presence of contamination was prepared by copolymerisation from a solution containing 10 mg ml^{-1} GOx and 300 mmol dm^{-3} p(pd). The spectra at TOA's of 10° and 90° are shown in Figure 3.2.

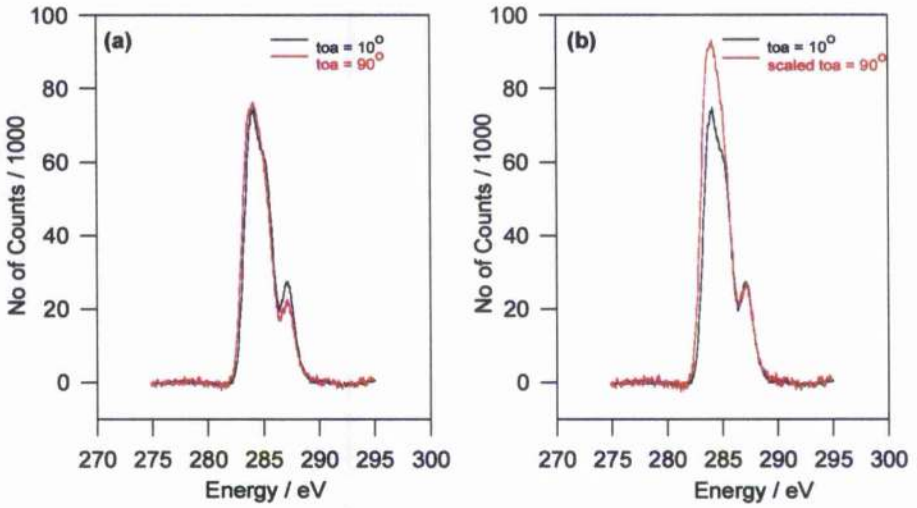

Figure 3.2 - (a) The C(1s) spectra for the Au/p(pd) (300 mmol dm^{-3})/GOx (10 mg ml^{-1}) sample at TOA's of 10° and 90° and (b) the same spectra but with the 90° spectrum multiplied by a scaling factor in order to align the peak at 287 eV, corresponding to the amount of enzyme present within the whole sample. The spectra in (b) show that there is an increased amount of low energy contamination when the sample is analysed at an angle of 90° i.e. the whole depth of the sample is probed, perhaps incorporating contamination from the electrode surface.

By examining firstly the spectra in Figure 3.2(a) it can be seen that at a TOA of 10° there appears to be more GOx present than in the spectrum at a TOA of 90°. This is indicated by a higher number of counts at the peak located around 287.0 eV which is representative of the amount of carbonyl groups of the enzyme. One possible explanation for this would be that the enzyme protrudes from the surface of the polymer and, therefore, at a shallow take-off angle, where only the outermost surface is analysed, all the carbonyl groups on the enzyme can be freely counted. At 90°, where the incident X-rays are perpendicular to the sample, only the carbonyl groups on the top of the enzyme are counted thus misrepresenting the proportion of enzyme within the sample.

In order to obtain a fair assessment of the proportion of contamination within the sample, the 90° TOA spectrum was scaled by an appropriate factor (in this case 1.22) to allow overlaying of the carbonyl peak at 288.0 eV. This indicates that the total amount of enzyme within the sample should remain constant irrespective of the angle at which it is analysed. The scaled spectrum is shown in Figure 3.2 (b) together with the 10° spectrum for the same sample. By looking at both spectra in the low energy region i.e. approximately 284.8 eV as quoted by Briggs and Seah[145] it is obvious that there is a higher number of counts and, therefore, more 'dirt' observable when the full depth of the sample is analysed at a TOA of 90°. This could be explained by the fact that the films used in these studies are thin which therefore allows any material i.e. contamination directly on the electrode surface to be counted. This result is not what perhaps would have been expected since at a TOA of 10° it would be reasonable to observe more contamination from 'dirt' on the surface. Therefore, contamination of the electrode surface is a very real possibility.

This effect is observed for each sample probed and highlights the importance of maintaining as clean an environment as possible for the samples both during preparation and analysis.

3.2.1.3 - Effect of Variation of Enzyme Solution Concentration:

This section investigates the ability of XPS to identify samples prepared with different solution enzyme concentrations by examination of the individual carbon C(1s) spectra. By overlaying the spectra of the samples prepared from solutions containing 10 mg ml^{-1} and 1 mg ml^{-1} GOx it is possible to see the effect that altering the enzyme solution concentration has on the amount of both polymer and enzyme retained at the electrode surface (the assumption is made that the enzyme concentration is equivalent to the number of C=O counts). This is shown diagrammatically in Figure 3.3.

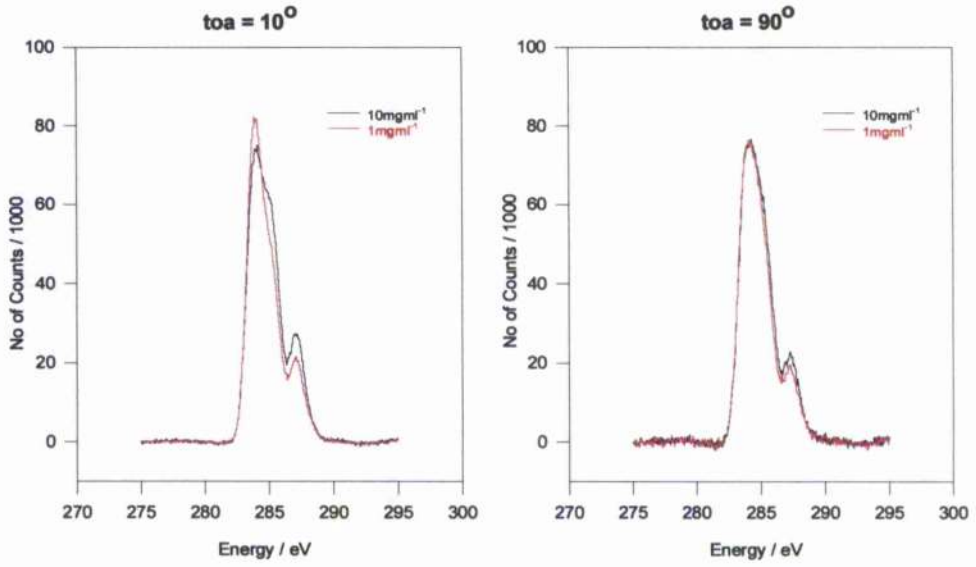

Figure 3.3 - The effect of variation of the enzyme polymerisation solution concentration on the amount of enzyme retained within the polymer film. This is shown in both (a) and (b) for concentrations of 10 mg ml^{-1} and 1 mg ml^{-1}. Also shown is the variation in the enzyme quantity with take-off angle at angles of (a) 10° and (b) 90° to provide an additional analytical perspective.

The attractive feature of the XPS technique that is of significance within these studies is its ability to identify particular functional groups on the sample being analysed. In this case the functional group of interest is the carbonyl (C=O) group which is characteristic to the enzyme within the polymer film (which has no such group). These features are visible at binding energies of approximately 287.0 eV on the C(1s) spectra[141] of the composite samples and can be used to indicate the variation of the enzyme content within the polymer film.

On examination of this region of the spectra in Figure 3.3(a) and (b) it can be seen that the carbonyl peak height decreases as the sample solution enzyme concentration is decreased from 10 mg ml^{-1} to 1 mg ml^{-1} suggesting that the concentration of GOx entrapped within the polymer film i.e. surface enzyme concentration is subsequently reduced. This effect is independent of the take-off angle at which the sample is measured.

This preliminary study uses only two enzyme concentrations, although a more detailed analysis of the effect of enzyme solution concentration on enzyme surface

concentration is described in Chapter 4 where a wider range of concentrations are examined using the same technique but with a different polymer.

It would be informative to take this work forward and transform the qualitative results obtained from looking at the C(1s) spectra into quantitative numerical results, and thus provide an indication of the proportion of polymer and enzyme within the sensing layer. However, due to the difficulty in distinguishing between individual enzyme and polymer peaks on the composite sample C(1s) spectra, quantification could only be performed using the simplest of protocols. Additionally, the presence of 'defects' and 'impurities' within the sample can present a problem in consistent quantitative analysis.

As stated, the fitting protocol involved manually altering the proportions of both the individual enzyme and polymer spectra until a 'best-fit' to the composite sample spectra was obtained. Estimated values for the proportions of both polymer and enzyme were determined for samples polymerised from a solution containing 300 mmol dm^{-3} p(pd) and either 10 mg ml^{-1} or 1 mg ml^{-1} GOx. Ideally the proportions of both should total 100% but due to the simplicity of the fitting process and unavoidable experimental error this is not the case. Therefore, the proportions have been normalised in order to allow clearer extraction of information from the data. Figure 3.4 uses the sample prepared by copolymerisation from a solution containing 300 mmol dm^{-3} p(pd) and 10 mg ml^{-1} GOx and analysed at a take-off angle of 90° to illustrate the fitting procedure.

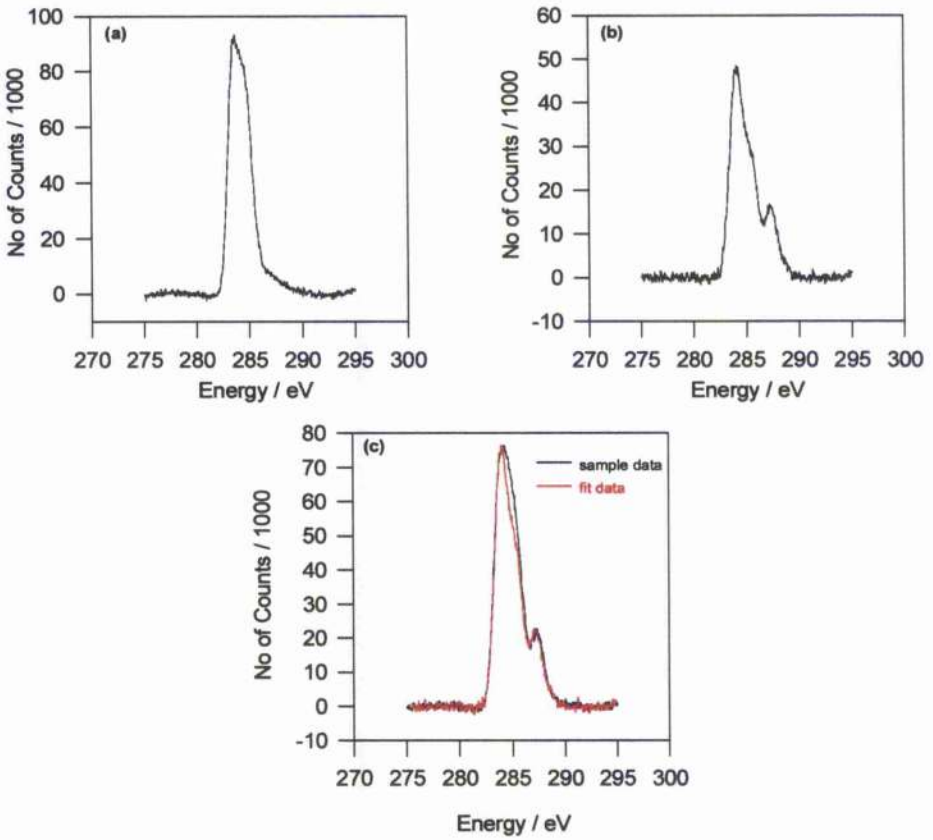

Figure 3.4 shows the simple fitting technique used to establish the percentages of both polymer and enzyme contained within samples: (a) shows the C(1s) spectrum for the p(pd) only sample, (b) shows the C(1s) spectrum for the GOx only sample and (c) shows the sample data for the composite sample (prepared by copolymerisation from a solution containing 300 mmol dm^{-3} p(pd) and 10 mg ml^{-1} GOx at +700 mV *vs.* Ag|AgCl and measured at a TOA = 90°) and the fitted curve obtained using the procedure of manually adjusting the percentage of (a) & (b), adding them together and fitting to the sample data.

This fitting procedure was performed on samples, analysed at take-off angles of both 10° and 90°, which were prepared from solutions containing both 10 and 1 mg ml^{-1}. The breakdown of the composite samples into their polymer and enzyme component percentages provides a good indication of the likelihood of there being more enzyme in the sample when the polymerisation solution contains a higher enzyme concentration, as shown in Table 3.1.

SAMPLE	% DAB	% GOx
10 mg ml^{-1} , TOA = 10°	3	97
10 mg ml^{-1} , TOA = 90°	11	89
1 mg ml^{-1} , TOA = 10°	19	81
1 mg ml^{-1} , TOA = 90°	23	77

Table 3.1 - The relative percentages of polymer and enzyme that comprise each sample (prepared as described in section 3.1.1.) as measured by manually fitting the C(1s) polymer and enzyme spectra to the sample C(1s) spectra.

The figures in Table 3.1 show that for a shallow take-off angle of 10°, when the GOx solution concentration is decreased from 10 mg ml^{-1} to 1 mg ml^{-1} there is a corresponding drop from 97% to 81% in the quantity of protein (as determined by the amount of C=O) within the polymer-enzyme film. As a consequence, there is an increase in the percentage of polymer present in the layer from 3% to 19%. Similarly, for a sharper take-off angle of 90° the percentages follow the same trend i.e. the GOx film content falls from 89% to 77% and the p(pd) film content rises from 11% to 23% as the solution enzyme concentration is decreased.

Normalisation in this manner makes the assumption that the volume of the film remains constant. This raises the question: does the increase in enzyme surface concentration decrease the polymerisation efficiency and, hence, amount of polymer on the electrode surface? Observation of the XPS spectra and the corresponding iR spectra indicate that this is not the case i.e. the film volume varies as a function of the preparation conditions. The ability to know the amount of material on an electrode surface and subsequently control it, is extremely advantageous when considering the preparation and reliability of enzyme-electrodes.

The capability of the XPS technique to look at samples at varied angles enables information on the structure of the polymer-enzyme profile (with respect to depth) to be obtained, as discussed previously in Section 3.2.1.1. By using a take-off angle of 10° it is possible to obtain information on the outermost layer of the film and by changing the angle to 90° information is acquired on the structure of the whole film.

Using this data it can be shown that since there is a higher percentage of GOx when using a TOA of 10°, that the enzyme is protruding through the polymer film. This possesses advantages when considering the ability of the enzyme-electrode to produce an electrochemical current in response to the analyte of interest. Also, this has particular relevance for constructing interference-free sensors based upon the polymer charge exclusion properties.[43] As the most predominant interferents are charged, if the polymer possesses an opposite charge and the polymer-enzyme layer construction is as suggested above (i.e. enzyme protruding from the film), then charged analytes, e.g. glutamate, can access the enzyme easily whilst the polymer excludes any interfering species from being measured at the electrode surface. This is discussed in more detail in Chapter 4.

3.2.1.4 - Effect of Variation of the Method of Enzyme Immobilisation:

Having established that the concentration of the enzyme in the polymerisation solution plays a key role in the composition of the polymer-enzyme sensing layer, the next step in the optimisation process is to consider different methods of immobilising the enzyme within the film. The three methods investigated were as follows:

- 10 minute adsorption of the GOx onto the electrode surface followed by a 10 minute polymerisation of p(pd)
- 10 minute copolymerisation from a solution containing both GOx and p(pd)
- 10 minute p(pd) film growth followed by a 10 minute adsorption of the GOx

Once again, the relevant information was obtained from the carbon C(1s) spectra, using data from experiments with enzyme solution concentrations of both 10 mg ml^{-1} and 1 mg ml^{-1}.

Figure 3.5 shows the C(1s) spectra acquired from samples prepared using all three immobilisation methods with enzyme solution concentrations of (a) & (c) 10 mg ml^{-1} and (b) & (d) 1 mg ml^{-1}. The spectra shown in this figure were measured at take-off angles of both 10° ((a) & (b)) and 90° ((c) & (d)).

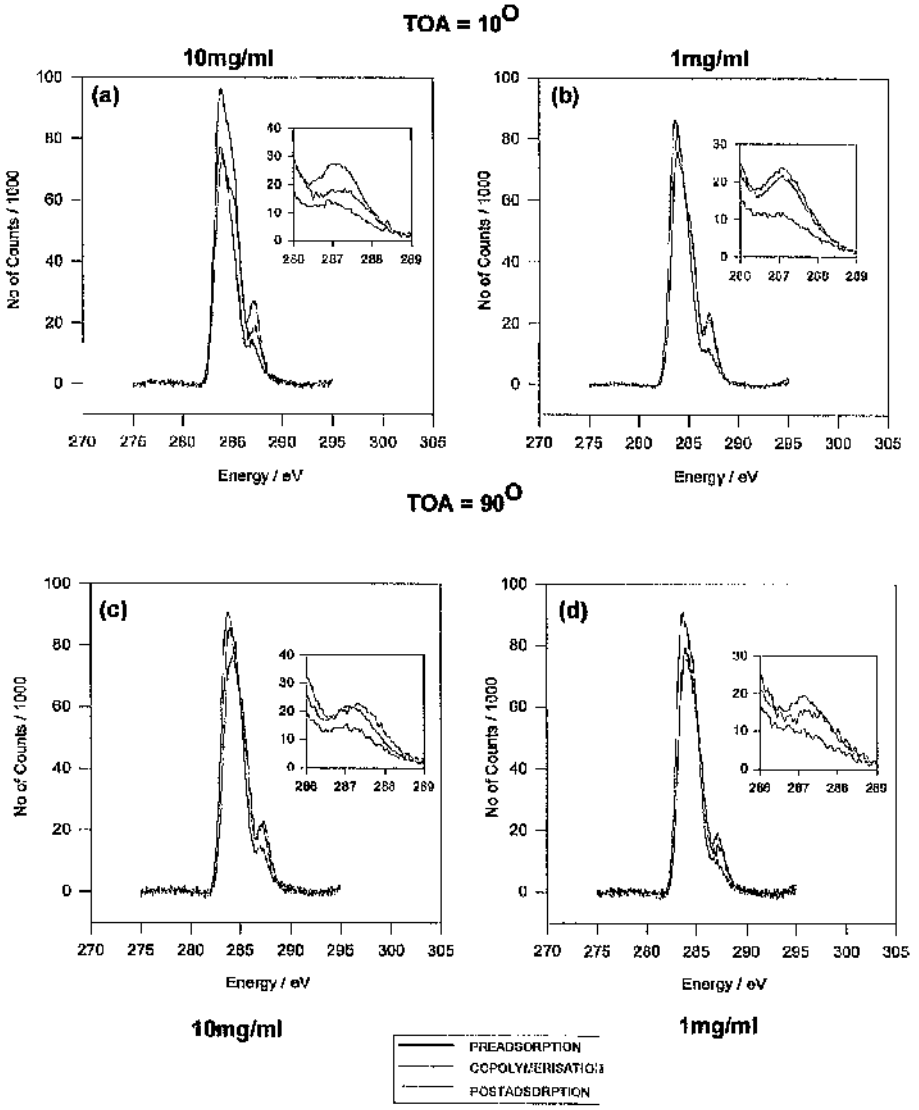

Figure 3.5 - Carbon C(1s) spectra obtained using the three immobilisation techniques (detailed in the text), enzyme solution concentrations and take-off angles. By examining the region of the spectra corresponding to the GOx in the sample at a TOA of 90° for both concentrations (c) 10 mg ml^{-1} and (d) 1 mg ml^{-1} it can be seen that the copolymerisation technique yields a higher amount of enzyme. When the TOA is changed to 10° the same effect is observed for (a) 10 mg ml^{-1} enzyme but not for (b) 1 mg ml^{-1}. The set of spectra shown in (b) indicates that the postadsorption technique yields a higher GOx content. See text for details.

The results shown in Figure 3.5 are displayed by measurement angle to allow clearer presentation. By inspecting initially those obtained at a TOA of 90° i.e. Figure 3.5 (c) and (d), and by expanding the region where the carbonyl groups are to be found, it is seen that irrespective of enzyme solution concentration the immobilisation method which yields the highest amount of GOx in the sample is that involving copolymerisation of the enzyme and the polymer. The method involving

postadsorption of enzyme also contains a relatively large proportion of enzyme, while the least 'successful' method of entrapping enzyme within the biosensor was that of preadsorption of enzyme onto the electrode surface. For all three methods the number of counts decreased when the enzyme solution concentration was decreased (as expected), although the reduction of the amount of enzyme in the polymer was not as substantial as would have initially been expected from the electrochemistry.(See Chapter 2)

In considering the results in Figure 3.5 (a) and (b) where TOA of 10° was used, the results differ from the trend observed at 90°. For a solution enzyme concentration of 10 mg ml^{-1} the highest number of carbonyl counts appear in the copolymerised sample followed by the postadsorbed sample and finally the preadsorbed sample; the same trend that was observed for the 90° analysis. However, for the samples prepared with an enzyme solution concentration of 1 mg ml^{-1}, the maximum amount of enzyme (carbonyl counts) appear to be from the postadsorbed sample. This can be explained since at a 10° angle only the top surface of the sample is measured, which is where the GOx is located for the postadsorbed samples. Also when considering the copolymerised sample in Figure 3.5(b), by decreasing the solution enzyme concentration there will be less GOx on the surface. Therefore, although it can be limitedly seen at 10° the sample will produce a large electrochemical response (as seen in Chapter 2) since the enzyme is distributed throughout the depth of the film.

3.2.1.5 - Summary of the XPS Results:

The results presented in Sections 3.2.1.3 - 3.2.1.4 use the spectroscopic XPS analysis of various different samples to discover the optimum polymer-enzyme preparation conditions and, hence, achieve maximum sensor response (see Chapter 2). The outcome of this analysis can be summarised best with the aid of histograms, as shown in Figure 3.6 (a) and (b).

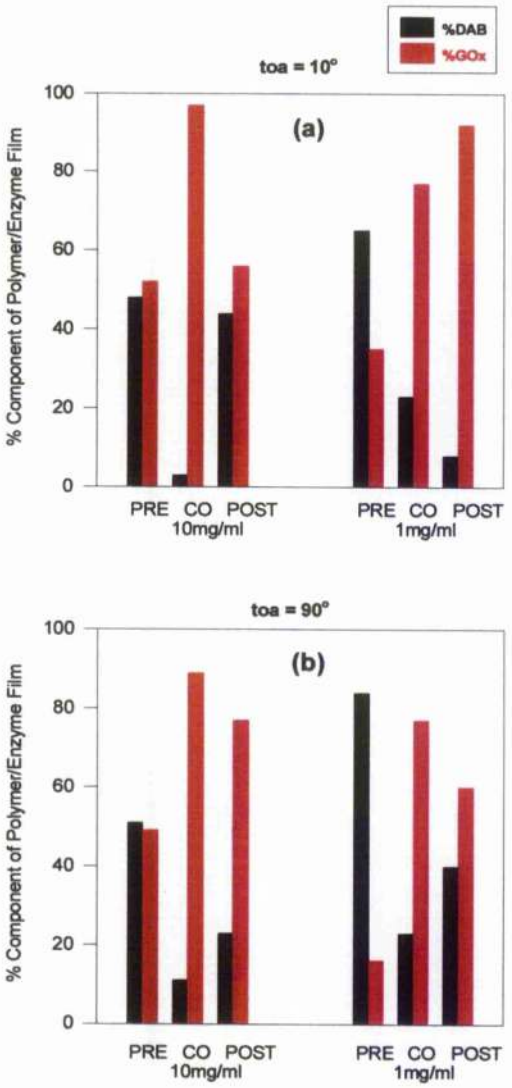

Figure 3.6 - Histograms showing the percentage composition of the polymer-enzyme films as a function of the preparation conditions, obtained using XPS. The graphs are separated by take-off angle i.e. (a) shows a TOA = 10° while (b) shows a TOA = 90°. The important point to notice from both is that the maximum percentage of enzyme retained within the polymer-enzyme layer is achieved when the sample is polymerised from a solution containing both polymer and enzyme i.e. copolymerisation. Also of interest is the expected observation that the percentage of enzyme in the film decreases with decreasing enzyme solution concentration.

The set of experimental results obtained using XPS, as shown in Figure 3.6 (a) and (b), indicate that the most efficient method of enzyme immobilisation is to prepare the sample by polymerisation from a solution containing both enzyme and monomer.

This is best illustrated in Figure 3.6(b) where the samples are analysed at a take-off angle of 90° i.e. more of the depth of the polymer-enzyme film is sampled, not just

the surface composition. Samples prepared using the copolymerisation technique with different enzyme solution concentrations gave the highest percentage of enzyme within the sensing layer.

The information contained in this section correlates well with the electrochemical results obtained for Au/p(pd)/GOx sensors as presented in Chapter 2 (and those of FT-iR experimentation, detailed in the following sections). Therefore, electrode preparation by the method of copolymerisation from a solution containing both monomer and enzyme not only produces the highest electrochemical response but the samples are also shown to contain the highest percentage of enzyme within the sensing layer. This method has been used by many others to optimise the electrochemical response of various types of sensors.[97]

3.2.2 - FT-iR Analysis

As a complementary technique to the XPS studies, analysis using FT-iR was performed to examine the samples prepared as described previously in this Chapter. Once again the effect of variation of enzyme solution concentration and immobilisation technique on the proportions of polymer and enzyme within the films was investigated. FT-iR analysis isolates the characteristic group and bond frequencies of particular functional groups contained within the bulk film thereby making it possible to determine the relative proportions of polymer and enzyme contained within it. The technique contrasts with XPS in that there is an increase in the depth of penetration such that information on the composition of the entire layer can be determined.

3.2.2.1 - Collection of the Raw Transmission Data:

Initially each sample was scanned over a wide region from 1000 to 4000 cm^{-1} to examine the position of all the absorbance peaks and also the size and shape of the background signal. An example of the raw transmission data obtained from such

experiments is shown in Figure 3.7 which illustrates the FT-iR spectra for the sample prepared by copolymerisation from a solution containing 300 mmol dm^{-3} p(pd) and 10 mg ml^{-1} GOx.

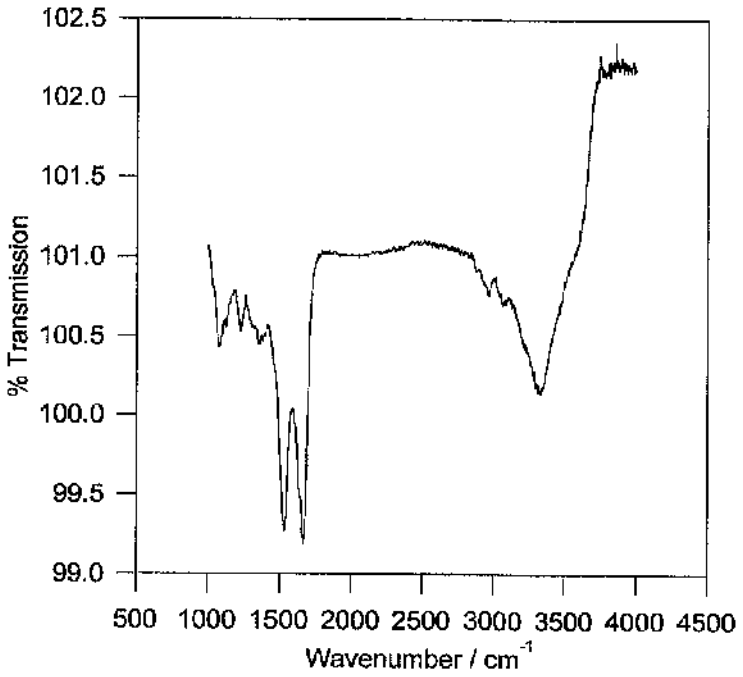

Figure 3.7 - The raw FT-iR transmission data collected for a sample prepared by copolymerisation from a solution containing 300 mmol dm^{-3} p(pd) and 10 mg ml^{-1} GOx. Note the distinct peaks around the area 1400 - 1750 cm^{-1} corresponding to the amide groups of the enzyme

The raw transmission data collected from each sample was subjected to a degree of data processing which involved conversion from transmission into absorbance values and subsequently normalised by correcting for variation in sample area. Once the data was in this form it was possible to compare the peaks on the spectra from the differently prepared samples.

The major problem with FT-iR analysis is the presence of water vapour in the sample chamber which is highly absorbent of iR radiation and thus provides large interfering background contributions to the analysis spectra. Before either qualitative or quantitative analysis can be performed it is essential to carry out an accurate background subtraction. A 'best-fit' cubic baseline was subtracted from the

data between 1400 and 1750 cm^{-1} using PeakFit. More advanced methods have been incorporated into quantification and curve-fit algorithms.[161, 189]

3.2.2.2 - Analysis of the p(pd) and GOx Reference Spectra:

The area of interest for these studies encompasses the region where the amide I and II groups of the GOx are found i.e. 1400 - 1750 cm^{-1}. This region, however, also contains peaks of significant interest for the p(pd) polymer. Therefore, both qualitative and quantitative analyses were performed with the data restricted purely to this region. The reference spectra for pure p(pd) and GOx are shown in Figure 3.8.

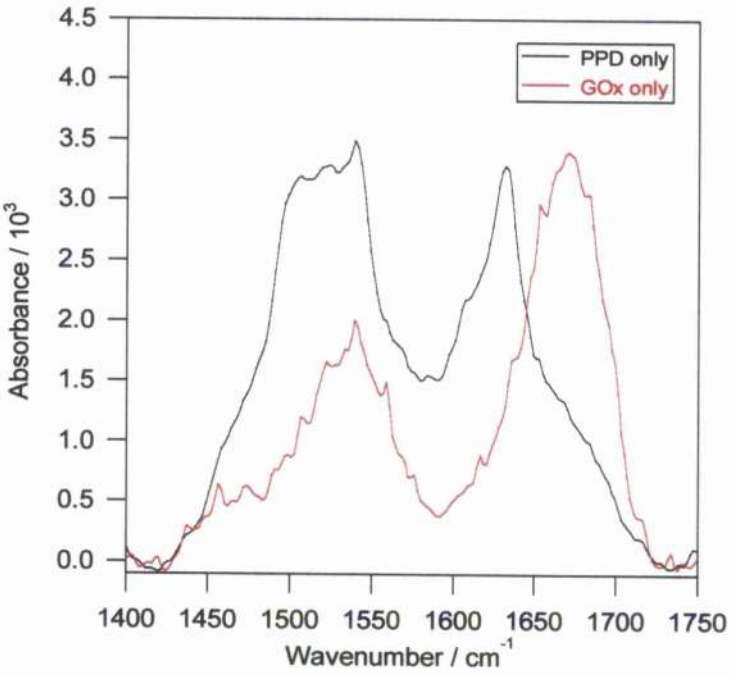

Figure 3.8 - Reference spectra for pure p(pd) (300 mmol dm^{-2} , 10 min @ 700 mV *vs.* Ag|AgCl) and pure GOx (10 mg ml^{-1} , 30 min cycle over range 0 - 700 mV *vs.* Ag|AgCl). The region of interest expanded from 1400 - 1750 cm^{-1} to cover the amide I and II bands of the GOx and characteristic ring-breathing and secondary amine bands of the p(pd).

Educated assumptions can be made as to the origination of the peaks shown in the spectrum for pure p(pd) in Figure 3.8. (The structure of the p(pd) polymer is shown in Figure 1.7, Introduction). The peak around 1500 cm^{-1} is characteristic of the three

aromatic ring-breathing modes of the benzene on the polymer chain while the peak around 1650 cm^{-1} could be attributable to the secondary amines of the polymer. A similar analysis was performed by Lin *et al.* which investigated p(pd) films coated on platinum electrodes and corroborates the iR band assignment illustrated above.[165]

The peaks in the pure GOx spectrum in Figure 3.8 can be more confidently assigned since there are many previous reports that have used FT-iR spectroscopy to study enzymes and proteins.[155, 161, 163, 167, 189] In general, proteins have broad, strong bands which, due to considerable overlap, are difficult to differentiate. However, the amide bands that arise from the vibration of the peptide groups provide information on the secondary structure of the protein and are, therefore, characteristic of the protein. The different amide stretches most commonly used in protein analysis are the amide I (1600 - 1700 cm^{-1}), amide II (1500 - 1600 cm^{-1}) and amide III (1200 - 1300 cm^{-1}) bands. The amide III band is usually very weak (due to the nature of the vibrations associated with it) and so the analysis in this chapter concentrates only on the amide I and II bands, characteristic of the C=O stretching vibration and N-H bending vibrations respectively, as can be seen in Figure 3.8. A more detailed description of the origination of amide bands in proteins can be found in many reports in the literature.[152, 155]

3.2.2.3 - Fitting of FT-iR Data:

As is the case for the corresponding XPS analysis of the samples, it was considered unrealistic to try to predict accurately the percentage composition of the polymer-enzyme sensing layer since FT-iR spectroscopy has the potential to measure many of the polymer functional groups and bonds corresponding to unknown peaks at various frequencies. The polymer and hence composite samples examined in these studies provide a complex interactive system which produces spectra that contain a convoluted series of peaks which could be affected by the method of sample preparation. The spectra collected for composite samples prepared under varied immobilisation conditions exhibit inconsistent peaks due to the fact that unlike XPS

where the core electrons are counted, FT-iR concentrates on the outer electrons of the molecules which could easily be altered by, for example, polarisation due to postadsorption of enzyme. Therefore a simplistic fitting procedure was adopted (in preference to more complicated Gaussian fitting techniques[189] for quantitative interpretation of this data).

Thus, the fitting technique was identical to that performed on the XPS data in that the proportions of p(pd) and GOx reference spectra were altered manually to provide a 'best-fit' to the sample spectra. One example of the technique is shown in Figure 3.9 for the sample prepared by copolymerisation from a solution of p(pd) and 10 mg ml^{-1} GOx.

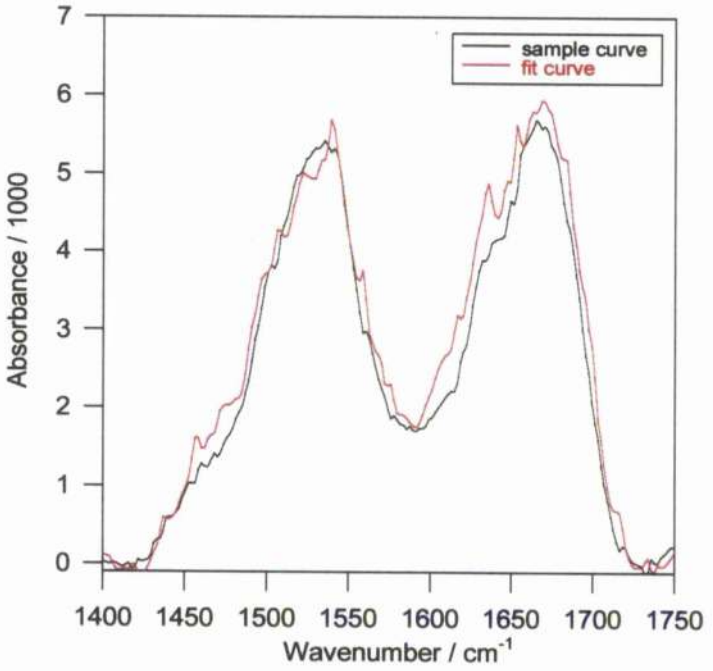

Figure 3.9 - Example of the fitting procedure used for the FT-iR sample analysis. The percentages of pure p(pd) and GOx reference spectra were multiplied and summed in order to provide a 'best-fit' curve to the sample spectrum. This spectrum was obtained for the sample prepared by copolymerisation from a solution of 300 mmol dm^{-3} p(pd) and 10 mg ml^{-1} GOx. The most successful fit parameters indicated a film composition of 64% GOx and 36% p(pd).

This fitting procedure was performed for all the samples analysed using both electrochemical methods (Chapter 2) and XPS (Chapter 3) i.e. prepared by either preadsorption, copolymerisation or postadsorption of either 10 mg ml^{-1} or 1 mg ml^{-1}

enzyme. The percentage composition of the films prepared for each of the samples mentioned above is best represented in graphical format as shown in Figure 3.10.

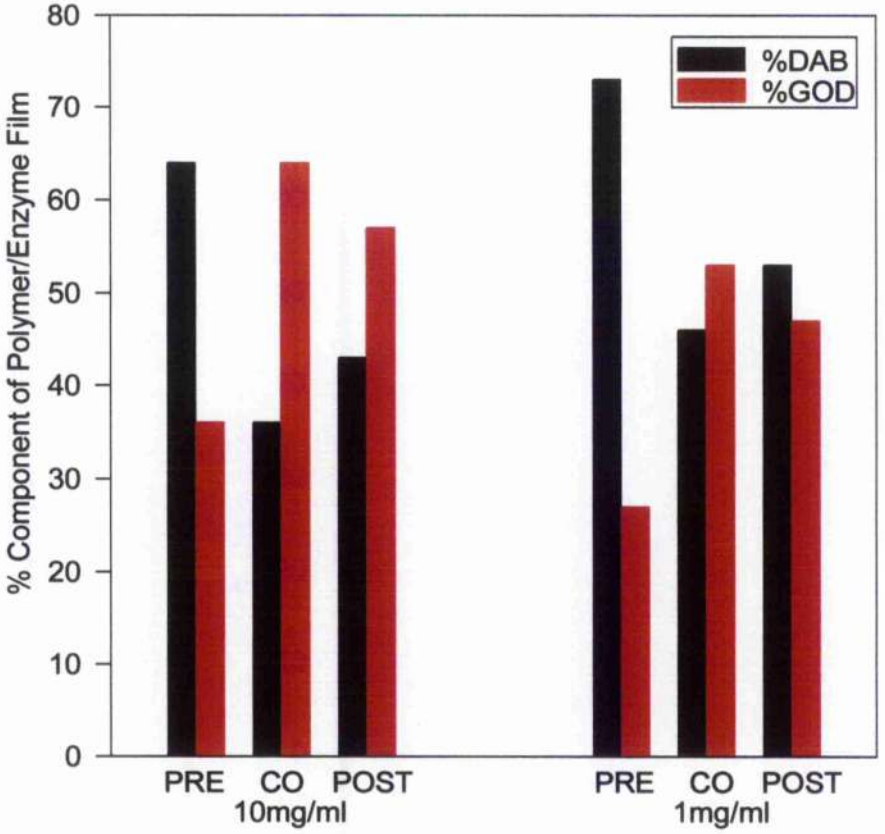

Figure 3.10 - Histogram showing the variation in percentage composition of polymer and enzyme contained (determined from numerical curve-fitting analysis) within the different samples prepared (as described in section 3.1.1).

The values in Figure 3.10 show that for samples prepared with solution concentrations of both 10 mg ml^{-1} and 1 mg ml^{-1} GOx, the surface GOx concentration is at a maximum when the sample is prepared using the copolymersiation technique. The sequence continues with postadsorption being the next most successful method followed by preadsorption.

When this sequence is correlated with both the electrochemical results from Chapter 2 and the XPS results from this chapter, it is possible to predict that the most effective method for enzyme immobilisation within polymer-enzyme sensing layers is that of copolymerisation from a solution containing both monomer and enzyme.

3.3 Summary

The work completed in this chapter uses the spectroscopic techniques of X-ray Photoelectron Spectroscopy (XPS) and Fourier Transform Infra-red (FT-iR) spectroscopy to analyse the composition of the polymer-enzyme film. This analysis was performed on samples which varied not only in the method of immobilisation of enzyme but also the concentration of the enzyme in the immobilisation solution.

The XPS results showed, through measurement at two different take-off angles, that a maximum enzyme loading could be achieved by copolymerising from a solution containing 300 mmol dm^{-3} phenylene diamine monomer and either 10 mg ml^{-1} or 1 mg ml^{-1} glucose oxidase. Additionally, the XPS results highlighted that (as expected) by decreasing the concentration of enzyme within the preparation solution the percentage of enzyme observed within the polymer-enzyme film was subsequently decreased.

FT-iR allowed the bulk of the polymer-enzyme films to be investigated and the results supported the views that copolymerisation produced a higher percentage of enzyme within the film and that this percentage was reduced as the enzyme concentration of the preparation solution was reduced. However, for both techniques (XPS and FT-iR) it would be advisable to expand the range of enzyme and polymer concentrations further to see if the same effect is observed - such a study is performed in the following chapter, Chapter 4.

The results of this chapter can be substantiated with those from the electrochemical analysis of the samples in Chapter 2 to confidently state that the most effective method of enzyme immobilisation is that of copolymerisation from a solution of both monomer and enzyme.

CHAPTER 4 - ELECTROCHEMICAL AND SPECTROSCOPIC ANALYSIS OF POLY(*m*-FLUORO PHENOL) BASED SENSORS

In this chapter the three complimentary techniques of electrochemical assay analysis, X-ray Photoelectron Spectroscopy (XPS) and Fourier Transform Infra-Red Spectroscopy (FT-iR) were used to characterise the bulk and surface composition of glucose biosensors, prepared using electro-entrapped thin insulating films of poly(fluorophenol) (p(fp)). These sensors are similar to those described in Chapters 2 and 3 in that they retain the enzyme glucose oxidase at a gold electrode surface (Au/p(fp)/GOx) in a non-conducting polymer matrix. However, in this chapter we are able to use the fluorine content of the p(fp) polymer to provide information on the position and the relative amounts of both enzyme and polymer within the sensing layer structure.

Although we have established in the preceding chapters that the most effective method of enzyme immobilisation within films of poly(*o*-phenylenediamine) is that of copolymerisation from a solution containing both monomer and enzyme, the sensors described in this chapter were again prepared using three different immobilisation techniques in order to confirm that the efficiency of a particular copolymerisation method was not dependent upon the polymer. Additionally, as in other chapters, the immobilisation procedure was explored in more detail by firstly examining the effect of variation in the duration of polymerisation and finally by altering the concentration of enzyme within the immobilisation solution over the range 0.01 - 10.00 mg ml^{-1}.

As stated, in this chapter a more sophisticated method of analysis was adopted which permitted quantification of the composition of the polymer-enzyme layer. The electrochemical assay results obtained were fitted to the theoretical algorithm for enzymes entrapped within thin films, as reported by Bartlett[132], which enabled the kinetic parameters of the biosensing system to be elucidated. Also, the fluorine and

nitrogen in the enzyme and polymer, which are identified in both the XPS and FT-iR spectra, can be used to apportion their relative amounts in the samples.

4.1 Experimental

The samples prepared for analysis in this chapter were similar to those constructed in Chapter 2 with the exception of the type of polymer used. The preparation technique is reiterated in this section illustrating the slight procedural differences for the Au/p(fp)/GOx electrodes.

4.1.1 Materials

Meta-fluorophenol (F1,300-2) was purchased from Aldrich (Poole, England) and was used without further purification. Phosphate buffer solutions (40 mmol dm^{-3}) were prepared from stock solutions of disodium hydrogen phosphate and sodium dihydrogen phosphate (Sigma). KCl was added to the buffers (50 mmol dm^{-3}) as the supporting electrolyte, and the pH of the buffer was adjusted to pH 7.4. All solutions were freshly prepared using reverse osmosis ultra-pure water (Millipore, U.K). Stock solutions of *D*-glucose (G-7528), also purchased from Sigma, were prepared in appropriate buffers immediately prior to use. Glucose oxidase, GOx, (EC 1.1.3.4., 245 U mg^{-1}) from *Aspergillus niger* was a gift from MediSense (Birmingham) and was prepared as a buffered solution and stored at -20°C.

Gold working electrodes of area 1 cm^2 were fabricated using standard photolithographic techniques as described in Chapter 2, Section 2.1.2. The materials used: titanium, palladium and gold were purchased from Goodfellows (Cambridge, U.K.). The Ag|AgCl reference electrode (MF-2063) was purchased from BAS Technicol, Cheshire.

4.1.2 Methods

4.1.2.1 - Polymer-Enzyme Layer Preparation:

Three different approaches to polymer-enzyme layer preparation were investigated in which films of poly(*m*-fluorophenol) were grown in order to retain the enzyme GOx at gold electrode surfaces. For each of these techniques, the concentration of GOx in the immobilisation solution was 10 mg ml^{-1} and the polymer was grown by cycling the electrode from 0 to +700 mV *vs.* Ag|AgCl in a solution of 10 mmol dm^{-3} fluorophenol for a period of 5 minutes. The maximum peak current value on the forward or oxidation sweep of the cyclic voltammogram decreased between the first sweep and the final sweep indicating the growth of a non-conducting, self-limiting film. The voltammogram is shown in Figure 4.1.

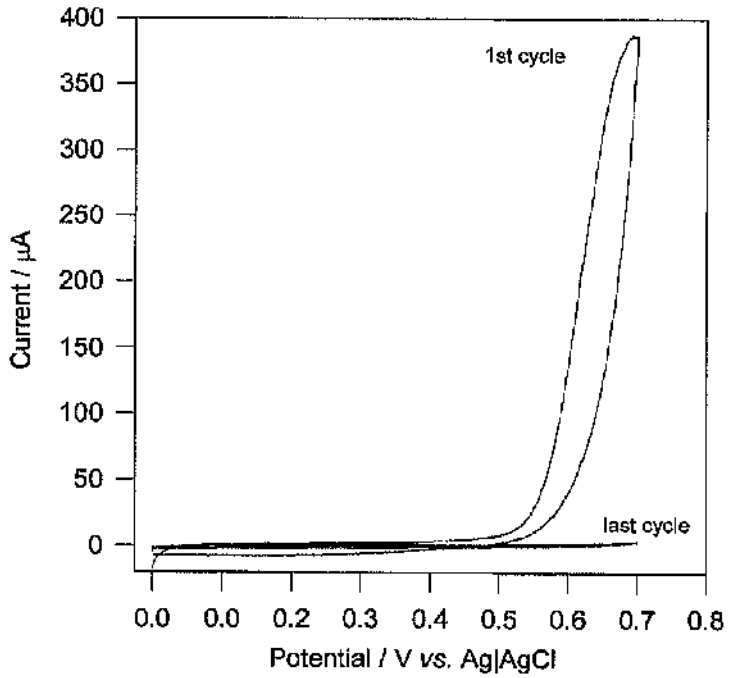

Figure 4.1 shows the cyclic voltammogram obtained during the electropolymerisation of poly(fluorophenol) films. The electrode is swept between 0 and +700 mV *vs.* Ag|AgCl for a period of 5 minutes to allow the insulating film to grow to a self-limiting thickness of approximately 10 nm, as indicated by the fall in maximum current between the first and last scans.

The first immobilisation method involved a 5 minute preadsorption of 10 mg ml^{-1} GOx (in PBS) onto the cleaned bare gold electrode followed by electrodeposition of a layer of p(fp). The second, known as copolymerisation, consisted of a 5 minute

polymerisation from a solution containing both 10 mmol dm^{-3} monomer and 10 mg ml^{-1} enzyme. Finally, in the third method a layer of p(fp) was grown directly onto the electrode surface and then the enzyme was adsorbed on top of the polymer for 5 minutes. Subsequently, after later comparison of the three methods, the second method was adopted to examine the effect of polymerisation time i.e. samples were prepared by copolymerising as described above for a either 5, 15, 30 or 60 minutes.

Samples were also prepared to investigate the effect of enzyme solution concentration using a 5 minute copolymerisation from solutions containing either 10.00, 1.00, 0.10 or 0.01 mg ml^{-1} GOx and 10 mmol dm^{-3} fluorophenol.

4.1.2.2 - Electrochemical Measurements:

A standard three-electrode electrochemical cell connected to a PC-controlled PAR 273 potentiostat (EG&G Princeton Applied Research, U.K.) was used to collect the amperometric current profiles of the sensors in response to glucose. The electrodes were maintained at a constant potential of +700 mV *vs.* Ag|AgCl and, after a steady-state baseline had been achieved, the current response was monitored when additions of glucose in the range 0 - 100 mmol dm^{-3} were introduced into the solution. A steady-state current value for each concentration was recorded before the next was introduced.

The electrochemical assay results for the response of the electrodes to glucose were fitted using SigmaPlot (Jandel Scientific) to a theoretical expression for enzymes entrapped within thin, non-conducting polymer membranes[132]. From such fits it is subsequently possible to realise and compare the kinetic parameters of the sensors.

4.1.2.3 - XPS and FT-iR Measurements:

The XPS and FT-iR spectra were collected using the same spectrometer settings as described for the analyses in Chapter 3, using the high-resolution SCIENTA ESCA 300 spectrometer and software located at RUSTI, Daresbury Laboratories

(Warrington, U.K.). The slit width of the source was maintained at 0.8 mm to obtain a consistent sampling area and the take of angle was varied from 10° to 90° for each interface measured. Prior to analysis, each sample was rinsed in RO water, blown dry and immediately loaded into the sample chamber of the instrument. All measurements were performed with a pressure of ca. 10^{-9} Torr in the main sampling chamber.

Analysis of each sample was performed by first taking a survey scan spectrum covering a wide (1300 eV) range of energies. Subsequently, individual spectra (e.g. C(1s), N(1s) etc.) were examined in more detail over smaller ranges (20 eV) at specific features/regions of interest. As the samples were insulated from the analyser (due to the underlying glass substrate) flood-gun energy was required to compensate for the build up of positive charge from photoelectron emission. Therefore, before analysis, the individual spectra obtained had to be corrected for the offset due to the flood-gun electron kinetic energy, using the Au(4f) energy (85.00 eV) as a reference.

The instrument used to collect the FT-iR spectra was a BOMEM MB-102 FT-iR spectrometer with a mercury cadmium telenide (MCT) detector running BOMEM GRAMS/32 (Version 4.04) software (Gallactic Industries Corporation). Data were recorded in specular reflectance mode using p-polarised light at an incident angle of 80°, with a 4 cm^{-1} resolution and an iris aperture of 8 mm.

Nitrogen purging was maintained throughout the experiments to flush the atmosphere of any water, which would produce strong adsorption bands at 3300 cm^{-1} and 1600 cm^{-1}. The spectrometer output data was collected as transmission spectra and converted into absorbance data before analysis.

4.1.2.4 - Quantification and Curve Fitting of XPS and FT-iR Spectra:

The raw data obtained from the XPS and FT-iR experiments was manipulated in the same manner as is described in Chapter 3, Sections 3.1.1.3 and 3.1.1.5 in order to obtain data in a processable format. However, the fitting procedure for the XPS

spectra was varied slightly in light of the additional information that could be extracted from the results.

The XPS data was initially referenced to compensate for the flood-gun charging effects and then a linear baseline was subtracted. By examining the peak heights of both the nitrogen N(1s) and fluorine F(1s) spectra collected for each sample with respect to the reference polymer and enzyme spectra, it is possible to estimate the percentage of polymer and enzyme within the samples. These percentages were then applied as multipliers of the polymer and enzyme C(1s) reference spectra using SigmaPlot software in order to obtain a 'best-fit' spectra for the sample C(1s) spectra. This method uses the fluorine and nitrogen signals as distinguishing features of the polymer and enzyme respectively, allowing educated quantification of the content of polymer and enzyme within the sensing layer.

Unfortunately, the characteristic fluorine and nitrogen 'labelling' does not provide any assistance for the fitting of the FT-iR sample spectra, since the principal error in this technique is attributable to the method of baseline/background subtraction.[157] Thus, after the conversion from transmission to percentage absorbance using the Equation (3.1), a cubic baseline was subtracted from the FT-iR spectra and then this data was normalised for variations in the sample area. The data analysed was again restricted to the region 1550 - 1750 cm^{-1} which contains the protein dependent amide bands, and SigmaPlot was used to manually alter the percentages of reference polymer and enzyme spectra in order to obtain a 'best-fit' to each sample spectra.

4.2 Results and Discussion

The results obtained are described as the electrochemical assay analysis, the XPS analysis and the FT-iR analysis. Within each area, the results for the individual techniques have been separated further according to the aspect of the polymer-enzyme layer being examined.

4.2.1 Electrochemical Assay Results

The aspects of glucose enzyme-electrode preparation in this chapter initially investigated the effect on sensor response when the polymer-enzyme layer was prepared using a variety of techniques. Having subsequently established the best 'general' preparation procedure, this was then optimised by varying both the duration of the electropolymerisation and the concentration of enzyme in the polymerisation solution. Although this has been previously accomplished for many other polymer matrices[75, 77, 103, 107], this work appears to be unique for polyfluorophenol films.

4.2.1.1 - Effect of Variation of the Method of Enzyme Immobilisation:

As described previously in Chapter 3 for samples prepared with the thin, non-conducting p(pd) polymer, the effect of the polymer-enzyme layer preparation on sensor response was investigated. For the p(pd) films this effect was examined using only XPS and FT-iR while this chapter additionally includes the variation in the electrochemical response of the sensors.

The three preparation methods compared were (a) a 5 minute *preadsorption* of 10 mg ml^{-1} GOx onto the electrode surface followed by 5 minute electrodeposition of 10 mmol dm^{-3} p(fp), (b) a 5 minute *copolymerisation* of both 10 mg ml^{-1} GOx and 10 mmol dm^{-3} p(fp) simultaneously and (c) a 5 minute deposition of 10 mmol dm^{-3} p(fp) onto the electrode surface followed by a 5 minute *postadsorption* of 10 mg ml^{-1} GOx. Samples were prepared using the three techniques and the amperometric current profiles measured in response to glucose over the range 0 - 100 mmol dm^{-3}. The results are shown in Figure 4.2.

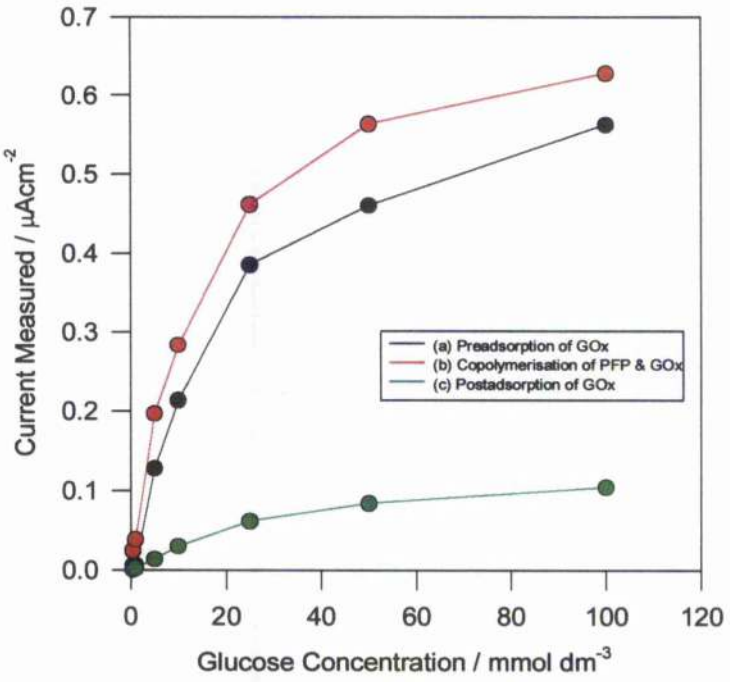

Figure 4.2 - Variation of enzyme immobilisation method and the subsequent effect on sensor response. The methods investigated all used 10 mmol dm^{-3} p(fp) and a GOx solution concentration of 10 mg ml^{-1} and were prepared as follows: (a) 5 minute preadsorption of GOx followed by a 5 minute polymerisation of p(fp), (b) 5 minute copolymerisation from a solution containing both enzyme and polymer and (c) 5 minute polymer growth followed by a 5 minute GOx postadsorption. From these electrochemical assay results the most productive method i.e. the one which entraps most enzyme at the electrode surface appears to be the copolymerisation technique.

The electrochemical current profiles observed in Figure 4.2 show that the immobilisation procedure which yields the largest maximal sensor response (i_{max}) is that of copolymerisation from a solution containing both enzyme and monomer. This also suggests that by simultaneously immobilising the enzyme and electro-depositing the polymer it is possible to achieve the most favourable environment for effective enzyme/analyte reaction. This hypothesis can be substantiated by the other results in this chapter obtained from the XPS and FT-iR analyses and was found to be true also for the poly(phenylenediamine) sensors described in Chapters 2 and 3.

The data in Figure 4.2 can also be used, to a limited extent, to predict the composition and, hence, the sensitivity of the polymer-enzyme layer. When the enzyme is absorbed onto an underlying polymer layer, unless there is a strong adhesion between the two it is not unreasonable to suppose that there will be some degree of desorption when the sensor is operated under aqueous conditions. This

may be the reason for the substantial decrease in sensor response, Figure 4.2 (c), when prepared in this manner. Alternatively, when the enzyme is preadsorbed onto the bare gold electrode and covered by a layer of polymer, it is proposed that the polymer layer will encapsulate the enzyme, making it increasingly difficult for the analyte of interest, in this case glucose, to diffuse through the polymer and react with the enzyme. This may account for the drop in electrochemical response for sensors prepared using this technique i.e. Figure 4.2 (b).

The two situations described above can be supported by the concept behind the copolymerisation technique. By including enzyme in the electropolymerisation solution (as a polycation to aid polymerisation) it is likely that as the polymer forms it encases the enzyme molecules within it and fills up any gaps between enzyme molecules. Such a configuration may allow the enzyme to protrude from the polymer layer making it easy for reaction with glucose.

This concept of establishing the polymer-enzyme micro-environment in which the enzyme is either 'proud of' or 'buried within' the entrapment matrix is of considerable interest when considering sensor fabrication, particularly if the membrane is permselective and/or the enzyme's substrates are charged. Therefore, the composition of the polymer-enzyme matrix is examined in some detail within this chapter using electrochemical assay responses and, in particular, XPS later in this Chapter where the penetration depth into the layer can be varied.

4.2.1.2 - Effect of Variation of Electropolymerisation Time:

Having established that the most effective method of sensor preparation is that of copolymerisation of the enzyme and polymer, this section now explores the effect of varying one of the parameters of the technique. The electrochemical responses to glucose were recorded when the electrodes were prepared by copolymerisation for periods of 5, 15, 30 and 60 minutes. The consequence of such variation is shown in Figure 4.3.

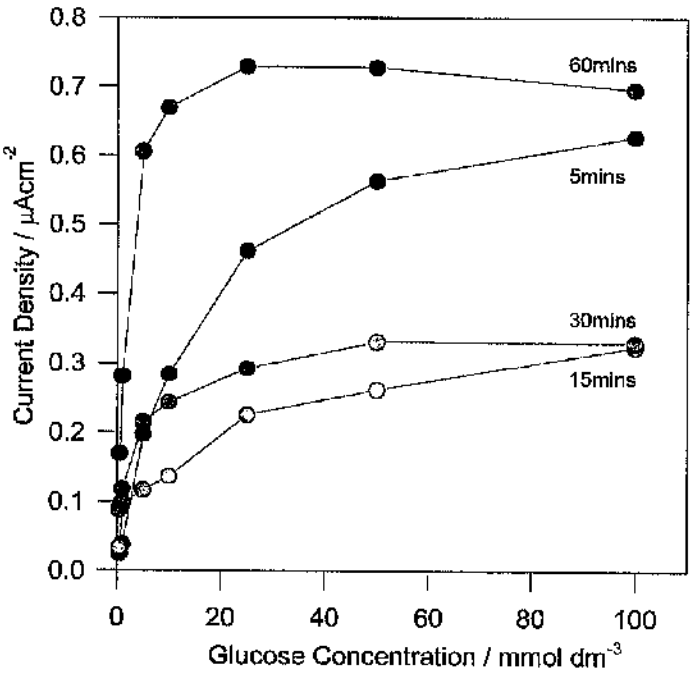

Figure 4.3 - The effect on sensor response caused by variation in the duration of electropolymerisation. By increasing the length of electrodeposition of the polymer-enzyme layer from 5 minutes to 1 hour, the corresponding electrochemical response of the sensors does not appear to follow an obvious trend. The choice of 5 minutes as the value for this parameter for subsequent experiments was based upon it possessing the best electrochemical profile.

The current profiles corresponding to an increase in the electrodeposition time from 5 minutes to 1 hour, represented in Figure 4.3, illustrate that no distinct trend emerged as this polymerisation parameter was altered. Although each plot follows an asymptotic curve i.e. a sharp initial increase followed by a kinetically saturated response which is independent of substrate concentration, the calibration curve formed by the 5 minute polymerisation best follows the expected response of an ideal sensor. The operating characteristics of such an ideal sensor can be described by Michaelis-Menten kinetics, as detailed in the Introduction, and exhibit a relatively large linear/dynamic range which eventually saturates as the system becomes mass transfer or kinetically limited.

These results must be viewed in connection with those in Section 4.2.2.3 obtained from XPS on the same samples which show very little variation in the percentage of polymer and enzyme present in each of the films (also the results in Section 4.2.3.2 obtained by FT-iR analysis should be considered.) Therefore, for this reason the

method of 5 minute polymerisation was adopted for subsequent sensor preparations. Several similar time-dependence studies have been performed for sensors prepared with conducting polymer matrices. Fortier *et al* varied the polymerisation time for GOx immobilised within p(py) films and found that, since this polymer is not self-limiting, the current response of the sensor diminished as the thickness of the polymer layer increased. This is related to the fact that a large fraction of the enzymatically produced H_2O_2 is lost in solution and, therefore, unable to be measured at the electrode surface. However, since the polymerisation of non-conducting films show a degree of molecular self-assembly, i.e. the film grows only thick enough to become an insulator, studies have never been performed that extend the polymerisation beyond the point at which the current decreases to a minimum, signalling complete surface coverage.

4.2.1.3 - Effect of Variation of Enzyme Solution Concentration:

The final and most important polymerisation parameter studied in this work was the effect on amperometric sensor response due to variation of enzyme concentration in the polymerisation solution and, hence, in the polymer-enzyme film.

Samples were prepared from polymerisation solutions containing 10.00, 1.00, 0.01 and 0.01 mg ml^{-1} GOx and their electrochemical response to glucose observed. The current profiles obtained are shown in Figure 4.4.

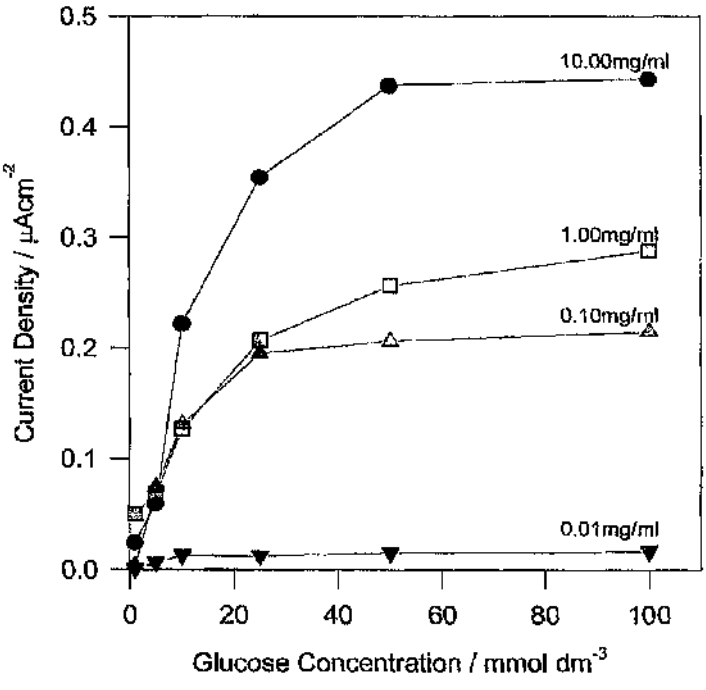

Figure 4.4 – The GOx solution concentration dependence of the sensor response. The samples were prepared by copolymerisation at 700 mV *vs.* Ag|AgCl from a solution containing 10 mmol dm^{-3} fluorophenol and either 10, 1, 0.1 or 0.01 mg ml^{-1} GOx. The maximum current densities of the sensors, at a given substrate concentration, decrease as the GOx solution concentration is decreased, indicating that there is less enzyme entrapped within the polymer-enzyme film.

By comparing the plots in Figure 4.4 it can be seen that as the concentration of GOx is decreased from 10.00 mg ml^{-1} to 0.01 mg ml^{-1} at a given glucose concentration, the maximum current density response decreases accordingly from 0.45 μA cm^{-2} to 0.02 μA cm^{-2}. The decreasing response, as the current density, suggests that there is a subsequent reduction in the concentration of GOx retained within the polymer-enzyme layer during the copolymerisation procedure, a function of the amount of GOx in the loading solution.

To provide a more in-depth picture of the sensor interface, the kinetics of the immobilised enzyme at the electrode surface were established for each sample. This was carried out in the same way as the p(pd) film analysis in Chapter 2, using Equation (1.11) (Chapter 1) to describe the kinetic behaviour of enzymes immobilised in thin films. As described in the Introduction, this equation can be rearranged in order to extract parameters of kinetic interest. These are shown in Table 4.1.

$[GOx]_{soln}$ Conc. / mg ml^{-1}	$\frac{K_S k_{cat} e_\Sigma}{K_m}$ / s^{-1}	$\frac{k_{cat} e_\Sigma}{(1+{k_{cat}}/{kK_A a_\infty})}$ / mol cm^{-3} s^{-1}	$\frac{K_m}{K_S(1+{k_{cat}}/{kK_A a_\infty})}$ / mmol cm^{-3}
10	5.23	1.85 x 10^3	2.83
1	2.63	2.88 x 10^3	0.91
0.1	7.48	1.30 x 10^3	5.75
0.01	0.80	1.08 x 10^3	0.74

Table 4.1 - Kinetic parameters for Au/p(fp)/GOx electrodes (prepared as described in the text) as a function of the concentration of GOx in the polymerisation solution.

The values in Table 4.1 draw together the gradients, intercepts and ratio of gradient to intercept of the reciprocal plots obtained from the current/time profiles in Figure 4.4. The term $\frac{K_S k_{cat} e_\Sigma}{K_m}$ can be regarded as the first order rate constant of the system (equivalent to the k_{cat} of Michaelis-Menten kinetics) and similarly the term $\frac{k_{cat} e_\Sigma}{(1+{k_{cat}}/{kK_A a_\infty})}$ represents the second order rate constant of the system. The third term in the table, $\frac{K_m}{K_S(1+{k_{cat}}/{kK_A a_\infty})}$, is considered as the K_m of the system which changes as a function of the enzyme loading in the sensing layer. This indicates that the physical nature and, hence, the mass transfer characteristics of the polymer-enzyme layer also vary as a function of enzyme surface concentration. This is as expected since at low enzyme concentrations the layer is predominantly composed of polymer and hence less substrate partitions into it, resulting in an increase in the K_m of the system. Subsequently, when there is only a low concentration of enzyme present the system may be expected to be less 'enzymatically active' as illustrated by a drop in the first order rate constant, k_{cat}. This reduction in k_{cat} is shown in the first column of Table 4.1.

The kinetic parameter values in Table 4.1 can be used to produce a 'best fit' curve for each of the data sets. The data collected for the sample containing 10 mg ml^{-1}

GOx is used in Figure 4.5 to illustrate the 'best-fit' curves obtained by fitting using the immobilised enzyme method of kinetic analysis and additionally the Michaelis-Menten kinetic method which assumes the enzyme is in solution.

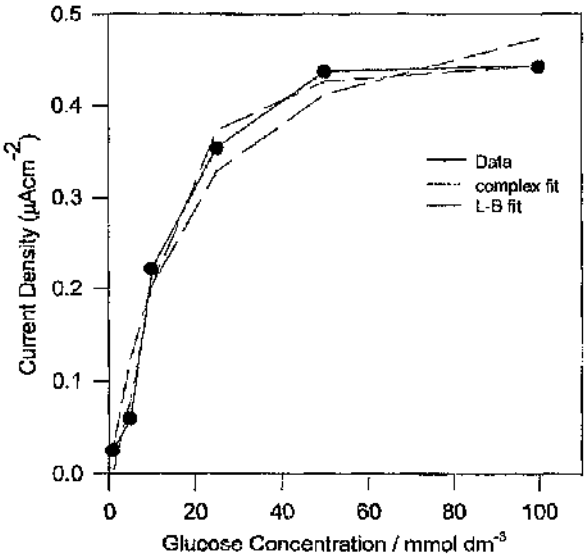

Figure 4.5 -The 'best-fit' curves obtained using the kinetic parameters from the data analysis using both the Michaelis-Menten and complex analysis equations. In this figure the sample with 10 mg ml^{-1} GOx is used as an example to illustrate the variation in curves due to the method of kinetic analysis and fitting.

A similar method of fitting was carried out for each of the sample data sets and is shown in Figure 4.6 (a) and (b) for the two methods of analysis respectively.

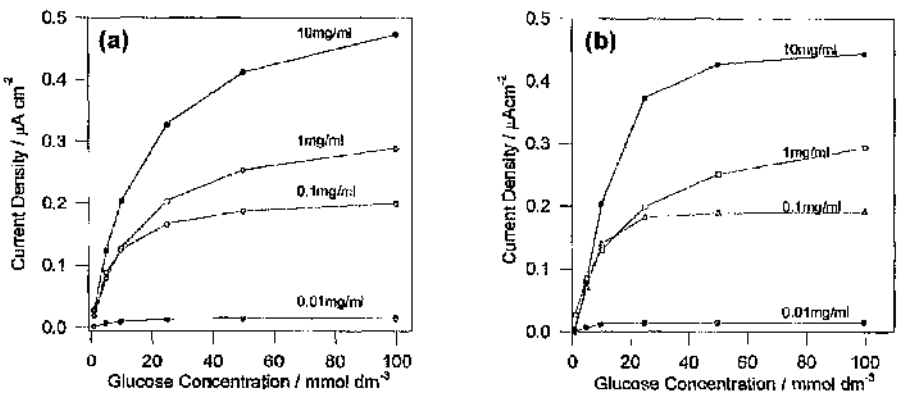

Figure 4.6 - The 'best-fit' curves to the experimental data for the samples with varying enzyme solution concentration. These were obtained using two different kinetic analysis models: (a) using the complex model for enzymes immobilised within thin films, Equation (1.11) and (b) using the simpler Michaelis-Menten model for enzyme kinetic activity, Equation (4.1).

4.2.2 XPS Analysis

The XPS analysis of results addressed four important issues: (a) the problem of analysing data for the biofilm in the presence of contamination; (b) differences in the amount of enzyme immobilised in the polymer-enzyme film as a function of the immobilisation method; (c) the time dependence of immobilisation; (d) the dependence on the concentration of enzyme in the film on the concentration of the enzyme in the solution (and subsequent comparison with electrochemical results).

4.2.2.1 - Effect of Sample Surface Contamination :

The need to maintain a 'clean' sample surface was highlighted in Section 3.2.1.1 where the amount of gold substrate visible through the polymer-enzyme layer was examined at the two different take-off angles, 10° and 90° (see Figure 3.1). This can be substantiated by looking at the polymer-enzyme surface layer after the sample has been stored in a relatively 'clean' atmosphere for a period of two days. The C(1s) spectra of the sample prepared by copolymerisation from a solution containing 10 mg ml^{-1} GOx and 10 mmol dm^{-3} p(fp) were collected on two occasions, separated by 48 hours. The resulting spectra are shown in Figure 4.7.

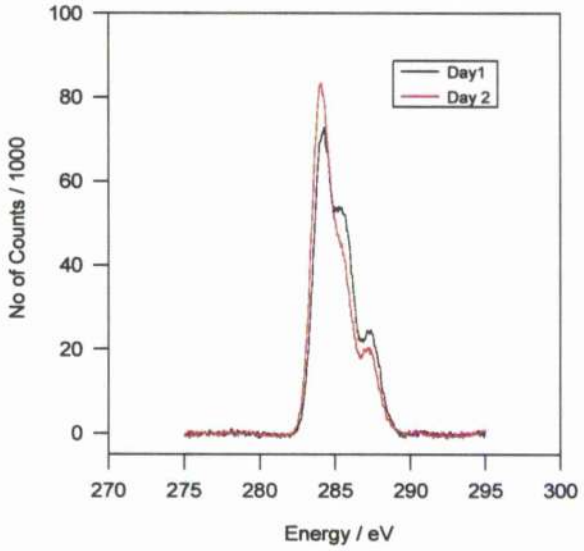

Figure 4.7 - Increased contamination at the low energy end of the spectra (~284 eV) due to sample exposure to atmosphere over a period of 2 days. The C(1s) spectra were obtained for the sample prepared by copolymerisation from a solution containing 10 mg ml^{-1} GOx and 10 mmol dm^{-3} p(fp) at a take-off angle of 10°.

The graph in Figure 4.7 shows that after exposure of the samples to air for a period of approximately 24 hours, the amount of contamination observed at the lower energies on the spectra is increased by approximately 10% as a consequence of hydrocarbon adsorption from the atmosphere.

Concurrently, there appears to be a reduction in the amount of polymer and enzyme observed on the spectra collected on the second day i.e. the peak heights at 286.0 eV and 287.5 eV corresponding to p(fp) and GOx respectively are both reduced. This loss in amount of material from the sensor surface may be caused by any of the following three factors: (a) hydrocarbon adsorption obscuring the polymer; (b) bacterial degradation of the enzyme; (c) sample damage by the bombardment of X-rays in the XPS technique. The Au(4f) spectra, collected on the two occasions, are shown in Figure 4.8. These spectra display a noticeable decrease in the amount of material on the electrode surface which is consistent with reasons (b) and (c) above.

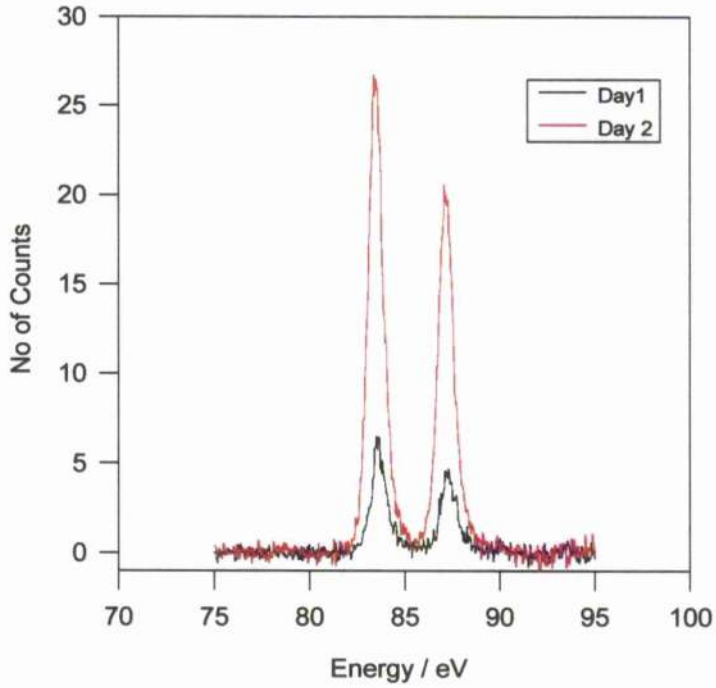

Figure 4.8 - The Au(4f) spectra collected at a TOA = 10° for the Au/p(fp)/GOx sample prepared by 5 minute copolymerisation from a solution containing 10 mg ml^{-1} GOx and 10 mmol dm^{-3} p(fp). The increase in gold observed on the second day illustrates that there appears to be a reduction in the total amount of polymer and enzyme contained within the sensing layer. This can most likely be attributed to damage caused by x-ray bombardment of the surface.

The idea of a reduction in total mass of the polymer-enzyme layer due to bombardment of x-rays during the XPS measurements has been described by Ratner[147] where he suggests that the damage may be due to the electrons emitted in response to the x-rays. As the samples in these experiments were only measured once, this was not, however, considered to be important in the analyses described in this thesis.

4.2.2.2 - Effect of Variation in Enzyme Immobilisation Method :

The first parameter of the polymer-enzyme layer preparation to be examined with the XPS technique was that of variation in the method of enzyme immobilisation in order to maximise enzyme loading. As described in previous sections, the three immobilisation methods investigated were (a) preadsorption of GOx followed by electrodeposition of a p(fp) layer, (b) copolymerisation from a solution containing both GOx and p(fp) and (c) electrodeposition of the p(fp) layer proceeded by a postadsorption of GOx. Samples were prepared using each of these methods and the C(1s), N(1s) and F(1s) spectra were obtained at take-off angles of both 10° and 90° in order to examine a depth profiling of the relative amounts of enzyme (C(1s) and N(1s)) and polymer.

In order to extract quantitative information from the spectral results, the percentage of both polymer and enzyme were estimated from the reference p(fp) F(1s) and GOx N(1s) spectra which were subsequently used to find the 'best fit' to the individual sample C(1s) spectra. By performing this fitting process, it is possible to obtain values for the percentages of p(fp) and GOx contained within the polymer-enzyme layer.

As stated, the initial step of the fitting process involved estimating the percentage of p(fp) and GOx contained within the samples by measuring the ratio of F(1s) and N(1s) in the sample spectra to that in the reference F(1s) and N(1s) spectra. These ratios were calculated from the peak heights of the sample and reference spectra and were used as initial estimates for the fitting parameters. The fitting was subsequently

performed by multiplying the reference p(fp) and GOx C(1s) spectra by an appropriate ratio and summing them to obtain a curve that best represented the C(1s) spectra obtained for the sample. The multiplier values were then altered manually until values which gave a 'best fit' were noted and used to indicate the percentage composition of the sensing layer. This is shown diagrammatically in Figure 4.9 for a TOA = 10° i.e. looking at the surface of the polymer-enzyme layer.

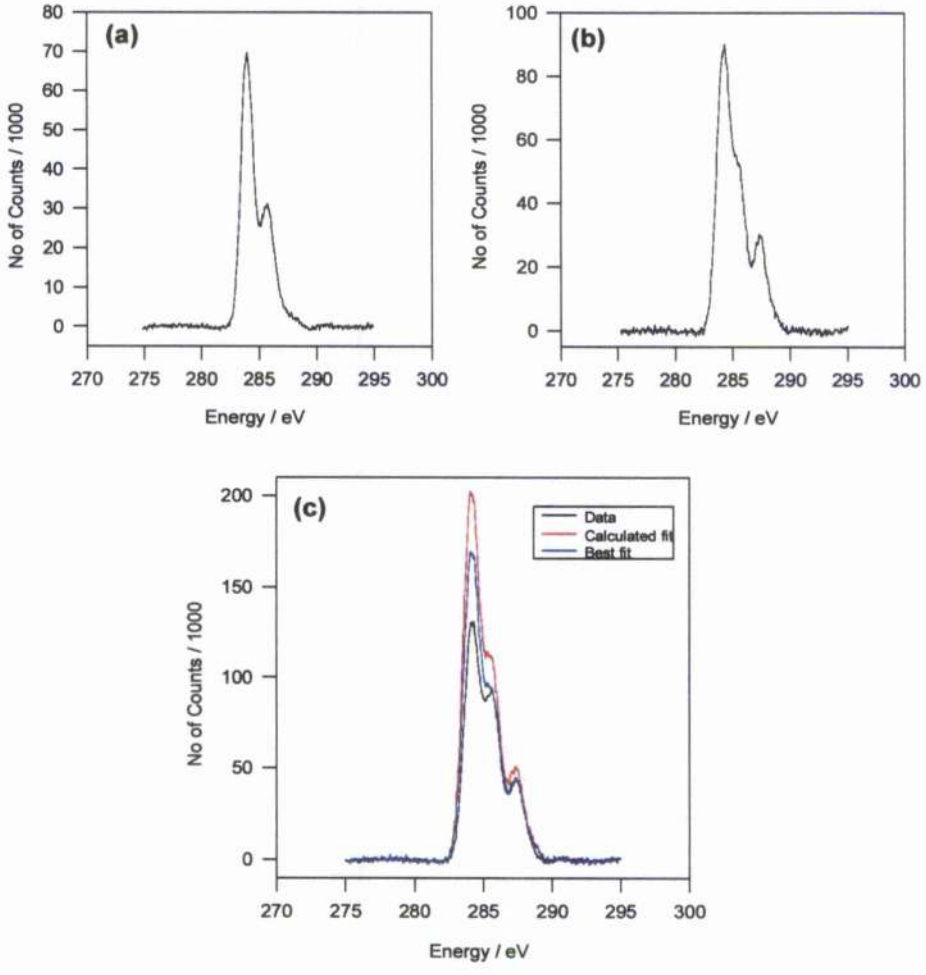

Figure 4.9 illustrates the fitting technique used to establish the percentage composition of the polymer-enzyme sensing layer. The plot in (a) shows the C(1s) reference spectrum for the sample prepared by 5 minute polymerisation from a solution containing only 10 mmol dm^{-3} p(fp), (b) shows the C(1s) reference spectrum for the sample prepared by 5 minute electrosorption of 10 mg ml^{-1} GOx at +700 mV *vs.* Ag|AgCl and (c) shows the C(1s) spectra obtained for the sample prepared by 5 minute copolymerisation from a solution containing 300 mmol dm^{-3} and 10 mg ml^{-1} GOx. The percentages of (a) and (b) were estimated by the ratio of fluorine in the sample to that in the reference sample and similarly for nitrogen and the fit shown in (c). Also shown in (c) is the 'best fit' obtained by manually varying the percentages of (a) and (b).

The plots in Figure 4.9 (c) emphasises that the 'best fit' to the sample data is best achieved by manually altering the fitting parameters rather than using the calculated percentages of polymer and enzyme. Percentage compositions were obtained at TOAs of both 10° and 90° for samples prepared using the three possible immobilisation methods and an enzyme solution concentration of 10 mg ml^{-1}. These are best represented in tabular form as in Table 4.3.

SAMPLE	% p(fp)	% GOx
10 mg ml^{-1}, PRE, TOA = 10°	92	8
10 mg ml^{-1}, CO, TOA = 10°	35	65
10 mg ml^{-1}, POST, TOA = 10°	50	50
10 mg ml^{-1}, PRE, TOA = 90°	66	34
10 mg ml^{-1}, CO, TOA = 90°	21	79
10 mg ml^{-1}, POST, TOA = 90°	51	49

Table 4.3 - The relative percentages of polymer and enzyme that are contained within each sample as obtained by manually fitting the reference polymer and enzyme C(1s) spectra to the sample C(1s) spectra.

The values shown in both Table 4.3 and Figure 4.10 (where values are shown only for an enzyme solution concentration of 10 mg ml^{-1}) indicate that the method of immobilisation which yields the greatest percentage of enzyme within the polymer-enzyme sensing layer is that involving the copolymerisation of 10 mg ml^{-1} GOx and 10 mmol dm^{-3} fluorophenol.

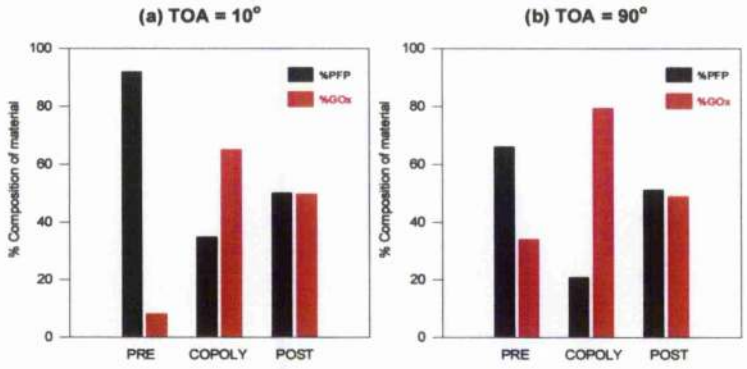

Figure 4.10 - The variation in percentage composition of samples prepared using different sensing layer preparation techniques as tabulated in Table 4.3. The three methods investigated were (a) preadsorption of GOx followed by electrodeposition of p(fp), (b) copolymerisation from a solution containing both enzyme and polymer and (c) electrodeposition of p(fp) followed by postadsorption of GOx. The results are shown for 1 cm^2 samples prepared as described in Section 4.1.2.1 for enzyme solution concentration of 10 mg ml^{-1}.

By initially examining the samples at a low TOA (10°) to place an emphasis on the analysis of the surface of the layer, the copolymerisation method results in the entrapment of 30% more enzyme than the next most successful method of postadsorption. When the TOA is changed to 90°, where more of the depth of the film is being examined, this percentage increase rises to 61%. The hypothesis that the preadsorption method produces a low GOx percentage due to insufficient XPS penetration depth at both angles is not supported by electrochemical experimentation in Section 4.2.1.1. Therefore, as was the case with the p(pd) polymer system, the immobilisation of enzymes was performed henceforth by copolymerisation from a solution containing both enzyme and p(fp).

4.2.2.3 - Effect of Variation of Electropolymerisation Time:

XPS was used to investigate the effect of varying the duration of copolymerisation on the polymer-enzyme sensing layer composition. The electrochemical results obtained from the same set of experiments, as shown in Section 4.2.1.2, showed that there was a poor correlation between electropolymerisation time and maximum current densities at saturated substrate concentrations, results which are corroborated by XPS analysis, Figure 4.11.

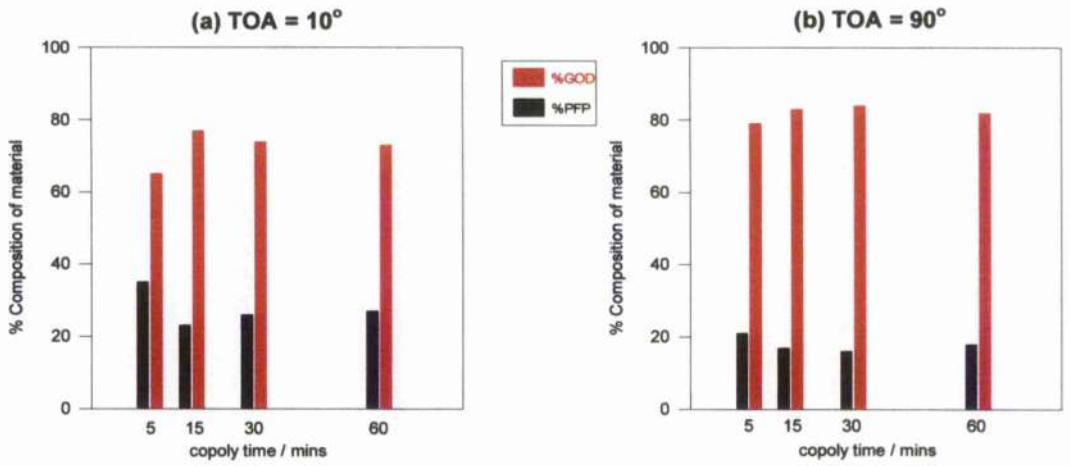

Figure 4.11 - The time independence property of the copolymerisation immobilisation process. The plots are taken for measurements made on the sample prepared by copolymerisation from a solution containing 10 mg ml^{-1} GOx and 10 mmol dm^{-3} p(fp) for 5, 15, 30 and 60 minute durations. The samples were measured at TOAs of both 10° and 90° as shown in (a) and (b) respectively. The variation in the GOx percentage composition of samples does not appear to rely on any particular length of polymerisation. Therefore, 5 minute preparations were subsequently used.

Indeed, examination of Figure 4.11 reveals that the peak heights in neither plot (a) nor (b) exhibit any particular trend to suggest an optimum duration for the polymerisation procedure. The percentage composition of GOx is maintained within the ranges 65 - 77 % for a TOA of 10° and 79 - 84 % when the angle is changed to 90°. Correspondingly, the polymer percentage composition varies only within the ranges 23 - 35 % and 16 - 21 % for the same angles. The values obtained when the TOA is at 90° show a higher percentage of enzyme within the film due to the entire depth of the sample being probed.

As a consequence, a 5 minute polymerisation duration was adopted for all subsequent assays, for the ease of preparation.

Further testing on the p(fp) sensors with extended polymerisation times should be performed in the future to establish if longer electrodepositions provide the advantage of increased elimination of electro-active interferents that was shown to be the case for the p(pd) sensors described in Chapter 2.

4.2.2.3 - Effect of Variation of Enzyme Solution Concentration:

The most significant parameter of the polymer-enzyme preparation procedure to be examined is that of variation in the concentration of enzyme contained within the polymerisation solution and the subsequent effect this has on the sensor response. In this work four concentrations of enzyme were investigated i.e. 10.00, 1.00, 0.10 & 0.01 mg ml^{-1} and the percentage of each contained in the sample after preparation was estimated by spectral decomposition of data obtained using XPS.

In the analysis of these data sets the fluorine on the p(fp) chain acts as a marker for the polymer, allowing the measured F(1s) spectra to represent the amount of polymer contained within the sample. In contrast with the analyses of the p(pd) samples, the polymer contains no nitrogen, and thus the N(1s) spectra collected from the sample is representative of the enzyme content of the sample. As the enzyme concentration of the polymerisation solution is reduced, if the concentration of enzyme in the film also decreases then there should be a decrease in the peak height of the N(1s) spectra and a corresponding increase in the peak height of the F(1s) spectra. This was found to be the case and is shown in Figure 4.12. Also illustrated in Figure 4.12 is the C(1s) sample spectra showing a decrease in the peak height at ~ 287 eV which corresponds to a decreasing enzyme concentration. The plots in this figure show only the spectra obtained at a TOA of 90° but a similar picture was observed at a shallower TOA of 10°.

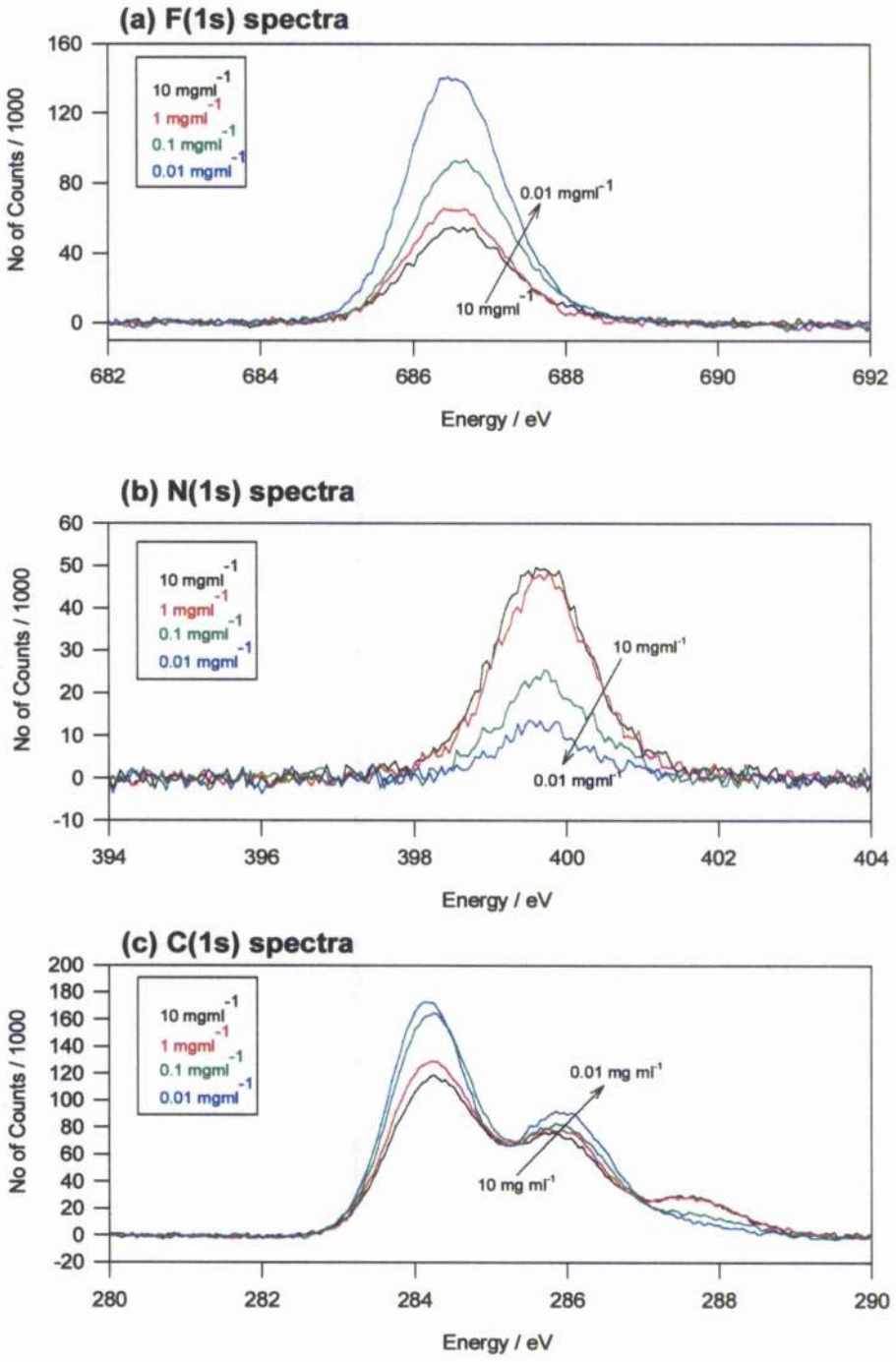

Figure 4.12 - The (a) F(1s), (b) N(1s) and (c) C(1s) XPS spectra, measured at a TOA = 90°, of the samples prepared as Au/p(fp)(10 mmol dm^{-3})/GOx where the GOx solution concentration was varied between 10 and 0.01 mg ml^{-1} (as described in Section 4.1.2.1). As the GOx concentration is decreased the peak heights in (a) and (b) increase and decrease respectively, indicating a rise in the polymer content of the film and a drop in the enzyme content. The plot in (c) shows the peak at ~ 287 eV, corresponding to the enzyme, decreases with decreasing GOx concentration.

The results presented in Figure 4.12 provide qualitative information confirming an increase in the amount of GOx immobilised within the polymer-enzyme layer as the GOx concentration in the polymerisation solution is increased. However, it is advantageous to have a measure of the true amount of GOx (and p(fp)) within the film of each sample. Quantification of the polymer-enzyme interface for each sample was, therefore, performed by fitting the C(1s) GOx and p(fp) reference spectra to that of the experimental data. The fitting procedure was identical to that explained earlier in this chapter where initial estimates for the percentage of both GOx and p(fp) contained within the sample were extracted from the N(1s) and F(1s) ratios and then altered until a 'best fit' was obtained. The spectra were fitted for data collected at TOAs of 10° and 90°. The 'best fit' percentages of polymer and enzyme are shown in Figure 4.13.

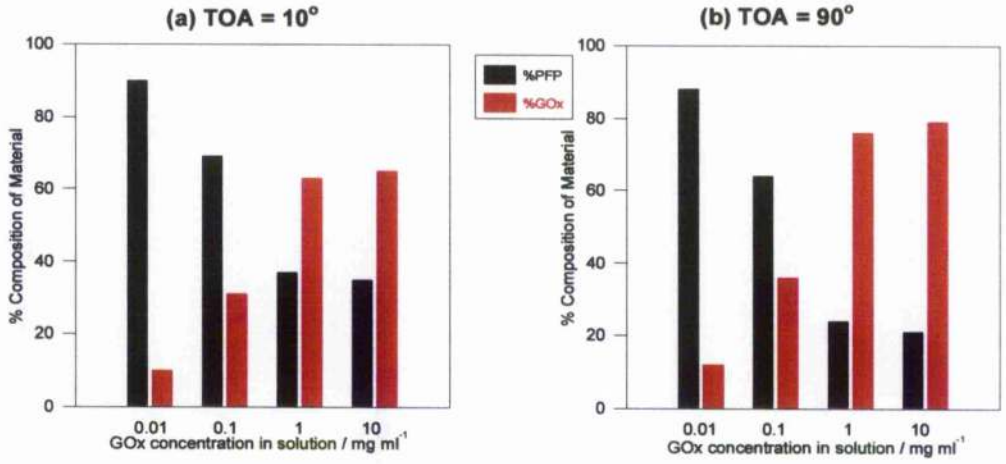

Figure 4.13 - The effect that varying the concentration of GOx in solution has on the percentage composition of the samples. The values are collected for samples prepared as described in section 4.1.2.1 and at TOAs of (a) 10° and (b) 90° using GOx solution concentrations of 10, 1, 0.1 and 0.01 mg ml^{-1} for each angle. In both (a) and (b) it is clear to see that the percentage of enzyme contained within the sample increases as the GOx solution concentration is increased. Correspondingly the polymer content of the films is reduced with increasing enzyme solution concentration.

By examining the plots in Figure 4.13 it is clear that there is an obvious trend in the percentage composition of the polymer-enzyme layer. The values obtained from Figure 4.13 show that at a TOA of 10° there is a 55% increase in the amount of GOx contained within the polymer-enzyme at 10.00 mg ml^{-1} when compared to that at 0.01 mg ml^{-1}. This is supported by a similar decrease in the amount of polymer in

the film. The value of this percentage increase rises to 67% when the TOA is 90°, indicating that the surface composition (at 10° TOA) is not the same as that in the bulk of the polymer (at 90° TOA).

The advantage of using the p(fp) polymer becomes more apparent at this stage of the polymer-enzyme film analysis. The presence of the fluorine in the polymer enables estimates to be made for the percentage composition of the polymer and, hence, GOx in the samples. This provides a method for obtaining a value for e_Σ within Equation (1.11).

Using the assumption that the coverage of GOx on the electrode surface is one enzyme layer thick and equivalent to 1.3 x 10^{-11} mol cm^{-2}[95] and assuming the polymer-enzyme layers are sufficiently thin that this single enzyme layer assumption is realistic, the GOx percentages obtained from XPS analysis can be used to estimate e_Σ, as shown in Table 4.3 for the different enzyme solution concentrations investigated.

$[GOx]_{solution}$ / mg ml^{-1}	XPS Best Fit GOx %	e_Σ / mol cm^{-2}
10	79	1.03 x 10^{-11}
1	76	0.99 x 10^{-11}
0.1	36	0.47 x 10^{-11}
0.01	12	0.16 x 10^{-11}

Table 4.3 - Estimates of the amount of GOx immobilised within the polymer-enzyme films as predicted by the percentage composition of GOx obtained by XPS analysis. The samples were prepared as described in section 4.1.2.1 using GOx solution concentrations of 10, 1, 0.1 and 0.01 mg ml^{-1} and examined at a TOA of 90°. These values are based upon the assumption that a single enzyme layer coverage of GOx on the bare electrode surface is equivalent to 1.3 x 10^{-11} mol cm^{-2}.

The values in Table 4.3 display the trend that the GOx surface concentration decreases with decreasing GOx solution concentration when measured at a TOA of 90°. The values of GOx surface concentration can then be used with the XPS results

to predict the distribution of enzyme within the sensing layer film. Figure 4.14 shows the plot of the ratio of polymer to enzyme i.e. N(1s):F(1s) against surface GOx concentration for samples measured at TOAs of 10° and 90°.

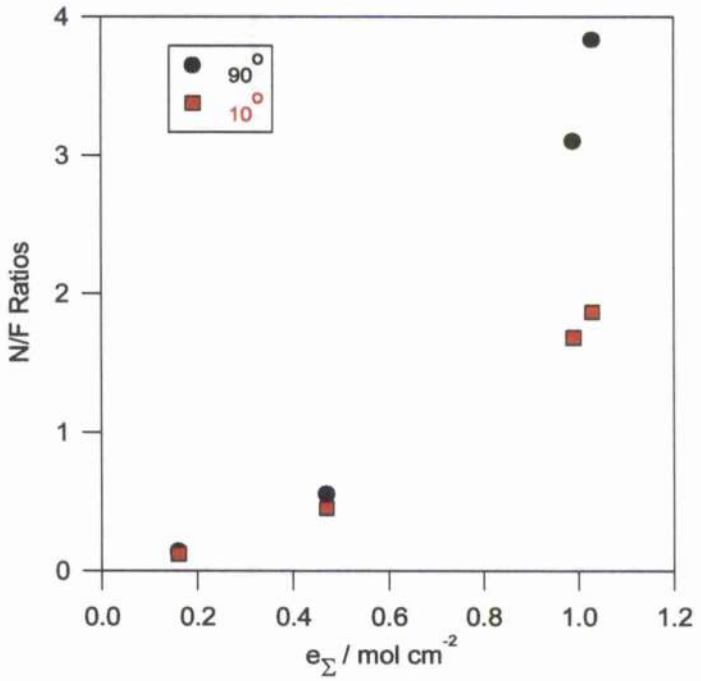

Figure 4.14 - The plot of the ratio of enzyme to polymer content in the films against the concentration of GOx retained at the electrode surface for TOAs of both 10° and 90°. Samples were prepared as described in section 4.1.2.1 for GOx solution concentrations of 10.00, 1.00 0.10 and 0.01 mg ml^{-1} and the surface concentrations were determined by using the XPS resulting percentage compositions and assuming a monolayer coverage of 1.3 x 10^{-11} mol cm^{-3}. Note that the plot at TOA = 90° is greater than that at TOA = 10° providing information on the construction of the polymer-enzyme layer.

The data in Figure 4.14 illustrates that at a TOA of 90° the N(1s):F(1s) ratio is greater than that at a TOA of 10° suggesting that by examining the samples at a steep angle there is more enzyme than polymer detected. Similarly, shallow angle analysis yields a ratio which implies a greater amount of polymer than enzyme in the film. This becomes more apparent as the concentration of enzyme within the film, e_Σ, increases. These results suggest that the enzyme is entrapped within in the film as described in Figure 1.15 where the enzyme is 'buried' within the polymer film. This effect is most obvious at high surface GOx concentrations which would substantiate the hypothesis that there is an outer covering of polymer over the top of the enzyme

(at 10° and a high surface loading of enzyme, the same outer layer of polymer is measured whilst at 90° the enzyme contained throughout the entire penetration depth of the film is measured).

Additional information on the micro-environment of the sensing layer can be extracted from the data by looking at the method of enzyme adsorption within the polymer.[138, 140]. By plotting the ratio of GOx concentration in solution to that at the electrode surface against the GOx concentration in solution, it is possible to diagnose whether GOx is entrapped within the p(fp) film as a Langmuir adsorption isotherm, see Figure 4.15.

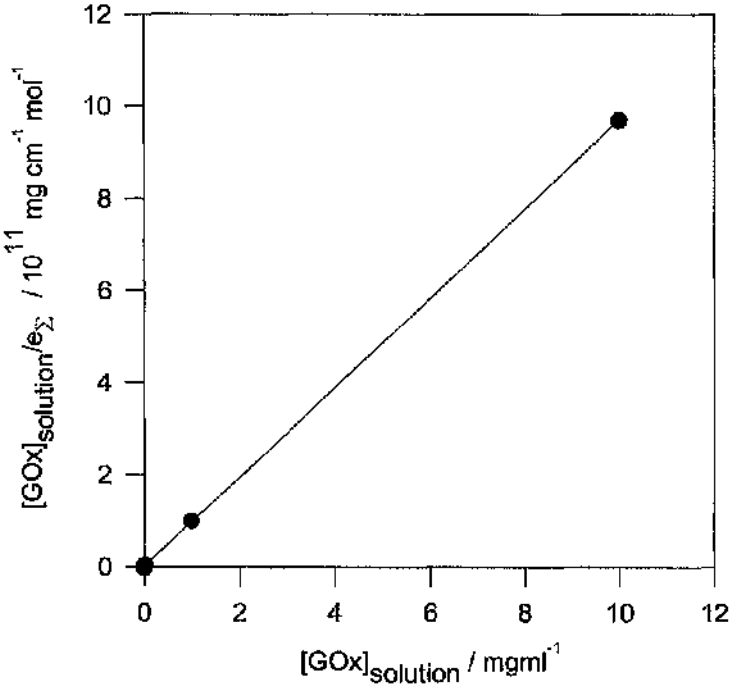

Figure 4.15 - Plot showing that by immobilising the GOx in the p(fp) film using the method of 5 minute copolymerisation from a solution containing 10 mmol dm^{-3} p(fp) and a range of either 10, 1, 0,1 or 0.01 mg ml^{-1} GOx the enzyme is adsorbed within the film as a Langmuir adsorption isotherm.

The concept of the adsorption isotherms is one which relates the amount of substance adsorbed per unit area to the concentration of adsorbate in the bulk solution and the free energy of adsorption. There are many isotherms (e.g. Frumkin, Gibbs and Temkin)[140] the difference between which can be attributed to their method and

extent of taking into account lateral interactions between adjacent adsorbed species. The Langmuir isotherm assumes that the adsorption process is reversible and that there are no lateral interactions and, hence, the energy of adsorption is not a function of surface coverage. However, although enzyme adsorption on surfaces cannot be regarded as an irreversible process and it is unlikely that there will not be any interactions between adjacent enzyme molecules, the Langmuir isotherm can still provide a more reliable model for the method of adsorption than the other possible isotherms. (Examples of other systems where Langmuir isotherms have been used as a good approximation for adsorption can be found in the literature.)[190, 191] The linearity of the plot in Figure 4.15, measured using a regression coefficient (r^2 = 0.99), illustrates that irrespective of the concentration of GOx in the polymerisation solution, there is an equal likelihood of any molecule of GOx being adsorbed into the polymer film. Similarly, because of the assumptions made for Langmuir isotherms, this holds true for the desorption of GOx from the polymer-enzyme layer.

Using this information it is possible to display the electrochemical results, as shown in Figure 4.6 (b), which were obtained by fitting the experimental data to the algorithm in Equation 1.11, as a function of the enzyme surface concentration and, hence, enable the further elucidation of the kinetic parameters. The plot in Figure 4.16 shows the responses of the samples prepared with different enzyme surface concentrations to a concentration of glucose in the saturated region i.e. 100 mmol dm^{-3} glucose.

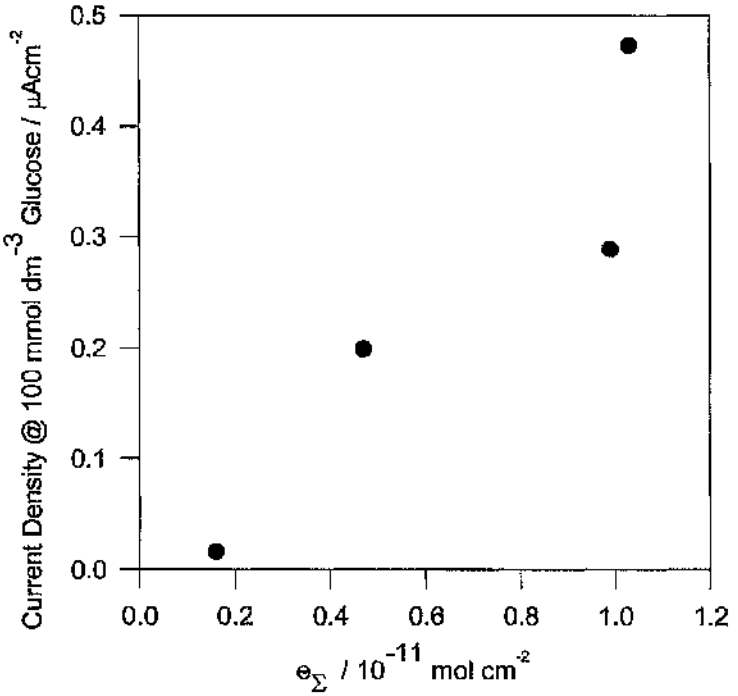

Figure 4.16 - Plot illustrating the trend in electrode response to 100 mmol dm^{-3} glucose as the concentration of GOx entrapped within the polymer-enzyme layer is increased in the range 0 - 1 mol cm^{-3}. This enzyme surface concentration range is equivalent to an enzyme polymerisation solution concentration range of 0 - 10 mmol dm^{-3} assuming that a one-enzyme layer thick coverage of GOx is equivalent to 1.3 x 10^{-11} mol cm^{-3}. The samples examined were prepared as described in section 4.1.2.1 and electrochemical measurements were collected at a potential of + 700 mV *vs.* Ag|AgCl in response to glucose aliquots in the range 0 - 100 mmol dm^{-3}.

It is obvious from the trend in Figure 4.16 that, as the concentration of GOx in the polymerisation solution and, therefore, the concentration of GOx entrapped by the p(fp) at the electrode surface, is increased, there is an increase in the current response of the sensors. Therefore, the elementary factor in obtaining higher sensor response is to increase the concentration of enzyme within the electropolymerisation solution during sensor preparation.

As described previously, the fitting equation, Equation (1.11), provides a kinetic description of the sensors using a more complex algorithm than that of the Michaelis-Menten and incorporates a wide range of kinetic parameters, the measurement of some of which is outwith the scope of this work. However, having obtained an estimate of the surface concentration of enzyme, e_Σ, from the

experimental results, the final piece of analysis performed in this section is to elucidate the relationship between the remaining parameters of Equation (1.11) and the surface enzyme concentration.

Ideally, the sensor response should be modelled using known values for each term in the algorithm but by plotting the parameters m and c, as shown in Equations 4.2 (a) and (b), (See Introduction, Section 1.1.7) as a function of the sample surface enzyme concentration, the simplistic assumption can be made of the existence of a linear relationship as described by the equation of a straight line.

$$m = \frac{K_m}{\alpha K_s k_{cat} e_\Sigma l} \qquad c = \frac{1 + {k_{cat}}/{kK_A a_\infty}}{\alpha k_{cat} e_\Sigma l} \qquad \textbf{Equation 4.2 (a) \& (b)}$$

The plots showing such a relationship are shown in Figure 4.17.

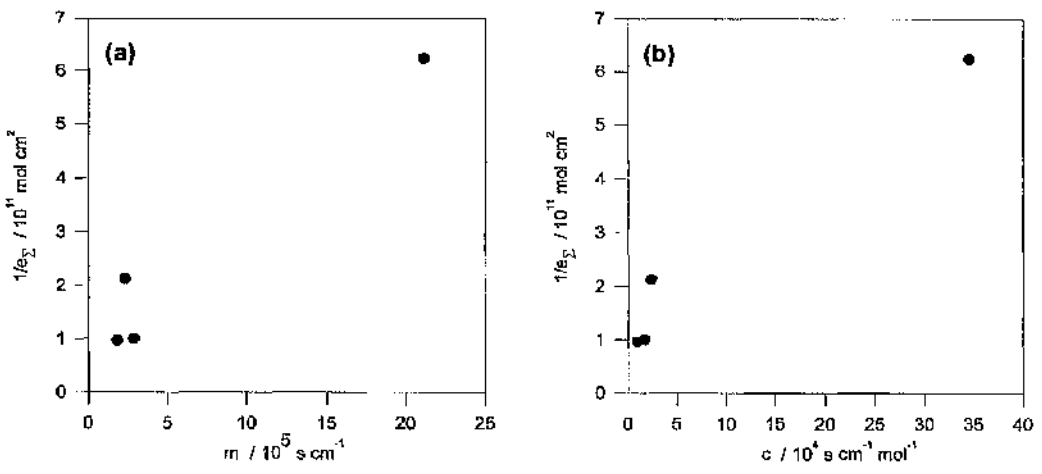

Figure 4.17 - Plots showing the relationship between the kinetic parameters (a) m and (b) c with enzyme surface concentration as described by linear analysis of Equation 4.2 (a) & (b).

The plots are clearly not linear and can be used only to suggest a trend for the variation in enzyme surface concentration with varying terms m and c. More data points are required before any further information can be extracted. They may also be used in this context to provide estimates for the remaining terms of the fit

equation, namely K_m, K_s, k_{cat}, k, K_A and a_∞ which as yet are unable to be measured for this type of experiment because the physical properties of the polymer are not yet known.

4.2.3 FT-iR Analysis

The electrochemical and XPS analyses of the samples under examination in this chapter were augmented with results obtained by FT-iR investigation. There is, however, little advantage of using the p(fp) polymer for this technique because of the difficulty in assigning fluorine signals on the FT-iR spectra. The information from FT-iR analysis is collected as transmission data and the reference spectra for the GOx and p(fp) are shown in Figure 4.18. These can be used to identify the specific peak profiles attributable entirely to polymer or enzyme.

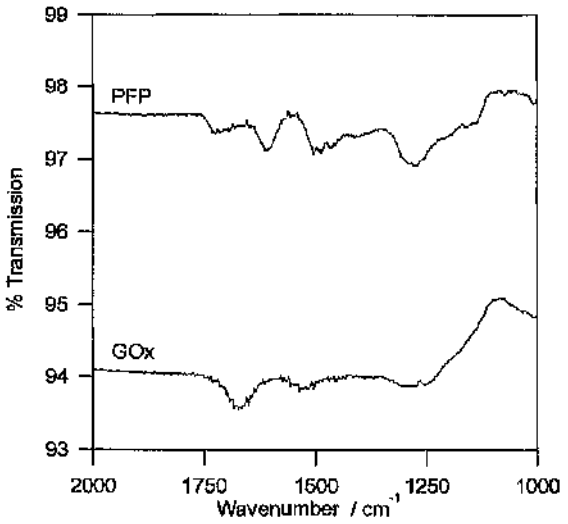

Figure 4.18 - The raw transmission data as obtained from the FT-iR analysis of the reference GOx sample prepared by 30 minute electrosorption of 10 mg ml^{-1} GOx and the reference p(fp) sample prepared by 5 minute polymerisation from a solution containing 10 mmol dm^{-3} fluorophenol monomer. Both spectra show individual peaks corresponding to the functional groups of their structure.

By looking at the reference spectra individually, the main peaks of interest on the GOx spectra are, as described in Chapter 3, those corresponding to the amide groups

on the enzyme. As before, the amide I and II peaks can be used to identify the presence of enzyme in the samples.

When considering the spectra of the p(fp) reference sample (and that of the fluorophenol monomer, not shown here[168]) there are a variety of distinct peaks which can be attributed to different bonds within the polymer structure. The peaks at 1600 cm^{-1} are characteristic of the C-H and C=C stretching vibrations, whilst the peaks between 1400 and 1500 cm^{-1} can be attributed to the ring breathing modes of the benzene-like ring within the phenol. The peak at approximately 1300 cm^{-1} arises from the phenyl ether (C-O-C) bond stretching between the monomers.

Additionally, there are numerous peaks below 1100 cm^{-1} which can be attributed to the C-F stretching vibrations of the p(fp) chain which, theoretically, are able to provide information on the content of polymer within the samples. However, at such low wavenumbers, the transmission data values will incur large errors, due to the background subtraction function of the spectrometer (errors are exaggerated greatly by the differential between the collected sample spectrum and the background). As a consequence of the uncertainty in the low wavenumber data, the sample spectra cannot be compared reliably using the peaks below 1100 cm^{-1}.

For the purpose of the analysis in this chapter the data of quantitative interest was confined to the region containing the most analytically significant peaks, seen in both reference spectra i.e. 1550 - 1750 cm^{-1}.

The samples investigated with the FT-iR technique looked at the factors of the preparation process previously examined with both electrochemical assays and XPS. For example, the three enzyme immobilisation methods were tested together with variation in the duration of polymerisation and the concentration of enzyme contained within the polymerisation solution.

4.2.3.1 - Effect of Variation of Method of Enzyme Immobilisation:

Initially samples were prepared, as described in Section 4.1.2.1, using the three techniques. Data were collected over the range 1000 - 2000 cm^{-1} from samples prepared using each of these methods and with a GOx solution concentration of 10 mg ml^{-1}. The resulting spectra were restricted to the region of interest and plotted in Figure 4.19.

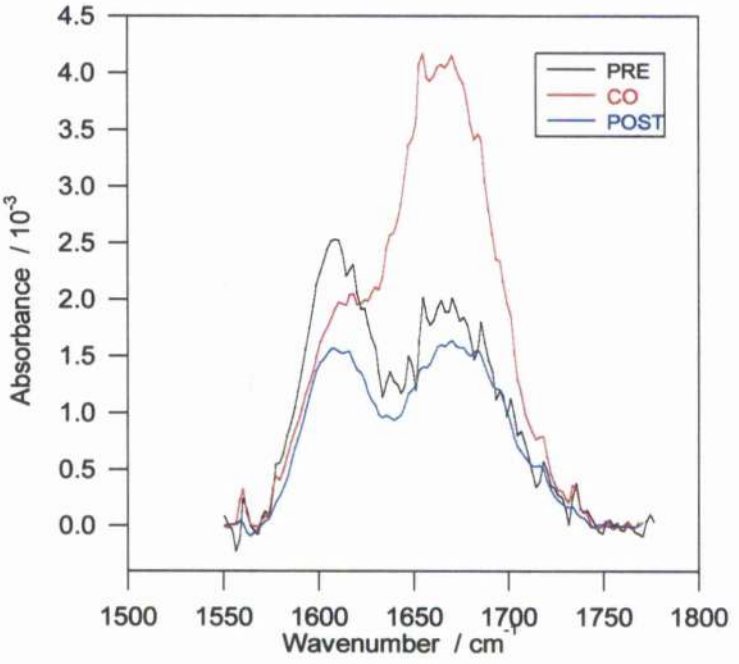

Figure 4.19 - The effect of variation of method of enzyme immobilisation using FT-iR spectral analysis. The samples were prepared as described in Section 4.1.2.1 using the three techniques: (a) preadsorption of GOx followed by electrodeposition of p(fp), (b) copolymerisation from a solution containing both GOx and p(fp) monomer and (c) postadsorption of GOx onto an electro-deposited layer of p(fp). The range shown highlights the vibrations of the amide I band of the enzyme and the C-C & C-H stretching vibrations of the p(fp).

By inspection of the three traces in Figure 4.19 it is clear that the immobilisation technique which corresponds to the largest amide I peak height and, therefore, the greatest amount of GOx within the sample is that of copolymerisation. Similarly, although the postadsorption and preadsorption techniques yield similar amounts of GOx, the technique which produces the largest C-H/C-C peak height is that of preadsorption. This might suggest that the by having the enzyme on the surface of the electrode the polymer has a larger surface area over which to grow. These

results corroborate those obtained from both electrochemical assays and XPS and indicate the optimum method of immobilisation for future biosensing interfaces.

4.2.3.2 - Effect of Variation of Length of Polymerisation Time:

In order to examine the importance of the length of polymerisation time, samples were prepared by copolymerisation from a solution containing both GOx and fluorophenol monomer for periods of 5, 15, 30 and 60 minutes and the effect of this on the sensor composition measured by FT-iR spectral analysis. This variation is illustrated with the spectra shown in Figure 4.20.

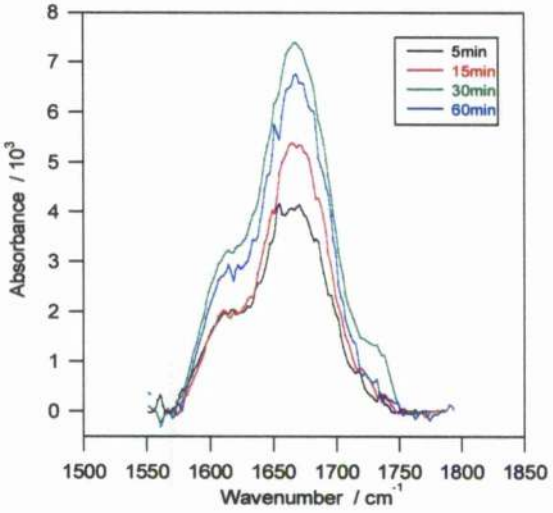

Figure 4.20 - The effect of variation in electropolymerisation duration as observed from the FT-iR spectra over the range 1550 - 1750 cm^{-1}. The samples were prepared by copolymerisation (see section 4.1.2.1) for periods of 5, 15, 30 and 60 minutes cycling. The amide I peak and the C-C/C-H peak from the GOx and p(fp) correspondingly are subject to change due to this variation.

By looking at the amide I peaks for the plots in Figure 4.20 it can be noticed that a short polymerisation time does not produce as much GOx within the polymer-enzyme layer as does a longer polymerisation. Also, as the polymerisation duration is increased the amount of polymer, as indicated by the peaks at ~ 1630 cm^{-1}, increases accordingly. This suggests that extended polymerisation should give a more favourable method for sensor preparation. However, this increased time also deposits a greater total amount of polymeric material on the surface. Thus, a scaling

factor of 1.6 can be calculated from the ratio of both peaks at 5 minutes and 60 minutes indicating that in fact there appears to be no advantage of increased GOx concentration within the film with increased polymerisation time.

4.2.3.3 - Effect of Variation of Enzyme Solution Concentration:

The final parameter of the polymer-enzyme layer preparation procedure examined using FT-iR was the change in composition of the layer due to variation in the concentration of GOx in the polymerisation solution. Samples were prepared (as described in Section 4.1.2.1) from solutions containing 0.01, 0.10, 1.00 and 10.00 mg ml^{-1} GOx and FT-iR spectra collected over the range 1000 - 2000 cm^{-1}. For the reasons stated earlier the range of interest was restricted to 1550 - 1750 cm^{-1} and the amount of enzyme and polymer contained within the film was qualitatively measured from the change in peak heights. The spectra collected are plotted in Figure 4.21.

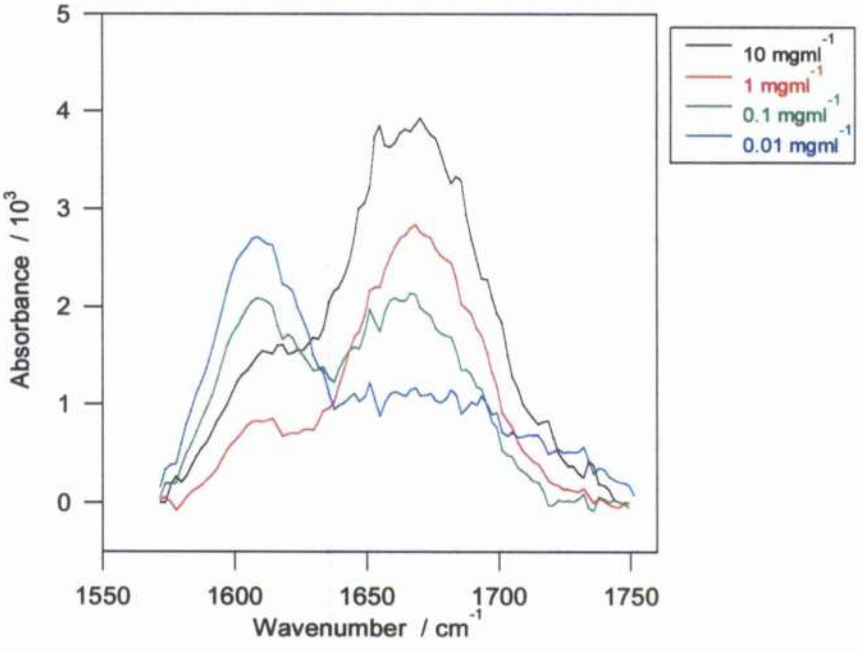

Figure 4.21 - The variation in peak heights for samples prepared (as described in Section 4.2) using polymerisation GOx solution concentrations of 0.01, 0.1, 1 & 10 mg ml^{-1}. The FT-iR spectra collected show that as the GOx solution concentration is increased the peak due to the stretching vibrations of amide I increases while the C-C/C-H peak, indicative of the p(fp), decreases correspondingly.

As the concentration of GOx in the polymerisation solution is increased it is presumed that the concentration immobilised within the polymer film will also increase accordingly. The amide I peaks on the plots in Figure 4.21 suggest that the samples follow this trend. Similarly, as the concentration of enzyme in the sample increases, to maintain a constant sensing layer volume, there should be a decrease in the amount of p(fp) observed on the sample surface. The peaks corresponding to the C-C/C-H stretching vibrations of the p(fp) show such a decrease with increasing amide I peak heights. It is, however, unfortunate that in this sequence of peaks the 10 mg ml^{-1} value is greater than that for the 1 mg ml^{-1} sample. This may be due to any number of reasons relating to, for example, experimental error or uneven film growth.

It is possible to extract quantitative information concerning the polymer-enzyme layer composition by using the reference p(fp) and GOx spectra to fit the data to that of the sample spectra. This fitting procedure is an unrefined method, identical to that used for the XPS fitting in the previous chapter. By manually altering the percentage components of the p(fp) and GOx reference spectra to obtain a 'best-fit' to the sample spectra, it is possible to obtain a measure of the amount of material within the sensing layer. The plot in Figure 4.22 (a) shows the reference p(fp) spectra, (b) shows the GOx reference spectra and (c) shows the sample spectra for a GOx solution concentration of 10 mg ml^{-1}.

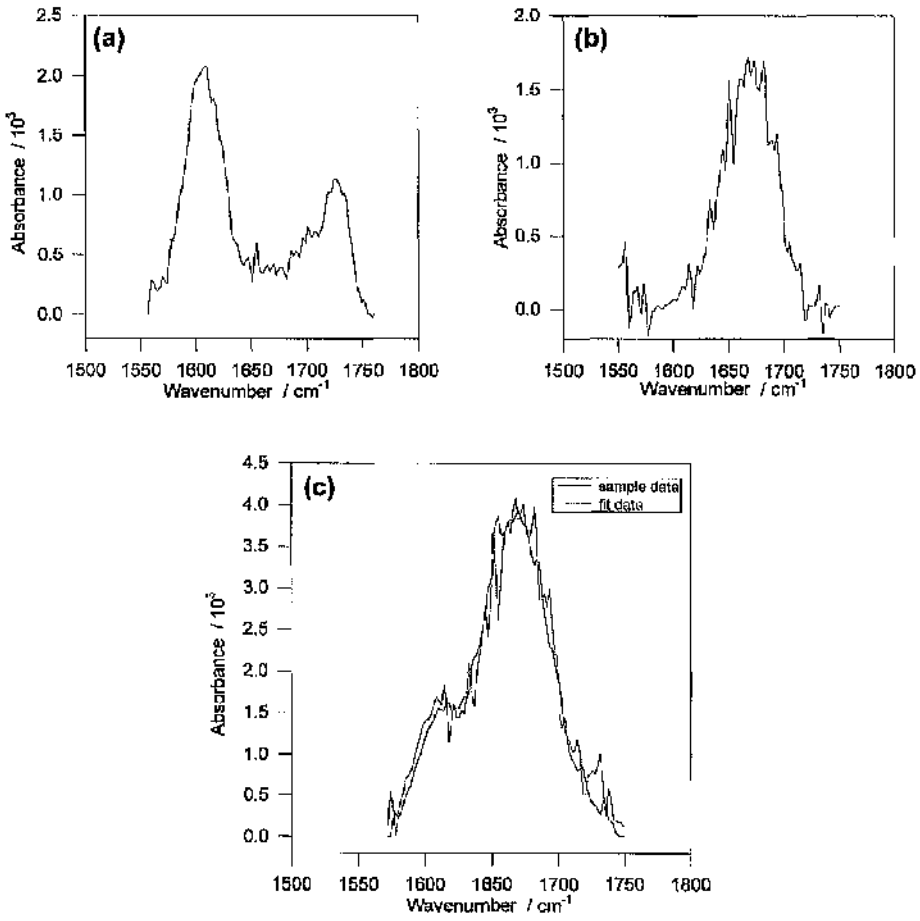

Figure 4.22 - The data fitting procedure for the FT-iR spectra obtained for samples prepared (see section 4.1.2.1) by copolymerisation from solutions containing varying concentrations of GOx. The percentages of p(fp) reference spectrum (a) and GOx reference spectrum (b) are altered in order to obtain a best fit curve to the sample data (c).

The fitting procedure was performed for the samples prepared from different GOx solution concentrations and the values obtained used to indicate the relative amount of material on the sensor surface. As in previous sections, the percentage composition of each sample is displayed using a bar chart in Figure 4.23 (a) and diagrammatically in Figure 4.23 (b).

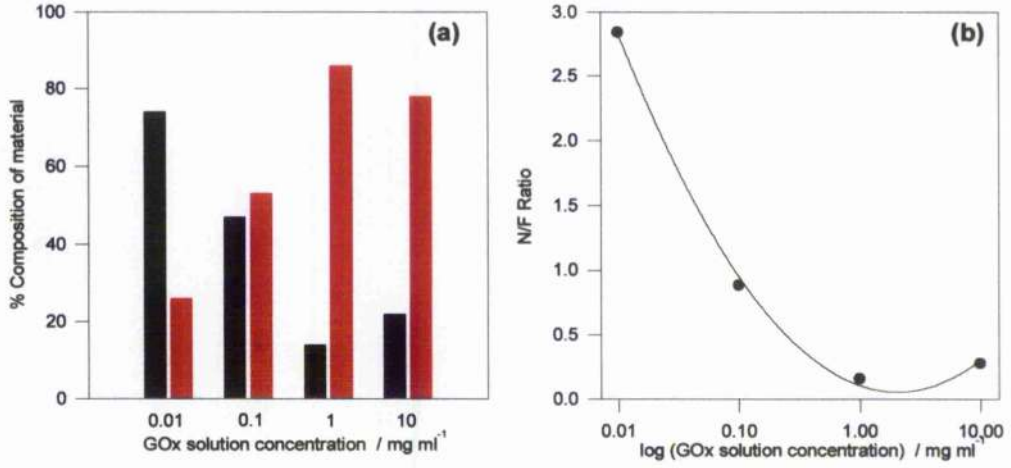

Figure 4.23 --The percentage composition of the polymer-enzyme layer as deduced from the best-fit curves to the sample FT-iR spectra for samples prepared from varying GOx solution concentrations. The plot in (a) shows the percentage values of p(fp) and GOx for each sample while (b) shows the data as ratios of enzyme to polymer, and fitted using a second order regression function with $r^2 = 0.998$.

The values from Figure 4.23 (a) and (b) show there is at least a 50% increase in the percentage of GOx contained within the film when the solution enzyme concentration is increased from low to high values. As is expected, there is a simultaneous decrease of approximately 50% in the percentage of p(fp) within the film. However, the values indicate that there is more enzyme in the film when the solution concentration is 1 mg ml^{-1} than when it is 10 mg ml^{-1}. Although this has not been the case for the other analytical techniques used for this polymer-enzyme combination and, therefore, may be due to experimental error of the FT-iR technique, it does agree with the electrochemical data obtained for the p(pd) sensors in Chapter 2. When considering only the data in this chapter, however, the same trend is followed as predicted from the alternative techniques and so can be quoted reliably.

The absence of error bars on the experimental data, which may show if this is an artefact or not, was as a result of both long data collection times for some of the techniques (XPS) and the difficulties in producing identical samples. Great care had to be taken in producing standardised protocols for sensor preparation, for example,

polymer growth conditions, in order to minimise any errors due to preparation method.

4.3 Summary

The results presented in this chapter have been collected using a variety of different analytical techniques, each of which has the ability to analyse a different aspect of the polymer-enzyme sensing layer. The preparation conditions of the polymer-enzyme film were altered by varying the method and duration of enzyme immobilisation and the concentration of enzyme within the polymerisation solution and the effect of such alterations was monitored using three different analytical tools. Initially electrochemical assays were performed which provided information on the sensor response as a function of the polymerisation parameters. Analysis was subsequently performed using the spectroscopic techniques of XPS and FT-iR where the surface and bulk composition of the samples were examined for the amount of polymer and enzyme entrapped within the sensing layer.

The samples which generated the best sensor response were those prepared by copolymerisation from a solution containing both enzyme and monomer. This response was maximised by increasing the concentration of enzyme contained in the polymerisation solution which effectively increases the amount of enzyme retained within the film. There appeared to be no obvious trend in the effect of increased polymerisation time.

In detail, using XPS analysis there was found to be a greater amount of GOx contained within the polymer-enzyme layer when the samples were prepared by copolymerisation from a solution containing the largest concentration of enzyme. Similarly, as the amount of GOx increased the corresponding amount of p(fp) in the sensing layer decreased accordingly. Data was collected at TOAs of 10° and 90° and the results suggest that since there is a smaller ratio of enzyme to polymer at a shallow angle i.e. when the surface of the sample is analysed, the film forms with the enzyme 'buried within' the polymer film. This case appears to be contrary to the situation described in Chapters 2 and 3 with sensors prepared using

polyphenylenediamine where the ratios suggest that the enzyme 'stands proud' of the polymer. This may be due to any of many possible factors but the most conceivable hypothesis could be that the individual polymers have different states of hydration when placed in solution which may cause one to swell more than the other, allowing the enzyme to protrude rather than be encased.

The presence of the fluorine in the polymer structure allowed kinetic analysis of the system to be performed. Using the assumption of monolayer coverage of enzyme, the enzyme surface concentration was able to be calculated which subsequently allowed the conclusion that the enzyme is entrapped within the film as a Langmuir isotherm. Also, the kinetics of the sensor were able to be elucidated from Equation (1.11) and their dependence on enzyme surface concentration illustrated.

The final technique applied to the sensors was that of FT-iR. The results obtained from this set of experiments illustrated also that copolymerisation from a solution containing monomer and a maximum amount of enzyme yielded the highest proportions of GOx and p(fp) within the samples. As this technique samples the entire volume of the sensor it also highlighted that the amount of material on the surface of the electrode is subject to variation in the preparation procedure. This was illustrated best by the experiments where the polymerisation time was increased. Although there appeared to be an increase in the amount of enzyme and polymer in the film as the duration was increased, the ratio of polymer to enzyme remained constant irrespective of the length of time polymerised. Therefore, there is no advantage to be achieved by polymerising for longer periods of time.

In summary of the results contained in this chapter, using the three complimentary techniques it has been possible to determine the following information on the polymer-enzyme film:

- the concentration of enzyme (*eS*) within the polymer entrapment matrix
- the micro-environment of *eS* within the film
- the mechanism of enzyme entrapment
- the dependence of kinetic parameters on *eS*.

CHAPTER 5 - OSMIUM BASED GLUTAMATE SENSORS

This chapter describes the development of a glutamate microsensor employing the technique of enzyme wiring within osmium based polymers.[94, 116] Initially, assays were performed on macroelectrodes due to the ease of polymer deposition and electrode characterisation. The initial aim of this work involved wiring the enzyme directly to a glassy carbon electrode surface using a polymer of poly(vinylpyridine)-containing Os(dimethylbipyridine)$_2$Cl$_2$, known as POs-EA. The development of this system hereafter led to the development of a bienzyme electrode prepared by the co-immobilisation of GLOx with soybean peroxidase (SBP) in the same redox-hypoxy network of POs-EA, as described in Section 1.1.6 and Figure 1.10 of Chapter 1. As described in Chapter 1, the advantage of the bienzyme system is that a cathodic current (as opposed to anodic current for the single enzyme system) is measured as the Os^{III} is reduced to Os^{II}, thus allowing the electrode potential to be maintained at values where electro-active interference need not be a problem. This sensor was further developed for use on microelectrodes and their ability to block interfering substances investigated.

5.1 Experimental

5.1.1 Materials:

Poly(ethylene glycol) diglycidyl ether (Polysciences, PEGDGE 400, catalog No 08210), ascorbic acid (Aldrich Cat # 25,556-4), glutamic acid (Cat # G-1626), glucose (Cat # G-7528), uric acid (Cat # U-2625) and cellulose acetate, prepared in hexaquinone, (Cat # C-3782) were purchased from Sigma. Soybean peroxidase, SBP, was purchased from Enzymol International Inc. (HP grade, 130 pyrogallol

Units mg^{-1}). Glutamate oxidase, GLOx, (EC 1.4.3.11., from *Streptomyces* species, 30 Units mg^{-1}) was a gift from Yamasa Shoyu (Chiba, Japan). Glucose oxidase, GOx, (EC 1.1.3.4., from *Aspergillus niger*, 245 Units mg^{-1}) was a gift from MediSense (Birmingham, U.K.). The redox polymer, poly(vinylpyridine)-containing Os(dimethylbipyridine)$_2$Cl$_2$ (POs-EA) was prepared as reported.[91, 122] All other chemicals were purchased from Sigma.

The structures of both the POs-EA polymer and the PEGDGE 400 crosslinker are shown in Figure 5.1.

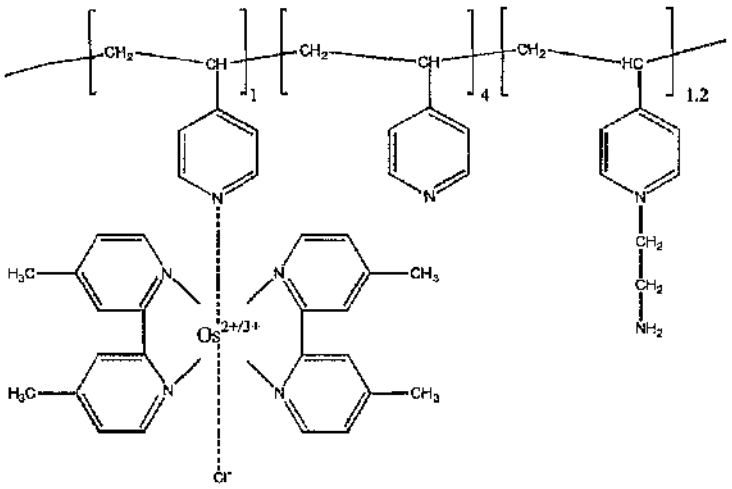

(a) Poly(vinyl pyridine) containing Os(dimethyl bipyridine)$_2$Cl$_2$

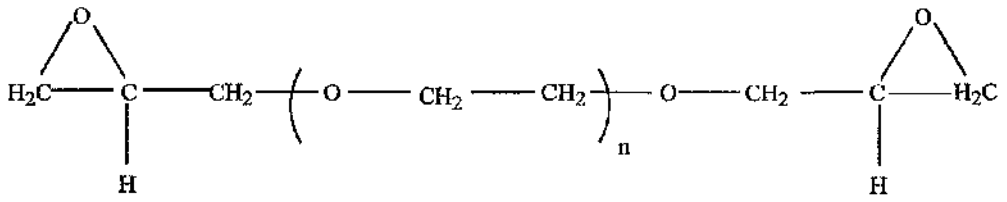

(b) Poly(ethylene glycol) diclycidly ether (PEGDGE 400)

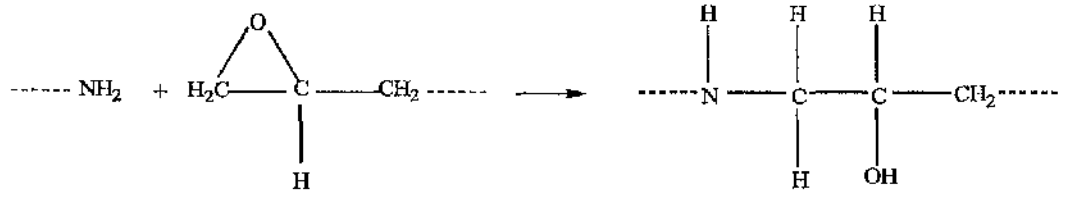

(c) Reaction between the amine group of either the polymer or enzyme and the epoxy group of the PEGDGE 400

Figure 5.1 - (a) The chemical structure of the osmium-containing redox polymer backbone, Poly(vinyl pyridine) containing Os(dimethyl bipyridine)$_2$Cl$_2$, (b) The chemical structure of the di-epoxide crosslinking agent Poly(ethylene glycol) diclycidly ether (PEGDGE 400) and (c) The general reaction scheme of an epoxide with an amine.

5.1.2 - Methods

5.1.2.1 Electrode Preparation:

Rotating disk electrodes were prepared by embedding vitreous carbon rods (3 mm diameter, V10 Atomergic) in a Teflon shroud using a low viscosity epoxy resin (Polyscience, catalog No 01916). Electrodes were cleaned and successively polished using two grades of alumina slurry (1 and 0.3 μm) with 5 minute sonication and rinsing with RO water after each grade. Before use, electrodes were cycled in buffer between 0 and 600 mV *vs.* Ag|AgCl at a scan rate of 100 mV s^{-1} (featureless electrochemistry with a low non-Faradaic background current being both desirable as well as indicative of a clean operational surface).

Microelectrodes were prepared by inserting 8 μm diameter carbon fibres in polypropylene micropipette tips. The pipette tip was melted allowing the protruding fibre to be sealed. The tip was then cut perpendicularly to the fibre to obtain a flat working surface with an outside diameter of approximately 1 mm. Electrical contact was established with the carbon fibre by filling the tip with a (2:1) mixture of carbon powder and mineral oil and inserting a copper wire. A layer of cellulose acetate was added on top of the sensing layer by dropping 0.5 μl of 0.05% cellulose acetate, prepared in hexaquinone, onto the surface of the dry sensor and left to cure overnight.

Also used were 8 μm glassy carbon electrodes encased within glass to give an outer diameter of 2 mm (purchased from Cypress Systems Inc.). The cleaning procedure was the same as for the macroelectrodes described above.

All direct-wired enzyme electrodes were prepared by mixing the POs-EA polymer (5 mg ml^{-1} in reverse osmosis (RO) water), glutamate oxidase (6.7 mg ml^{-1} in 20 mmol dm^{-3} phosphate buffer containing 0.14 mol dm^{-3} NaCl, pH=7.4) and PEGDGE crosslinker (2.5 mg ml^{-1} in water) and then applying 5 μl of the mixture to the electrode surface The electrodes were allowed to cure slowly for at least 24 hours in air at room temperature before use.

Preparation of the bienzyme electrodes was performed in a similar manner to the direct-wired electrodes. A 5 µl drop of the following mixture was applied to the electrode surface: POs-EA polymer (5 mg ml^{-1} in RO water), glutamate oxidase (6.7 mg ml^{-1} in phosphate buffer containing 0.14 mol dm^{-3} NaCl, pH=7.4), soybean peroxidase (20 mg ml^{-1} in water) and PEGDGE crosslinker (2.5 mg ml^{-1} in water). The electrodes were allowed to dry slowly for at least 24 hours in air at room temperature before use.

Wired SBP glutamate microelectrodes were prepared on both the 8 µm glassy carbon fibres and graphite carbon fibre electrodes. The 2 µl drop of solution applied to the electrode surface contained 0.9 µl POs-EA (1 mg ml^{-1}), 0.45 µl SBP (2 mg ml^{-1}), 0.15 µl GLOx (0.67 mg ml^{-1}) and 0.5 µl PEGDGE (0.25 mg ml^{-1}), giving a percentage weight distribution of 45%:45%:5%:5% respectively.

5.1.2.2 Measurement of Enzyme Activity:

The activities of both GLOx and GOx were tested by detection of their ability to produce H_2O_2, on reaction with their appropriate substrate, using a QUANTOFIX Peroxide 100 strip test (EM Science, New Jersey, USA) which contains a peroxidase enzyme. Known concentrations of both GOx and GLOx were prepared and a drop added to individual test strips. On the introduction of either glucose or glutamate, the H_2O_2 produced by the reaction turned the test strips a discrete shade of blue. Visual comparison of the colour of each strip and consideration of their corresponding enzyme concentrations meant it was possible to estimate the ratio of glucose oxidase activity and turnover and relate it to that of glutamate oxidase.

5.1.2.3 Electrochemical Measurements:

Initial tests were performed on the single enzyme system, using cyclic voltammetry (at 100 mV s^{-1}) between -300 to +600 mV *vs.* Ag|AgCl, to establish the sensing potential at which to poise the electrode. All experiments were carried out in 20 mmol dm^{-3} phosphate buffer using a standard three electrode cell, with a glassy

carbon working electrode of area 0.07 cm^2, Ag|AgCl reference electrode (BAS, 3 mol dm^{-3} NaCl) and a platinum counter electrode.

Both voltammetric and amperometric responses were recorded using a BAS Model CV-1 B potentiostat and the signal was recorded on a BAS x-y recorder. Rotating disk electrode experiments were also performed, using a speed of 1000 rpm with a Pine Instruments AFMSRX rotator with an MSRS speed controller.

For the amperometric experiments on the direct-wired enzyme electrodes the potential of the working electrode, with respect to the reference electrode, was maintained at +415 mV *vs.* Ag|AgCl and the corresponding anodic current profile recorded for varying glutamate concentrations. A stock solution of 500 mmol dm^{-3} glutamate was prepared and known aliquots were added to the buffer solution to provide specific solution concentrations of glutamate. The current value was allowed to stabilise after each addition.

Interference measurements were carried out in the same manner. Amperometric current (anodic) responses were measured as a result of additions of physiological concentrations of ascorbic acid and uric acid (0.2 and 0.4 mmol dm^{-3} respectively) at a potential of +415 mV *vs.* Ag|AgCl.

For the bienzyme electrodes, amperometric measurements were carried out using an identical approach except with a reducing working electrode potential of +50 mV *vs.* Ag|AgCl.[125] The magnitude of the currents measured using the microelectrode sensors required a much more sensitive detection system. Additionally, in order to reduce the amount of electrical interference, the experiments were performed with the three electrode cell inside a Faraday cage and the data was collected using a PC controlled CH Instruments electrochemical detector Model 700.

In order to examine the effect of oxygen on the electrodes responses, the electrodes were operated under air-saturated, nitrogen-saturated and oxygen-saturated conditions. This was achieved by purging the cell with nitrogen or oxygen for a

length of time between 20-30 minutes. A blanket of nitrogen or oxygen was maintained over the solution surface whilst performing the experiments, as appropriate.

5.1.2.4 Data Analysis:

All the amperometric data collected from the electrochemical experiments was analysed using SigmaPlot (Jandel Scientific) and presented as current densities *vs.* concentration profiles.

5.2 Results and Discussion

This section focuses on the electrochemical responses obtained using the two different electrically wired GLOx sensors. The apparent advantage of the latter system, based upon a bienzyme construction, is discussed and the subsequent development of this for microelectrodes is described in section 5.2.3.

5.2.1 - Direct-Wired GLOx Electrodes

5.2.1.1 Enzyme Activities:

The work of Heller *et al.*[94, 116, 118] on electrical wiring of GOx onto electrode surfaces using osmium based hydrogels provided a model system for the glutamate sensors described in the following sections.

As little is known about the enzyme glutamate oxidase, initial tests were carried out to assess its ability to be 'wired'. It's enzymatic activity was compared to that of the well characterised glucose oxidase model.[86] The activities of both enzymes (in solution) were tested by detection of their hydrogen peroxide production using a QUANTOFIX test strip as described in section 5.1.2. The peroxide-induced colour change and the corresponding enzyme concentrations were considered and revealed that the H_2O_2 produced by GLOx was equivalent to that produced by a concentration of GOx of an order of magnitude greater, suggesting the GLOx activity appears to be

an order of magnitude smaller than that of GOx. This is supported by the values reported for GLOx of 30 Units mg^{-1} (Kusakabe[87]) and for GOx of 300 Units mg^{-1} (Sigma[192]).

These qualitative results suggested that GLOx could be successfully 'wired' using hydrogels. On calibration of glutamate sensors prepared in such a manner, it was found that the magnitude of the GLOx sensor response was smaller than that of wired GOx sensors, which can most likely be attributed either to the lower enzyme activity or to a different interaction between the hydrogel and the enzyme. Results which address these two hypotheses are presented later in this section.

5.2.1.2 Electrochemical Response:

Electrochemical assays were performed for first glucose and then glutamate sensors prepared using the direct-wired enzyme technique. As a model system, the glucose response of GOx-Os electrodes was first investigated.

- Glucose: The steady state current response of a typical glucose sensor to successive increments of glucose concentration in the range 0 to 100 mmol dm^{-3} was measured and the amperometric anodic current density response is shown in Figure 5.2 as a function of substrate concentration. A saturation current density of 600 μA cm^{-2} was obtained and at low glucose concentrations the response followed a linear trend. Although these results were lower than those obtained by Heller *et al* [94], they are within experimental limits of comparison, given that the two systems were investigated using GOx from different sources.

- Glutamate: Using the same osmium polymer, glutamate electrodes were prepared and their electrochemical responses monitored and compared to those of the glucose sensors. A calibration plot of the response to various glutamate solution concentration over the range 0 to 50 mmol dm^{-3} was prepared and is shown in Figure 5.3. The response is linear at concentrations below 0.5 mmol dm^{-3} with an average sensitivity within this region of 8 μA cm^{-2} (mmol dm^{-3})$^{-1}$. The Michaelis-Menten

kinetic parameter (K_m) was determined from the x-axis intercept of a Lineweaver-Burke plot, shown in Figure 5.4, and has a value of 4.4 mmol dm^{-3}.

The linearity of the sensor in the range 0 - 0.5 mmol dm^{-3} justifies their suitability for application *in vivo* since current estimates for the concentration of glutamate in the extracellular space in the brain vary between 4 - 350 μmol dm^{-3}, increasing by 20 - 30% during phases of increased brain activity.[193-195]

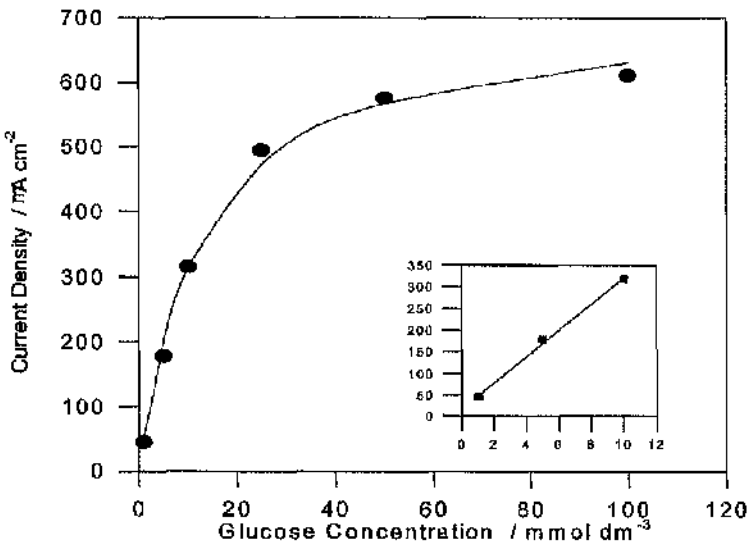

Figure 5.2 - Dependence of the steady-state anodic current on the glucose concentration of a POs-Ea/GOx/PEGDGE electrode. The electrode diameter was 3 mm, the sensing potential was maintained at +415 mV *vs.* Ag|AgCl and the response was measured over a range of 0 to 100 mmol dm^{-3} glucose.

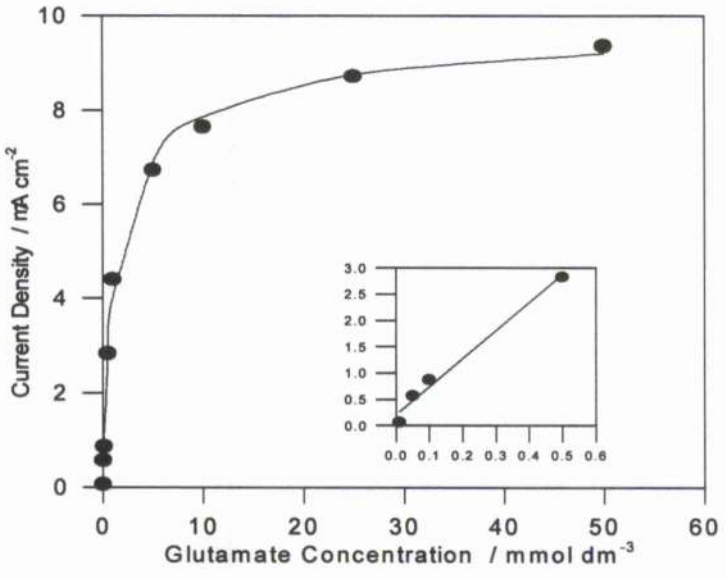

Figure 5.3 - Anodic current density profile of a POs-EA/GLOx/PEGDGE electrode. The electrode was prepared with POs-EA/GLOx/PEGDGE. The electrode diameter was 3 mm, the sensing potential was maintained at +415 mV *vs.* Ag|AgCl and the response was measured over a range of 0 to 50 mmol dm^{-3} glutamate.

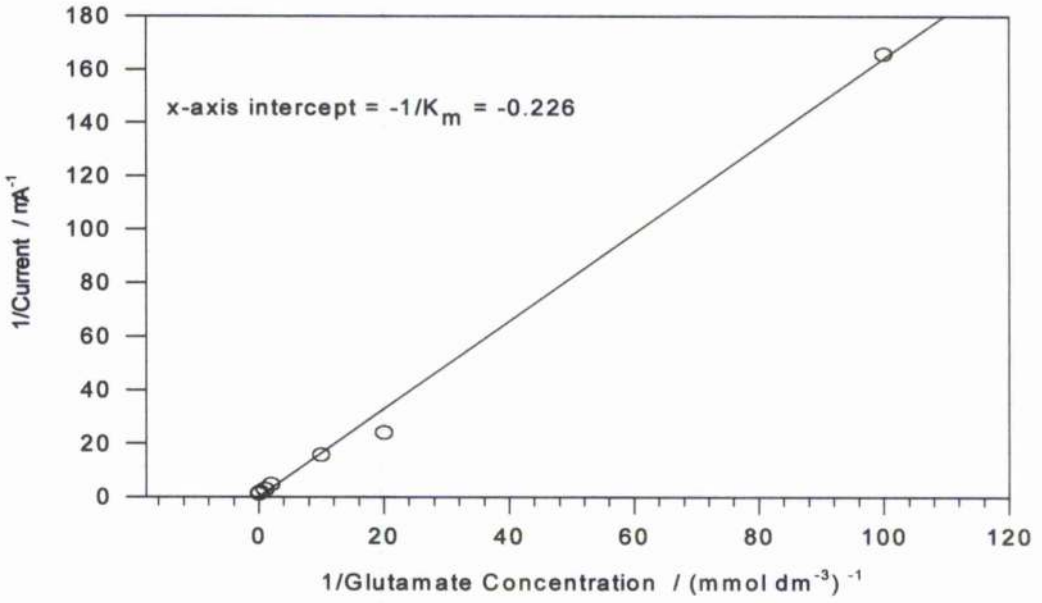

Figure 5.4 - Lineweaver-Burke plot for the POs-EA/GLOx/PEGDGE electrode. Regression determined by least squares fit, r^2=0.996. The x-axis intercept can be analysed to provide information about the kinetic parameters of the electrode system.

As expected, the K_m of 4.42 mmol dm^{-3} obtained experimentally is larger than the value reported by Kusakabe[87] of 0.21 mmol dm^{-3} for glutamate oxidase in solution; a fact that can be attributed to mass transfer limitation. A recent review paper[32], which analyses alternative glutamate electrode configurations developed in previous years shows that the biosensor characteristics, including the apparent K_m value, are highly dependent on the electrode material and the composition of the sensing layer. The values range from 28 μmol dm^{-3}[196] to 9.1 mmol dm^{-3} [135]. Whilst Lineweaver-Burke plots are of considerable value to characterising enzyme kinetics, one weakness of the analysis is that the linear regression is skewed by kinetic measurements made at low concentrations (which are the most sensitive to error). For example, if the point on Figure 5.4 at 100 (mmol dm^{-3})$^{-1}$, which corresponds to a glutamate concentration of 0.1 mmol dm^{-3} , is not considered then the estimated K_m value is reduced to 0.5 mmol dm^{-3}. It is feasible to remove this point because the low glutamate concentration signals are most likely to contribute the largest errors into the response.

The saturation current density of 19 μA cm^{-2} obtained for the glutamate electrodes can be compared to the value of 600 μA cm^{-2} for glucose oxidase wired in the same hydrogel. This variation in magnitude may be due to the lower specific activity of the GLOx or to a poorer wiring of the enzyme to the polymer. The results do however demonstrate that GLOx can successfully be wired within an osmium-based hydrogel matrix.

5.2.1.3 Oxygen Dependence of the GLOx-Osmium Electrodes:

For *in vivo* glutamate concentration measurements, it is desirable that the electrode be insensitive to changes in dissolved oxygen concentration. Oxygen is a natural co-substrate for glutamate oxidase and will, therefore, compete effectively with the oxidised osmium sites, Os^{III}, to re-oxidise the substrate-reduced active site of the enzyme. The competition scheme is shown in Equations (5.1) - (5.3).

$$glutamate + O_2 + H_2O \xrightarrow{GLOx} \alpha - ketoglutaric\ \ acid + H_2O_2 + NH_3 \qquad \textbf{(5.1)}$$

$$GLOx - FADH_2 + 2Os^{III} \longrightarrow GLOx - FAD + 2Os^{II} + 2H^+ \qquad \textbf{(5.2)}$$

$$GLOx - FADH_2 + O_2 \longrightarrow GLOx - FAD + H_2O_2 \qquad \textbf{(5.3)}$$

If the electrode is characterised under oxygen-rich conditions then the steady-state response current is substantially lowered since there is a direct competition between the oxygen and the Os^{III} to act as an electron acceptor. The steady-state glutamate response is shown in Figure 5.5 for a wired electrode under air, N_2 and O_2 saturated conditions.

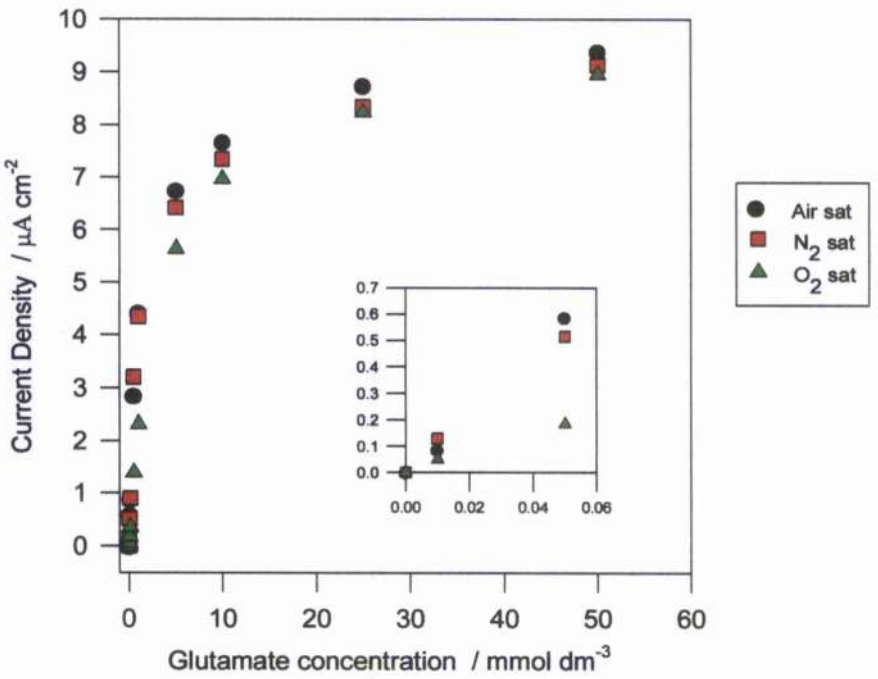

Figure 5.5 - Effect of low oxygen conditions on the glutamate saturation current density. Electrodes were prepared with POs-EA/GOx/PEGDGE sensing layers. Solutions were deareated with pure N_2, O_2 and air for 20 - 30 minutes and a blanket of gas maintained over the cell while measurements were made. A sensing potential of +415 mV *vs.* Ag|AgCl was maintained.

At a glutamate concentration of 50 mmol dm^{-3} the electro-oxidation current response decreased by 2.7% when the bubbled gas was changed from air to N_2 and then by a further 1.8% when the bubbled gas was changed from N_2 to O_2. At 0.05 mmol dm^{-3}

glutamate the corresponding decreases were 12.3% then 63.8% from air to N_2 to O_2. This can be explained as follows: the maximum current densities under all three gaseous conditions (i.e. air, N_2 and O_2 saturated) remained approximately equal when the concentration of glutamate was saturating, which suggests that the enzyme-glutamate reaction is the limiting step and that there are sufficient electron acceptors, as Os^{III}, present in the vicinity of the enzyme to carry the current. At lower glutamate concentrations the reaction between the enzyme and the Os^{III} becomes limiting and the rate is dependent upon the availability of the Os^{III} sites (as well as its competition with O_2). For the same solution oxygen concentration, there is a higher probability that the oxygen will react with the reduced enzyme if the solution concentration of glutamate is low rather than if the glutamate is in excess.

5.2.1.4 Electrode Selectivity:

Glutamate sensors are often insufficiently selective when operated at potentials where ascorbate and urate can be electro-oxidised. The direct-wired glutamate sensors discussed in this chapter have a sensing potential of +415 mV *vs.* Ag|AgCl which is capable of oxidising these interfering substances and so the selectivity (i.e. the equivalent glutamate response to a physiological amount of interferent) of these sensors was tested against ascorbate and urate concentrations of (physiological conditions) 0.2 and 0.4 mmol dm^{-3} respectively. In the presence of 5 mmol dm^{-3} glutamate, the electrooxidation current density of which was 7 $\mu A\ cm^{-2}$, a known concentration of 0.2 mmol dm^{-3} ascorbate was introduced into the assay. The electrooxidation current of the sensor increased to 146 $\mu A\ cm^{-2}$ indicating a *ca.* 95% rise in sensor response. Similarly, on addition of 0.4 mmol dm^{-3} urate into a solution of 5 mmol dm^{-3} glutamate the sensor response increased to approximately 157 $\mu A\ cm^{-2}$; another 95% enlargement. One possible explanation could be that the negatively charged interferents are being actively partitioned into the positively charged redox hydrogel and subsequently oxidised at the electrode surface. Clearly it is unsatisfactory to have such a poor signal to noise ratios; therefore it is necessary to find a method of reducing the electrode potential as low as possible. This is discussed in the following section.

5.2.2 - Single Layer, Bienzyme Glutamate Electrodes Based on Electrically Wired Soybean Peroxidase

In order to reduce the electrochemical potential of the sensor and, therefore, enhance the signal:noise ratio, electrodes were prepared where SBP was wired to a redox polymer and GLOx immobilised within it.[129] With such a configuration the electrode potential was able to be decreased to +50 mV *vs.* Ag|AgCl, producing a electro-reductive current. This section presents the results obtained from such sensors and highlights their advantages over the directly wired GLOx electrodes discussed previously.

5.2.2.1 Electrochemical Response:

The steady-state cathodic current profile of electrodes constructed using the combination of POs-EA/SBP/GLOx/PEGDGE were recorded in response to various concentrations of glutamate. The calibration plot for one such sensor in response to glutamate concentrations in the range 0 to 10 mmol dm^{-3} is shown in Figure 5.6.

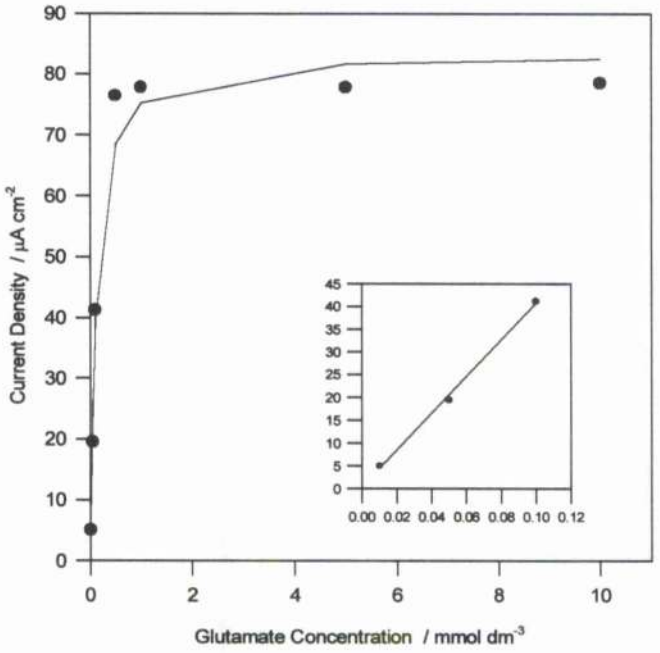

Figure 5.6 The glutamate calibration plot for an electrode prepared by wiring SBP and immobilising GLOx within an osmium-based hydrogel. The cathodic current response to glutamate in the concentration range 0 to 50 mmol dm^{-3} is presented along with the limit to which the linear range extends. The electrode area had a diameter of 8 μm and the potential it was held at was +50 mV *vs.* Ag|AgCl.

Maximum cathodic current densities of 80 μA cm^{-2} were obtained, showing a ten-fold increase over electrodes prepared by direct wiring of glutamate oxidase. The maximum current density is achieved at a much lower glutamate concentration and the linear region is reduced to 0.1 mmol dm^{-3}. In this region there is a sensitivity of 400 μA cm^{-2} (mmol dm^{-3})$^{-1}$ and the Michaelis-Menten kinetic parameter K_m has a value of 0.17 mmol dm^{-3}. The Lineweaver-Burke plot for this data is shown in Figure 5.7.

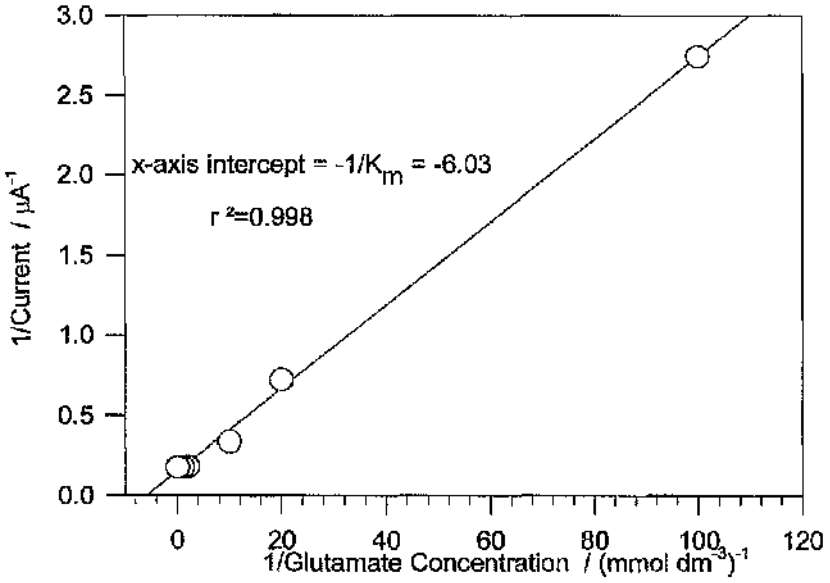

Figure 5.7 - Lineweaver-Burke plot for GLOx electrode based on wired SBP. The regression was based upon a least squares fit with r^2=0.998. The x-axis intercept was examined to determine the kinetic parameter K_m.

The K_m value obtained is closer to that of 0.21 mmol dm^{-3} reported for solution GLOx[88], indicating that responses are closer to that for a diffusion limited model. In the case of the SBP wired glutamate sensors the GLOx is not bound to the polymer and the sensing principle relies on its physical entrapment, without alteration of its surface composition. This theory could be supported by the occurrence of a saturation current density greater than that for direct wired GLOx sensors.

5.2.2.2 Oxygen Dependence of the GLOx-SBP-Osmium Electrodes:

In contrast to the direct wired GLOx electrodes described in the previous section which are relatively oxygen independent, the electrodes based on wired SBP require an oxygen-rich environment in which to operate. Glutamate, in the presence of oxygen, oxidises the substrate-reduced immobilised glutamate oxidase to form hydrogen peroxide which is electro-reduced at the SBP-wired modified electrode surface.

To illustrate this effect, Figure 5.8 shows the current density response when the sensor is operated under air and nitrogen saturated conditions.

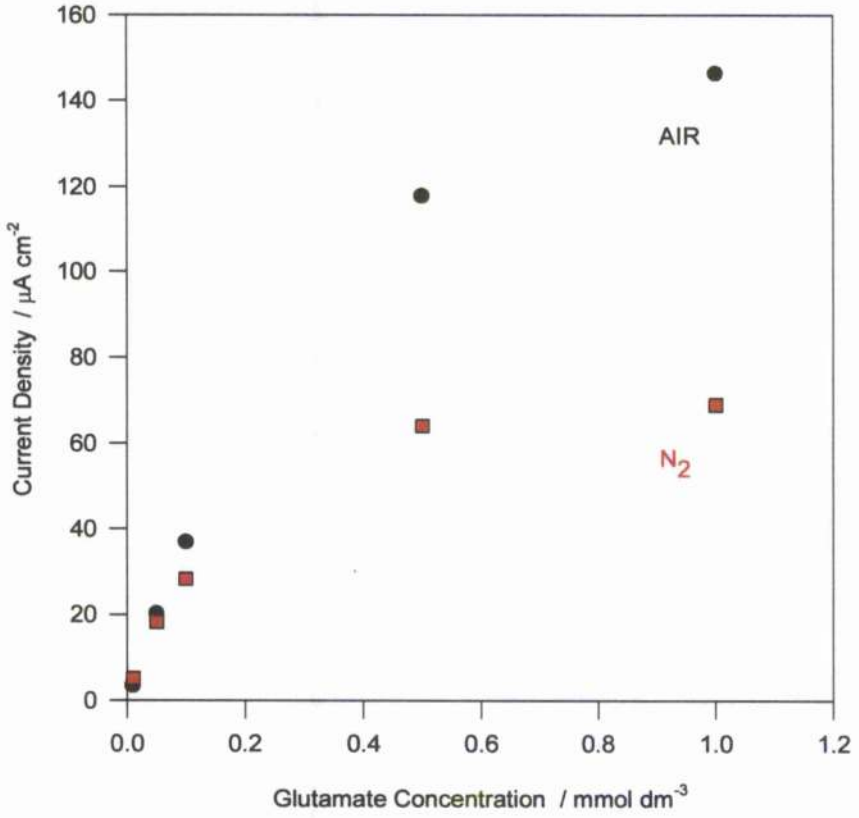

Figure 5.8 - Dependence of the SBP wired glutamate sensor on oxygen. The electro-reductive current response to glutamate over the range 0 - 1 mmol dm^{-3} was measured under both air and nitrogen saturated conditions. Solutions were deareated for 20 - 30 minutes and the responses were measured at a potential of +50 mV *vs.* Ag|AgCl.

As expected, the electro-reduction current was observed to be much larger in aerated solutions. This effect is most exaggerated at higher glutamate concentrations where

the signal dropped by 53% (glutamate concentration = 1 mmol dm^{-3}) when the solution was bubbled first with air and then with nitrogen. At lower concentrations, for example 0.05 mmol dm^{-3}, the signal was subjected to only an 11% decrease. This variation in percentage signal decrease could be attributed to a residual amount of oxygen maintained within the polymer matrix after degassing which is sufficient to oxidise low concentrations of glutamate but not abundant enough to oxidise larger concentrations.

As the ultimate aim of this work is to obtain a sensor for reliable operation *in vivo*, where there will be limited oxygen and typically glutamate concentrations in the micromolar range, the system described above would appear to have a response which is adequately reliable and unaffected by such conditions.

5.2.2.3 Electrode Selectivity:

The most obvious advantage of the bienzyme, wired-SBP sensors is the ability to hold the electrode at a reducing potential of +50 mV *vs.* Ag|AgCl. At such a low potential the common interferents, ascorbate and urate, should not be electro-oxidised. There is, however, still an interfering signal observed with these sensors but its magnitude (with respect to an appropriate glutamate concentration response) is substantially lower than that for the direct-wired GLOx system. Experimental results showed that the signal due to the ascorbate is equivalent to 50% of the 5 mmol dm^{-3} glutamate signal and the signal due to the urate is equivalent to 65% of the glutamate signal. This corresponds to signal to noise ratios, for 0.2 mmol dm^{-3} ascorbate and 0.4 mmol dm^{-3} urate introduced into a 5 mmol dm^{-3} glutamate solution, of 2.0 and 2.9 respectively.

Alternative methods are currently being investigated to reduce this electro-interference by designing multi-layer electrodes which include barrier membranes. An example of this is the recent work by Heller *et al.* where a four-layer sensing structure is constructed[129]. This consists of a wired SBP layer, adjacent to the electrode surface; a second insulating layer of cellulose acetate membrane, allowing

hydrogen peroxide controlled transport; a third layer of immobilised oxidase enzyme, where the substrate is reacted with oxygen to produce hydrogen peroxide; and a fourth layer of cellulose acetate to control the substrate transport. Such systems appear to virtually eradicate responses due to interfering species.

5.2.3 - Glutamate Microsensors Based Upon Wired Soybean Peroxidase

The development of miniaturised glutamate enzyme electrodes is essential for *in vivo* measurements to provide spatially discrete measurements in defined positions within tissue. In this section the single layer, bienzyme technique described in the previous section for preparing glutamate sensors is applied to microelectrodes and their performance discussed in comparison with that of macroelectrode sensors.

The microelectrodes prepared in this chapter consisted of a poly(vinylpyridine) containing Os(dimethylbipyridine)$_2$Cl$_2$ polymer matrix containing wired SBP and immobilised but not wired GLOx. In order to decrease the proportion of the current due to interfering solution species, a transport controlling layer of cellulose acetate was added to the electrodes on top of the sensing layer. This acts as a barrier to the unwanted species, which are electro-oxidised at the electrode surface, and allows the glutamate to diffuse readily through to the sensing layer.

5.2.3.1 Electrochemical Response:

Microelectrodes were prepared with POs-EA/SBP/GLOx/PEGDGE on two different carbon electrode surfaces with working area 5×10^{-7} cm^2. The first were prepared on glassy carbon electrodes, purchased encased in a 2 mm diameter glass coating, and the second on carbon fibre electrodes enclosed in plastic, fabricated within the laboratory. This section reports not only the comparison between glutamate responses at macro and microelectrodes with the same sensing layer composition but also the variation of response at microelectrodes with respect to the type of electrode surface.

Figure 5.9 shows the calibration plots for both types of microelectrode in response to different solution concentration of glutamate. Figure 5.9(a) shows the glutamate electro-reduction current density variation for POs-EA/SBP/GLOx/PEGDGE for the carbon fibre microelectrodes and Figure 5.9(b) shows a similar plot for the glassy carbon based electrodes

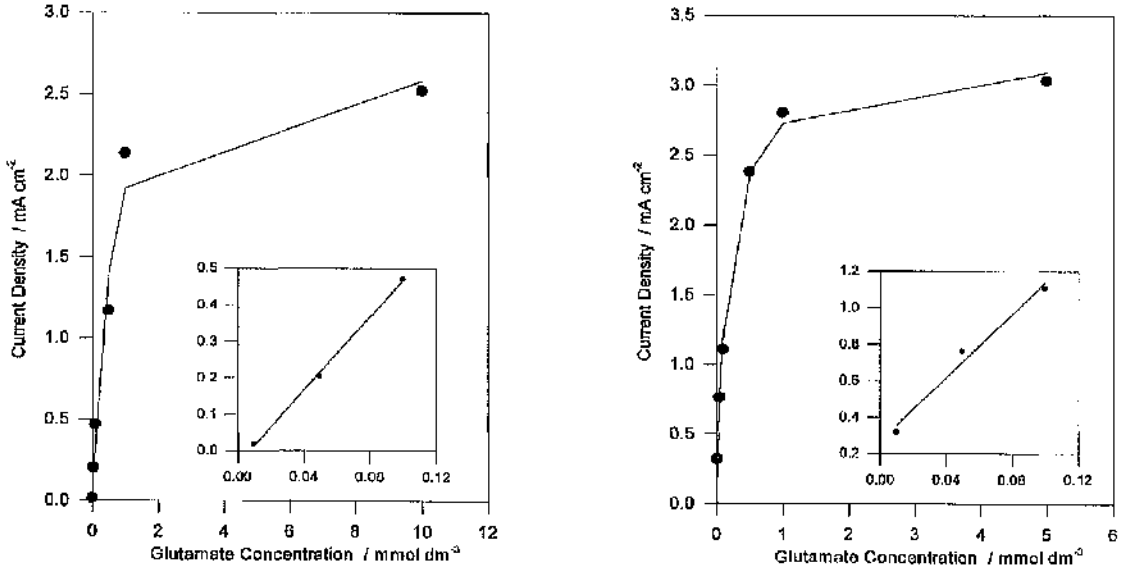

Figure 5.9 - (a) Glutamate cathodic current variation for POs-EA/GLOx/SBP/PEGDGE sensors prepared upon carbon fibre microelectrodes. (b) Electrodes prepared with the same sensing layer but on glassy carbon microelectrodes. For both, the sensing area was 5.0 x 10^{-7} cm^2 and the electrode potential was maintained at +50 mV *vs.* Ag|AgCl. Responses were measured over the range 0 to 10 mmol dm^{-3} glutamate..

The limiting cathodic current densities achieved on both microelectrode sensors were similar, both lying in the range 2 - 3 mA cm^{-2}. These values are higher than those observed with the same polymer/enzyme network on macroelectrodes, which is consistent with the theory that the current density increases at least ten-fold under radial diffusion conditions at microelectrodes[197], when the response is diffusion limited.

For both electrodes the linear region extends to 0.1 mmol dm^{-3} and the sensitivities in this region are 4.1 mA cm^{-2} (mmol dm^{-3})$^{-1}$ and 15.31 mA cm^{-2} (mmol dm^{-3})$^{-1}$ for the carbon fibre and glassy carbon microelectrodes respectively. The Michaelis-Menten

kinetic parameter K_m was calculated for both systems by analysis of the Lineweaver-Burke plots shown in Figure 5.10(a) and (b). Values of 0.81 mmol dm^{-3} and 0.16 mmol dm^{-3} were obtained for the carbon fibre and glassy carbon sensors respectively. These compare well with the reported value of 0.21 mmol dm^{-3} for the enzyme in solution.[88]

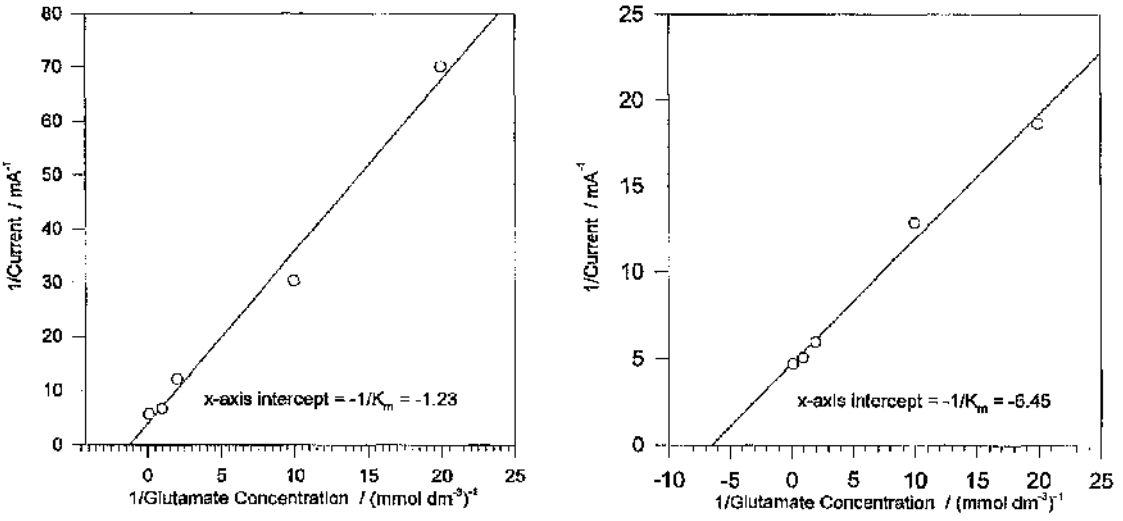

Figure 5.10 - (a) and (b) - Lineweaver-Burke plots for the carbon fibre and glassy carbon microelectrode systems respectively. Regression was calculated by least squares fit with r^2=0.986 and 0.991 for the two systems. Values due to 0.01 mmol dm^{-3} glutamate removed to reduce the error in the kinetic parameter.

In order to assess the similarity of the two microelectrode systems, an unpaired students t-test was performed (using SigmaPlot)[177] with a 95% confidence level. The value of t obtained from comparison of the experimental data in Figure 5.10 (a) & (b) was calculated to be 1.64 which is significantly lower than the theoretically predicted figure of 2.31 (for 8 degrees of freedom)[198] , indicating that there is a 95% probability that there is no variation between the two systems. (For the same statistical analysis, the value of P = 0.18 which is greater than 0.05 and hence the 95 % confidence level). Any differences that do exist can be attributed to the reliability of producing carbon fibre electrodes with a surface area of exactly 8 μm. Therefore, the principal consideration in developing these sensors further is the ability to

decrease the dimensions for use in *in vivo* monitoring; restricted only by photolithographic limitations.

5.2.3.2 Electrode Selectivity:

The determination of neurotransmitters, such as glutamate, *in vivo* is dependent on a high signal to noise ratio of the microsensor. Therefore, the elimination of interfering species which can be electro-oxidised at the electrode surface is of prime importance when designing the sensors. One of the most prevalent interferents is ascorbate. The glutamate microelectrodes prepared and tested as described in the previous section, i.e. POs-EA/SBP/GLOx/PEGDGE modified by addition of a layer of cellulose acetate, (see Figure 5.9(b)) were investigated for their response to ascorbate.

The response to 0.2 mmol dm^{-3} ascorbate was equivalent to the response observed for an approximate glutamate concentration of 0.08 mmol dm^{-3}. Although the interfering current was still not totally eliminated, the signal to noise ratio was increased to 3.15; a substantial improvement over the initial direct-wired GLOx systems where the glutamate signal was completely 'drowned out' by the ascorbate signal. As mentioned previously, a quad-layer system is currently under investigation to maximise interferent elimination.

5.3 Summary

The work in this chapter focused on enzyme attachment and immobilisation within osmium based polymers and has shown that by direct electrochemical contact, i.e. wiring of the enzyme to the electrode surface, a substantial increase in the sensor current response can be achieved over other previously reported electrochemical glutamate sensors where the enzyme is immobilised within an electropolymerised matrix.

By considering the maximisation of the current densities for wired systems on macroelectrodes and transferring this to microelectrodes, a significant step has been made towards the development of a highly sensitive *in vivo* glutamate sensor.

The most attractive system investigated consisted of a single layer, bienzyme electrode where GLOx is incorporated within a wired POs-EA/SBP cross-linked polymer layer. This enables the electrode to be poised at a lower, reducing potential (e.g. +50 mV *vs.* Ag|AgCl) which diminishes the likelihood of interference from any electro-active substance present in physiological fluids. Another advantage of this system is that it is able to operate satisfactorily for low glutamate concentrations under deoxygenated conditions. When considering operating conditions *in vivo*, the concentration of oxygen is very low and so this system would appear to be suitable for such purposes.

Finally, although the microelectrode system described has not been optimised fully, it is hoped that the results presented within this chapter can provide a basis for ideas for future improvements. These may include variation of the percentage composition of polymer, enzyme, crosslinker and cellulose acetate within the sensing layer and increasing the length of drying time once this layer has been applied to the electrode surface. The most significant improvement, however, would be the modification of design in order to totally eliminate the electrooxidation of interfering species. As described in previous sections, the on-going development of a quad-layer arrangement may be capable of achieving exactly this.

CHAPTER 6 - ELECTROCHEMICAL AND SPECTROSCOPIC ANALYSIS OF THE PREPARATION AND OPERATION OF OSMIUM HYDROGEL BASED GLUTAMATE SENSORS

In this chapter glutamate biosensors were prepared using osmium redox hydrogels[91, 114] and examined using electrochemical and spectroscopic techniques to probe the effect of altering various sensor parameters (e.g. preparation methods, hydration state of the binder). For example, as the hydrogels rely on their ability to swell for efficient conduction, the effect of soaking the sensors in buffer for prolonged periods of time was investigated using both electrochemical assay analysis and XPS[141]. Additionally, the percentage of crosslinking component of the sensor, polyethylene glycol diglycidyl ether (PEGDGE), which binds the entire sensing layer together, was varied and also studied using electrochemical assay analysis and XPS.

The sensors were prepared as the single layer, bienzyme electrodes described in Chapter 5 using osmium based polymers to 'wire' the enzyme soybean peroxidase to the electrode surface and simultaneously immobilise the enzyme glutamate oxidase at the electrode surface. A polyethylene glycol diglycidyl ether (PEGDGE) crosslinker was employed to entrap the components together and to prevent the polymer-enzyme layer from lifting off the surface of the electrode. The results presented in previous chapters for non-conducting polymer sensors, prepared under specific conditions, used electrochemical analysis to determine their response over a range of glutamate concentrations, their operation under oxygen-saturated conditions and the effect of interfering species on their response. This chapter examines the consequence of varying the preparation conditions of hydrogel-based sensors using electrochemical analysis to explore changes in sensor response and XPS to investigate changes in polymer-enzyme layer composition.

6.1 Experimental

The bienzyme electrode systems examined in this chapter were prepared using the same technique as described in Chapter 5, Section 5.1.2 with the exception of variation in the percentage of crosslinker contained within the film.

6.1.1 Materials

Poly(ethylene glycol) diglycidyl ether (Polysciences, PEGDGE 400, catalog No 08210), ascorbic acid (Aldrich Cat # 25,556-4) and glutamic acid (Cat # G-1626) were purchased from Sigma. Soybean peroxidase (SBP) was purchased from Enzymol International Inc. (HP grade, 130 pyrogallol Units mg^{-1}). Glutamate oxidase (GLOx) (EC 1.4.3.11., from *Streptomyces* species, 30 Units mg^{-1}) was a gift from Yamasa Shoyu (Chiba, Japan). The redox polymer, poly(vinylpyridine)-containing Os(dimethylbipyridine)$_2$Cl$_2$ (POs-EA) was prepared in Department of Chemical Engineering, University of Texas at Austin, Texas as reported[91, 122]. All other chemicals were purchased from Sigma. Titanium, palladium and gold were purchased from Goodfellows (Cambridge, U.K.). The Ag|AgCl reference electrode (MF-2063) was purchased from BAS Technicol, Cheshire.

The structures of both the POs-EA polymer and the PEGDGE 400 crosslinker are shown in Chapter 5, Figure 5.1.

6.1.2 Methods

6.1.2.1 Electrode Preparation:

Unlike the carbon paste sensors prepared in Chapter 5, the analysis in this chapter was performed on evaporated gold electrodes. Gold working electrodes of area 1 cm^2 were fabricated using standard photolithographic techniques as described in Chapter 2, Section 2.1.2.

Preparation of the bienzyme electrodes was performed as described in Chapter 5, Section 5.1.2. To summarise the procedure, a 5 μl drop of the following mixture: POs-Ea polymer (5 mg ml^{-1} in RO water), glutamate oxidase (6.7 mg ml^{-1} in phosphate buffer containing 0.14 mol dm^{-3} NaCl, pH=7.4), soybean peroxidase (20 mg ml^{-1} in water) and PEGDGE crosslinker (2.5 mg ml^{-1} in water) was applied to the electrode surface. The ratio of each 'component' of the mixture is 45% polymer:45% SBP:5% GLOx:either 5% or 1% PEGDGE. The electrodes were allowed to dry slowly for at least 24 hours in air at room temperature before use.

The experiments in this chapter investigated the sensors response immediately after drying and then the effect of soaking the sensors in 20 mmol dm^{-3} phosphate buffer (containing 0.14 mol dm^{-3} NaCl, pH=7.4) for periods of 1 hour and 10 hours was also investigated, in both cases using electrochemistry and XPS.

6.1.2.2 Electrochemical Measurements:

The sensors were tested for their response to glutamate over the range 0 - 25 mmol dm^{-3} using a standard three electrode arrangement containing the working electrode, a Ag|AgCl reference electrode and a platinum counter electrode. The set-up was controlled by a PC and the cathodic current responses measured at a constant potential of +50 mV *vs.* Ag|AgCl. Calibration plots were obtained for each of the sensors prepared using 1% or 5% PEGDGE and in different states of hydration.

Additionally, cyclic voltammograms were recorded for each of the sensors in phosphate buffer by sweeping the potential from -100 mV up to +600 mV (*vs.* Ag|AgCl) at scan rates of 1, 20 and 100 mV s^{-1} to obtain information on the amount of redox material (i.e. the number of osmium centres) on the surface.

6.1.2.3 XPS Measurements:

As for the XPS analyses in preceding chapters, the XPS spectra were collected using the high-resolution SCIENTA ESCA 300 spectrometer and software located at RUSTI, Daresbury Laboratories (Warrington, U.K.). The slit width of the source

was maintained at 0.8 mm to obtain a consistent sampling area and the take of angle was varied from 10° to 90° for each sample measured. Prior to measurement, each sample was rinsed in RO water, blown dry and immediately loaded into the sample chamber of the instrument. All measurements were performed with a pressure of ca. 10^{-9} Torr in the main analytical vacuum chamber.

Analysis of each sample was performed by first taking a survey scan spectrum covering a wide range of approximately 1300 eV and then examining in more detail scans over smaller ranges (20 eV) to investigate specific features/regions found in the wide spectrum. As before, the samples were insulated from the analyser due to their glass substrate, and so flood-gun energy was required to compensate for the build up of positive charge from photoelectron emission. Therefore, before analysis, the individual spectra obtained had to be corrected for the offset due to the flood-gun electron kinetic energy using the Au(4f) energy as a reference. Additionally, a cubic baseline was subtracted from the spectra to allow for background correction.

As these sensors are multi-component systems i.e. they are comprised not simply of polymer and enzyme, quantification of the XPS spectra by fitting the sample spectra using the reference spectra would prove extremely complicated. Therefore, the characteristic spectra (i.e. N(1s), S(2s) and Au(4f)) were used to provide quantitative information of the amount of polymeric and enzymatic material on the electrode surface.

6.2 Results and Discussion

The results in this chapter are divided into three sections each of which use a different analytical technique to obtain information about the structure and function of the bienzyme sensing layer. The first two techniques, chronoamperometry and cyclic voltammetry, are electrochemical methods which provide information on the sensor response and the amount of redox material within the layer respectively. The final tool is the spectroscopic technique of XPS which was used to examine the surface composition of the sensors. Each of these techniques was used to examine the sensors when the percentage of crosslinker and the hydration state were varied.

6.2.1 - Chronoamperometric Analysis

Different bienzyme glutamate sensors were prepared as described in Section 6.1.2.1; three containing 5% PEGDGE and three containing 1% PEGDGE. One sample representing each percentage was measured for their amperometric cathodic current responses to glutamate over the range 0 - 25 mmol dm^{-3} immediately after preparation (i.e. dry) and the others measured after soaking in phosphate buffer for periods of 1 hour and 10 hours. These assays allow the strength of the crosslinker and the effect of hydrogel swelling on the sensor response to be explored.

The amperometric current profiles for each sensor were recorded for samples prepared using 1 % and 5% PEGDGE crosslinker and are shown in Figure 6.1 (a) for 'as prepared' samples, (b) for samples soaked in phosphate buffer for 1 hour and (c) for samples soaked for 10 hours.

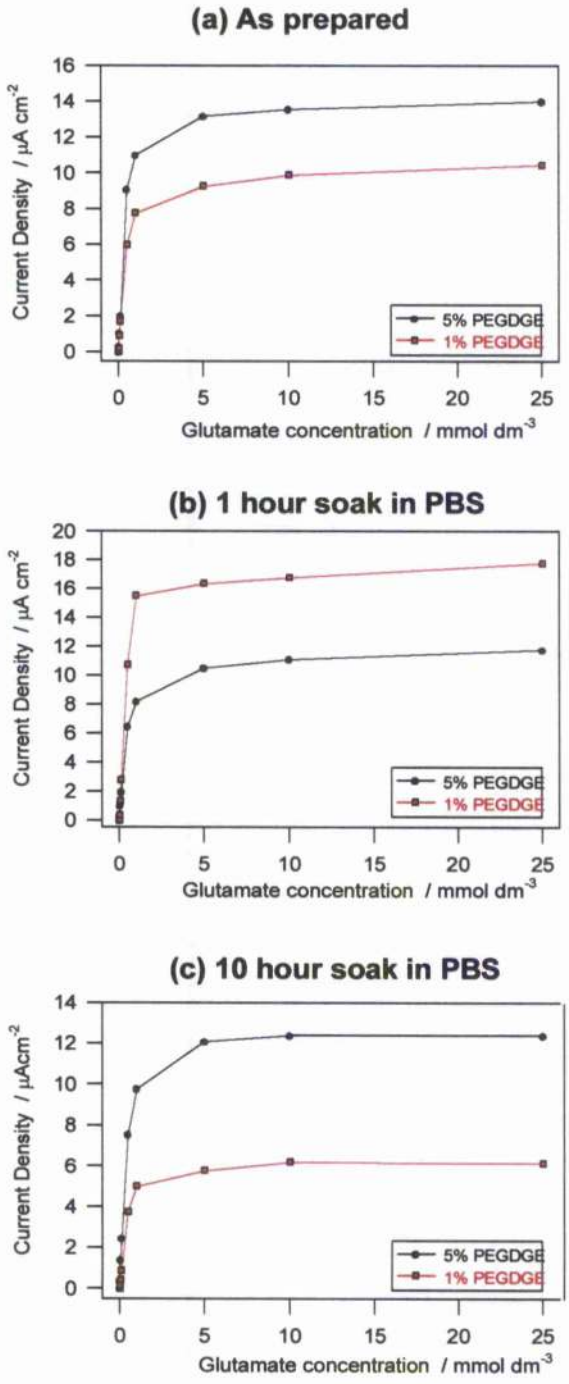

Figure 6.1 - Comparison of the sensor cathodic current responses to glutamate in the range 0 - 25 mmol dm^{-3} for samples prepared with either a 1% or 5% PEGDGE crosslinking solution. The plots in (a) show the trend for the sensors tested immediately after preparation i.e. dry while those in (b) illustrate the trend for sensors soaked in PBS for 1 hour and (c) for sensors soaked for a period of 10 hours. All the electrodes were prepared as described in Section 6.1.2.1 and their responses measured amperometrically at +50 mV *vs.* Ag|AgCl.

The amperometric current profiles were compared as a function of the percentage of PEGDGE used during preparation and the duration of immersion in phosphate buffer. When the sensors were prepared with 5% PEGDGE the maximum current densities obtained from the 'as prepared' and hydrated sensors all lie within the relatively narrow range of 11.5 - 14 $\mu A\ cm^{-2}$. However, with a 1% PEGDGE composition, the sensor responses are far less consistent, lying within the wide range of 6 - 18 $\mu A\ cm^{-2}$. This suggests that by using a higher proportion of crosslinker during preparation there is a greater stability in the wiring of the enzyme to the hydrogel network even under conditions of prolonged hydration i.e. when the hydrogel is greatly swollen.

Additionally, it is noticeable that the maximum sensor response for an unsoaked 5% PEGDGE sample is at least 10% larger than those obtained after immersion for either 1 hour or 10 hours. It appears inevitable that when placed in solution and the hydrogel swells, a small but possibly negligible amount of enzyme is lost to solution.

6.2.2 - Cyclic Voltammetric Analysis

Cyclic voltammetry at various scan rates was employed to determine the effect of crosslinking and hydration state variation on the electrochemical behaviour of the sensors. This set of experiments illustrates the usefulness of cyclic voltammetry as a tool for estimating the amount of electrochemically active material present on the electrode surface.

Cyclic voltammograms covering the range -100 mV to +600 mV *vs.* Ag|AgCl were recorded for samples prepared using both 1% and 5% PEGDGE which were 'as prepared', or had been immersed in buffer for periods of 1 or 10 hours. The plots in Figure 6.2 show representative examples of these voltammograms for the samples prepared with 5% PEGDGE and examined 'as prepared'.

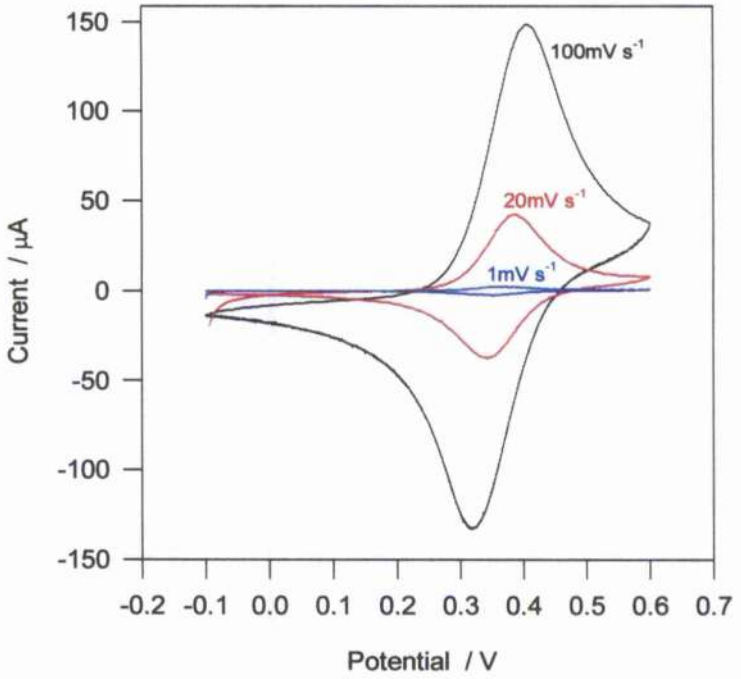

Figure 6.2 - Cyclic voltammograms of the sample prepared with 5% PEGDGE, analysed as prepared and recorded at scan rates of 1, 20 and 100 mV s^{-1}. The scan rate dependence of the current/potential plots are representative of the trend shown for all the samples measured i.e. 5% PEGDGE after soaking for 1 and 10 hours and 1% PEGDGE as prepared and after 1 and 10 hour soaks in phosphate buffer. The oxidative and reductive peak heights are used to obtain quantitative information on the content of osmium hydrogel material present on the surface composition.

By examining the voltammograms in Figure 6.2 it is obvious that the scan rate has a significant effect on the peak oxidation and reduction currents. This variation in peak current can be used to compare the number of osmium centres on the surface of the samples as a function of the percentage of crosslinker and hydration state of the sensor.

At low scan rates the voltammograms exhibit the classic symmetric shape, showing reversible oxidation and reduction of a surface bound species with an approximate standard potential (ΔE) of +350 mV *vs.* Ag|AgCl (ideally the ΔE should equal zero for an immobilised species but the potential of the redox polymer ensures that this is not the case here). As the scan rate is increased the voltammograms illustrate an increase in the redox peak separation and assume the shape characteristic of a diffusion-limited process[139]. Information on the amount of electro-active material on the electrode surface i.e. the number of osmium redox sites within the polymer

can be obtained by analysis of the parameters extracted from the cyclic voltammograms. The values in Table 6.1 show representative oxidation and reduction peak current values ($I_{peak\ (ox)}$ and $I_{peak\ (red)}$) obtained from the whole range of samples at scan rates of 1, 20 and 100 mV s^{-1}.

SAMPLE	1 mV s^{-1}		20 mV s^{-1}		100 mV s^{-1}	
	$I_{peak\ (ox)}$ / μA	$I_{peak\ (red)}$ / μA	$I_{peak\ (ox)}$ / μA	$I_{peak\ (red)}$ / μA	$I_{peak\ (ox)}$ / μA	$I_{peak\ (red)}$ / μA
1%, 0 hr	0.70	0.55	20.00	12.10	117.50	75.00
1%, 1 hr	1.45	0.80	20.00	20.70	75.00	57.50
1%, 10 hr	3.00	1.80	30.70	21.40	100.00	67.50
5%, 0 hr	2.35	2.25	48.60	31.40	157.50	140.00
5%, 1 hr	3.10	2.30	25.00	18.60	117.50	92.50
5%, 10 hr	2.10	1.35	25.00	20.70	112.50	85.00

Table 6.1 - Peak current values for the oxidation and reduction of the bienzyme glutamate electrodes prepared as described in Section 6.1.2.1 and scanned over a 700 mV range at rates of 1, 20 and 100 mV s^{-1}. The difference between the samples prepared with 1% and 5% PEGDGE were examined as were those in various states of hydration. The $I_{peak\ (ox)}$ and $I_{peak\ (red)}$ values can be used to indicate the number of osmium centres present in the samples.

The variation in peak responses obtained in Table 6.1 due to increasing scan rate can be explained as follows. The electrochemistry of the swollen osmium hydrogel is slow which implies that at high scan rates only the layers of the polymer film directly adjacent to the electrode will be oxidised and reduced. Therefore, by decreasing the scan rate, material from the entire polymer depth has the opportunity to participate in the interfacial redox reaction. In order to illustrate this relationship between scan rate and amount of osmium polymer on the electrode surface, the oxidation peak current values ($I_{peak\ (ox)}$) obtained for the 'as prepared' 5% PEGDGE sample at the three different scan rates were investigated. Table 6.2 shows the values of interest.

Scan Rate / mV s^{-1}	$I_{peak\ (ox)}$/Scan Rate / μA s mV^{-1}
1	2.35
20	2.43
100	1.58

Table 6.2 - Relationship between the peak oxidation currents and the scan rate using as an example the values obtained for the sample prepared using 5% PEGDGE and with 0 hour PBS soak.

Theory would dictate that there is a proportionality between the scan rate and the height of the oxidation/reduction peak currents of a sample where the electron transfer process is slow[69, 70, 138]. This suggests that the ratio of peak height to scan rate should remain as a constant value. From the values in Table 6.2, at lower scan rates this value is consistently 2.4 ± 2% but decreases by approximately 30% when the scan rate is increased to 100 mV s^{-1}. This decrease indicates that not all the osmium redox sites within the polymer layer are able to react at such high scan rates. Additionally, since the ratio in Table 6.2 is constant for lower scan rates, it is possible that at 20 mV s^{-1} all the sites are able to react and no further information would be gained by dropping the rate to 1 mV s^{-1}. However, for the purpose of this work the values obtained at the slowest scan rate, 1 mV s^{-1}, were used for subsequent analysis.

The values in Table 6.1 which correspond to those collected at a scan rate of 1 mV s^{-1} were used to investigate the effect of variation in PEGDGE composition of the sensor and hydration state of the polymer. It is possible to estimate the surface coverage of each sample by representing their maximum current responses to glutamate (I_{max} which is attributable to both the amount of polymer and GLOx present in the sample) as a function of the number of osmium redox sites in the polymer layer (obtained from the $I_{peak\ (ox)}$ values), as shown in Table 6.3.

SAMPLE	I_{max} / μA	$\frac{I_{max}}{I_{peak(ox)}}$
1% PEGDGE, 0 hr	10.44	14.92
1% PEGDGE, 1 hr	17.78	12.26
1% PEGDGE, 10 hr	6.15	2.05
5% PEGDGE, 0 hr	14.00	5.96
5% PEGDGE, 1 hr	11.77	3.80
5% PEGDGE, 10 hr	12.39	5.90

Table 6.3 - Comparison of the ratio between maximum sensor current in response to 100 mmol dm^{-3} glutamate (I_{max}) and oxidation current peak height ($I_{peak(ox)}$) at a scan rate of 1 mV s^{-1}. Such a ratio indicates the number of osmium redox sites available on the electrode surface and how this value changes when the percentage of crosslinker is varied from 1% to 5% and also when the sensors have been soaked in buffer for periods of 0, 1 and 10 hours.

Inspection of the values in Table 6.3 for the samples prepared with a 1% PEGDGE crosslinking composition, reveals a decreasing ratio of maximum current response to oxidation peak height with an increased soak time in phosphate buffer. This indicates that after a prolonged period of immersion the number of active osmium redox sites on the electrode is reduced, suggesting that there is a detachment of polymeric material from the electrode surface. In contrast, the number of osmium sites calculated for the 5% PEGDGE samples appears to fluctuate very little with increased immersion time, implying minimal loss of polymer into solution.

These results, therefore, indicate that the use of 5% PEGDGE when preparing the bienzyme glutamate electrodes employing the POs-EA osmium hydrogel produces a more consistent/stable number of active redox sites than sensors prepared with a 1% PEGDGE crosslinking composition, especially if the sensors are to be operated for prolonged periods of time in aqueous solutions. This corroborates the chronoamperometric results of Section 6.2.1 which illustrate that a 5% PEGDGE composition is more effective at providing a strongly wired osmium hydrogel, glutamate oxidase and soybean peroxidase layer on the electrode surface. Sensors

bound with 5% crosslinker obtain their strength from an increased structural integrity of the polymer film which subsequently allows increased electrical connection of the enzyme entrapped within it.

Similar experiments have been performed by Heller *et al*[92] using cyclic voltammetry to estimate the amount of material on the surface when the percentage of PEGDGE was varied between 1.6% and 18.5%. The results, which were obtained from different enzyme systems on carbon paste electrodes, indicated that there was no discernible effect on the electrochemical properties of the sensors over this range. However, such carbon electrodes are reported to have excellent adherence to redox hydrogels[116]. The electrodes used in this set of experiments were prepared by electro-depositing gold onto glass and may possess different hydrogel adherence properties when immersed in solution i.e. when the hydrogel is swollen.

6.2.3 - XPS Analysis

The final technique employed to investigate the surface composition of osmium hydrogel sensors prepared with different percentages of crosslinker and after increased periods of immersion in phosphate buffer was that of XPS. As in previous chapters, individual elemental spectra, C(1s), N(1s), S(2p), Os(4f) and Au(4f), were collected and compared with each other to provide information on the sensing layer composition. All measurements were performed at a take-off angle of 90° to maximise the volume being sampled.

Initially the gold Au(4f) spectra were examined for both sets of samples, i.e. using 1% and 5% PEGDGE, in order to quantify the amount of underlying gold electrode which can be observed. Experiments were performed as a function of increased time of incubation in PBS. The background subtracted spectra for each crosslinking percentage are shown in Figure 6.3.

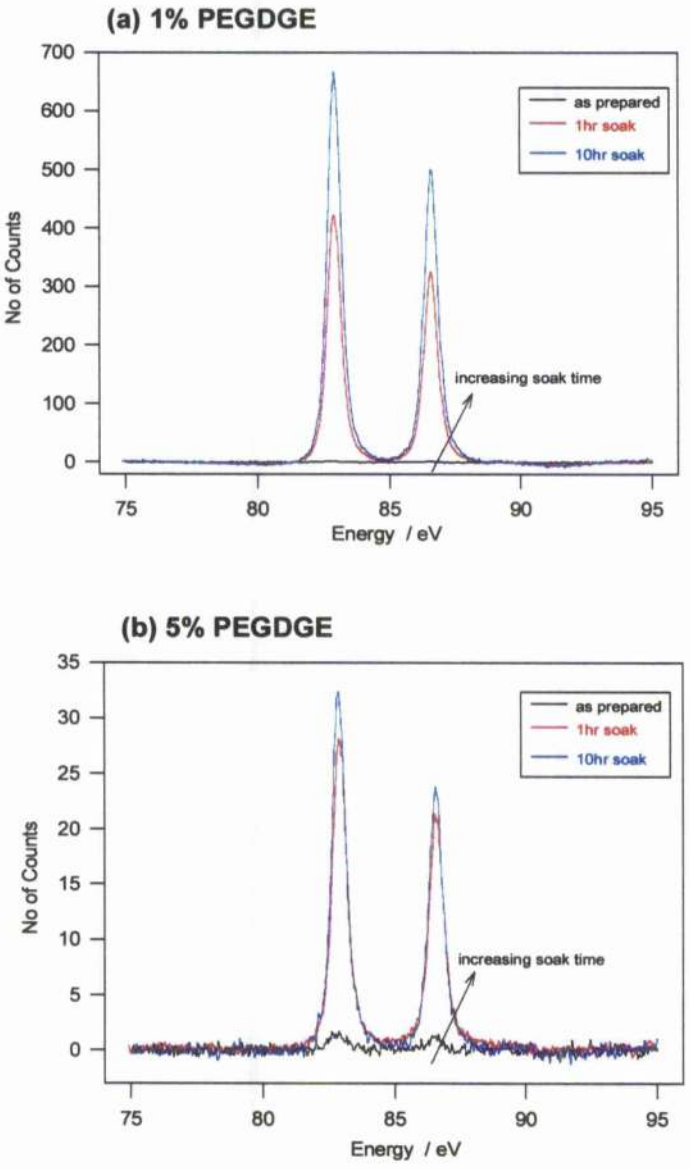

Figure 6.3 - Comparison of the Au(4f) spectra for samples prepared using (a) 1% and (b) 5% PEGDGE crosslinker which have been soaked in phosphate buffer for periods of 0, 1 and 10 hours. The spectra were collected as described in section 6.1.2.3. Note the decrease in scales and increase in noise levels from (a) to (b) as a function of increased sensitivity of the lower measurement

Examination of the spectra in Figure 6.3 show clearly that for both crosslinker percentages there is a marked increase in the amount of gold detected as the samples are soaked for longer periods of time. The implication, corroborated by electrochemistry, is that material is lost from the surface when the electrodes are immersed for extended periods in aqueous solutions. This effect is observed to a

greater extent for those samples prepared with a 1% PEGDGE composition, as compared with those at 5% PEGDGE.

In comparison with the effectively zero amount of gold detected in the 'as prepared' samples, the values obtained for the 1% samples show a 700% increase, with respect to peak height, whereas those obtained from the 5% samples rise only by 35%, with respect to peak height. Therefore, it appears that as the polymer swells in solution a higher percentage of crosslinker is required in order to minimise the amount of material (enzyme and/or polymer) being lost from the sensing layer.

This result can be substantiated by comparing the background values obtained for the measured sample spectra for each element. For example, the C(1s) spectra obtained for each sample (both 1% and 5% PEGDGE) are shown in Figure 6.4 (a) and (b) before baseline subtraction was performed. The background measured from the as prepared samples are considerably lower than those for the soaked samples at the low PEGDGE percentage. Such a difference in background can be accounted for by a difference in sample density i.e. higher background values are produced by thinner or less dense films. This too can, therefore, be used as an indication that there is less material on the surface after a long soak time and this becomes increasingly less if the samples are prepared using a low percentage of crosslinker.

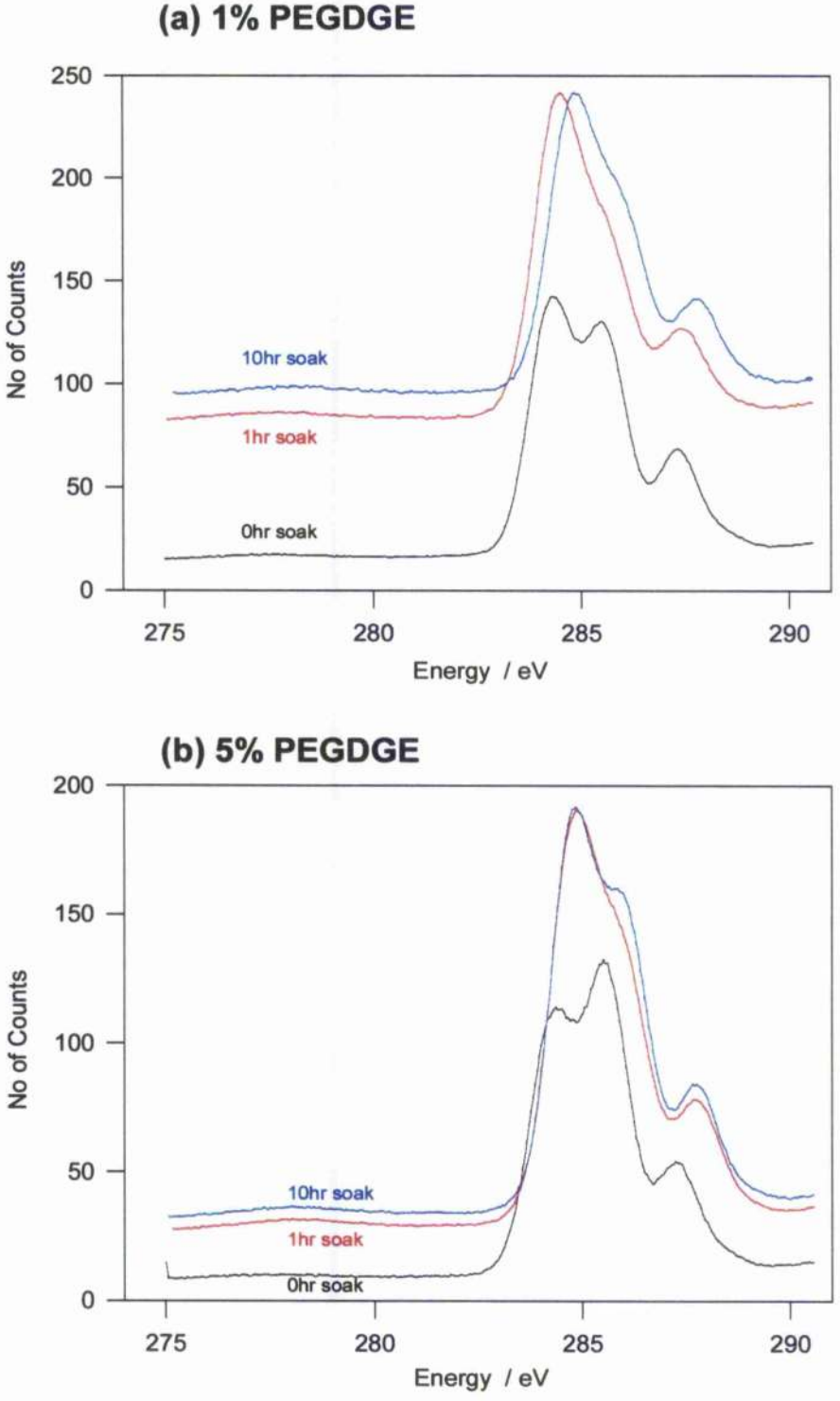

Figure 6.4 - Comparison of the carbon C(1s) spectra obtained by XPS (as described in section 6.1.2.3) for samples prepared with (a) 1% and (b) 5% PEGDGE crosslinker. Each set of plots shows the spectra for samples under various stages of hydration i.e. soaked in buffer for 0, 1 and 10 hours.

The peaks in the C(1s) spectra in Figure 6.4 can also be used to observe this 'falling off'/desorption of material from the electrode surface. The peak that occurs around 286 eV corresponds to the C-O and C-N bonding within the polymer layer and its height can be seen to be reduced substantially as the immersion time is increased, indicating a reduction in the amount of polymer on the electrode. The extent of the polymer detachment i.e. the 286 eV peak height decrease, is reduced when the percentage of crosslinker is increased to 5%. Also, the peak that occurs at 288 eV, which can be used as a marker for the enzyme content of the film, implies a substantially reduced detachment of material. This has consequence when considering the ratio of maximum sensor response current, I_{max}, to CV peak oxidation current, I_{peak}, as in Table 6.3, and, therefore, the volume of polymer and enzyme within the sensing layer. The values of I_{max} are affected by the amount of both enzyme and polymer whereas the I_{peak} values are affected only by the polymer. By examining the XPS carbon spectra it is possible to observe the change in amount of both polymer and enzyme which are responsible for the variation in this ratio.

Similarly, the osmium Os(4f), nitrogen N(1s) and sulphur S(2p) spectra, as shown in Figure 6.5, were examined by eye, to provide information on the amount of polymer and enzyme contained within the films before and after soaking. Once again, as mentioned above, increasing background values for each set of spectra followed an increasing soak time. The spectra were also examined after background subtraction had been performed (data not shown here) to ascertain the peak height variation.

By considering the sets of Os(4f) spectra corresponding to 1% and 5% PEGDGE it can be seen that the peaks corresponding to different osmium bond groups vary notably in height as a function of immersion time. For both the 1% and 5% PEGDGE samples, an increase in the height of the two main peaks at 50 and 53 eV is observed as the samples are soaked for longer periods of time. The peak present at 56 eV, which is seen to increase greatly with soak time, can be attributed not to osmium but to electrons in a different energy level in the underlying gold, Au(5p). The growth of this signal with increasing soak time is in agreement with the result obtained from the Au(4f) spectra, as described previously.

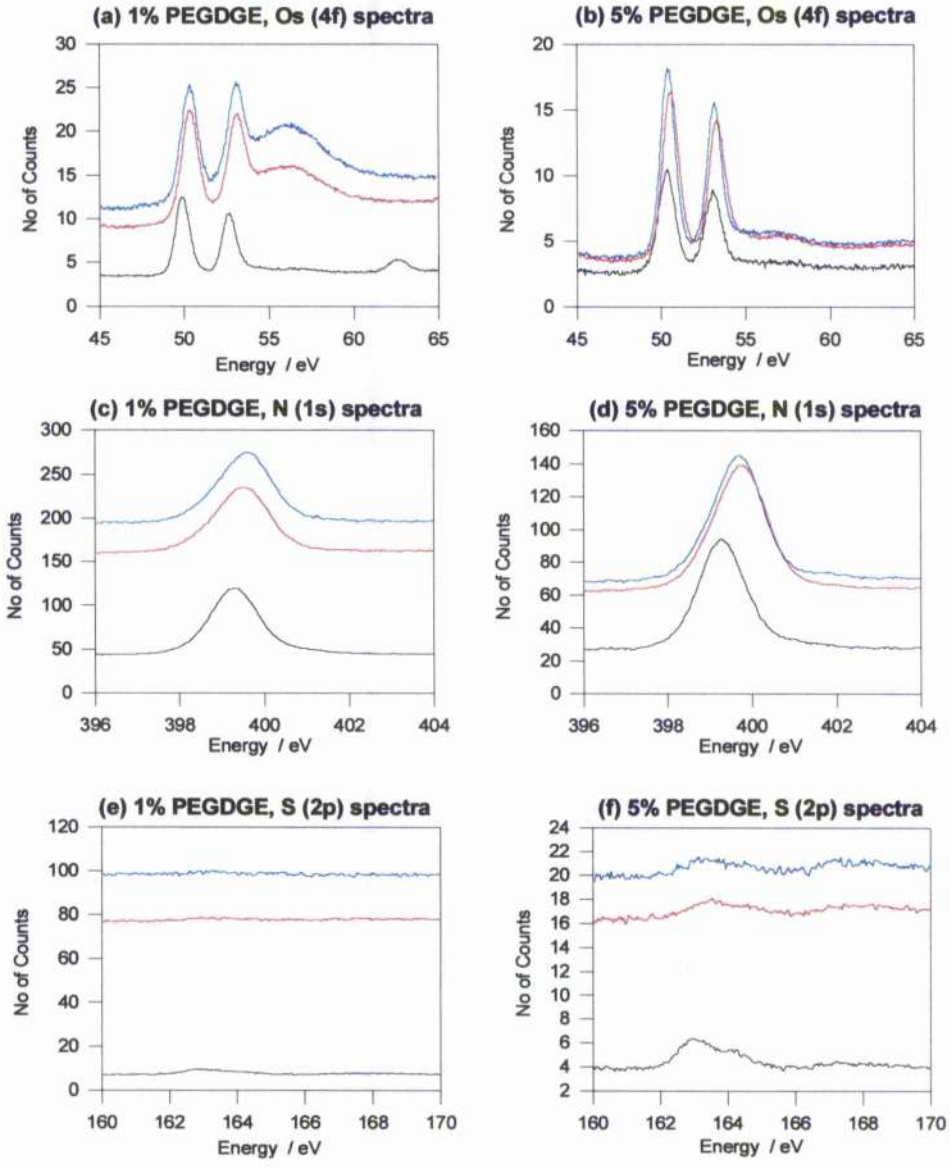

Figure 6.5 - XPS spectra obtained for various elements: (a) osmium, characteristic purely of polymer, Os(4f) for samples prepared with 1% PEGDGE, (b) as for (a) but with a 5% PEGDGE, (c) nitrogen, characteristic of enzyme, N(1s) for 1% PEGDGE, (d) N(1s) for 5% PEGDGE, (e) sulphur, characteristic of amino acids in the enzyme, S(2p) for 1% PEGDGE and (f) S(2p) for 5% PEGDGE.

The peak heights of the N(1s) spectra from both sets of samples do not show any considerable variation and, therefore, do not provide a great deal of information on the sensing layer configuration. However, as this is a bienzyme system the nitrogen spectra contain counts obtained for both glutamate oxidase and soybean peroxidase. It is essential for optimisation of the sensors that the amount of the analyte-specific

enzyme, GLOx, can be determined. This may be possible by examining the XPS spectra for the sulphur S(2p) present in the enzymes.

Two of the most common amino acids which contain sulphur groups are cysteine, recognisable by a (-SH) group and methionine which possesses a ($-S-CH_3$) group. By examining the amino acid structure of both the enzymes, GLOx and SBP, it may be possible to identify the number of cysteines and methionines in each. Although it is difficult to resolve from Figure 6.5 (e) and (f), the sulphur spectra can be decomposed into two sulphur environments corresponding to each of these amino acid end groups. The heights of these peaks could be used with the ratio of cysteine to methionine for each enzyme to provide estimates of the amount of each enzyme within the sensing layer. Unfortunately, the amino acid structures of both enzymes were unavailable and so this theory was not able to be tested.

In general, the spectra obtained from the 5% PEGDGE samples appeared to be more visually consistent than those from the 1% samples indicating a more strongly wired system.

The final piece of analysis performed on the XPS data used the area under the spectra to provide a quantitative estimate of the amount of material on the electrode surface. The number of counts under the peaks were measured over a 10 eV energy range for the Au(4f), Os(4f), N(1s) and S(2p) spectra and compared for each sample. These results are shown in Figure 6.6.

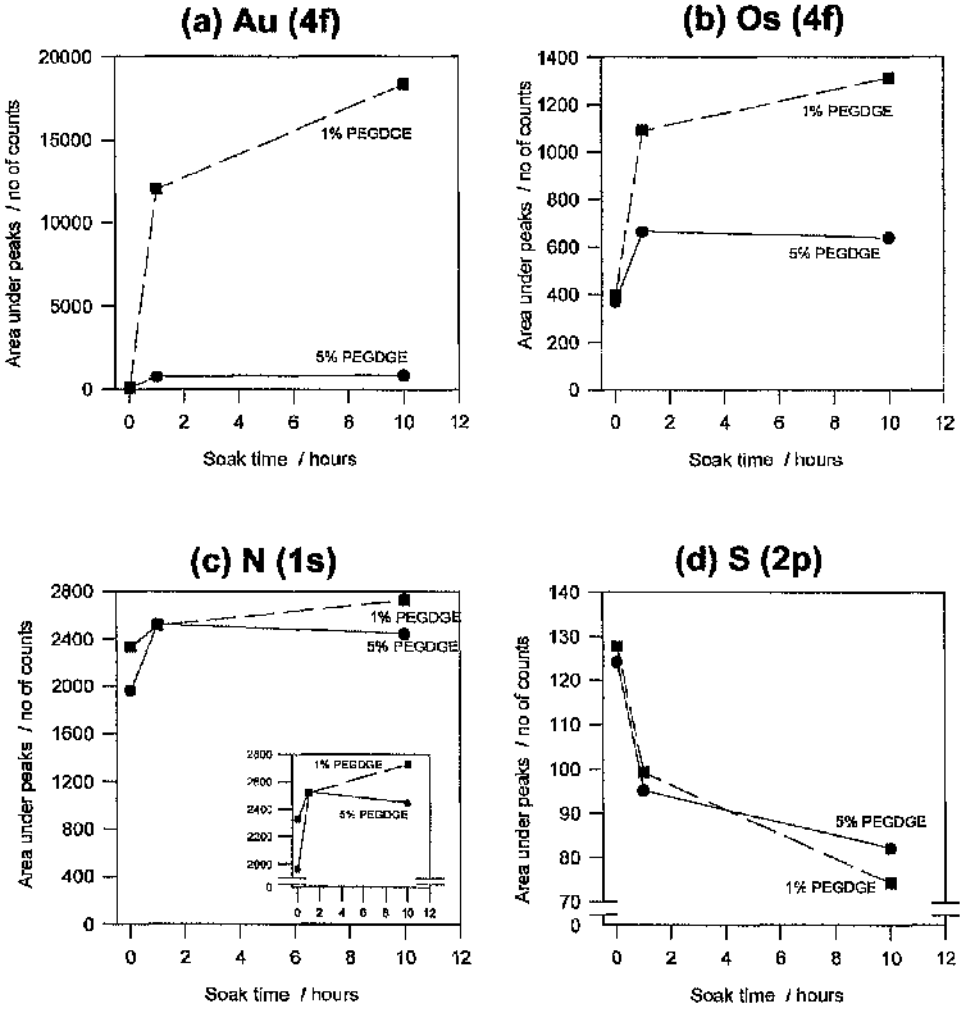

Figure 6.6 - Comparison of area under the peaks i.e. amount of material on the surface of samples prepared with 1% and 5% PEGDGE. Plots are shown for the values obtained from (a) Au(4f), (b) Os(4f), (c) N(1s) and (d) S(2p) spectra.

By looking separately at each of the plots in Figure 6.6 it is possible to obtain an idea of the amount of each material on the sample surface as a function of both crosslinker concentration and soak time. The data for the gold spectra integrations in Figure 6.6 (a) show that although when the samples are measured 'as prepared' there is little variation between the 1% and 5% samples in the amount of gold surface exposed; but the increase in variation is considerably larger as a result of increased immersion time. After a 10 hour soak in buffer both samples show a considerable increase in the amount of gold electrode detected, however, the sample prepared with 1% PEGDGE shows a 95% increase over that for the sample prepared with 5%

PEGDGE. This corroborates well with the electrochemical results obtained for the samples.

Examination of the Os(4f) spectra values in Figure 6.6 (b) shows that after a 10 hour soak in buffer there appears to be more polymeric material on the surface of the 1% PEGDGE sample than the 5% sample. This is most likely to be an effect of the swelling properties of the osmium hydrogel increasing the density of sites within the interfacial region.

The amount of enzymatic material on the surface was provided by the plots in Figure 6.6 (c) and (d). The nitrogen N(1s) values indicated that there was a consistent amount of enzyme on the surface irrespective of crosslinker percentage. However, the sulphur S(2p) values showed a 34% and 42% drop between the 'as prepared' and 10 hour soak for the 5% and 1% PEGDGE samples respectively, (with respect to scales on the other graphs in the figure) showing that there is in fact a decrease in the amount of enzyme wired within the hydrogel as it swells in solution.

6.3 Summary

The work completed in this chapter compliments that of Chapter 5 by examining the effect of varying the proportion of PEGDGE crosslinker that holds the enzymes within the osmium hydrogel. Additionally the sensors were immersed in phosphate buffer for periods of up to 10 hours and the effect of this on their response and composition assessed. This analysis was performed using three techniques: chronoamperometry, cyclic voltammetry and X-ray photoelectron spectroscopy.

The electrochemical responses of the sensors to glutamate over the range 0 - 25 mmol dm^{-3} was determined by chronoamperometry. The results showed that the electrochemical responses to glutamate were lower for those sensors prepared with a 1% PEGDGE crosslinker procedure and also decreased when left soaking for

prolonged periods of time, suggesting that a higher concentration of crosslinker is required to achieve a strongly bound hydrogel sensor.

Cyclic voltammetric experimental results showed that the number of active osmium sites on the surface is reduced when the proportion of crosslinker in the sensors is decreased from 5% to 1%. This reduction in active sites was also found when the sensors were immersed in buffer for long periods of time indicating that there is a 'falling off'/desorption of material from the electrode surface.

Finally, the technique of XPS looked at the amount of each individual component of the sensing layer. As the crosslinker percentage in the hydrogel film is decreased and the soak time increased there is a substantial rise in the amount of gold electrode observed through the sensing layer. This indicates that polymeric and/or enzymatic material is becoming detached from the electrode surface. By examining the amount of nitrogen and sulphur in the samples, corresponding to the amount of enzyme present, a decrease was observed with increasing soak time for both 1% and 5% samples but the size of this decrease was substantially larger for the 1% samples. The amount of osmium observed in both 1% and 5% samples appeared to rise with increased soak time which is attributable to the swelling effects of the hydrogel. Therefore, the results in this chapter suggest that samples prepared with a 5% PEGDGE crosslinker composition will provide a much more stable and strongly wired hydrogel sensor.

CHAPTER 7 - CONCLUSIONS

The work completed in the course of this thesis investigated the composition of glucose biosensor interfaces using the novel combination of electrochemical and spectroscopic techniques in order to generate a 'model' system upon which to base the development of glutamate biosensors.

Initially glucose sensors were prepared by electro-entrapment of the enzyme glucose oxidase (GOx) within thin, non-conducting films of poly(o-phenylenediamine) (p(pd)). Their electrochemical responses to glucose over the range 0 - 100 mmol dm^{-3} were examined as a function of electrode material, method of enzyme entrapment, enzyme solution concentration and solution oxygen concentration. The method of preparation which produced optimal electrochemical response and maximal enzyme loading within the film, for both gold and platinum electrode-based sensors, was that of copolymerisation from a solution containing both enzyme and monomer. However, it was found that although the use of higher concentrations of enzyme in the polymerisation solution produced larger current responses, this was only true up to a point, after which the current response was reduced by increasing enzyme solution concentration. Investigation of the dependence of the platinum-based sensors on solution oxygen was performed, as the result of a European Fellowship, in the Department of Chemistry, University College Dublin, Dublin (Eire) under the supervision of Dr. R. O'Neill who has looked extensively at the operation of p(pd) glucose sensors under anaerobic conditions[115]. This work highlighted the interesting feature of such sensors to operate under anaerobic conditions.

Additionally, the specificity of the sensors was examined by determination of their ability to successfully exclude electro-active interferents such as ascorbate. This has particular application when considering their operation *in vivo*, where the sensing fluid is a complex matrix such as blood or extra-cellular fluid. Sensors were prepared with a lipid layer (phosphatidylcholine) below the polymer-enzyme sensing

layer to complement the size exclusion properties of the p(pd) films and, hence, minimise further the proportion of the current response due to interfering electro-active species such as ascorbate. Preliminary investigations were performed which involved extending the duration of polymerisation in order to fill in any 'gaps' in the polymer layer and further reduce the signal due to electro-active interferents.

X-ray photoelectron spectroscopic (XPS) and Fourier Transform infra-red (FT-iR) spectroscopic analysis of the same samples (prepared on gold electrodes) at two different take-off angles (i.e. a shallow 10° and a steeper 90°), not only corroborated the electrochemical results, but also suggested the micro-environment of the polymer and enzyme within the sensing layer, i.e. the enzyme may 'stand proud' of the polymer matrix.

In order to quantify the XPS results, the polymer matrix was changed to poly(fluorophenol), (p(fp)), which also forms a thin, non-conducting film but its fluorine content has a higher intensity on the XPS spectra. Identical experiments to those prepared with p(pd) films were performed and the results indicated that with this polymer the enzyme appeared to be 'buried' within the film. Once again electrochemical analysis of the sensors' response indicated that by using the procedure of copolymerisation of monomer and a high solution concentration of enzyme, it was possible to maximise the sensor operation. Using an expression that models the theoretical steady-state response of enzymes entrapped within thin polymer films[132], estimates were able to be made for the kinetic parameters of the system.

Finally, in order to overcome the problems associated with electropolymerised sensors, i.e. the high operating potentials and corresponding large signals due to electro-active interference, led to the development of hydrogel based systems which operate at much lower potentials and have a greatly increased response to analyte. Glutamate sensors were prepared using the osmium based hydrogel, poly(vinylpyridine)-containing Os(dimethylbipyridine)$_2$Cl$_2$, in both single and bienzyme layer formats. The most effective method was the bienzyme system which

contained the polymer, both GOx and soybean peroxidase (SBP) and was held together with a crosslinker of polyethyleneglycol diglycidyl ether (PEGDGE). This method of enzyme immobilisation was transferred successfully to microelectrodes (carbon fibre, 8 μm diameter) and produced, consistently, current densities in the order of 3 mA cm^{-2}. The addition of a layer of cellulose acetate enhanced the selectivity of the sensor such that a 60% increase in the signal to noise ratio was observed. This hydrogel work was performed, as a result of a Foreign Exchange programme, in the Department of Chemical Engineering, University of Texas at Austin, Austin, Texas under the supervision of Professor Adam Heller. Additional spectroscopic analyses were performed using XPS (Daresbury Laboratories) and FT-iR (in-house) facilities to examine the effect that variation of the preparation parameters had on the sensor composition. The result of such analyses suggested that a crosslinker percentage of 5% PEGDGE was required to ensure the stability of the wiring of the sensor, especially if it is to be operated in aqueous solution for prolonged periods of time.

7.1 Suggestions for Further Work

In order to obtain highly sensitive and selective glutamate microsensors for applications *in vivo*, future developments should concentrate on the improved development of the hydrogel based microelectrodes. This would involve varying the percentage composition of the components in the bienzyme construction (GLOx, SBP, PEGDGE & POs-EA) as well as investigations into the length of drying/curing time of the sensing layer in order to maximise the sensor response. However, the most substantial improvement that could be achieved for this type of sensor, and for every construction of sensor, is the elimination of the interfering signal, due to oxidation of electro-active species present in the physiological fluids, which reduces the signal to noise ratio of the sensors. Therefore, this effect should be investigated in more detail, perhaps using the quad layer construction suggested by Heller *et al.*[129]. This was based on carbon macroelectrodes using a sandwich type

construction containing two layers of cellulose acetate and was found to be relatively insensitive to interferents. The application of such a construction to microelectrodes would have to be considered.

Further investigations into the non-conducting polymer based sensors would also be advantageous as the information on the positioning of the enzyme within the polymer layer has great application for enzyme immobilisation and characterisation of biosensor interfaces. Although the XPS and FT-iR studies provided the basis for the extraction of information on the relationship between enzyme solution and surface concentration, more extensive quantitative analysis of the XPS and FT-iR data is required involving the discovery and use of superior fitting routines and baseline subtraction/correction methods.

Additionally, the technique of iodination of the enzyme in the sensing layer, initial investigations into which were performed during this project, for the purpose of XPS measurements is worth exploring further. In a similar manner to the use of the fluorine in the polyfluorophenol polymer, iodination of the enzyme glucose oxidase was performed which provided a label for the enzyme in the sensing layer. Like fluorine, iodine produces a strong signal on the XPS spectra, allowing the distinction of polymer and enzyme by the fluorine and iodine spectra as opposed to the nitrogen or carbon spectra. Although the preliminary XPS results obtained for iodinated GOx in a p(fp) polymer matrix produced an unidentified secondary peak in the iodine spectra which may have been caused by insufficient dialysis of the enzyme, the electroactivity of the enzyme did not seem to be altered. However, others have successfully iodinated enzymes and so further progression of this technique would be encouraged as it has prospect of providing detailed information on enzyme entrapment within thin polymer films.

7.2 Publications and Conference Contributions Arising from this Work

- 'Glutamate oxidase enzyme electrodes: microsensors for neurotransmitter determination using electrochemically polymerised permselective films', Cooper, J.M., Foreman, P.L., Glidle, A., Ling, T.W. & Pritchard, D.J., *Journal of Electroanalytical Chemistry* (388):143-149, 1995.

- 'Probing Thin Layer Enzyme-Polymer Matrices Using XPS', Foreman, P.L., Cooper, J.M. & Glidle, A., Presented as a poster at Electrochem 96 Conference: Bath, England 14 - 17th September 1996

- 'XPS and FT-iR to Probe Thin Layer Biosensor Interfaces', Foreman, P.L., Cooper, J.M. & Glidle, A., Presented as a poster at Artificial Biosensor Interfaces, European Union Network Conference at Tubingen, Germany 10 - 12th October 1996.
- 'Characterisation of Biosensor Interfaces Using Spectroscopic Techniques', Foreman, P.L., Cooper, J.M. & Glidle, A., Presented as a poster at Artificial Biosensor Interfaces, European Union Network Conference Sitges, Barcelona, Spain 23 - 25th October 1997.

- 'Spectroscopic Characterisation of Biosensor Interfaces: The Applications of XPS and FT-iR to the Determination of Enzymes in Polymer Films, Foreman, P.L., Cooper, J.M., Glidle, A., and Beamson, G, To be submitted to *Langmuir*, 1998.

REFERENCES

1. Collings, A.F. and F. Caruso, *Biosensors: Recent Trends.* Reports on Progress in Physics, 1997. **60**(11): p. 1397-1445.
2. Rouhi, A.M., *Biosensors Send Mixed Signals - Despite remarkable breadth of biosensor research, commercial success has been limited.* Chemical and Engineering News, 1997. **75**(19): p. 41-45.
3. Scheller, F.W., *et al.*, *Biosensors: trends and commercialisation.* Biosensors, 1985. **1**: p. 135-160.
4. Vadgama, P. and P.W. Crump, *Biosensors: Recent Trends.* Analyst, 1992. **117**: p. 1657-1670.
5. Alcock, S.J. and A.P.F. Turner, *Continuous analyte monitoring to aid clinical practice.* IEEE Engineering in Medicine and Biology, 1994: p. 319-325.
6. Connolly, P., *Clinical diagnostics opportunities for biosensors and bioelectronics.* Biosensors & Bioelectronics, 1995. **10**: p. 1-6.
7. Tamiya, E. and I. Karube, *Micro-biosensors for clinical analyses.* Sensors and Actuators, 1988. **15**: p. 199-207.
8. Fischer, U., S. Alcock, and A.P.F. Turner, *Assessment of devices for in vivo monitoring of chemical species.* Biosensors & Bioelectronics, 1995. **10**(5): p. xxiii-xxx.
9. Nicolini, C., *From neural chip and engineered biomolecules to bioelectronic devices: An overview.* Biosensors & Bioelectronics, 1995. **10**: p. 105-127.
10. Reach, G., J. Feijen, and S. Alcock, *BIOMED concerted action chemical sensors for in vivo monitoring. The biocompatibility issue.* Biosensors & Bioelectronics, 1994. **9**(6): p. xxi-xxviii.
11. Sethi, R.S., *Transducer aspects of biosensors.* Biosensors & Bioelectronics, 1994. **9**(3): p. 243-264.
12. Vadgama, P., *Biosensors: Adaptation for Practical Use.* Sensors and Actuators B, 1990. **1**: p. 1-7.

13. Brunner, G.A., *et al.*, *Validation of home blood glucose meters with respect to clinical and analytical approaches.* Diabetes Care, 1998. **21**(4): p. 585-590.

14. King, J.M., C.A. Eigenmann, and S. Colagiuri, *Effect of ambient temperature and humidity on performance of blood glucose meters.* Diabetic Medicine, 1995. **12**(4): p. 337-340.

15. Tieszen, K.L., *et al.*, *Evaluation of a second-generation electrochemical blood glucose monitoring system.* Diabetic Medicine, 1995. **12**: p. 173-176.

16. Trajanoski, Z., *et al.*, *Accuracy of home blood glucose meters during hypoglycemia.* Diabetes Care, 1996. **19**(12): p. 1412-1415.

17. Clark, R.A., P.B. Hietpas, and A.G. Ewing, *Electrochemical analysis in picoliter microvials.* Analytical Chemistry, 1997. **69**(2): p. 259-263.

18. Dietrich, T.R., *et al.*, *Fabrication technologies for microsystems utilizing photoetchable glass.* Microelectronic Engineering, 1996. **30**: p. 497-504.

19. Dawson, D.A., *et al.*, *Anti-ischaemic efficacy of a nitric oxide synthase inhibitor and a N-methyl-D-aspartate receptor antagonist in models of transient and permanent focal cerebral ischaemia.* British Journal of Pharmacology, 1994. **113**: p. 247-253.

20. Katayama, Y., *et al.*, *Calcium-dependent glutamate release concomitant with massive potassium flux during cerebral ischaemia in vivo.* Brain Research, 1991. **558**: p. 136-139.

21. Szatkowski, M. and D. Attwell, *Triggering and execution of neuronal death in brain ischaemia: two phases of glutamate release by different mechanisms.* Trends in Neuroscience, 1994. **17**(9): p. 359-364.

22. Todd, A.J., *et al.*, *Immunocytochemical evidence that neurotensin is present in glutamatergic neurons in the superficial dorsal horn of the rat.* The Journal of Neuroscience, 1994. **14**(2): p. 774-784.

23. Todd, A.J. and R.C. Spike, *The localisation of classical transmitters and neuropeptides within neurons in laminae I-III of the mammalian spinal dorsal horn.* Progress in Neurobiology, 1993. **41**(5): p. 609-645.

24. Wahl, F., *et al.*, *Extracellular glutamate during focal cerebral ischaemia in rats: time course and calcium dependency.* Journal of Neurochemistry, 1994. **63**(3): p. 1003-1010.

25. Almeida, N.F. and A.K. Mulchandani, *A mediated amperometric enzyme electrode using tetrathiafulvalene and L-glutamate oxidase for the determination of L-glutamic acid.* Analytica Chimica Acta, 1993. **282**: p. 353-361.

26. Alvarez-Crespo, S.L., *et al.*, *Amperometric glutamate biosensor based on poly(o-phenylenediamine) film electrogenerated onto modified carbon paste electrodes.* Biosensors & Bioelectronics, 1997. **12**(8): p. 739-747.

27. Berners, M.O.M., M.G. Boutelle, and M. Fillenz, *On-line measurement of brain glutamate with an enzyme/polymer-coated tubular electrode.* Analytical Chemistry, 1994. **66**(13): p. 2017-2021.

28. Chen, C.Y. and Y.C. Su, *Amperometric L-glutamate sensor using a novel L-glutamate oxidase from Streptomyces platensis NTU 3304.* Analytica Chimica Acta, 1991. **243**: p. 9-15.

29. Cooper, J.M., *et al.*, *Glutamate oxidase enzyme electrodes: microsensors for neurotransmitter determination using electrochemically polymerised permselective films.* Journal of Electroanalytical Chemistry, 1995(388): p. 143-149.

30. Olson Cosford, R.J. and W.G. Kuhr, *Capillary biosensors for glutamate.* Analytical Chemistry, 1996. **68**(13): p. 2164-2169.

31. Cosnier, S., *et al.*, *An electrochemical method for making enzyme microsensors. Application to the detection of dopamine and glutamate.* Analytical Chemistry, 1997. **69**(5): p. 968-971.

32. Ghobadi, S., *et al.*, *Bienzyme Carbon Paste Electrodes for L-Glutamate Determination.* Current Separations, 1996. **14**(3/4): p. 94-102.

33. Hale, P.D., *et al.*, *Glutamate biosensors based on electrical communication between L-glutamate oxidase and a flexible redox polymer.* Analytical Letters, 1991. **24**(3): p. 345-356.

34. Kacaniklic, V., *et al.*, *Amperometric biosensors for detection of L- and D-amino acids based on coimmobilized peroxidase and L- and D- amino acid oxidases in carbon paste electrodes.* Electroanalysis, 1994. **6**: p. 381-390.

35. Moser, I., *et al.*, *Miniaturised Thin Film Glutamate and Glutamine Biosensors.* Biosensors & Bioelectronics, 1995. **10**: p. 527-532.

36. Mulchandani, A. and A.S. Bassi, *Determination of glutamine and glutamic acid in mammalian cell cultures using tetrathiafulvalene modified enzyme electrodes.* Biosensors & Bioelectronics, 1996. **11**(3): p. 271-280.

37. Osborne, P.G., *et al.*, *On-line, real time measurements of extracellular brain glucose using microdialysis and electrochemical detection.* Current Separations, 1996. **15**(1): p. 1-7.

38. Zilkha, E., *et al.*, *Amperometric biosensors for on-line monitoring of extracellular glucose and glutamate in the brain.* Analytical Letters , 1994. **27**(3): p. 453-473.

39. Schubert, F., *et al.*, *Enzyme electrodes for L-glutamate using chemical redox mediators and enzymatic substrate amplification.* Analytical Letters, 1986. **19**(11 & 12): p. 1273-1288.

40. Vahjen, W., *et al.*, *Mediated enzyme electrode for the determination of L-glutamate.* Analytical Letters, 1991. **24**(8): p. 1445-1452.

41. Villarta, R.L., D.D. Cunningham, and G.G. Guilbault, *Amperometric enzyme electrodes for the determination of L-glutamate.* Talanta, 1991. **38**(1): p. 49-55.

42. White, S.F., *et al.*, *On-line monitoring of glucose, glutamate and glutamine during mammalian cell cultivations.* Biosensors & Bioelectronics, 1995. **10**: p. 543-551.

43. Hu, Y., *et al.*, *Direct measurement of glutamate release in the brain using a dual enzyme-based electrochemical sensor.* Brain Research, 1994. **659**: p. 117-125.

44. Aizawa, M., *Biosensors for molecular identification*, in *Intelligent Sensors*, H. Yamasaki, Editor. 1996, Elsevier Science. p. 85-97.

45. Aizawa, M., *Molecular Interfacing for Protein Molecular Devices and Neurodevices.* IEEE Engineering in Medicine and Biology, 1994. **February/March**: p. 94-102.

46. Cooper, J.M. and C.J. McNeil, *Biosensors*, in *The Encyclopaedia of Advanced Materials*, D. Bloor, *et al.*, Editors. 1994, Pergamon. p. 257-264.

47. Ghindilis, A.L., *et al.*, *Immunosensors: Electrochemical Sensing and Other Engineering Approaches.* Biosensors & Bioelectronics, 1998. **13**(1): p. 113-131.

48. Giuliano, K.A. and D.L. Taylor, *Fluorescent-Protein Biosensors: New Tools for Drug Discovery.* Trends in Biotechnology, 1998. **16**(3): p. 135-140.

49. Hellinga, H.W. and J.S. Marvin, *Protein Engineering and the Development of Generic Biosensors.* Trends in Biotechnology, 1998. **16**(4): p. 183-189.

50. Byfield, M.P. and R.A. Abukeshna, *Biochemical aspects of biosensors.* G.E.C. J. of Research, 1991. **9**(2): p. 97-1117.

51. Holden Thorp, H., *Cutting Out the Middleman: DNA Biosensors Based on Electrochemical Oxidation.* Trends in Biotechnology, 1998. **16**(3): p. 117-121.

52. Anderson, G.P., *et al.*, *Development of an evanescent wave fiber optic biosensor.* IEEE Engineering in Medicine and Biology, 1994: p. 358-363.

53. Barker, S.L.R., *et al.*, *Fiber-Optic Nitric Oxide-Selective Biosensors and Nanosensors.* Analytical Chemistry, 1998. **70**(5): p. 971-976.

54. Bond, A.M., *Past, present and future contributions of microelectrodes to analytical studies employing voltammetric detection.* Analyst, 1994. **119**: p. R1-R21.

55. Bruckenstein, S. and M. Shay, *Experimental aspects of use of the quartz crystal microbalance in solution.* Electrochimica Acta, 1985. **30**(10): p. 1295-1300.

56. Keese, C.R. and I. Giaever, *A biosensor that monitors cell morphology with electric fields.* IEEE Engineering in Medicine and Biology, 1994: p. 402-407.

57. Muehlbauer, M.J., *et al.*, *Thermoelectric enzyme sensor for measuring blood glucose.* Biosensors & Bioelectronics, 1990. **5**: p. 1-12.

58. Nabauer, A., *et al.*, *Biosensors based on piezoelectric crystals.* Sensors and Actuators B, 1990. **1**: p. 508-509.

59. Soller, B.R., *Design of intravascular fiber optic blood gas sensors.* IEEE Engineering in Medicine and Biology, 1994: p. 327-335.

60. Turner, A.P.F., I. Karube, and G.S. Wilson, *Biosensors: Fundamentals and Applications*. 1 ed. 1987, Oxford: Oxford University Press. 747.

61. Hall, E.A.H., *Biosensors*. 1 ed. Open University Press Biotechnology Series, ed. J.A. Bryant and J.F. Kennedy. 1990, Milton Keynes: Open University Press Biotechnology Series. 351.

62. Clark, L.C. and C. Lyons, *Electrode systems for continuous monitoring in cardiovascular surgery.* Annals New York Academy of Sciences, 1962. **102**: p. 29-45.

63. Holme, D.J. and H. Peck, *Chapter 8 - Enzymes*, in *Analytical Biochemistry*, D.J. Holme and H. Peck, Editors. 1998, Addison Wesley Longman: Harlow. p. 257-305.

64. Lehninger, A.L., *Principles of Biochemistry*. 1 ed. 1982, New York: Worth Publishers Ltd. 1-983.

65. Cooper, J.M. and G. Moores, *Bioelectronics IV - Undergraduate Course Notes*, . 1992-3.

66. Stryer, L., *Biochemistry*. 1 ed. 1988, New York: W.H. Freeman and Company. 1-1065.

67. Alberts, B., *et al.*, *Molecular Biology of the Cell*. 2 ed, ed. R. Adams. 1989, New York: Garland Publishing Inc. 1-1218.

68. Dixon, M. and E.C. Webb, *Enzymes*. 2 ed. 1966, London: Longmans, Green and Co. Ltd. 950.

69. Davis, G., *Electrochemical Techniques for the Development of Amperometric Biosensors.* Biosensors, 1985. **1**: p. 161-178.

70. Kissinger, P.T. and W.R. Heineman, *Cyclic Voltammetry.* Journal of Chemical Education, 1983. **60**(9): p. 702-706.

71. Cooper, J.M., C.J. McNeil, and J.A. Spoors, *Amperometric enzyme electrode for the determination of aspartate aminotransferase and alanine aminotransferase in serum.* Analytica Chimica Acta, 1991. **245**: p. 57-62.

72. Newman, J.D., *et al., Catalytic materials, membranes and fabrication technologies suitable for the construction of amperometric biosensors.* Analytical Chemistry, 1995. **67**(24): p. 4594-4599.

73. Abdel-Hamid, I., P. Atanasov, and E. Wilkins, *Development of a needle-type biosensor for intravascular glucose monitoring.* Analytica Chimica Acta, 1995. **313**: p. 45-54.

74. Bott, A.W., *Electrochemical Methods for the Determination of Glucose.* Current Separations, 1998. **17**(1): p. 25-31.

75. Fortier, G., E. Brassard, and D. Belanger, *Optimisation of a polypyrrole glucose oxidase biosensor.* Biosensors & Bioelectronics, 1990. **5**: p. 473-490.

76. Gilligan, B.J., *et al., Evaluation of a Subcutaneous Glucose Sensor out to 3 Months in a Dog Model.* Diabetes Care, 1994. **17**(8): p. 882-887.

77. Gilmartin, M.A.T., J.P. Hart, and D.T. Patton, *Prototype, solid-phase glucose biosensor.* Analyst, 1995. **120**: p. 1973-1981.

78. Guerrieri, A., *et al., Electrosynthesized Non-Conducting Polymers as Permselective Membranes in Amperometric Enzyme Electrodes: A Glucose Biosensor Based on a Co-Crosslinked Glucose Oxidase/Overoxidised Polypyrrole Bilayer.* Biosensors & Bioelectronics, 1998. **13**(1): p. 103-112.

79. Labat-Allietta, N. and D.R. Thevenot, *Influence of Calcium on Glucose Biosensor Response and on Hydrogen Peroxide Detection.* Biosensors & Bioelectronics, 1998. **13**(1): p. 19-29.

80. Mann-Buxbaum, E., *et al., New microminiaturised glucose sensors using covalent immobilisation techniques.* Sensors and Actuators B, 1990. **1**: p. 518-522.

81. Mercado, R.C. and F. Moussy, *In vitro and in vivo Mineralization of Nafion Membrane Used for Implantable Glucose Sensors.* Biosensors & Bioelectronics, 1998. **13**(2): p. 133-145.

82. Pickup, J.C., G.W. Shaw, and D.J. Claremont, *Implantable glucose sensors: Choosing the appropriate sensing strategy.* Biosensors, 1988. **3**: p. 335-346.

83. Reynolds, E.R. and A.M. Yacynych, *Platinized carbon ultarmicroelectrodes as glucose biosensors.* Electroanalysis, 1993. **5**: p. 405-411.

84. Svorc, J., *et al.*, *Composite Transducers for Amperometric Biosensors. The Glucose Sensor.* Analytical Chemistry, 1997. **69**(11): p. 2086-2090.

85. Yokoyama, K., *et al.*, *Mediated Micro-glucose Sensor using 2uM Platinum Electrodes.* Electroanalysis, 1992. **4**: p. 859-864.

86. Wilson, R. and A.P.F. Turner, *Glucose oxidase: an ideal enzyme.* Biosensors & Bioelectronics, 1992. **7**(3): p. 165-185.

87. Kusakabe, H., *et al.*, *Purification and properties of a new enzyme L-glutamate oxidase, from Streptomyces sp. X-119-6 grown on wheat bran.* Agricultural & Biological Chemistry, 1983. **47**(6): p. 1323-1328.

88. Kusakabe, H., Y. Midorikawa, and T. Fujishima, *Methods for determining L-glutamate in soy sauce with L-glutamate oxidase.* Agricultural & Biological Chemistry, 1984. **48**(1): p. 181-184.

89. Rolfe, P., *Intra-vascular oxygen sensors for neonatal monitoring.* IEEE Engineering in Medicine and Biology, 1994: p. 336-345.

90. Geise, R.J., S.Y. Rao, and A.M. Yacynych, *Electropolymerised 1,3-diaminobenzene for the construction of a 1,1'-dimethylferrocene mediated glucose biosensor.* Analytica Chimica Acta, 1993. **281**: p. 467-473.

91. Gregg, B.A. and A. Heller, *Redox polymer films containing enzymes. 1. A redox-conducting epoxy cement: synthesis, characterisation and electrocatalytic oxidation of hydroquinone.* The Journal of Physical Chemistry, 1991. **95**(15): p. 5970-5975.

92. Gregg, B.A. and A. Heller, *Redox polymer films containing enzymes. 2. Glucose oxidase containing enzyme electrodes.* The Journal of Physical Chemistry, 1991. **95**(15): p. 5976-5980.

93. Heller, A. and Y. Degani. *Direct electrical communication between redox enzymes and metal electrodes.* 1989. MRS International Meeting on Advanced Materials: Materials Research Society.

94. Heller, A., *Electrical connection of enzyme redox centres to electrodes.* The Journal of Physical Chemistry, 1992. **96**(9): p. 3579-3587.

95. Jiang, L., C.J. McNeil, and J.M. Cooper, *Direct electron transfer reactions of glucose oxidase immobilised at a self-assembled monolayer.* Journal of the Chemical Society, Chemical Communications, 1995. **12**: p. 1293-1294.

96. Geckeler, K.E. and B. Muller, *Polymer Materials in Biosensors.* Naturwissenschaften, 1993. **80**: p. 18-24.

97. Bartlett, P.N. and J.M. Cooper, *A review of the immobilisation of enzymes in electropolymerised films.* Journal of Electroanalytical Chemistry, 1993. **362**(1-2): p. 1-12.

98. Imisides, M.D., *et al.*, *The use of electropolymerisation to produce new sensing surfaces: A review emphasising electrodeposition of heteroaromatic compounds.* Electroanalysis, 1991. **3**: p. 879-889.

99. Ivaska, A., *Analytical Applications of Conducting Polymers.* Electroanalysis, 1991. **3**: p. 247-254.

100. Geise, R.J. and A.M. Yacynych, *Electropolymerized films in the construction of biosensors.* ACS Symposium Series, 1989. **403**: p. 64-77.

101. Emr, S.A. and A.M. Yacynych, *Use of polymer films in amperometric biosensors.* Electroanalysis, 1995. **7**(10): p. 913-923.

102. Treloar, P.H., I.M. Christie, and P.M. Vadgama, *Engineering the right membranes for electrodes at the biological interface; solvent cast and electropolymerised.* Biosensors & Bioelectronics, 1995. **10**: p. 195-201.

103. Dempsey, E., J. Wang, and M.R. Smyth, *Electropolymerised o-phenylenediamine film as means of immobilising lactate oxidase for a l-lactate biosensor.* Talanta, 1993. **40**(3): p. 445-451.

104. Geise, R.J., *et al.*, *Electropolymerised films to prevent interferences and electrode fouling in biosensors.* Biosensors & Bioelectronics, 1991. **6**: p. 151-160.

105. Lowry, J.P. and R.D. O'Neill, *Partial characterisation in vitro of glucose oxidase-modified poly(phenylenediamine)-coated electrodes for neurochemical analysis in vivo.* Electroanalysis, 1994. **6**: p. 369-379.

106. Sasso, S.V., *et al.*, *Electropolymerized 1,2-diaminobenzene as a means to prevent interferences and fouling and to stabilize immobilised enzyme in electrochemical biosensors.* Analytical Chemistry, 1990. **62**(11): p. 1111-1117.

107. Wang, J. and H. Wu, *Permselective lipid-poly(o-phenylenediamine) coatings for amperometric biosensing of glucose.* Analytica Chimica Acta, 1993. **283**: p. 683-688.

108. Yano, J., *Electrochemical and structural studies on soluble and conducting polymer from o-phenylenediamine.* Journal of Polymer Science: Part A: Polymer Chemistry, 1995. **33**: p. 2435-2441.

109. Chiba, K., *et al.*, *Electrochemical preparation of a ladder polymer containing phenazine rings.* Journal of Electroanalytical Chemistry, 1987. **219**(1-2): p. 117-124.

110. Caruana, D.J., *Electrochemical Immobilisation of Enzymes on Microelectrodes*, in *Chemistry Department*. 1994, University of Southampton. p. 1-213.

111. Plonsey, R., *The Biomedical Engineering Handbook.* 1 ed. The Electrical Engineering Handbook Series, ed. J.D. Bronzino. 1995, Connecticut: CRC Press & IEEE Press. 2819.

112. Palmisano, F., *et al.*, *Correlation between permselectivity and chemical structure of overoxidised polypyrrole membranes used in electroproduced enzyme biosensors.* Analytical Chemistry, 1995. **67**(13): p. 2207-2211.

113. Moussy, F., D.J. Harrison, and R.V. Rajotte, *A Miniaturised Nafion-based glucose sensor: in vitro and in vivo evaluation in dogs.* International Journal of Artificial Organs, 1994. **17**(2): p. 88-94.

114. Gregg, B.A. and A. Heller, *Cross-linked redox gels containing glucose oxidase for amperometric biosensor applications.* Analytical Chemistry, 1990. **62**(3): p. 258-263.

115. Lowry, J.P., *et al.*, *Efficient Glucose detection in anaerobic solutions using an enzyme-modified electrode designed to detect H_2O_2: Implications for biomedical applications.* Journal of the Chemical Society, Chemical Communications, 1994(21): p. 2483-2484.

116. Heller, A., *Electrical wiring of redox enzymes.* Accounts of Chemical Research, 1990. **23**(5): p. 128-134.

117. Katakis, I. and A. Heller, *Electron transfer via redox hydrogels between electrodes and enzymes*, in *Frontiers in Biosensorics I: Fundamental Aspects*,

F.W. Scheller, F. Schubert, and J. Fedrowitz, Editors. 1997, Birkhauser Verlag: Basel, Switzerland. p. 229-241.

118. Heller, A., R. Maidan, and D.L. Wang, *Amperometric biosensors based on three-dimensional hydrogel-forming epoxy networks.* Sensors and Actuators B, 1993. **13-14**: p. 180-183.

119. Heller, A., *Amperometric biosensors.* Current Opinion in Biotechnology, 1996. **7**: p. 50-54.

120. Linke, B., *et al.*, *Amperometric biosensor for in vivo glucose sensing based on glucose oxidase immobilised in a redox hydrogel.* Biosensors & Bioelectronics, 1994. **9**: p. 151-158.

121. Ohara, T.J., R. Rajagopalan, and A. Heller, *Glucose electrodes based on cross-linked $[Os(bpy)_2Cl]^{+/2+}$ complexed with poly(1-vinylimidazole) films.* Analytical Chemistry, 1993. **65**(23): p. 3512-3517.

122. Aoki, A., R. Rajagopalan, and A. Heller, *Effect of quaternization on electron diffusion coefficients for redox hydrogels based on poly(4-vinylpyridine).* The Journal of Physical Chemistry, 1995. **99**(14): p. 5102-5110.

123. Vreeke, M.S. and A. Heller, *Hydrogen Peroxide Electrodes Based on Electrical Connection of Redox Centers of Various Peroxidases to Electrodes through a Three-Dimensional Electron-Relaying Polymer Network.* ACS Symposium Series: Diagnostic Biosensor Polymers, 1994. **556**: p. 180-193.

124. Ohara, T.J., R. Rajagopalan, and A. Heller, *"Wired" enzyme electrodes for amperometric determination of glucose or lactate in the presence of interfering substances.* Analytical Chemistry, 1994. **66**(15): p. 2451-2457.

125. Ohara, T.J., *et al.*, *Bienzyme sensors based on "electrically wired" peroxidase.* Electroanalysis, 1993. **5**: p. 825-831.

126. Maidan, R. and A. Heller, *Elimination of electrooxidizable interferant-produced currents in amperometric biosensors.* Analytical Chemistry, 1992. **64**(23): p. 2889-2896.

127. Vreeke, M., R. Maidan, and A. Heller, *Hydrogen peroxide and β-nicotinamide adenine dinucleotide sensing amperometric electrodes based on electrical connection of horseradish peroxidase redox centres to electrodes*

through a three-dimensional electron relaying polymer network. Analytical Chemistry, 1992. **64**(24): p. 3084-3090.

128. Vijayakumar, A.R., *et al.*, *Alcohol biosensors based on coupled oxidase-peroxidase systems.* Analytica Chimica Acta, 1996. **327**: p. 223-234.

129. Kenausis, G., C. Chen, and A. Heller, *Electrochemical glucose and lactate sensors based on "wired" thermostable soybean peroxidase operating continuously and stably at 37°C.* Analytical Chemistry, 1997. **69**(6): p. 1054-1060.

130. Wightman, M.R. and D.O. Wipf, *Voltammetry at ultramicroelectrodes.* Electroanalytical Chemistry, 1989. **15**: p. 267-353.

131. Malitesta, C., *et al.*, *Glucose fast-response amperometric sensor based on glucose-oxidase immobilised in an electropolymerised poly(ortho-phenylenediamine) film.* Analytical Chemistry, 1990. **62**(24): p. 2735-2740.

132. Bartlett, P.N., P. Tebbutt, and C.H. Tyrrell, *Electrochemical Immobilisation of Enzymes. 3. Immobilisation of Glucose Oxidase in Thin Films of Electrochemically Polymerised Phenols.* Analytical Chemistry, 1992. **64**(2): p. 138-142.

133. Bartlett, P.N. and D.J. Caruana, *Electrochemical Immobilisation of Enzymes Part V: Microelectrodes for the Detection of Glucose Based on Glucose Oxidase Immobilised in a Poly(phenol) Film.* Analyst, 1992. **117**: p. 1287-1292.

134. Bartlett, P.N. and D. Caruana, *Electrochemical immobilisation of enzymes. 6. Microelectrodes for the detection of L-lactate based on flavocytochrome B(2) immobilised in a poly(phenol) film.* Analyst, 1994. **119**: p. 175-180.

135. Cooper, J.M. and D.J. Pritchard, *Biomolecular sensors for neurotransmitter determination - electrochemical immobilisation of glutamate oxidase at microelectrodes in a poly(o-phenylenediamine) film.* Journal of Material Science, 1994. **5**(2): p. 111-116.

136. Faulkner, L.R., *Understanding Electrochemistry: Some Distinctive Concepts.* Journal of Chemical Education, 1983. **60**(4): p. 262-268.

137. O'Neill, R.D., *Microvoltammetric Techniques and Sensors for Monitoring Neurochemical Dynamics in vivo.* Analyst, 1994. **119**: p. 767-779.

138. Pletcher, D., *A First Course in Electrode Processes*. 1 ed. 1991, Alresford: Alresford Press Ltd. 1-271.

139. Fisher, A.C., *Electrode Dynamics*. 1 ed. Oxford Chemistry Primers, ed. S.G. Davies, *et al.* 1996, Oxford: Oxford University Press. 1-85.

140. Bard, A.J. and L.R. Faulkner, *Electrochemical Methods: Fundamentals and Applications*. 1 ed. 1980, New York: John Wiley & Sons. 703.

141. Vickerman, J.C., *et al.*, *Surface Analysis: The Principal Techniques*. 1 ed. 1997, Chichester: John Wiley & Sons Ltd. 1-451.

142. Fitzgerald, S., *Analysis of thin films and surfaces*. Microscopy and Analysis, 1995: p. 5-7.

143. Willard, H.H., *Chemical analysis of surfaces*, in *Instrumental Methods of Analysis*. 1974, Van Nostrand: London. p. 379-402.

144. Berkowitz, J., *Photoabsorption, Photoionization and Photoelectron Spectrscopy*. 1 ed. 1979, New York: Academic Press Inc. 1-465.

145. Briggs, D., *et al.*, *Practical Surface Analysis by Auger and X-ray Photoelectron Spectrscopy*. 1 ed. 1983, Chichester: John Wiley & Sons Ltd. 1-527.

146. Carlson, T.A., *Photoelectron and Auger Spectroscopy*. 1 ed. Modern Analytical Chemistry, ed. D. Hercules. 1975, New York: Plenum Press. 1-411.

147. Ratner, B., *Advances in the Analysis of Surfaces of Biomedical Interest*. Surface and Interface Analysis, 1995. **23**: p. 521-528.

148. Siegbahn, K., *ESCA Atomic Molecular and Solid State Structure Studies by Means of Electron Spectroscopy*. 1967, Uppsala: Almquist and Wiksells.

149. Sears, F.W., M.W. Zemansky, and H.D. Young, *University Physics*. 7 ed, ed. J.M. Dormitzer. 1987, Reading: Addison-Wesley Publishing Company.

150. Moulder, J.F., *et al.*, *Handbook of X-ray Photoelectron Spectroscopy*. 1992, Minnesota: Perking-elmer Corp.

151. Beamson, G. and D. Briggs, *High Resolution XPS of Organic Polymers: The Scienta ESCA300 Database*. 1992, Chichester: John Wiley & Sons.

152. Kemp, W., *Organic Spectroscopy*. 3 ed. 1991, London: MacMillan Education Ltd. 1-384.

153. Williams, H.D. and I. Fleming, *Infrared spectra,* in *Spectroscopic Methods in Organic Chemistry.* 1980, McGraw-Hill: London. p. 29-62.

154. Allara, D.L., *A summary of critical issues for application of IR spectroscopy to characterization of surface processing.* Critical Reviews in Surface Chemistry, 1993. **2**(1.2): p. 91-110.

155. Haris, P.I. and D. Chapman, *Does Fourier-transform infrared spectroscopy provide useful information on protein structures?* Trends in Biochemical Sciences, 1992. **17**(9): p. 328-333.

156. Porter, M.D., *IR external reflection spectroscopy: a probe for chemically modified surfaces.* Analytical Chemistry, 1988. **60**(20): p. 1143A-1155A.

157. van der Maas, J.H. and G. Dijkstra, *Basic Infrared Spectroscopy.* 1 ed. 1969, London: Heyden & Sons Ltd. 1-105.

158. Davies, M., *et al.*, *Infra-red Spectroscopy and Molecular Structure: An Outline of the Principles.* 1 ed. 1963, New York: Elsevier Publishing Company. 1-459.

159. Singh, B.R. and M.P. Fuller, *FT-iR in combination with the attenuated total reflectance technique: a very sensitive method for the structural analysis of polypeptides.* Applied Spectroscopy, 1991. **45**(6): p. 1017-1021.

160. Surewicz, W.K. and H.H. Mantsch, *New insight into protein secondary structure from resolution-enhanced infrared spectra.* Biochimica et Biophysica Acta, 1988. **952**(2): p. 115-130.

161. Susi, H. and D.M. Byler, *Resolution-enhanced fourier transform infrared spectroscopy of enzymes.* Methods in Enzymology, 1986. **130**(13): p. 290-311.

162. Fu, F.N., *et al.*, *Secondary structure estimation of proteins using the amide III region of Fourier Transform Infrared Spectroscopy: application to analyze calcium-binding-induced structural changes in calsequestrin.* Applied Spectroscopy, 1994. **48**(11): p. 1432-1441.

163. Yu, T., *et al.*, *Characterization of regenerated silk fibroin membranes for immobilizing glucose oxidase and construction of a tetrathiafulvalene-mediating glucose sensor.* Journal of Applied Polymer Science, 1995. **58**: p. 973-980.

164. Griffith, A., *et al., Determination of the biomolecular composition of an enzyme-polymer biosensor.* The Journal of Physical Chemistry B, 1997. **101**(11): p. 2092-2100.

165. Lin, X. and H. Zhang, *In situ external reflection FT-iR spectroelectrochemical investigation of poly(o-phenylenediamine) film coated on a platinum electrode.* Electrochimica Acta, 1996. **41**(13): p. 2019-2024.

166. McBride, M.B. and K.H. Kung, *Adsorption of phenol and substituted phenols by iron oxides.* Environmental Toxicology and Chemistry, 1991. **10**: p. 441-448.

167. Fiol, C., *et al., Characterization of behenic acid/glucose oxidase Langmuir-Blodgett films by spectrophotometry: a tentative model of their organization.* Thin Solid Films, 1995. **261**: p. 287-295.

168. Pouchert, C.J., *The Aldrich Library of FT-iR Spectra.* 1985, Milwaukee: Aldrich Chemical. 4800.

169. Brendel, R., *Quantitative infrared study of ultrathin MIS structures by grazing internal reflection.* Applied Physics A, 1990. **50**: p. 587-593.

170. Rabolt, J.F., M. Jurich, and J.D. Swalen, *Infrared reflection-absorption studies of thin films at grazing incidence.* Applied Spectroscopy, 1985. **39**(2): p. 269-272.

171. Lowry, J.P., *et al., Characterisation of carbon paste electrodes in vitro for simultaneous amperometric measurements of change in oxygen and ascorbic acid concentrations in vivo.* Analyst, 1996. **121**(6): p. 761-766.

172. Lowry, J.P., *et al., Characterisation of glucose oxidase-modified poly(phenylenediamine)-coated electrodes in vitro and in vivo: homogenous interference by ascorbic acid in hydrogen peroxide detection.* Analytical Chemistry, 1994. **66**(10): p. 1754-1761.

173. Cammack, J., B. Ghasemzedah, and R.N. Adams, *The pharmacological profile of glutamate-evoked ascorbic acid efflux measured by in vivo electrochemistry.* Brain Research, 1991. **565**: p. 17-22.

174. Szucs, A., G.D. Hitchens, and J.O. Bockris, *On the adsorption of glucose-oxidase at a gold electrode.* Journal of the Electrochemical Society, 1989. **136**(12): p. 3748-3755.

175. Dong, X.D. and J.T. Lu, *Characteristics of the glucose oxidase at different surfaces.* Bioelectrochemistry and Bioenergetics, 1997. **42**(1): p. 63-69.

176. Fortier, G. and D. Belanger, *Characterisation of the biochemical behaviour of glucose-oxidase entrapped in a polypyrrole film.* Biotechnology and Bioengineering, 1991. **37**(9): p. 854-858.

177. *SigmaPlot 4.0 - User's Manual.* 1997, Chicago: Prentice Hall.

178. Wang, J. and Z. Lu, *Highly stable phospholipid cholesterol electrode coatings for amperometric monitoring of hydrophobic substances in flowing streams.* Analytical Chemistry, 1990. **62**(8): p. 826-829.

179. de Gier, J., *Permeability barriers formed by membrane-lipids.* Bioelectrochemistry and Bioenergetics, 1992. **27**(1): p. 1-10.

180. Amine, A., *et al.*, *Electrochemical behaviour of a lipid modified enzyme electrode.* Analytical Letters, 1989. **22**(11-1): p. 2403-2411.

181. Salmeron, M., L. Brewer, and G.A. Somorjai, *The structure and stability of surface platinum oxide and of oxides of other noble metals.* Surface Science, 1981. **112**(3): p. 207-228.

182. Farebrother, M., *et al.*, *Early stages of growth of hydrous platinum-oxide films.* Journal of Electroanalytical Chemistry, 1991. **297**(2): p. 469-488.

183. Bolzan, A.E. and A.J. Arvia, *Fast electrochemical reactions during the anodization of platinum-electrodes in aqueous-solutions - detection of a reversible charge storage process at platinum-oxide coated electrodes.* Journal of Electroanalytical Chemistry, 1992. **341**(1-2): p. 93-109.

184. Birss, V.I. and M. Goledzinowski, *The unusual reduction behaviour of thin, hydrous platinum oxide-films.* Journal of Electroanalytical Chemistry, 1993. **351**(1-2): p. 227-243.

185. Dicks, J.M., *et al.*, *Ferrocene modified polypyrrole with immobilised glucose-oxidase and its application in amperometric glucose microbiosensors.* Annales de Biologie Clinique, 1989. **47**(10): p. 607-619.

186. Reffner, J.A. and W.T. Wihlborg, *Microanalysis by reflectance FT-iR microscopy.* American Laboratory, 1990. **22**(6): p. 19-26.

187. Socrates, G., *Infrared Characteristic Group Frequencies: Tables and Charts.* 2 ed. 1980, Chichester: John Wiley & Sons Ltd. 1-246.

188. Radhakrishnan, S. and A.B. Mandale, *Polypyrrole growth on crystalline PEO complexes - characterisation by WAXD and XPS.* Synthetic Metals, 1994. **62**(3): p. 217-221.

189. Williams, R.W., *Protein secondary structure analysis using Raman amide I and amide II spectra.* Methods in Enzymology, 1986. **130**(14): p. 311-331.

190. Duff, D.G., S.M.C. Ross, and D.H. Vaughan, *Adsorption from Solution - An experiment to illustrate the Langmuir Adsorption-Isotherm.* Journal of Chemical Education, 1988. **65**(9): p. 815-816.

191. Eckl, K. and H. Gruler, *Description of cell-adhesion by the Langmuir Adsorption-isotherm.* Zeitschrift fur Naturforschung C - A Journal of Biosciences, 1988. **43**(9-10): p. 769-776.

192. *Sigma Catalogue.* 1998, Poole, Dorset: Sigma-Aldrich Company Ltd.

193. Benveniste, H. and P.C. Huttemeier, *Microdialysis - Theory and Application.* Progress in Neurobiology, 1990. **35**(3): p. 195-215.

194. Obrenovitch, T.P., *et al.*, *Extracellular neuroactive amino-acids in the rat striatum during ischaemia - comparison between penumbral conditions and ischaemia with sustained anoxic depolarization.* Journal of Neurochemistry, 1993. **61**(1): p. 178-186.

195. Albery, W.J., M.G. Boutelle, and P.T. Galley, *The dialysis electrode - a new method for in vivo monitoring.* Journal of the Chemical Society - Chemical Communications, 1992. **12**: p. 900-901.

196. Koshy, A., *et al.*, *Monitoring Molecules in Neuroscience*, , H. Rollema, B.H.C. Westernick, and W.J. Drijfhout, Editors. 1991, University Centre for Pharmacy: Groningen. p. 131-133.

197. Pishko, M.V., A.C. Michael, and A. Heller, *Amperometric glucose microelectrodes prepared through immobilization of glucose oxidase in redox hydrogels.* Analytical Chemistry, 1991. **63**(20): p. 2268-2272.

198. Manahan, S.E., *The Quantitative Treatment of Data*, in *Quantitative Chemical Analysis*, S. Ewing, Editor. 1986, Brooks/Cole Publishing Company: Belmont, California. p. 55-83.